An analysis of insulin- and non-insulin- stimulated glucose transport in rat skeletal muscle

A thesis submitted to the
FACULTY OF MEDICINE

For the degree of
DOCTOR OF PHILOSOPHY

By

Declan Jonathan James

Department of Biochemistry and Molecular Biology
The University of Glasgow

January 2002

Abstract

Skeletal muscle plays a crucial role in the insulin-mediated post-prandial disposal of blood glucose. Insulin resistance, that is a reduction in insulin's ability to stimulate glucose uptake, is of major pathogenic importance in several prevalent human disorders, including type 2 diabetes, hypertension and obesity. Interestingly, there is good evidence to suggest that in insulin-resistant individuals exercise-stimulated glucose uptake is unaffected. In an effort to explore these two mechanisms, I have examined insulin- and 5-aminoimidazole-4-carboxamide 1-β-D-ribonucleoside (AICAR)-stimulated glucose uptake in isolated skeletal muscle from the insulin-resistant stroke-prone spontaneously hypertensive rat (SHRSP) and the obese Zucker diabetic fatty rat (ZDF), a model of type 2 diabetes.

The data presented here will show that while the stroke-prone spontaneously hypertensive rat (SHRSP) and Zucker diabetic fatty rat display reduced insulin-stimulated glucose transport, their response to AICAR is unimpaired with respect to their insulin-sensitive controls, the Wistar Kyoto (WKY) and lean Zucker rats, respectively. Importantly, the observed insulin-resistance is also maintained in skeletal muscle cells cultured from SHRSP and ZDF rats, implying that the defect does not arise as a consequence of the tissue environment, but rather is a genetic characteristic of the muscle cells.

The expression and function of key molecules in the insulin-signalling cascade was also examined in these strains. Intriguingly, the total cellular expression levels of caveolin and flotillin, key proteins implicated in insulin signal transduction and compartmentalisation, are increased in the skeletal muscle from SHRSP compared to WKY but are unchanged between ZDF and lean Zucker rats. On the other hand the insulin-dependent activation of protein kinase B is markedly impaired in ZDF skeletal muscle with respect to lean Zucker rats, but is not different between SHRSP and WKY.

Taken together these results indicate that an inherent defect, at the level of skeletal muscle, is responsible for the observed insulin resistance. Moreover, this defect is confined to an insulin-specific step in the activation of glucose transport and is not a consequence of generalised resistance in the mechanism(s) of glucose transport. In addition, this underlying defect may be different between SHRSP and ZDF rats.

Finally, the molecular mechanism by which hyperglycaemia impairs insulin action was investigated in ZDF rats. Hyperglycaemia impairs insulin-stimulated glucose transport in lean Zucker muscle cells but does not lead to further impairment in the ZDF rat. The anti-diabetic drug, Rosiglitazone, was found to increase the basal glucose uptake by approximately two-fold but had no effect on insulin-stimulated glucose transport in lean or ZDF muscle cells cultured under normoglycaemic or hyperglycaemic conditions. These data are discussed within the context of present theories on the aetiology of insulin resistance.

Acknowledgements

I am eternally indebted to my poulaki Litsa, for her unending support and love throughout this odyssey. I would also like to say a special 'woof' to my dog, Erakli - Thank you for keeping my feet warm during the nights I was writing this, and for taking me for walks in the freezing cold (better than coffee anyday).

A big thanks goes to my supervisor, Prof. Gwyn Gould for always lightening the DOWNS and focusing the UPS - A great boss. I also wish to thank the Medical Research Council and SmithKline Beecham for providing me with a case award studentship.

I am especially grateful to Dr Luke Chamberlain and Dr Ian Salt for their invaluable technical support throughout this study and their advice and comments on improving this thesis. I would like to thank Fiona Cairns (a fellow muscler) and Delyth Graham for their help and technical assistance. Thanks to all members of Lab-C36 a great bunch of people to work with – Never a dull moment, always entertaining - to brighten up a day of pipetting. Thanks goes also to Dr. Francis Burton for the hours spent teaching me how to dissect muscles without mangling them up.

I would like to express my appreciation towards Dr. Greg Murphy for all his help and advice in things scientific and philosophical from the start. The Dominicans have a quality scientist, a great thinker and generous man but don't get him drunk and don't feed him after midnight. Thanks to everyone who helped in Vascular Biology at SmithKline Beecham now GlaxoSmithkline. Special thanks to Dr Stephen Smith for allowing me free reign of VB budget, Dr Paul Young, Dr Gary Moore (Mr TaqMan and molecular biology guru), Dr Carolyn Lister and the student posse and members of lab 007.

Finally, I would like to thank my Mum, Dad and my brothers Dominic and Kyle for their love and support they have always given me. And thanks to the BIG BOSS for letting me spin the decks.

Table of contents

List of Tables and Figures.

Abbreviations

AICAR	5-aminoimidazole-4-carboxamide 1-β-D-ribonucleoside
AMPK	AMP-activated protein kinase
ATP	Adenosine 5'-triphosphate
CEE	Chick embryo extract
DeGlc	2-deoxy-D-glucose
DTT	Dithiothreitol
ECL	Enhanced chemiluminescence
EDL	Extensor digitorum longus
EDTA	Diaminoethanetetra-acetic acid
eNOS	Endothelial nitric oxide synthase
FBS	Foetal bovine serum
FDB	Flexor digitorum brevis
FITC	Fluorescein isothiocyanate
Glut	Glucose transporter
HRP	Horse radish peroxidase
IRS	Insulin receptor substrate
mA	Milli Amps
min	Minutes
PDK1/2	3-Phosphoinositide-dependent kinase 1/2
PKB/cAKT	Protein kinase B
PI3K	Phosphatidylinositol 3'-kinase
SDS-PAGE	Sodium dodecyl sulphate-polyacrylamide gel electrophoresis
SHR	Spontaneously hypertensive rat
SHRSP	Stroke-prone spontaneously hypertensive rat
SNARE	Soluble N-ethylmaleimide attachment protein receptor
TEMED	N,N,N',N'-tetramethylethylenediamine.
Tx-100	TritonX-100
VAMP	Vesicle associated membrane protein
v/v	volume/volume ratio
WKY	Wistar Kyoto rat
w/v	weight/volume ratio
ZDF	Zucker diabetic fatty rat
ZMP	5-aminoimidazole-4-carboxamide ribonucleotide

Chapter 1

Introduction

1.1 Glucose homeostasis

Sugar metabolism describes the physical and chemical processes required for the transformation of carbohydrate into energy, vital for the various activities and survival of the cell (Banks et al., 1976). Metabolism of circulating dietary sugar is also essential for glucose homeostasis, i.e. the maintenance of blood glucose at normal levels (Banks et al., 1976); (Shulman and Rothman, 2001). In the post-prandial state, utilisation of the circulating glucose by the peripheral tissues of skeletal muscle and fat has to overcome some key constraints. These can be summarised as the physiological limitations of getting glucose from the blood into the interstitial space surrounding the muscle, and the cellular control in moving glucose from the interstitium across the plasma membrane into the cell (Vock et al., 1996). Finally, once inside the cell the utilisation of glucose is important in maintaining cellular function.

Movement of glucose from blood to interstitium.

The capillary bed that vascularises skeletal muscle is not a barrier to the glucose molecule since evidence suggests that glucose can freely move through the junctions between the capillary endothelial cells (Perry, 1980); (Vock et al., 1996). However, the amount of glucose moving into the interstitium and subsequently into the muscle cell is dependent on blood glucose concentration, blood flow and the degree of vascularisation of the muscle (Vock et al., 1996).

Skeletal muscle vascularisation influences the amount of interstitial glucose and distance between substrate (glucose) and target (skeletal muscle cell). The red in pigment type-1 muscle fibres are highly vascularised and have a higher oxidative capacity and more mitochondria (Wasserman and Halseth, 1998). In contrast, the white in pigment type-2b muscle fibres are poorly vascularised, have a low oxidative capacity with very few mitochondria and rely primarily upon the glycolytic pathway for energy production (Wasserman and Halseth, 1998). The above characteristics of type-1 muscle fibres give them the ability to work at a sustained level of output for longer periods, and therefore are referred to as slow-twitch fibres. Type-2b, are more suited to short powerful bursts of output and are referred to as fast-twitch fibres (Wasserman and Halseth, 1998). Studies have correlated insulin action with a greater increase in glucose uptake in the highly vascularised type-1 fibres in contrast to a negligible increase in the poorly vascularised

type-2b fibres (O'Doherty et al., 1998). Together with the extent of vascularisation, perfusion of the vasculature also determines extracellular glucose availability (Wasserman and Halseth, 1998). Both muscle contraction and exercise increase perfusion of skeletal muscle by as much as twenty-fold (Wasserman and Halseth, 1998). In addition, insulin through a haemodynamic effect is believed to increase skeletal muscle perfusion, thereby leading to an increase in extracellular substrate availability (Baron, 1994).

In summary, vascularisation and perfusion of skeletal muscle are important factors which influence the availability of extracellular glucose to the muscle cell and may in part explain the decreased rates of glucose disposal seen in poorly vascularised type-2b muscle in contrast to highly vascularised type-1 muscle.

Movement of glucose from interstitium across sarcolemma into the muscle cell.

The sarcolemma of the muscle cell/fibre is an effective barrier to the polar glucose molecule (Rea and James, 1997). As a consequence, glucose transfer across the sarcolemma requires a facilitative transport system (Gould and Seatter, 1997). Insulin maintains glucose homeostasis not only by facilitating the uptake of glucose molecules by the cells, but also by stimulating the conversion and storage of glucose in the form of glycogen (Yeaman et al., 2001). In the next few pages the signalling pathways by which insulin facilitates glucose transport and glycogen synthesis will be discussed.

1.2 Insulin-stimulated glucose transport

1.2.1 Insulin and the insulin receptor

Insulin is a polypeptide hormone that is synthesised and processed into the active form by the pancreatic β cells in the Islets of Langerhans. It was insulin's ability to reduce high levels of blood glucose in diabetics that attracted scientific interest after its discovery in 1922. This lead to the belief that lack of insulin was the primary defect in all patients with diabetes. Work by Himsworth in 1936 proved that lack of insulin was not the only form of the disease, indeed the more common form still prevailed in spite of insulin administration (Himsworth, 1936). He pointed to two forms of diabetes, the first he termed 'insulin sensitive' due to the ability of insulin to ameliorate the disease and the second 'insulin insensitive' or insulin resistant where insulin treatment was ineffective (Himsworth, 1936). Research since has been occupied with the challenging task of understanding the molecular events which insulin elicits in cells.

The unique ability of insulin to regulate glucose metabolism is brought about by its binding to the insulin receptor (Kasuga et al., 1982b). The insulin receptor belongs to the tyrosine kinase family of receptors and is widely expressed in many tissues including brain, liver, pancreas, cardiac muscle, skeletal muscle and fat (Siddle et al., 2001). Tyrosine kinase receptors are capable of phosphorylating intracellular substrates on tyrosine residues thus communicating an external signal into the cell (Siddle et al., 2001).

The insulin receptor (Figure 1.1) consists of two extracellular α–subunits and two membrane-spanning β-subunits that are held together by extracellular disulphide bonds to give a β–α–α–β subunit structure (Van Obberghen et al., 1981); (Kasuga et al., 1982a). Thus the insulin receptor is referred to as a heterotetrameric receptor. The α–subunits contain the ligand binding domains made up of two β helices and a cysteine rich region (Siddle et al., 2001). The β-subunits contain an extracellular domain, which also possesses ligand contact sites, a transmembrane domain and an intracellular domain (Siddle et al., 2001). This intracellular domain can be further subdivided into 3 functionally distinct regions: the juxta-membrane domain, the tyrosine kinase domain and the carboxyl terminal (C-terminal) domain (Siddle et al., 2001). The juxta-membrane

domain contains an internalisation NPXY motif that can be phosphorylated on the tyrosine residue and participates in insulin receptor substrate binding (White et al., 1988a). Site-directed mutagenesis of this tyrosine prevents receptor interaction with and phosphorylation of receptor substrates (White et al., 1988a). The tyrosine kinase domain contains binding sites for ATP and receptor substrates (Cheatham and Kahn, 1995). However, under basal conditions these sites are not available for ATP or receptor substrate binding (Hubbard et al., 1994). Insulin binding stimulates each β-subunit to phosphorylate the other on several residues. The subsequent autophosphorylation of three tyrosines in the tyrosine kinase domain is associated with the active form of the receptor (Kasuga et al., 1982c); (White et al., 1988b). This tris-autophosphorylation of the insulin receptor kinase domain reveals ATP and insulin receptor substrate binding sites (Hubbard et al., 1994); (Hubbard, 1997). Site-directed mutagenesis of the ATP-binding site within the kinase domain of human insulin receptors, abolishes subsequent tyrosine kinase activity toward insulin receptor substrates (Ebina et al., 1987); (Chou et al., 1987). In summary, the consequences of this tyrosine phosphorylation are twofold; it reveals recognition sites for and signals increased kinase activity toward cellular substrates.

As the insulin receptor is the first point of transmission and amplification of the insulin signal, any alteration in insulin binding, receptor expression, location, phosphorylation or kinase activity will drastically affect propagation of the insulin signal into the cell (Taira et al., 1989); (Williams et al., 1990); (Krook and O'Rahilly, 1996). Such alterations in the insulin receptor lead to severe insulin resistance as seen in Rabson-Mendenhall syndrome, in which a genetic deficiency of insulin receptors expression is observed (Rabson and Mendenhall, 1956); (Moncada et al., 1986). Such syndromes are rare in the general population and do not account for the majority of the insulin resistance seen, thus events downstream of the insulin receptor are suspected.

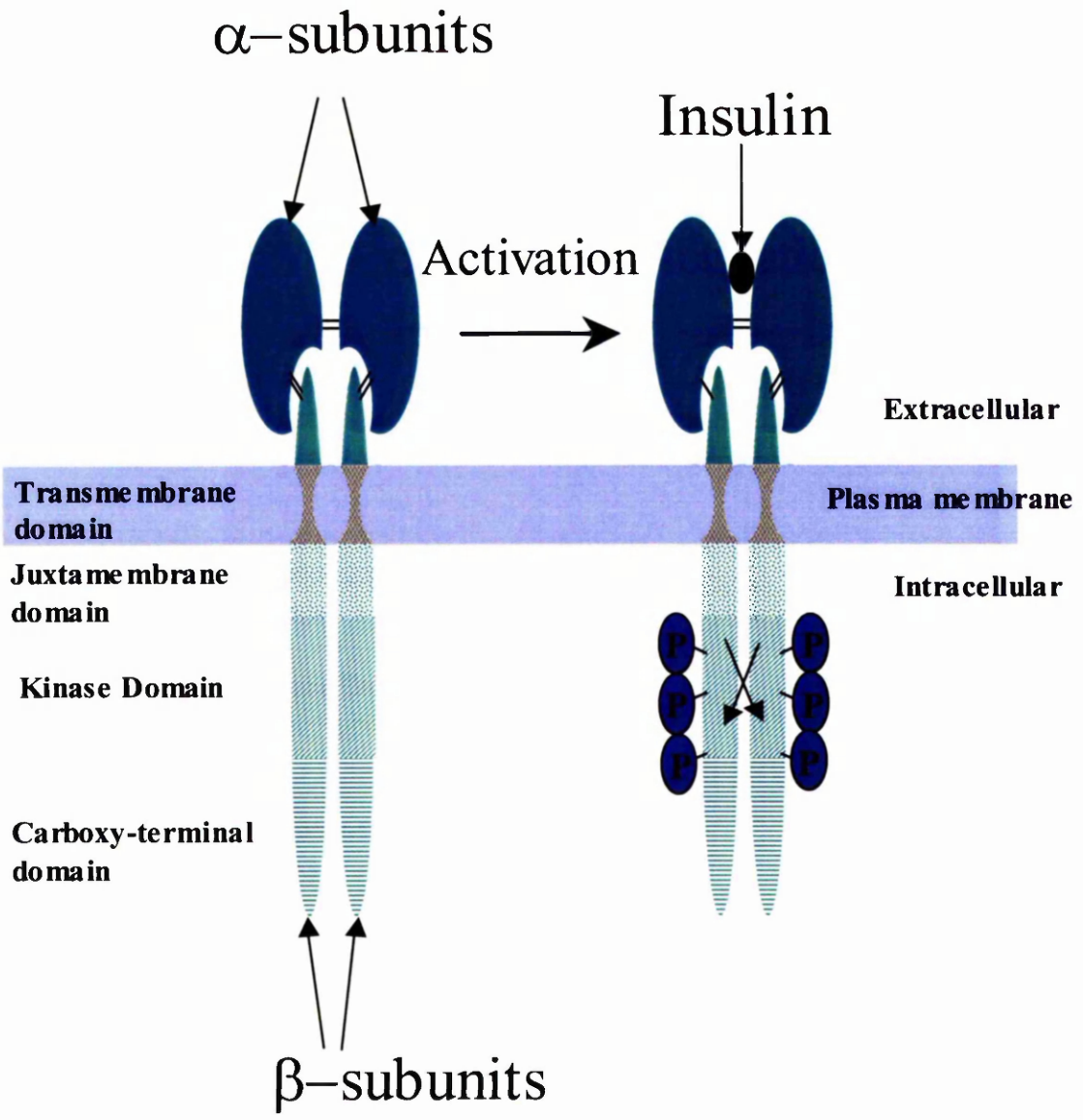

Figure 1.1 Structure and activation of the insulin receptor.

The insulin receptor is a heterotetramer composed of two identical α–subunits and two β–subunits. The α–subunits are disulphide linked to each other and to the β–subunits. The insulin receptor is activated by intramolecular trans-phosphorylation of the β–subunits upon binding of monomeric insulin ligand. Three tyrosine residues in the kinase domain become phosphorylated (indicated by circled letter P) and are associated with activated insulin receptor tyrosine kinase activity toward intracellular substrates.

1.2.2 Insulin receptor substrates and downstream events that lead to glucose transport.

The kinase domain of the insulin receptor was first shown to specifically phosphorylate a 185 KDa protein named IRS-1 (White et al., 1985); (Rothenberg et al., 1991); (Sun et al., 1992). Three other genetically and structurally homologous proteins, which are phosphorylated by the insulin receptor, have since been characterised: the 190 KDa IRS-2 (Sun et al., 1995), the 60 KDa IRS-3 (Lavan et al., 1997b) and the 160 KDa IRS-4 (Lavan et al., 1997a). Mutations in the insulin receptor juxtamembrane domain that disrupt insulin receptor-IRS-1 binding result in decreased insulin signalling (White et al., 1988a), whereas over expression of functional IRS-1 with these mutant insulin receptors restores the insulin response (Chen et al., 1995). Genetic ablation of either IRS-1 or IRS-2 in mice has deleterious effects on glucose transport (Araki et al., 1994); (Tamemoto et al., 1994); (Withers et al., 1998). Specifically, IRS-2 gene knock-out (KO) results in a diabetic phenotype whereas IRS-1 gene KO mice are insulin resistant (Araki et al., 1994); (Tamemoto et al., 1994); (Withers et al., 1998). The less severe insulin resistant phenotype seen in IRS-1 gene KO animals is attributed to the presence of other IRS isoforms (IRS–2 and –3), which are able to compensate for the lack of IRS-1 (Araki et al., 1994); (Tamemoto et al., 1994).

Each IRS isoform possesses an amino terminal (N-terminal) pleckstrin homology (PH) domain, capable of localising the protein toward charged phosphoinositide lipids in cellular membranes (White, 1998). Adjacent to the PH domain lies a phospho-tyrosine-binding domain (PTB domain), which binds the NPXpY motif present in the juxta-membrane domain of the insulin receptor β-subunit (White, 1998). The PH and PTB domains specifically target the substrates toward the insulin receptor where the activated insulin receptor tyrosine kinase domain phosphorylates multiple tyrosine residues C-terminal of the PH and PTB domains (Figure 1.2). Specifically, IRS-1 is phosphorylated on multiple tyrosine residues, which lie in YMxM or YxxM motifs (White, 1998). These tyrosine residues act as 'multiple docking sites' for proteins that contain PTB domains or Src homology-2 (SH-2) domains (White, 1997). SH-2 domains display great homology to the 60KDa viral sarcoma oncogene protein, $pp60^{v\text{-}src}$ that was first shown to have activity toward tyrosine residues.

In summary, the insulin receptor transduces its signal by recruitment and phosphorylation of IRS-1, -2, -3 and -4 (White, 1998). This permits multiple downstream events dependent on the recognition of pY motifs by SH2 or PTB containing effector proteins and on the repertoire of effector proteins present in the cell (White, 1998). The use of 'multiple docking proteins' like IRS's allows the insulin receptor to escape the stoichiometric constraints faced in ligand-receptor activation (one insulin molecule activating one insulin receptor) therefore amplifying the receptor signal (White, 1998).

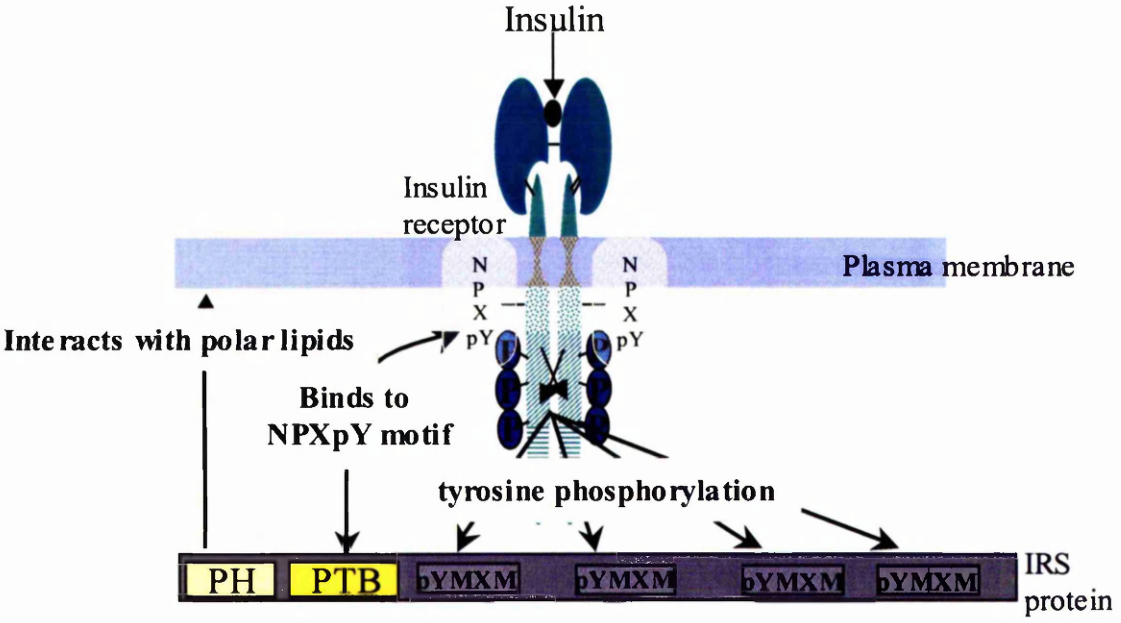

Figure 1.2 Protein-protein interaction domains involved in insulin signal transduction .

The amino-terminal PH domain is involved in the targeting of a typical IRS protein to the plasma membrane. The PTB domain is critical for the recognition of the juxta-membrane NPXpY sequence of the insulin receptor. Therefore both the PH and PTB domain contribute to the interaction of IRS with the insulin receptor. During interaction with the activated insulin receptor, the IRS proteins are phosphorylated on several tyrosine residues by the insulin receptor kinase domain. *Reproduced from Virkamaki, Ueki and Kahn, 1999*

Under insulin-stimulated conditions IRS-1 is found to co-immunoprecipitate with a heterodimeric protein consisting of an 85 KDa (p85) and a 110 KDa (p110) subunit (Shepherd et al., 1998). The p85 subunit acts as an adapter protein and interacts with phosphorylated tyrosine residues of IRS-1 via two SH2 domains (Rordorf-Nikolic et al.,

1995), and recruits the p110 subunit via a SH3 domain (Shepherd et al., 1998). The p110 subunit phosphorylates the D3 position of the inositol ring in phosphatidyl inositol-4,5-bisphosphate (PIP_2) lipids, thereby leading to an accumulation of phosphatidyl inositol-3,4,5-trisphosphate (PIP_3) lipids (Whitman et al., 1988); (Shepherd et al., 1998). Due to this specific activity it was named Phospho Inositide 3-Kinase (PI3K) (Figure 1.3). PI3K belongs to a large family of kinases categorised in four classes according to their function, structure and substrate specificity (Vanhaesebroeck et al., 1997). These enzymes are sub-classified in respect to the adapter and catalytic subunit isoforms they possess (Shepherd et al., 1998). Currently, the only PI3K form known to be implicated in insulin-stimulated glucose uptake is the Class I heterodimeric p85α / p110β PI3K (Wang et al., 1998; Wang et al., 1999).

Studies using a mutant adapter subunit (Δp85) in Chinese Hamster Ovary (CHO) and adipocyte cells showed that insulin-stimulated PI3K activity and glucose transport were impaired without affecting insulin receptor tyrosine kinase activity and IRS-1 phosphorylation (Hara et al., 1994); (Sharma et al., 1998). The PI3K inhibitor, wortmannin, inhibits insulin stimulation of glucose transport in skeletal muscle and fat cells (Cheatham et al., 1994); (Clarke et al., 1994); (Okada et al., 1994); (Kaliman et al., 1995); (Tsakiridis et al., 1995). Interestingly, the yeast PI3K homologue, vps34, is also involved in membrane trafficking events (Schu et al., 1993). In agreement, data regarding PI3K inhibition in mammalian systems found that treatment of cells with wortmannin prevented the sorting of proteins out of endosomes into a recycling or exocytic pathway and lead to their accumulation in large vacuolar-like bodies (Reaves et al., 1996). This suggested that PI3K activity facilitates vesicle budding from internal compartments and or vesicle fusion with target membranes, with possible implications for the insulin-sensitive glucose transporter, (Glut-4). Glut-4, as discussed in detail in the following sections (1.2.3 - 1.2.4.1), under basal conditions is sequestered intracellularly in a vesicular compartment and moves to the plasma membrane in response to insulin stimulation (Rea and James, 1997). In adipocytes, insulin-stimulation results in the specific targeting of IRS-1 along with recruited PI3K, from a cytosolic location to an intracellular protein matrix believed to be a cytoskeletal structure, which is distinct from but co-sediments with microsomal membranes (Yang et al., 1996); (Clark et al., 1998). Recent observations in myocytes, demonstrate that insulin stimulates a rapid re-

organisation of the actin cytoskeleton near the plasma membrane (Khayat et al., 2000). These actin cytoskeletal structures rapidly concentrate PI3K and subsequently recruit Glut-4 (Khayat et al., 2000).

In summary, these data suggest that PI3K activation is a point of convergence of insulin signalling and Glut-4 trafficking pathways, thus implying a necessity for PI3K activity in insulin-stimulated glucose transport (Shepherd et al., 1998). Therefore, the possibility exists that mutations in the PI3K gene could contribute to insulin resistance. Indeed, the mutation M326I, on the p85α coding sequence has been associated with glucose intolerance in humans (Hansen et al., 1997).

Recent investigations of downstream targets suggests that the product of PI3K activity, PI-3,4,5-P_3 (PIP_3) is necessary for glucose uptake (Jiang et al., 1998). This is borne out by overexpression experiments utilising PTEN (phosphatase and tensin homologue deleted on chromosome 10), which results in decreased PIP_3 levels in conjunction with an inhibition of insulin-stimulated glucose transport (Nakashima et al., 2000); (Ono et al., 2001). It has been proposed that localised production of phosphoinositides could promote budding and subsequent fusion of Glut4-containing vesicles with the plasma membrane (Heller-Harrison et al., 1996) (Glut4-containing vesicles are described in detail in 1.2.4.1).

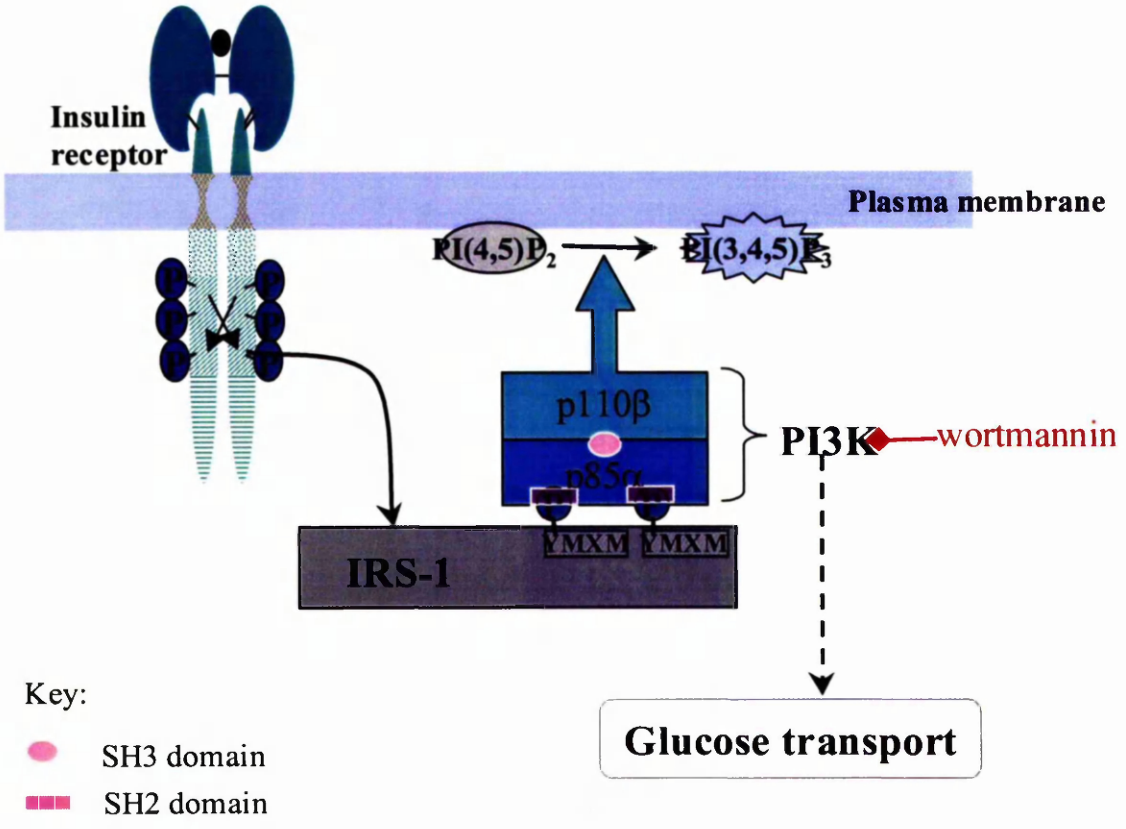

Figure 1.3 Schematic illustration of insulin signal transduction via IRS-1 and PI3K. .

The insulin receptor uses the IRS proteins to activate PI3K. The activated insulin receptor transiently binds and phosphorylates IRS-1 proteins. Phosphorylated tyrosine residues of IRS-1 interact with the p85α regulatory subunit of PI3K via two SH2 domains, which results in the activation of PI3K and increased glucose transport. The activated PI3K catalyses the phosphorylation of phosphoinositides on the 3-position to produce phosphatidylinositol-3-phosphate, especially $PI(3,4,5)P_3$. The fungal metabolite, wortmannin, specifically inhibits PI3K activity and insulin-stimulated glucose transport.

1.2.3 The glucose transporter family.

The family of glucose transporters (Gluts) consists of 12 members (Gluts1-12) (Table 1.1). The Gluts consist of 12 transmembrane spanning α–helices, which are arranged to form a central pore through which the bi-directional transport of monosaccharides can take place (Barrett et al., 1999). Studies indicate that regions of the transporters exposed to the extracellular or intracellular space have binding sites for monosaccharides (Barrett et al., 1999). Monosaccharide binding induces conformational changes in the transporter that results in the movement of the sugar molecule through the central pore and subsequent release on the other side of the membrane (Barrett et al., 1999). All the glucose transporters are post-translationally glycosylated on an asparagine residue of the exofacial loop between helices 1 and 2. The glucose transporters have a varied tissue distribution with Glut-1 being expressed in nearly all tissues. Skeletal muscle variably expresses Gluts-1, -3, -4, –5 and -11, all having marked differences in monosaccharide specificity (Table 1.1).

Protein	alias	Tissue distribution in humans	Hexose specificity
Glut 1		Erythrocytes, blood-tissue barriers, brain, low expression in all other tissues	Glucose
Glut 2		Liver, pancreatic β-cells, intestinal epithelia, kidney tubules	Low affinity but high capacity for glucose transport
Glut 3		Brain and neuronal tissues, placenta, liver, heart and skeletal muscle	High affinity for glucose
Glut 4		Fat cells, skeletal muscle, cardiac muscle, low expression in brain	High affinity for glucose
Glut 5		Small intestine epithelia, kidney, testis, spermatozoa, skeletal muscle	Fructose
Glut 6	Glut 9	Spleen, leukocytes, brain	Glucose
Glut 7		Uncharacterised	Unknown at present
Glut 8	GlutX1	Testis, blastocyst, brain	High affinity for glucose, can be specifically inhibited with fructose
Glut 9	GlutX	Liver, kidney	Unknown at present
Glut 10		Liver, pancreas	Unknown at present
Glut 11	Glut10	Cardiac and skeletal muscle	Low affinity for glucose, can be specifically inhibited with fructose (possible fructose transporter)
Glut 12	Glut8	Cardiac muscle and prostate	Unknown at present

Table 1.1 The facilitative glucose transporter isoforms. *Adapted from (Joost and Thorens, 2001).*

1.2.4 The muscle specific Gluts

Glut-1

Originally discovered as the abundant glucose transporter in erythrocyte membranes, this ubiquitous glucose transporter resides predominantly at the plasma membrane of most cells where it is responsible for the basal transport of glucose into the cell (Kasahara and Hinkle, 1977); (Baldwin et al., 1979); (Gorga et al., 1979). Glut-1 is highly expressed in brain, endothelial cells and erythrocytes, and is expressed (*in vitro*) in neo-natal and developing myoblasts but this expression is diminished in mature muscle and myotubes (*in vitro*) (Guillet-Deniau et al., 1994).

Glut-3

Glut-3 is expressed in nerves, pancreatic β-cells and embryonic tissues where it has a high affinity for glucose transport (Kayano et al., 1988); (Colville et al., 1993). Glut-3 is highly expressed during development of embryonic myoblasts and is restricted to intracellular compartments. However, during the early stages of myoblast alignment and fusion, Glut-3 is exclusively found at the plasma membrane. By three to four days post differentiation no Glut-3 (*in vitro)* is expressed in the mature myotube (Guillet-Deniau et al., 1994).

Glut-5

Glut-5 has a wide tissue distribution and can be found in the small intestine, skeletal muscle, adipose tissue, kidney, brain and spermatozoa (Kayano et al., 1990); (Mantych et al., 1993). Detailed functional characterisation showed Glut-5 to be a fructose specific transporter (Rand et al., 1993). Isolation of membrane fractions and immunocytochemistry revealed that Glut-5 localisation in skeletal muscle is restricted to the sarcolemma and is completely absent from internal membranes (Hundal et al., 1992); (Darakhshan et al., 1997); (Kristiansen et al., 1997). Glut-5 provides skeletal muscle with the ability to utilise fructose as a possible substrate.

Glut-4

The unique characteristic of Glut-4 is its high responsiveness to insulin. This transporter is predominantly expressed in cardiac muscle, skeletal muscle and fat (Fukumoto et al., 1989); (James et al., 1989); (Birnbaum, 1989). It is expressed late in the differentiation of

myoblasts but is the dominant glucose transporter isoform in mature myotubes (Guillet-Deniau et al., 1994). Glut-4 is unique among other glucose transporters in that under basal conditions it is sequestered intracellularly and localises to perinuclear compartments and large tubulo-vesicular aggregates within the centre of the muscle and fat cell (Friedman et al., 1991); (Slot et al., 1991b). This distribution of Glut-4 is also seen in whole skeletal muscle fibres and cultured differentiated skeletal muscle cells (Ploug et al., 1998), (Ralston and Ploug, 1996). In skeletal muscle fibres, contraction or insulin stimulation results in a redistribution of Glut-4 from these intracellular compartments to the sarcolemma and T-tubules and is concomitant with an increase in glucose uptake (Fushiki et al., 1989); (Roy and Marette, 1996); (Zorzano et al., 1996).

1.2.4.1 Subcellular localisation and translocation of Glut-4

Cushman and Suzuki were the first to show that insulin stimulated the recruitment of glucose transporters from an intracellular storage site to the cell surface (Cushman and Wardzala, 1980); (Suzuki and Kono, 1980); (Holman and Cushman, 1994). It has been the purpose of much research to define this intracellular storage site and thus discover how Glut-4 trafficking is regulated in response to insulin or contraction (Czech and Corvera, 1999); (Holman and Sandoval, 2001); (Ryder et al., 2001). Such information could aid in the rational design of drugs able to mimic the insulin and contraction responsiveness of this Glut-4 compartment. However, recent analyses have found that Glut-4 colocalises with numerous compartments of the cellular recycling system. These compartments include clathrin coated vesicles, endosomes, the trans-Golgi network and vesicles collectively referred to as Glut-4 storage vesicles (GSVs) that are enriched with Glut-4 and other insulin responsive proteins such as the insulin responsive amino peptidase (IRAP) and the vesicle associated membrane protein 2 (VAMP2) (Tanner and Lienhard, 1989); (Slot et al., 1991a); (Slot et al., 1991b); (Holman and Cushman, 1994); (Holman and Sandoval, 2001). Taken together these results indicate that Glut-4 utilises the endosomal-recycling pathway along with other integral membrane proteins (Figure 1.4). An example of one such protein is the transferrin receptor (TfR) that binds iron-loaded transferrin on the exofacial side of the plasma membrane and is internalised via clathrin-coated vesicles (Ponka and Lok, 1999). After disassembly of the clathrin coat these vesicles fuse with the early endosomes, where under an acidic environment iron dissociates from the receptor bound transferrin, which rapidly recycles back to the plasma

membrane (Ponka and Lok, 1999). In the absence of insulin the exocytic rate of Glut-4 is lower that TfR whereas in insulin-stimulated conditions the exocytic rate of Glut-4 is increased some 10-20 fold compared with TfR (Holman et al., 1994); (Yang and Holman, 1993). This data implies that Glut-4 is actively withdrawn from the recycling system in a compartment highly sensitive to insulin (Holman and Sandoval, 2001). (Livingstone et al., 1996) and (Martin et al., 1996), exploiting TfR's exclusive localisation to the endosomal recycling system and capacity to bind transferrin, chemically ablated the endosomal system using horseradish peroxidase (HRP)-conjugated transferrin, 3,3'-diaminobenzidine and hydrogen peroxide. Under these conditions HRP-conjugated transferrin forms a highly reactive cross-linker. They demonstrated that 60% of the Glut-4, which exists in a compartment devoid of transferrin receptors, was resistant to ablation (Livingstone et al., 1996). This data suggests that the unablatable Glut-4 is not part of the endosomal recycling system but is withdrawn into a specialised storage compartment referred to as the Glut-4 storage vesicles (GSVs) (Holman and Cushman, 1994); (Rea and James, 1997). Immunofluorescent confocal microscopy studies found that Glut-4 containing structures colocalised with VAMP2, however no overlap was observed with the TfR (Malide et al., 1997), a result consistent with data from TfR-HRP ablation studies by (Livingstone et al., 1996) and (Martin et al., 1996). Recent experiments, using low-density membrane fractions from adipocytes, efficiently separated GSVs from endosomal fractions based on their differential densities in iodixanol gradient material (Hashiramoto and James, 2000). These findings indicated that insulin stimulation leads to a decrease in GSV Glut-4 content as opposed to endosomal Glut-4 content.

In summary, these findings suggest that the majority of the Glut4-containing vesicles are sequestered from the plasma membrane under basal conditions in a sub-compartment that is distinct from the endosomal system and the trans-Golgi network (TGN). Morphological analyses show that this sub-compartment consists of tubulo-vesicular aggregates and is enriched in other insulin-responsive proteins like IRAP and VAMP2. On insulin stimulation, Glut4-containing vesicles preferentially move from this compartment and fuse with the plasma membrane. This compartment has therefore been aptly named 'Glut-4 storage vesicles' (GSVs) (Rea and James, 1997); (Simpson et al., 2001).

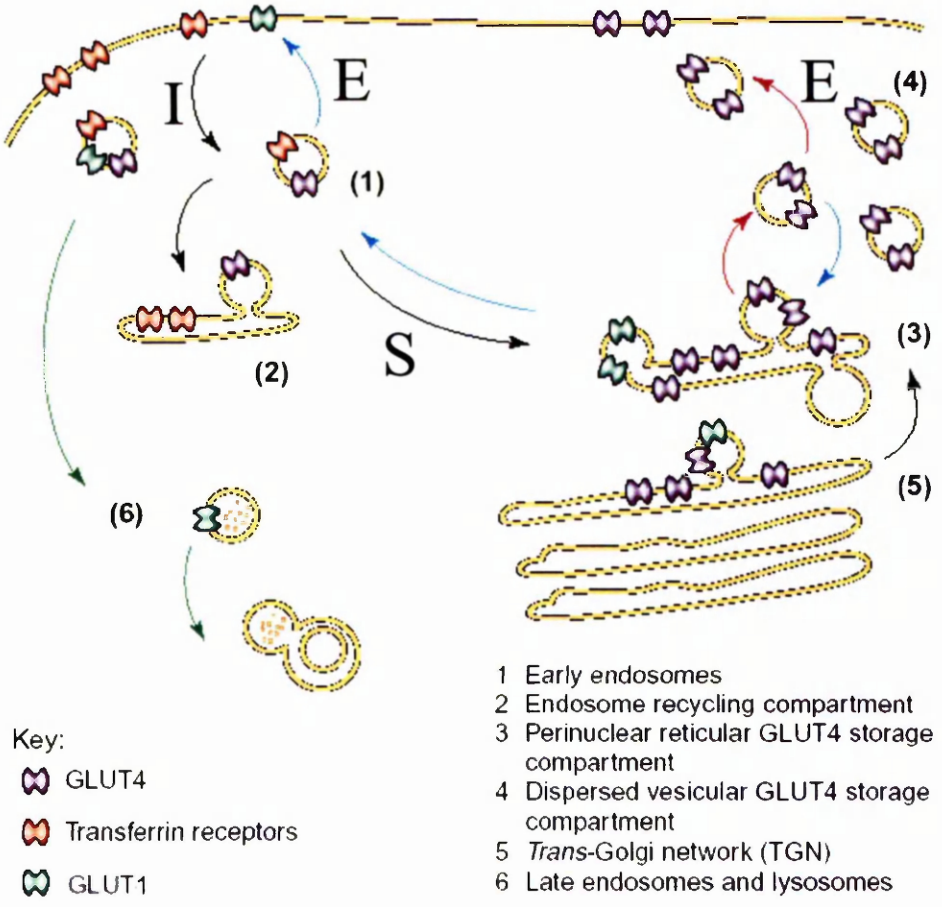

Figure 1.4 Trafficking of Glut-4

Under basal conditions Glut-4 is sequestered within the cell by efficient internalisation (**I**) from the plasma membrane and by intracellular retention in the Glut-4 storage compartment (GSVs) subsequent to sorting (**S**) out of the endosomes. Insulin stimulates the exocytosis (**E**) of the endosomal recycling compartment and the unique Glut-4 storage compartment. *Adapted from Holman, 2001.*

The insulin-stimulated movement and fusion of the GSVs with the plasma membrane is analogous to the mechanism of neurotransmitter release at the nerve synapse (Sudhof, 1995). In that system a specialised pool of small synaptic vesicles (SSVs) stimulated by the resultant Ca^{2+} influx due to nerve cell depolarisation, rapidly fuse with the presynaptic membrane releasing neurotransmitter into the nerve synapse (Sudhof, 1995); (Rothman and Warren, 1994). This membrane is rapidly recycled and refilled with neurotransmitter ready for another round of activity. Work by Rothman and colleagues identified several molecules mediating the targeting, docking and fusion of SSVs with the plasma membrane (Rothman and Warren, 1994). From their observations it was evident that a N-ethylmaleimide Sensitive Fusion protein (NSF) and its interaction with Soluble NSF Attachment Proteins (SNAPs) was central to the ATP-requiring fusion event (Sollner et al., 1993). However, the specificity of membrane fusion events is mediated by the pairing of the transport vesicle located SNAP receptor (vSNARE) with the target membrane SNAP receptor (tSNARE) (Sollner et al., 1993) (figure 1.5). This paradigm of membrane fusion known as the SNARE hypothesis prompted the search for homologues of v- and t-SNAREs in other systems in which membrane fusion occurred. Homologues of these SNARE proteins have been found in both myocytes and adipocytes suggesting that membrane fusion events analogous to those seen in neurones occur in these cell types (Cain et al., 1992); (Volchuk et al., 1994); (Volchuk et al., 1996).

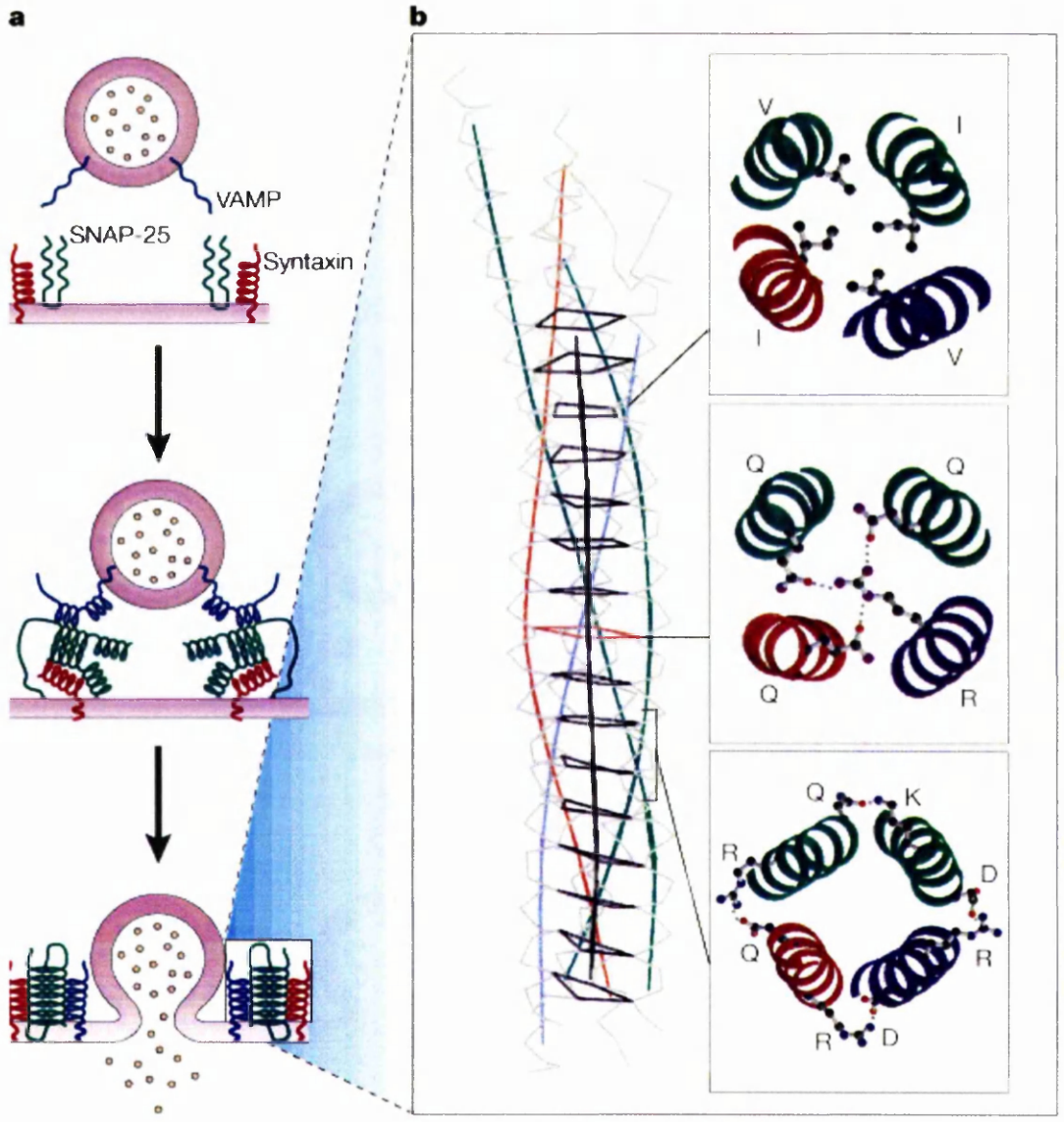

Figure 1.5 Model for SNARE complex formation.

Schematic showing the assembly of the neuronal SNARE complex during vesicle/plasma membrane fusion. (**a**) VAMP (blue) on the incoming vesicle interacts with syntaxin (red) and SNAP-25 (green) at the plasma membrane to form a four-helical bundle that 'zips' together pulling the two membranes together thus allowing membrane fusion to occur. (**b**) The left hand panel shows the four-helix bundle SNARE complex, the local helical axes (gray), the hydrophobic interaction layers (black boxes) and the middle layer (red box) containing a glutamine from SNAP-25. Cross-sectional views of the indicated positions are given on the right. *Reproduced from Chen & Scheller, 2001.*

In adipocytes and myocytes two vSNARES, vesicle associated membrane protein (VAMP2) and cellubrevin, were found to colocalise with Glut-4 vesicles (Cain et al., 1992). Further analysis found that VAMP2 localised with the unablated GSV pool (Martin et al., 1996) while cellubrevin localised to the ablated endosomal pool (McMahon et al., 1993). In agreement with these findings synthetic VAMP2 peptides prevented insulin-stimulated Glut-4 exocytosis in permeabilised fat cells whereas cellubrevin peptides did not inhibit Glut-4 translocation (Martin et al., 1996). As suggested by the SNARE hypothesis, these observations highlighted the suspected level of specificity of membrane fusion events afforded by the differential expression and localisation of the SNAREs. In this case a clear demarcation between the insulin-sensitive movement of GSVs to the plasma membrane was afforded by the vesicular localisation of the vSNARE VAMP2 in contrast to the endosomal trafficking of Glut-4 specified by cellubrevin.

Subsequently, the cognate target membrane SNARE (tSNARE) syntaxin-4 was found in fat and muscle cells (Volchuk et al., 1996). Syntaxin-4 bound VAMP2 with high affinity and was found to be highly expressed in and predominantly localised to the plasma membrane of muscle and fat cells (Volchuk et al., 1996). Further evidence of this interaction was obtained using synthetic peptides developed from the cytoplasmic tail of syntaxin-4 and antibodies raised to syntaxin-4. In both circumstances insulin-stimulated Glut-4 translocation to the plasma membrane in adipocytes was inhibited (Volchuk et al., 1996); (Tellam et al., 1997). This is convincing evidence that SNARE interaction is decisive in the regulation of Glut-4 vesicle fusion.

1.3 Insulin-stimulated glucose storage (glycogen synthesis)

After glucose is transported into the cell, the next step in glucose metabolism in skeletal muscle and fat is its phosphorylation by hexokinase II to produce glucose-6-phosphate (G6P) (Salway, 1994). The benefits of this action are twofold; it maintains a low intracellular glucose concentration essential in driving further transport, and traps the substrate inside the cell where it is utilised further in metabolism via the glycolytic or glycogenesis pathways. The choice of which pathways are used is dependent on the cellular energy demands. However, under insulin-stimulated conditions the storage of glucose, as glycogen is favoured (Salway, 1994).

Glycogen synthesis involves the incorporation of uridine diphosphate (UDP)-glucose, into the growing glycogen chain by the rate-limiting enzyme glycogen synthase (GS) (Salway, 1994). Interestingly, glycogen synthesis is found to be impaired in non-insulin-dependent diabetes mellitus (Shulman et al., 1990); (Rothman et al., 1995). This may come as no surprise as the tetrameric 85KDa protein GS, is regulated by an insulin-stimulated pathway involving kinase/ phosphatase activities (Cohen, 1999); (Yeaman et al., 2001). GS exists in an active (de-phosphorylated) and an inactive (phosphorylated) form. Inactivation of GS is catalysed by, among other enzymes, glycogen synthase kinase-3 (GSK-3) which phosphorylates key serine residues of the GS carboxyl terminal domain (Cohen, 1999). A consensus of opinion on the mechanism by which insulin brings about the de-phosphorylation and thus activation of GS during glycogen synthesis is described as follows (see also Figure 1.6). Recent studies have shown that wortmannin and LY294002 both block the insulin-stimulated activation of GS and PKB, and also prevents the inhibition of GSK3 (Burgering and Coffer, 1995); (Shepherd et al., 1995), (Yamamoto-Honda et al., 1995); (Cross et al., 1995). This evidence indicates that insulin-mediated inhibition of GSK-3 occurs via PKB phosphorylation through a PI3K-dependent pathway. PKB, also known as Akt, belongs to the AGC (cAMP-dependent protein kinase/protein kinase G/protein kinase C) extended family of protein kinases and exists as three isoforms, named PKB α, β and γ (Figure 1.7) (Hajduch et al., 2001). PKB contains an N-terminal pleckstrin homology (PH) domain followed by a catalytic kinase domain, and a C-terminal tail (Cohen, 1999). The PI3K phosphorylated membrane lipid products, PIP_2 and PIP_3, are believed to promote the recruitment of PKB to the cell

membrane through the interaction with the N-terminal PH domain (Frech et al., 1997). At the cell membrane a 63kDa monomeric kinase known as 3-phosphoinositide-dependent kinase-1 (PDK1) phosphorylates PKB (Alessi, 2001). PDK1 is expressed ubiquitously in human tissues and consists of an N-terminal catalytic domain similar to that of PKA, PKB and PKC, and has a C-terminal PH domain (Alessi et al., 1997a); (Stephens et al., 1998). PDK1 activates PKB by phosphorylation of a threonine residue specific to each of the three PKB isoforms (Alessi et al., 1997b); (Walker et al., 1998). It is in fact suggested that PIP_3 not only recruits PKB to the membrane but also alters the conformation of PKB such that the relevant threonine residue becomes accessible to PDK1 (Cohen, 1999) (Figure 1.8). As a consequence the activated PKB phosphorylates and inactivates GSK3, leading to the promotion of glycogenesis (Cohen, 1999). It should be noted that while this pathway explains much of insulin's effects on glycogen synthesis, other growth factors and stimuli such as glucose and amino acids are also able to stimulate glycogen synthesis via alternative and as yet not fully characterised pathways (Yeaman et al., 2001).

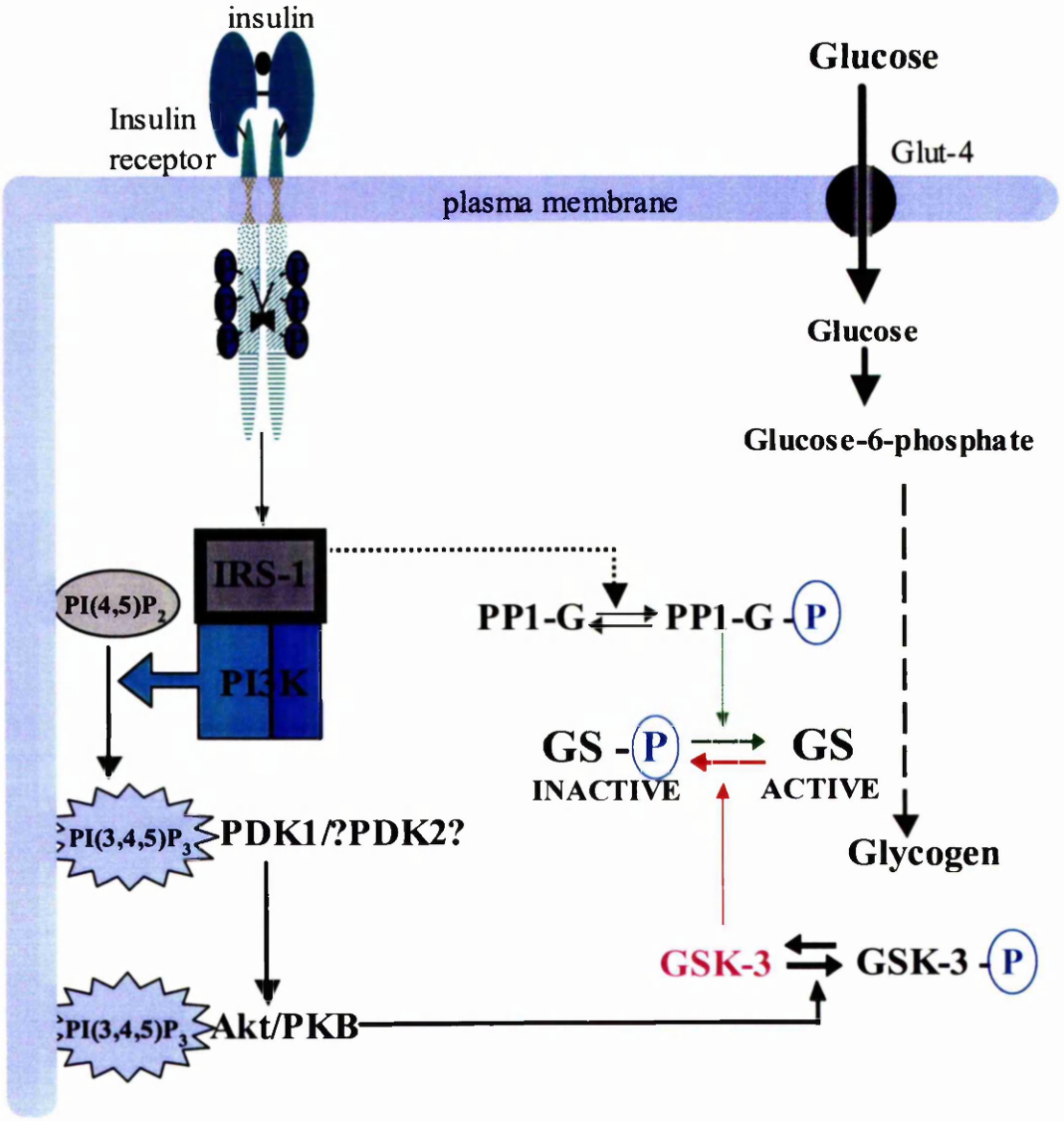

Figure 1.6 The regulation of glycogen synthesis by insulin.

Insulin stimulates glycogen accumulation through a coordinated increase in glucose transport and glycogen synthesis. Insulin activates glycogen synthase (GS) by promoting its dephosphorylation, through the inhibition of kinases such as GSK-3 and activation of the glycogen associated protein phosphatase-1 (PP1-G). Upon its activation downstream of PI3K, PKB phosphorylates and inactivates GSK-3, decreasing the rate of phosphorylation of glycogen synthase, therefore increasing its activity state. Insulin also specifically activates discrete pools of phosphatase, primarily increasing protein phosphatase-1 activity localised at the glycogen particle (PP1-G). Taken together insulin decreases the rate of phosphorylation of GS, increasing its activity state, which results in the increased incorporation of UDP-glucose into the growing glycogen molecule.

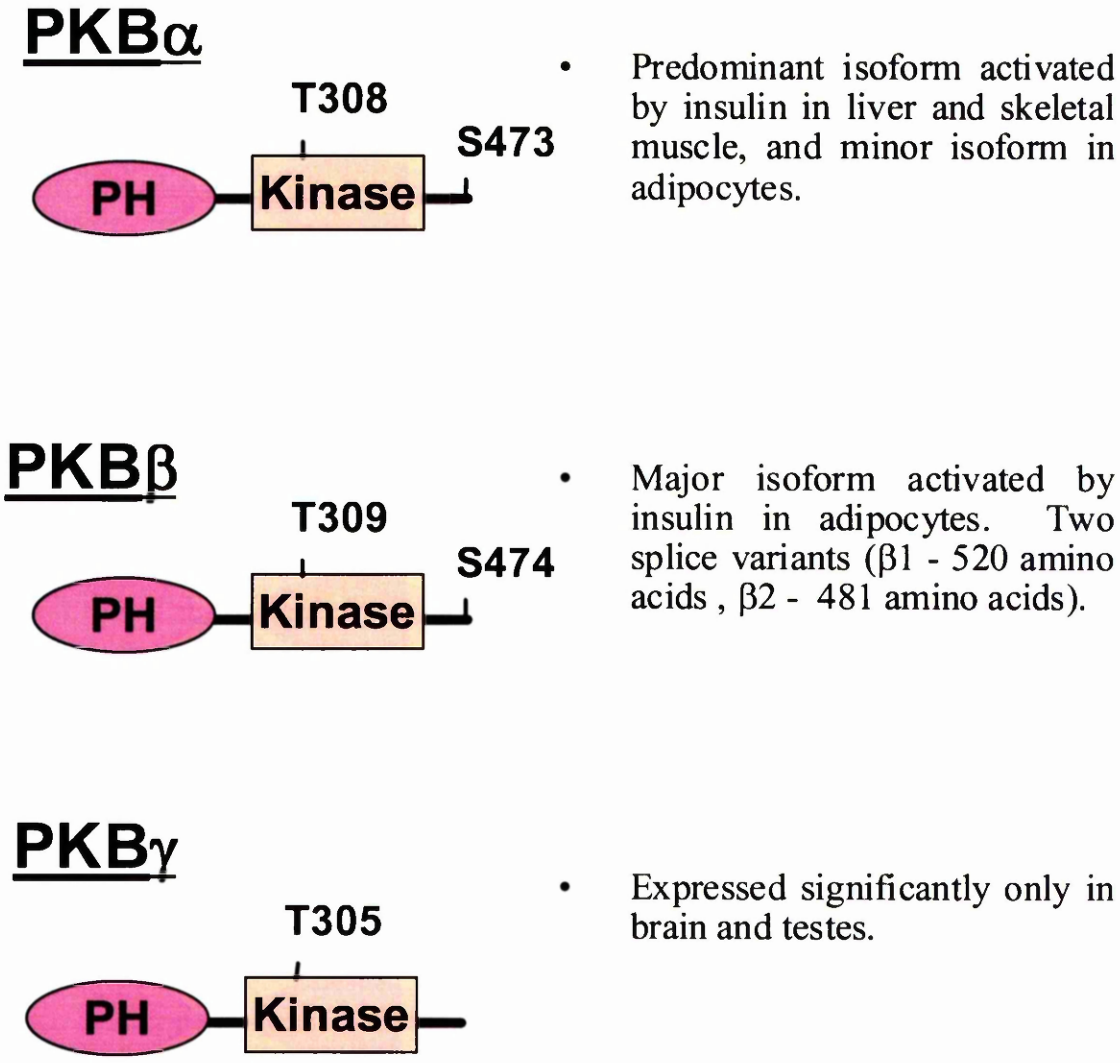

Figure 1.7 Structure of PKB isoforms

Schematic representation of the structure of the three PKB isoforms with the amino-terminal PH domain and kinase domain shown. The equivalent PDK1 threonine phosphorylation site and putative PDK2 serine phosphorylation site are indicated.

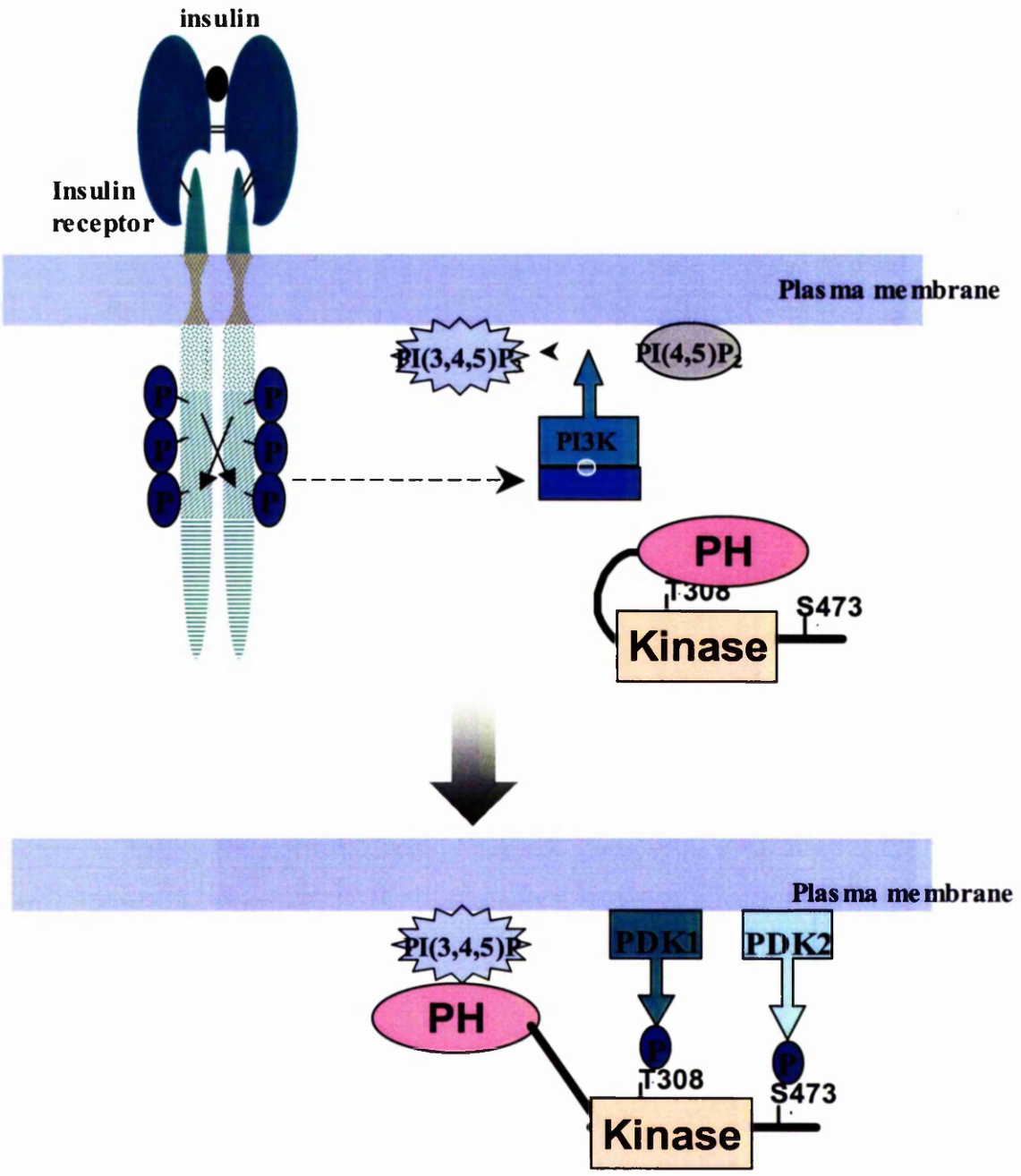

Figure 1.8 The mechanism of activation of PKB. .

The stimulation of cells with insulin activates PI3K and elevates the level of $PI(3,4,5)P_3$ at the plasma membrane. PIP_3 and or its intermediate breakdown product $PI(3,4)P_2$ then interacts with the PH domain of PKB, which has two effects. First it alters the conformation of PKB in such a way that Thr308 and (perhaps) Ser473 become accessible for phosphorylation by PDK1 and PDK2, respectively. Second, PKB is recruited from the cytosol to the plasma membrane where PDK1 and PDK2 are located. The phosphorylation of PKB at Thr308 and Ser473 (indicated by the circled letters Ps) activates PKB. *Reproduced from Cohen, 1999*

1.4 Alternative cascade events in insulin-stimulated glucose transport

Additional molecules that are potentially implicated in insulin–mediated glucose transport are the atypical Protein Kinase Cs (PKCs), PKB, the lipid raft-associated c-Cbl and the c-Cbl-associated protein (CAP) (Czech and Corvera, 1999). More specifically, the β isoform of PKB has been reported to be recruited to Glut4-containing vesicles upon stimulation by insulin (Calera et al., 1998). A number of studies have shown that overexpression of constitutively active PKCζ, PKCλ or membrane directed PKBα/β stimulates Glut-4 translocation in a number of insulin-sensitive cell culture models and tissues (Standaert et al., 1997); (Bandyopadhyay et al., 2000); (Kohn et al., 1996a); (Ueki et al., 1998); (Hajduch et al., 1998). In addition, overexpression of dominant negative PKCζ, PKCλ or PKB lead to a partial inhibition of Glut-4 translocation (Bandyopadhyay et al., 1997); (Kotani et al., 1998). The activation of PKCζ / λ and PKB in response to insulin is wortmannin sensitive, suggesting a PI3K-dependent mechanism (Standaert et al., 1997); (Nakanishi et al., 1993). Although these data support the involvement of PI3K activity, PKCζ / λ and PKBβ in insulin-stimulated Glut-4 translocation, evidence is emerging which raise important questions as to whether these molecules are sufficient or necessary for insulin-stimulated Glut-4 translocation and glucose transport (Baumann et al., 2000).

Recent studies have demonstrated that cell permeable PIP_3 esters were unable to stimulate glucose transport in the absence of insulin (Jiang et al., 1998). In contrast PIP_3 esters were able to overcome wortmannin inhibition of insulin-stimulated glucose transport (Jiang et al., 1998). In addition, β-integrin receptor clustering, platelet derived growth factor and interleukin-4 have been demonstrated to stimulate PI3K activity without increasing glucose transport (Guilherme and Czech, 1998); (Isakoff et al., 1995); (Wiese et al., 1995). These results suggest that at least one additional insulin-dependent but PI3K-independent pathway is necessary for insulin-stimulated glucose transport. Recent studies aimed at examining this wisely focused on a reassessment of other insulin receptor substrates that may be responsible for glucose transport (Ribon and Saltiel, 1997); (Baumann et al., 2000); (Watson et al., 2001); (Watson and Pessin, 2001). They found that insulin could tyrosine phosphorylate the proto-oncoprotein c-Cbl (Ribon and Saltiel,

1997). The *c-Cbl* proto-oncogene was first identified in haematopoietic tumours of mice infected with Casitas Br-M retrovirus (Thien and Langdon, 2001). The isolated retrovirus was able to induce pre- and pro-B lymphomas through the expression of the truncated viral protein product of the *v-Cbl* oncogene (Thien and Langdon, 2001). Therefore the name c-Cbl stands for cellular-Casitas B-lineage lymphoma. Cbl proteins are ubiquitously expressed and have been found to interact with a number of activated tyrosine kinases, targeting them for down regulation (Thien and Langdon, 2001). However, in insulin-responsive cells the c-Cbl protein was tyrosine phosphorylated by the insulin receptor through the interaction with the adapter protein with pleckstrin homology and src homology domains (APS) (Ahmed et al., 2000). Tyrosine phosphorylated c-Cbl is subsequently localised to plasma membrane lipid raft domains through the interaction with the SH3 domain of Cbl-associated protein (CAP) (Baumann et al., 2000). CAP specifically localises with caveolae through the interaction with the caveolae / lipid raft associated protein flotillin (Baumann et al., 2000). Moreover, this localisation is functionally important as a dominant interfering CAP mutant (CAPΔSH3), unable to interact with c-Cbl but able to bind flotillin, interfered with c-Cbl localisation to lipid raft domains and blocked insulin-stimulated Glut-4 translocation and glucose transport without any effect on PI3K activity (Baumann et al., 2000). The search for downstream molecules in the CAP/c-Cbl pathway has found that tyrosine phosphorylated c-Cbl recruits a small adapter protein c-CrkII that in turn binds the guanyl nucleotide exchange factor C3G, known to activate a number of small guanosine triphosphate (GTP) binding proteins (Ribon et al., 1996); (Reedquist et al., 1996). Interestingly, the small GTP binding Ras homologue (Rho) family member, TC10 was activated by C3G in an insulin-dependent but PI3K-independent manner (Chiang et al., 2001). Once activated TC10 was found to co-localise with CAP and c-Cbl in caveolae (Chiang et al., 2001). Disruption of TC10 activation inhibited insulin-stimulated glucose transport and Glut-4 translocation (Chiang et al., 2001).

The downstream effectors of TC10 are still unknown but their discovery may hold further clues to the mechanism by which insulin stimulates Glut-4 translocation (Figure 1.9). Intriguingly, the insulin receptor is also found localised to caveolae / lipid raft domains, suggesting that these domains may indicate a mechanism of compartmentalisation of the insulin signal (Gustavsson et al., 1999); (Nystrom et al., 1999). Lipid rafts are small

membranous microdomains that are preferentially enriched in cholesterol and sphingolipids (Smart et al., 1999); (Galbiati et al., 2001). This preferential lipid enrichment makes for a less fluid membrane that is resistant to non-ionic detergents as opposed to the bulk of the plasma membrane (Galbiati et al., 2001). These properties have aided in the isolation and characterisation of these lipid microdomains. Intriguingly, certain molecules such as glycosylphosphatidylinositiol-anchored and acylated proteins dynamically associate with rafts (Galbiati et al., 2001). As a consequence these lipid rafts concentrate molecules and act as platforms for conducting a variety of cellular functions such as signal transduction and membrane trafficking (Smart et al., 1999). Interestingly, a structural protein known as caveolin-1 directly binds cholesterol, a key component of lipid rafts, and promotes the invagination of the lipid raft to form caveolae (Smart et al., 1999); (Galbiati et al., 2001).

In summary, these data demonstrate that Glut-4 translocation and glucose transport, in adipocytes, require the inputs of both the insulin receptor⇨PI3K and insulin receptor/APS/c-Cbl/CAP⇨TC10 signalling pathways (Chiang et al., 2001). These pathways must at some point converge on the trafficking and membrane fusion machinery involved in Glut-4 vesicle translocation and plasma membrane localisation (Figure 1.9).

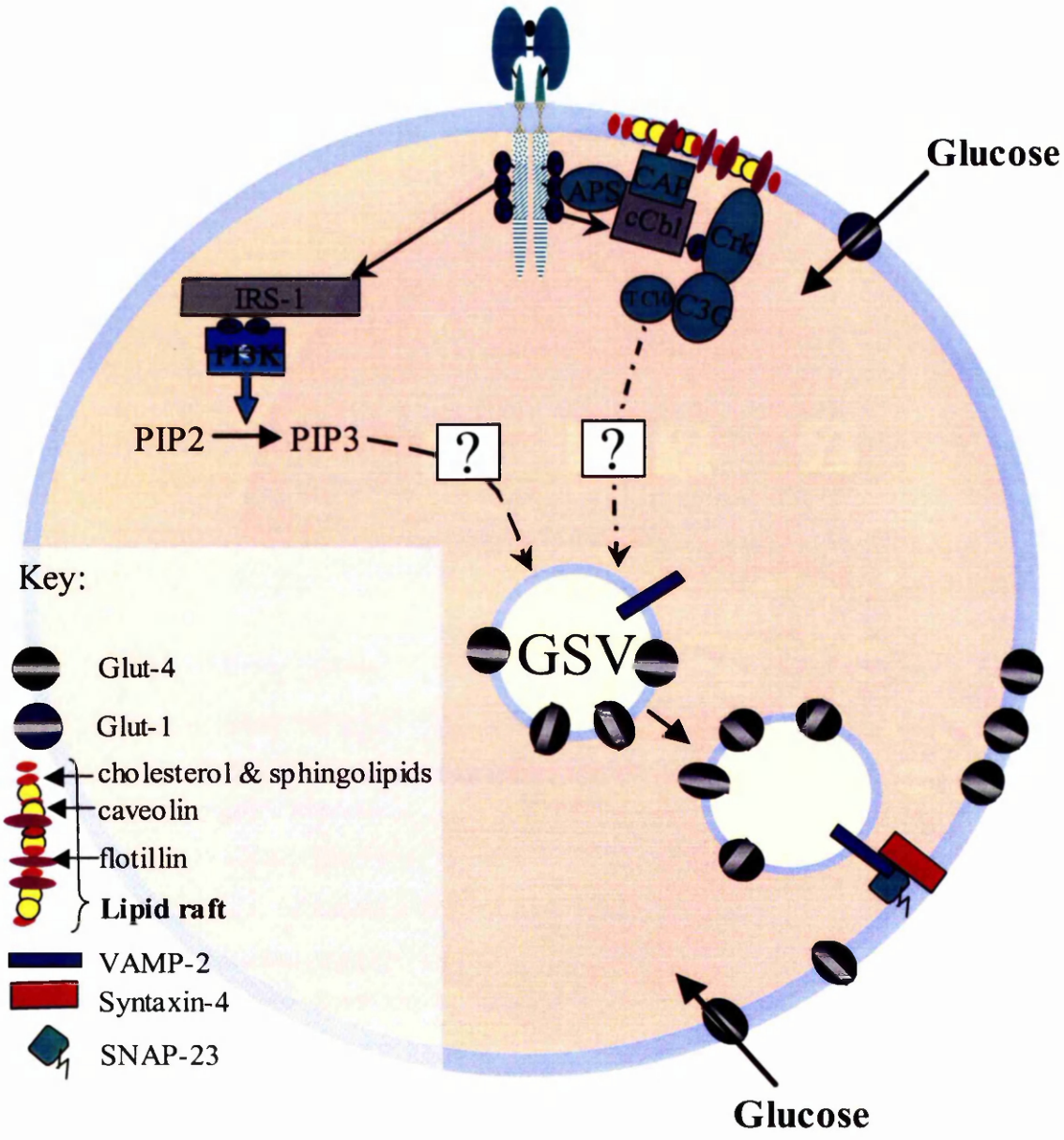

Figure 1.9 Insulin-stimulated pathways leading to Glut-4 translocation and glucose transport .

Insulin receptor autophosphorylation catalyses the phosphorylation of cellular proteins such as members of the IRS family and cCbl. Upon tyrosine phosphorylation (circled letter P), these proteins interact with signalling molecules through their SH2 domains resulting in the activation of a diverse series of signalling pathways including activation of PI3K and TC10. TC10 activation comes about by the tyrosine phosphorylation and subsequent recruitment of c-Cbl to the lipid raft through the adaptor protein CAP. Activated c-Cbl also recruits the CrkII/C3G complex into the lipid raft environment, where C3G can stimulate guanylnucleotide exchange on TC10. These pathways act in a concerted fashion to coordinate the regulation of Glut-4 vesicle trafficking, which results in increased glucose transport.

1.5 Exercise-stimulated glucose transport

It is currently widely believed that in addition to insulin, exercise promotes translocation of glucose transporters and glucose uptake ((Douen et al., 1990); reviewed in (Goodyear and Kahn, 1998)). However, the pathway through which exercise achieves this effect is believed to be different from that utilised by insulin (reviewed in (Hayashi et al., 1997); (Ryder et al., 2001)).

(Coderre et al., 1995) identified and characterised an exercise-sensitive pool of glucose transporters in rat skeletal muscle. By sucrose density gradient centrifugation, they isolated an insulin-sensitive Glut-4 pool (in the 32% fraction) and an exercise-stimulated pool (in the 36% fraction). No obvious differences in the protein composition between the two pools were found but further analysis by velocity gradient centrifugation revealed that the insulin-sensitive Glut-4 vesicles had a larger sedimentation coefficient (Coderre et al., 1995). In the same year, (Lund et al., 1995) provided supportive evidence on the contraction-stimulated translocation of Glut-4. By using the sensitive exofacial labelling technique with the impermeant photoaffinity reagent ATB-BMPA (2-N-[4-(1-azi-2,2,2-trifluoroethyl)benzoyl]-1,3-bis-(D-mannose-4-xyloxy)-2-propylamine), they demonstrated that contraction stimulates exocytosis of Glut-4. Furthermore, the combined effect of contraction and insulin on glucose uptake or Glut-4 translocation was greater than either stimulation alone (Lund et al., 1995); (Ploug et al., 1998). In contrast to the insulin-mediated pathway, contraction-mediated glucose uptake does not involve PI3-K, suggesting different signalling networks (Lund et al., 1995); (Yeh et al., 1995). Moreover, subcellular fractionation and immunofluorescence microscopy experiments suggest that insulin primarily recruits Glut-4 from a VAMP2 positive TfR-negative compartment whereas exercise/contractions primarily recruit Glut-4 from a TfR-positive compartment (Ploug et al., 1998); (Randhawa et al., 2000). This differential pattern of expression suggests that contraction mobilises an endosomal like pool of Glut-4 whilst insulin mobilises the GSV pool. A further level of distinction between exercise and insulin responsive Glut-4 vesicle fusion may come from a differential regulation of SNARE associated proteins which may have a preferential sensitivity to insulin or exercise stimulus. Examples of such proteins are munc-18c and syndet which interact closely with syntaxin-4 (Khan et al., 2001).

1.5.1 Signalling mechanisms involved in exercise-stimulated glucose transport

Although much progress has been made in elucidating the signal transduction mechanism for insulin-stimulated glucose uptake via Glut-4, little is known about the molecular signals that regulate Glut-4 recruitment during exercise. A molecule currently emerging as an important candidate component of exercise-mediated glucose transport in skeletal muscle is the AMP-activated protein kinase (Hardie and Carling, 1997).

1.5.1.1 AMPK - Role in exercise-stimulated glucose transport

AMP-activated protein kinase (AMPK) is a trimeric protein consisting of the catalytic subunit α, and the regulatory subunits β and γ. The kinase-containing subunit α, transfers a phosphate from the ATP to the target substrate (Hardie and Carling, 1997). Each subunit exists as two or three isoforms designated α1, α2 and β1, β2 and γ1, γ2 and γ3. The isoforms display differences in abundance, muscle type distribution and also sensitivity to AMP (Salt et al., 1998).

AMPK is considered to have a role in the maintenance of stable high-energy phosphate concentrations (ATP) and thus energy in muscle cells by promoting catabolic processes such as fatty acid oxidation and glucose transport, and inhibiting anabolic processes such as fatty acid and cholesterol synthesis (Hardie and Carling, 1997). During contraction and exercise the muscle utilises ATP as an energy source at increased rates. Depletion of ATP causes the elevation of the AMP:ATP ratio by displacement of the adenylate kinase (myokinase) reaction, and this activates AMPK via direct allosteric activation (Carling et al., 1989) and by multiple mechanisms which promote phosphorylation of AMPK by an upstream protein kinase, AMPK kinase (AMPKK) (Hawley et al., 1995) (Figure 1.10 & 1.11).

AMPK activity in the red region of rat quadriceps muscle has been found to be two- to three-fold increased during exercise, in a manner dependent on work rate (Winder and Hardie, 1996), (Rasmussen and Winder, 1997). Similarly, AMPK activity has been demonstrated to increase in rat epitrochlearis muscles stimulated with 5-aminoimidazole-4-carboxamide 1-β-D-ribonucleoside (AICAR), a molecule which after phosphorylation forms an AMP analogue called 5-aminoimidazole-4-carboxamide ribonucleotide (ZMP)

and can therefore activate AMPK and AMPKK (Hayashi et al., 1998) (Figure 1.11). In a study by (Hutber et al., 1997), contraction of rat gastrocnemius muscles was followed by a significant increase in AMPK levels and activity, as well as by a decline in creatine phosphate levels. These results taken together indicate a link between exercise-induced muscle contraction/AICAR treatment and elevation of AMPK activity in skeletal muscle. Similarly, studies on humans have also shown a direct response of AMPK to contraction (Chen et al., 2000); (Wojtaszewski et al., 2000b). More specifically, (Chen et al., 2000) have reported an increase in the activity of AMPK isoforms α1 and α2 and (Wojtaszewski et al., 2000b) found a three- to four- fold increase in the α2 isoform in the vastus lateralis muscle from 'healthy' humans under a high intensity exercise protocol.

A role of AMPK in glucose uptake was initially observed when AICAR was used in resting perfused muscle of rats, in an attempt to identify a potential role of AMPK in the regulation of muscle fatty acid oxidation (Merrill et al., 1997). In that particular study by Merrill and colleagues, it was found that AMPK activity after AICAR stimulation not only increased fatty acid oxidation but also resulted in increased glucose uptake (Merrill et al., 1997). In an attempt to throw light on the yet obscured contraction-mediated glucose uptake pathway, several teams have studied the effect of AICAR on glucose uptake by Glut-4, in the absence of insulin *in situ* and *in vivo* (Kurth-Kraczek et al., 1999); (Bergeron et al., 1999). Their results have provided evidence of a role for AMPK in contraction-stimulated glucose transport.

Not all effects of AMPK on glucose transported should be attributed to Glut-4. (Abbud et al., 2000) observed a two- to three- fold increase in glucose uptake in C2C12 cells treated with AICAR. This glucose uptake was said to be facilitated by Glut-1, the predominant Glut isoform in those cells (Abbud et al., 2000).

In summary, AMPK is implicated in Glut-4 mediated glucose uptake during exercise and contraction. However, the exact mechanism by which AMPK stimulates Glut-4 translocation is not known. In a review by Winder it has been suggested that AMPK could activate transcription factors that target the control elements of the Glut-4 gene favouring its expression (Winder, 2001). Indeed, (Zheng et al., 2001) using transgenic mice containing different segments of the human Glut-4 gene promoter linked to the

bacterial chloramphenicol acetyltransferase (CAT) reporter gene, showed that the region between 730 to 895 base pairs from the Glut-4 transcription start contains an element essential for induction of Glut-4 mRNA synthesis by AMPK, after AICAR stimulation.

Role of AMPK in type II diabetes and obesity.

An elevation in the activity of the AMPK α2 isoform in Type 2 diabetic patients subjected to exercise has been reported (Musi et al., 2001). Other studies have also suggested that some forms of type 2 diabetes are in fact due to abnormalities in signalling pathways that involve AMPK (Winder and Hardie, 1999). Taking into account the evidence for a role of AMPK in Glut-4 translocation and glucose transport during contraction and exercise, as well as the role of AMPK in muscle fatty acid oxidation (Merrill et al., 1997), it is natural to speculate that a deficiency in AMPK or a decrease in AMPK activity could lead to obesity and insulin resistance, and that exercise-stimulated AMPK activity could be significant in prevention of type 2 diabetes.

1.5.1.2 Nitric Oxide - Role in exercise signalling and muscle metabolism

It has been suggested that nitric oxide (NO) may regulate muscle metabolism, with most studies supporting a contribution of NO in glucose uptake, glycolysis, creatine kinase activity and mitochondrial oxygen consumption (Reid, 1998). Nitric oxide is produced in cells from L-arginine via the action of nitric oxide synthetase (NOS) (Palmer et al., 1988); (Marletta, 1994). One of the first studies to provide evidence on the existence of NOS in skeletal muscle was carried out by Balon and Nadler (Balon and Nadler, 1994). Using a chemiluminescent detection system, they monitored a 50-200% increase in NO efflux in rat extensor digitorum longus (EDL) muscle cultures incubated with L-arginine. Moreover, the NOS inhibitor NG-monomethyl-L-arginine monoacetate (L-NMMA) decreased NO efflux and the basal 2-deoxy-D-glucose (deGlc) transport, providing evidence for the existence of NOS in that tissue and a potential role of NO in carbohydrate metabolism (Balon and Nadler, 1994). In 1996, Balon and Nadler further extended their hypothesis of NO-induced glucose transport in skeletal muscle with additional data, which showed that NOS inhibition selectively inhibits contraction-stimulated glucose transport (Balon and Nadler, 1996). In agreement with this, EDL-muscles co-stimulated with maximal or sub-maximal concentrations of insulin and the NO donor sodium nitroprusside (SNP), showed an additive and dose-dependent increase

in glucose uptake (Balon and Nadler, 1997). Intriguingly, animals that underwent acute exercise showed increased NOS activity in skeletal muscle (Roberts et al., 1999). These findings suggested that NO may be a potential mediator of contraction induced glucose transport. Roberts and colleagues showed in rat sarcolemmal membrane preparations, that exercise- but not insulin-stimulated glucose transport was sensitive to another NOS inhibitor, N^{ω}-nitro-L-arginine-methyl-ester (L-NAME) (Roberts et al., 1997). These results further implicated NOS activity in exercise-stimulated glucose transport.

Young et al studying the *in vitro* effects of the nitric oxide donors, SNP and spermine NONOate, on glucose transport and utilisation in rat soleus muscle, suggested that nitric oxide may be able to specifically inhibit insulin-stimulated glycogen synthesis, or that glycogen synthase may be inactivated by a mechanism involving the NO-cGMP signalling pathway (Young et al., 1997). Finally, soleus muscle preparations incubated with SNP showed an eighty-fold increase in the cGMP content as well as an elevation in glucose transport and oxidation. This cGMP elevation was significantly decreased by LY-83583, a guanylate cyclase inhibitor (Young et al., 1997). These results suggest that NO increases glucose uptake and oxidation through a pathway that involves stimulation of guanylate cyclase and generation of cGMP.

In 1998, Young and Leighton investigated the effects of zaprinast on cGMP levels in soleus muscles isolated from lean, insulin-sensitive and obese, insulin-resistant rats (Young and Leighton, 1998). Zaprinast is a selective inhibitor of cGMP type V phosphodiesterase. The use of zaprinast results in the elevation of cGMP due to the inhibition of its hydrolysis by the cGMP type V phosphodiesterase. The results from this study showed that the cGMP content was significantly increased in lean rat muscles incubated with zaprinast, but not in the muscles of obese, insulin-resistant rats. (Young and Leighton, 1998) suggested that the lack of cGMP increase in zaprinast treated obese rat muscles could be due to a defect in NOS or due to a lack of stimulation of guanylate cyclase by NO. In both cases the result would be a decrease in cGMP generation, such that the inhibition of the cGMP phosphodiesterase would have little effect on the levels of intracellular cGMP. In fact, direct measurements illustrated impaired NOS activity in soleus, diaphragm, gastrocnemius and EDL muscles from obese rats (Young and Leighton, 1998). This finding indicates the presence of an endogenous cGMP

phosphodiesterase and an intrinsic guanylate cyclase activated by NO and that the sensitivity of this cyclase to NO and/or the function of NOS may be impaired in insulin-resistant muscle.

In summary, taken collectively the above data suggest that NO potentially mediates exercise-induced glucose transport through a pathway involving stimulation of guanylate cyclase and cGMP (Figure 1.11).

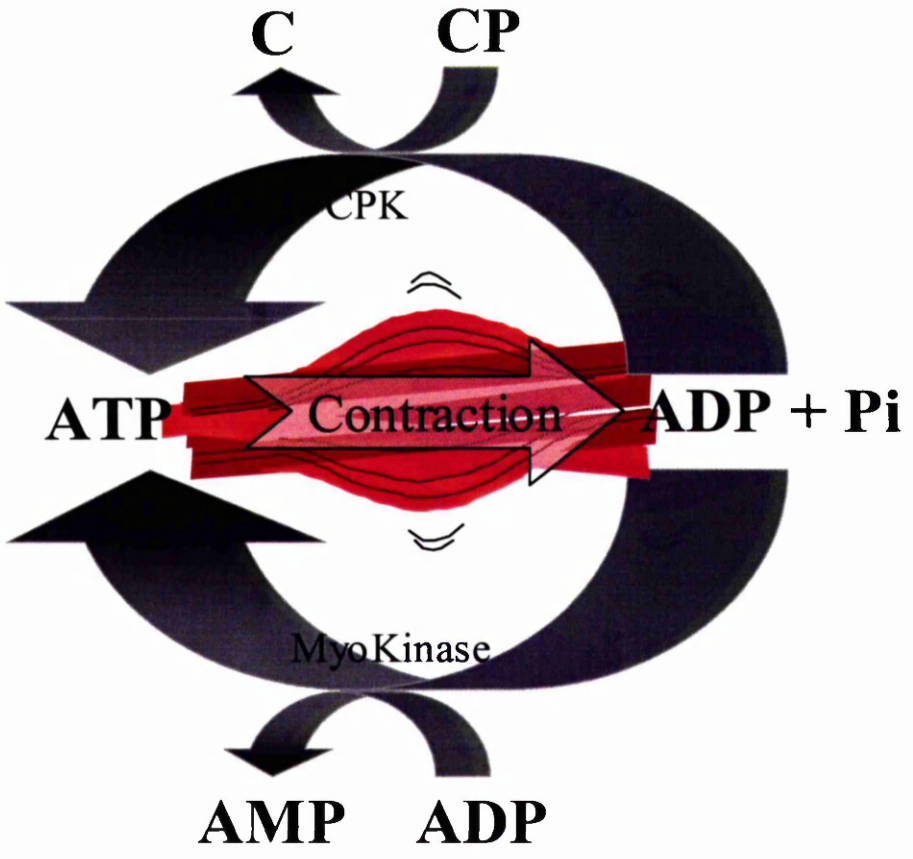

Figure 1.10 Maintenance of ATP levels during contraction.
Creatine phosphate (CP) decreases, creatine (C) increases and AMP increases in muscle during exercise/contraction as a result of actions of creatine phosphokinase (CPK) and myokinase (adenylate kinase). *Reproduced from Winder, 2001.*

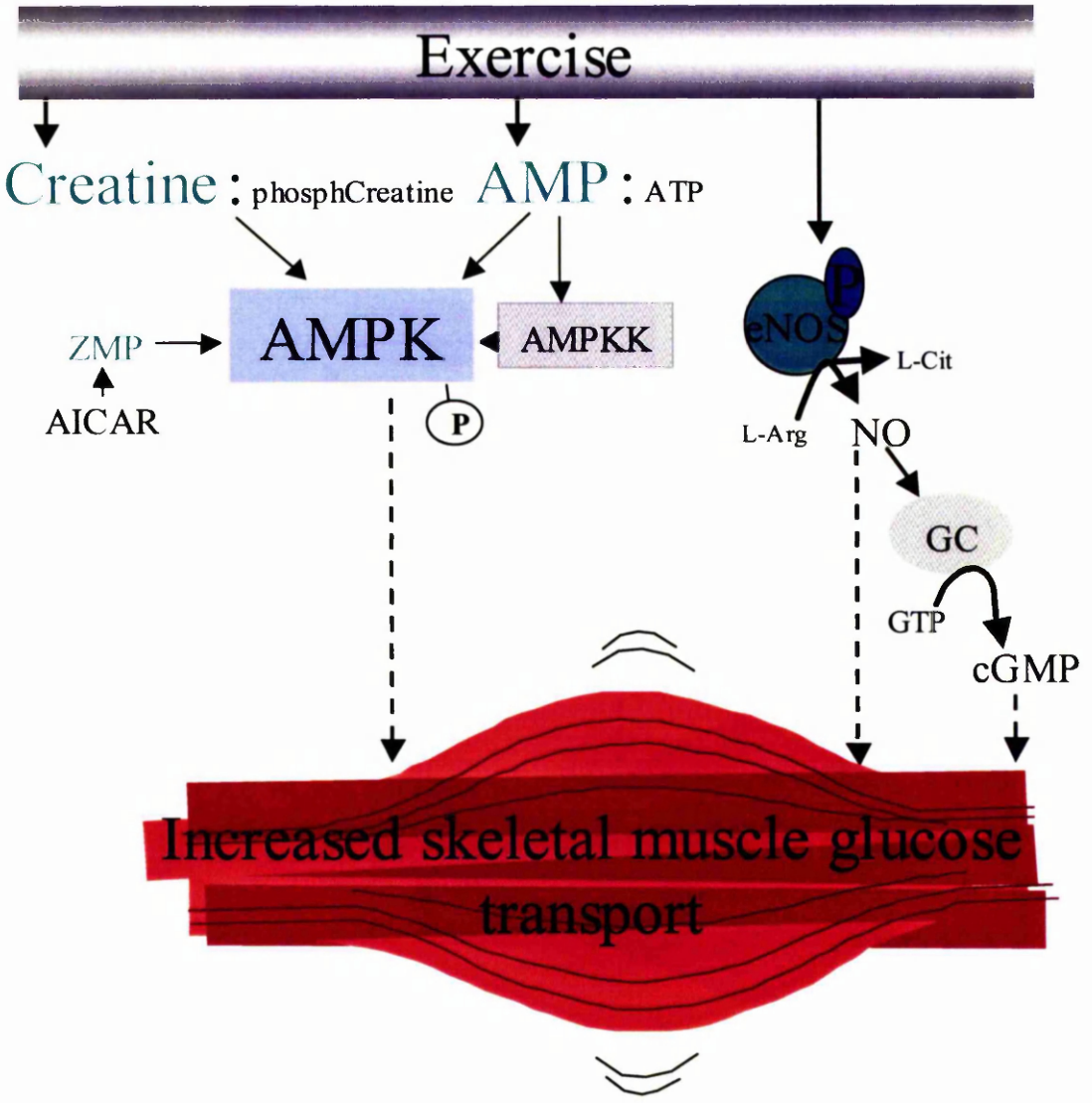

Figure 1.11 Signalling mechanisms involved in exercise-stimulated glucose transport.

The mechanisms by which exercise increases skeletal muscle glucose transport has not been precisely identified, however roles for nitric oxide (NO) and AMPK have been demonstrated. Exercise increases NO production, cGMP levels and AMPK activity in skeletal muscle. AMPK is activated allosterically in skeletal muscle by increases in the creatine-to-phosphocreatine and AMP-to-ATP ratios and is also activated by phosphorylation by an upstream kinase (AMPK-kinase). 5-aminoimidazole-4-carboxamide 1-β-D-ribonucleoside (AICAR), a compound which is converted to 5-aminoimidazole-4-carboxamide ribonucleotide (ZMP) within muscle, mimics the effect of AMP to increase AMPK activity and results in an increase in glucose transport.

1.6 Diabetes

1.6.1 Insulin-dependent diabetes mellitus (type 1 diabetes)

Insulin-dependent diabetes mellitus (IDDM), also known as type 1 diabetes, is the result of an abrupt cessation of insulin secretion from the pancreatic β-cells (Atkinson and Eisenbarth, 2001). This is usually caused by an autoimmune response of genetic or environmental origin that leads to the destruction of these cells (Atkinson and Eisenbarth, 2001). Consequently, the inability to regulate hepatic production of glucose together with reduced peripheral tissue glucose uptake due to the lack of insulin results in an abnormal accumulation of glucose in the blood (Zimmet et al., 2001). This abnormal accumulation of blood glucose or hyperglycaemia is the classical symptom of IDDM that accompanies excessive thirst, hunger, rapid weight loss, fatigue and polyuria (Atkinson and Eisenbarth, 2001). Long-term complications include retinopathy, nephropathy, neuropathy and peripheral vascular and coronary heart disease (Atkinson and Eisenbarth, 2001); (Zimmet et al., 2001). Variable combinations of the above complications are the main cause of morbidity and premature mortality in the IDDM population, which constitutes 10% of the total diabetic population (Zimmet et al., 2001). Daily insulin injections and dietary measures are employed in the management of this disease (Atkinson and Eisenbarth, 2001).

1.6.2 Non-Insulin-dependent diabetes mellitus (type 2 diabetes)

Non-insulin-dependent diabetes mellitus (NIDDM), alias type 2 diabetes comprises the remaining 90% of the total diabetes incidence and as in the case of IDDM, is also of environmental and genetic origin (Zimmet et al., 2001). NIDDM is particularly associated with obese individuals and it differs from IDDM in that patients do not suffer from the absence of insulin production. Instead, the insulin present, even when at highly elevated levels is unable to stimulate the utilisation of the accumulating blood glucose, either due to dysfunction of the insulin receptor/ insulin responsive cell or due to a blockade in the insulin-signalling pathway. NIDDM is characterised by insulin resistance in the liver, β-cells and peripheral tissues and is manifested as hyperglycaemia (Figure 1.12). As in the case of IDDM the long-term clinical complications of type 2 diabetes include heart disease, neuropathy, kidney failure and blindness. Type 2 diabetes

constitutes the majority of diabetes cases and as the number of affected individuals in the western cultures are increasing, pharmaceutical companies and health care systems are being urged to find a preventative measure for the onset of NIDDM. Currently, a low sugar/fat diet, exercise and anti-diabetic drugs are used to manage type 2 diabetes (Zimmet et al., 2001).

1.6.2.1 Therapeutic treatments for type 2 diabetes

There are three main classes of drugs aimed at maintaining normoglycaemia in NIDDM. These are the sulphonylureas, biguanides and the thaizolidinediones;

Sulphonylureas aim at enhancing β-cell insulin secretion. They do so by binding to a β-cell receptor causing closure of an ATP-dependent K^+ channel that results in membrane depolarisation. In response to membrane depolarisation, Ca^{2+} influx occurs and stimulates the exocytosis of insulin-containing vesicles. The biguanides act via an as yet undefined molecular target however their site of action is believed to be liver and skeletal muscle (Moller, 2001). The thiazolidinediones are oral hypoglycaemic drugs typified by rosiglitazone, pioglitazone, ciglitazone and troglitazone (Murphy and Holder, 2000). They promote peripheral glucose uptake and lower hepatic glucose output by increasing the sensitivity of these tissues to the action of insulin (Murphy and Holder, 2000). Indeed, it has been documented that administration of rosiglitazone to adipocytes provokes increase in insulin receptor expression along with enhancement of Glut-4 expression and translocation thus leading to an improvement in glucose metabolism (Young et al., 1995). The thiazolidinediones act as synthetic agonist of the peroxisome proliferator activated receptor gamma (PPARγ), a nuclear receptor involved in the formation of fat cells (adipogenesis) (Spiegelman, 1998). PPARγ belongs to a family of three nuclear receptors known as PPARα, γ and δ (Murphy and Holder, 2000). The family took their names from studies on mice that showed proliferation of fatty-acid oxidising peroxisomes when treated with fibrates (Murphy and Holder, 2000), a class of hypolipidaemic drugs that bind PPARα, the first receptor to be cloned (Murphy and Holder, 2000). When activated, the PPARs are capable of influencing transcription of a target gene by binding to a specific peroxisomal proliferator response element (PPRE) (Murphy and Holder, 2000). More specifically, PPARγ that exists as two isoforms 1 and

2 is expressed predominantly in adipose tissue and promotes differentiation of fibroblasts into adipocytes via the activation of adipogenic genes and also insulin receptor, IRS-1 and Glut-4. PPARγ is also expressed in liver and skeletal muscle but its predominant expression in fat cells is understandable as adipose tissue plays an important role in metabolic homeostasis and therefore activation of the above genes leads to an increased insulin sensitivity and glucose uptake.

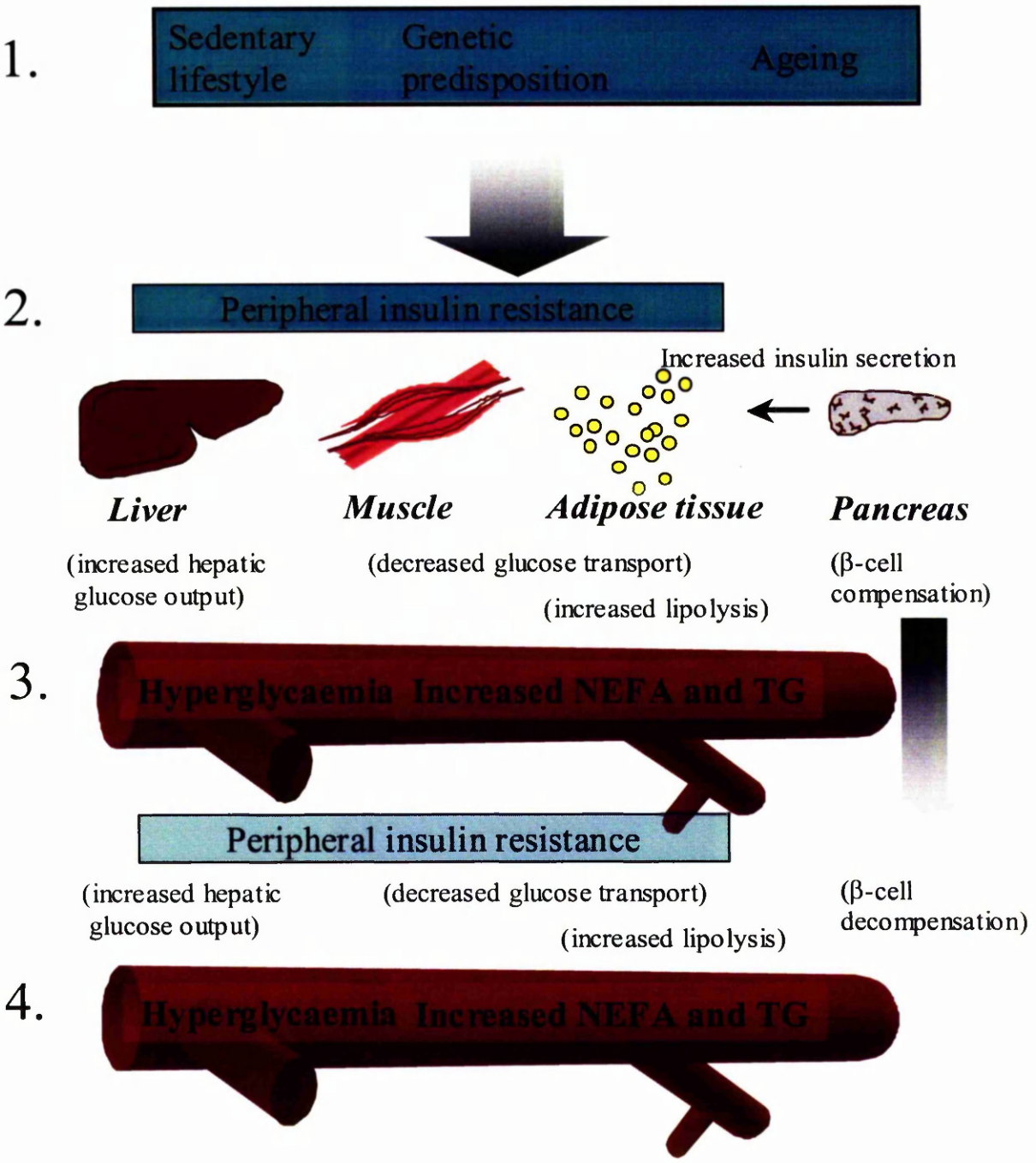

Figure 1.12 The development of type 2 diabetes

The contribution of insulin resistance in liver, muscle, fat and pancreatic β-cells to the development of type 2 diabetes. 1. Potential causative factors in early stages of the disease. 2. Peripheral insulin resistance in insulin-sensitve target tissues of skeletal muscle, adipose tissue and liver result in impaired glucose tolerance and is associated with increased insulin secretion by pancreatic β-cells. 3. Resultant blood anomalies of type 2 diabetes due to the persistent peripheral insulin resistance and the decreased insulin secretion by pancreatic β-cells. 4. Late stages of type 2 diabetes, with little or no insulin secretion and persistent peripheral insulin resistance.

1.7 Insulin resistance in relation to hypertension

Studies such as the one by Mitchel et al (1990) showing that lean, non-diabetic hypertensives are hyperinsulinaemic compared with normotensive controls have now established an association between insulin resistance, hypertension and associated conditions such as obesity. It has been commonly observed that hypertension is approximately twice as frequent in patients with diabetes compared with patients without the disease (Morris et al., 1994). Nevertheless a debate still exists on whether hypertension constitutes a clinical manifestation of insulin resistance and diabetes or whether it is hyperinsulinaemia that predisposes the organism to the development of diabetes. Currently there is available evidence in favour of both theories. (Julius et al., 1991) suggested that hypertension may precede the development of insulin resistance and hyperinsulinaemia and may in fact be the cause. They proposed that insulin resistance is secondary to the inability of blood glucose to be transported in the cells due to the reduced muscle blood flow and microvascular disease as occurs in hypertension and obesity. In contrast, studies have shown that insulin resistance is prevalent only in subjects with primary and not secondary hypertension (Donnelly and Connell, 1992). The lack of association between secondary hypertension and insulin resistance therefore suggests that elevated blood pressure does not lead to insulin resistance. Finally, it has been demonstrated that the spontaneously hypertensive rat (SHR), a genetic model of hypertension, develops insulin resistance (Reaven et al., 1989). This observation is of significance since the insulin resistance characterised by defective glucose transport into SHR adipocytes, develops long before any elevations in blood pressure are apparent (Reaven et al., 1989). Taken together these data suggest that hypertension is more likely to constitute a clinical manifestation secondary to the pre-existing condition of insulin resistance.

1.8 General aims of this thesis

It has been shown that glucose uptake can be mediated not only by insulin but also by a distinct mechanism regulated by exercise. Yet the individual steps that render the exercise-mediated pathway distinct from that mediated by insulin are not fully identified.

Aiming at better understanding the differences between the two pathways I compared and contrasted the deGlc transport under insulin and exercise-like conditions using the insulin-resistant SHRSP (stroke-prone spontaneously hypertensive rat), the type 2 diabetes rat model ZDF and their equivalent normal phenotypes. The results from these comparisons compose chapters 3 and 5 respectively while the work in chapter 4 aimed at identifying the origin of the insulin resistance observed in SHRSP animals. Is this defect secondary to a pathophysiological factor or is it due to a primary genetic defect? In order to answer this question, a model for the study of insulin resistance was developed in the form of skeletal muscle culture. The methodological development and characterisation of the skeletal muscle cell cultures along with the novel findings are detailed in chapter 4.

Chapter 2

Materials & Methods

2.1 Materials.

2.1.1 Animals

Male Wistar Kyoto (WKY) rats and Stroke Prone Spontaneously Hypertensive rats (SHRSP) were reared in house in the Joint Animal Facility at the University of Glasgow. Male Zucker *(fa/fa)* diabetic fatty (ZDF) rats and lean controls *(fa/+)* were purchased from Genetic Models Inc., USA.

2.1.2 Antibodies

Professor K. Siddle (University of Cambridge) supplied anti-IRS-1 antibodies. Anti-syntaxin-4 was a gift from Professor D.E. James (University of Queensland, Australia). Anti-AMPKα1 and α2 were provided by Professor D.G. Hardie (University of Dundee, UK). Anti-PKB (PH domain) was a gift from Professor P. Cohen (University of Dundee, UK). Dr. S.A Baldwin (University of Leeds, UK) donated anti-Glut-1 antibody. Anti-Glut-4 antibody raised against the C-terminal 14 amino acids of human Glut-4 was produced in house. Anti-caveolin-1 and Anti-flotillin antibodies were purchased from Becton Dickinson (Oxford, UK). Anti-Myogenin and anti-MyoD were purchased from Pharmingen (Oxford, UK). Anti-IRS-1 raised to carboxy terminus, Anti-IRS-2, and anti-p85α antibodies were from Upstate Biotechnology (TCS Biologicals, Bucks, UK). Anti-eNOS antibodies were from Sigma (Poole, Dorset, UK). Anti-VAMP-2 antibody was purchased from Synaptic Systems (Gottingen, Germany). Horse-radish peroxidase (HRP)-conjugated donkey anti-rabbit IgG and HRP-conjugated anti-mouse IgG antibodies were purchased from Amersham International plc, (Aylesbury, Buckinghamshire, UK).

2.1.2 Cells

L6 skeletal muscle cell line from American tissue culture collection was a gift from Dr E.M. Gibbs (Pfizer Central Research Groton, CT)

2.1.3 Cell Culture

Pederson Fetuin was supplied by Sigma (Poole, Dorset, UK). α-MEM, Chick embryo extract 60Å filtrate, Hams-F10, foetal bovine serum, 10000U/ml Penicillin, 10000U/ml streptomycin and trypsin/EDTA were from Gibco/Life Technologies, Inc (Paisley, UK).

13.5ml and 50ml centrifuge tubes and 1, 5, 10, 25ml sterile pipettes were supplied by Bibby Sterilin Ltd, (Stone, Staffordshire, UK). 25cm^2 Falcon Primaria flasks, 6-well Collagen type I BioCoat™ plates, 75cm^2 and 175 cm^2. Collagen type I BioCoat™ flasks were purchased from Becton & Dickinson (Franklin Lakes, NJ, USA).

2.1.4 General chemicals and reagents

ECL Western Blotting Detection Kit was purchased from Amersham International plc, (Aylesbury, Buckinghamshire, UK). Extra-thick filter paper, N, N, N', N', -tetramethylenediamine (TEMED) and non-fat blocking grade powdered milk were purchased from Bio-Rad Laboratories ltd, (Hemel Hempstead, Hertfordshire, UK). Bovine serum albumin-Fraction V (Low Hormone), Complete™ Protease Inhibitor Cocktail tablets and Tris were purchased from Boehringer Mannheim (GmbH, Germany). 10% Brij-35 solution, Hepes, MES, MOPS, NP-40 and 10% Tx-100 solution were obtained from Calbiochem (Nottingham, UK). 30% Acryl/Bis-acrylamide (35.7/1) solution was purchased from Fisons, (Loughborough, Leicestershire, UK). PIP_3 (1-*O*-stearoyl-2-*O*-arachidonoyl-*sn*-glycer-3-yl-D-*myo*-inositol-3,4,5-triphosphate.tetrasodium salt and MicrocystinLR were purchased from Alexis, (San Diego, California, USA). L-α-phosphatidylcholine and L-α-phosphatidylserine were purchased from Avanti Polar Lipids (Alabaster, Alabama, USA). Sterile Acrodisc® 0.2μm filters were purchased from Gelman Sciences Ltd, (Northampton, UK). RP X-Omat liquid fixer and developer and X-Omat AR film were purchased from Kodak Ltd, (Hemel Hempstead, Hertfordshire, UK). BCA protein assay reagent was purchased from Peribio (Cheshire, UK). Nitrocellulose membrane (0.45μm pore size) was supplied by Schleicher and Scheull, (Dassel, Germany). AICAR, collagenase type 1A, cytochalasin B, dexamethasone and wortmannin were supplied by Sigma (Poole, Dorset, UK). P-81 phosphocellulose paper was purchased from Whatman International Ltd. (Maidstone, UK). All other laboratory chemicals were of analytical reagent grade and purchased from either Sigma Chemical Company (Poole, Dorset, UK) or BDH (Loughborough, Leicestershire, UK).

2.1.5 Peptides

Dr G. Danielson (Novo Nordisk, Denmark) provided porcine insulin. PKB substrate peptide (RPRAATF) was from Dr. R. Plevin, (University of Strathclyde, U.K.). Protein Kinase A Inhibitor peptide (PKI) (TTYADFIASGRTGRRNAIHD) was purchased from Bachem (Merseyside, UK).

2.1.6 Radioactive chemicals

[γ^{32}P]-ATP, [^{14}C]-D-glucose, [^{14}C]sucrose, 2-deoxy-D-[2,6-^{3}H]glucose were purchased from NEN Dupont Ltd (Hertfordshire, UK)

2.2 Buffers

2.2.1 General Buffers

Hepes EDTA Sucrose Buffer (HES),
20mM Hepes (pH 7.4), 1mM EDTA, 225mM Sucrose

Immunoprecipitation buffer (IP buffer),
150mM NaCl, 50mM NaF, 1mM EDTA, 1mM EGTA, 10mM $Na_4P_2O_7$, 1.5mM $MgCl_2$, 1% (v/v) Glycerol, 50mM Hepes (pH 7.2), (1mM Activated $NaVO_4$, 1mM DTT, 1 Complete™ Protease Inhibitor Cocktail tablet and 2μM MicrocystinLR) added immediately prior to use.

Krebs Heinsleit Buffer (KH),
118mM NaCl, 4.7mM KCl, 1.2mM KH_2PO_4, 1.2mM $MgSO_4$, 25mM $NaHCO_3$ gassed with 95%O_2/5%CO_2 prior to addition of 2.5mM $CaCl_2$. Buffer will be pH 7.4.

Krebs Ringers HEPES buffer (KRH),
118mM NaCl, 5mM $NaHCO_3$, 4.7mM KCl, 1.2mM KH_2PO_4, 1.2mM $MgSO_4$, 25mM Hepes (pH 7.4), 2.5mM $CaCl_2$

Kinase Assay Buffer (KAB),
50mM Hepes (pH 7.4), 1mM DTT

2x Kinase Assay Buffer + Mg^{2+} (2x KAB+Mg)
100mM Hepes (pH 7.4), 2mM DTT, 40mM $MgCl_2$, 2μM MicrocystinLR

Mes Buffered Saline (MBS),
25mM MES (pH6.5), 150mM NaCl

Phosphate buffered saline (PBS),
137mM NaCl, 2.6mM KCl, 10mM Na_2HPO_4, 1.7mM KH_2PO_4 (pH7.4)

2.2.2 SDS-PAGE Buffers

Electrode buffer,

25mM Tris base; (pH 8.6) , 192mM glycine, 0.1%(w/v) SDS

Sample buffer,

93mM Tris.HCl; (pH 6.8), 1mM EDTA, 10% (v/v) glycerol, 2% (w/v) SDS, 0.002% (w/v) bromophenol blue and (20mM dithiothreitol added immediately prior to use).

2.2.3 Western Blotting Buffers

PBS-T,

PBS; (pH 7.4), 0.1% (v/v)Tween-20

Towbin buffer,

25mM Tris base; (pH 8.6), 192mM glycine, 20% (v/v) methanol

2.3 Methods

2.3.1 Growth and maintenance of WKY, SHRSP, lean Zuckers and ZDF rats.

Male Wistar Kyoto (WKY) rats, Stroke Prone Spontaneously Hypertensive rats, Zucker diabetic fatty rats and lean Zucker rats were housed under controlled conditions of temperature (21± 2°C) and light (12hr light-dark cycle) and fed on normal rat chow (rat and mouse no.1 maintenance diet, Special Diet Services, Waltham, Essex, UK) and water *ad libitum*. SHRSP and WKY blood pressure measurements were made by insertion of telemetry probes and by tail cuff measurements, according to standardised techniques (Jeffs et al., 1997). Glucose was measured by the glucose oxidase technique. Characteristics of the animals are presented in Table 3.1 and Table 5.1.

2.3.2 2-Deoxy-D-glucose (deGlc) transport assays in intact muscle.

Flexor digitorum brevis (FDB) muscles were dissected and cleaned of connective tissue without stretching and with tendons intact. Muscles were placed in KH buffer and were allowed to recover for 30 minutes at 37°C with continuous gassing with 95%O_2/5%CO_2. Muscles were pinned at resting length and incubated for 30 minutes in the presence or absence of 1μM insulin or 500μM AICAR after which time the muscles were rapidly washed three times with glucose-free KH buffer. Muscles were incubated for a further 10 minutes at 37°C in uptake buffer (KH buffer containing 1μM insulin, 10μM deGlc (1μCi/ml) and [^{14}C]-Sucrose (0.2μCi/ml; used as an extracellular marker) (in the presence or absence of 100nM wortmannin as indicated in the figure legends). Muscles were washed three times with ice-cold saline, blotted on filter paper, weighed and solubilised in 1ml of 0.5N NaOH at 60°C for 45 minutes and tissue associated radioactivity determined by scintillation spectrophotometry.

2.3.3 Preparation of muscle extracts.

Freshly dissected muscles were placed in a 50 ml Corning tube and homogenised in ice-cold immunoprecipitation buffer pH7.4, 1% NP40 using a Polytron (setting 5), followed by 20 strokes in a Dounce homogeniser. The homogenate was centrifuged at 14,000x*g* for 5 min at 4°C to remove unsolubilised material. The supernatant containing solubilised

protein was collected and assayed for protein as outlined in 2.3.5 prior to immunoprecipitation or immunoblot analysis as described below in 2.3.7 through to 2.3.10. The remainder of solubilised protein was aliquoted and stored at -80°C.

2.3.4 Fractionation of skeletal muscle.

Muscles were quickly dissected and snap frozen in liquid nitrogen. Frozen tissue was powdered using a mortar and pestle on dry-ice and resuspended in HES buffer supplemented with Complete™ protease inhibitor cocktail tablets prior to homogenisation. The homogenate was centrifuged at 12,000x*g* for 20 min at 4°C and the pellet collected (heavy membrane fraction). The supernatant was further centrifuged at 140,000x*g* for 1 hour at 4°C and the pellet (light membrane fraction) and supernatant (soluble protein fraction) collected. These fractions were assayed for protein and resuspended in SDS-PAGE sample buffer prior to immunoblot analysis.

2.3.5 Protein estimation using the Bichiconic Acid protocol

Protocol was carried out essentially as directed by manufacturer's instructions. A standard curve (ranging from 0 to 1mg/ml) was prepared from a 2mg/ml BSA solution. The standard curve was prepared in the same buffer as unknown sample to account for any interference from buffer constituents. Triplicate 10µl aliquots of each sample was then added to a 96 well plate, followed by 200µl of diluted BCA reagent (prepared by diluting 1 part of reagent A with 50 parts of reagent B). The plate was incubated at 37°C for 60 minutes, after this time the absorbance of the samples was read in an automated plate counter at 565nm. Using Microsoft Excel5.0 values of absorbance were plotted against their respective known standard BSA concentrations. A linear line of best fit was drawn, equation of line $y = mx + c$, intercept of x-axis set to zero. Unknown protein concentrations were interpolated from the linear fitted line.

2.3.6 In-vitro stimulation of extensor digitorum longus muscle

EDL muscles were isolated by dissection with tendons intact and were placed in KH buffer supplemented with 25 mM D-glucose and were allowed to recover for 30 minutes at 37°C with continuous gassing with 95%O_2/5%CO_2. Muscles were incubated under a

constant tension for 30 minutes in the presence or absence of 1 μM insulin after which time the muscles were rapidly washed three times with glucose-free KH Buffer and snap frozen.

2.3.7 Immunoprecipitation and assay of Protein kinase B.

Frozen tissue was powdered using a mortar and pestle on dry-ice and resuspended in immunoprecipitation buffer supplemented with 1% Tx-100. Muscle lysates were spun in a microfuge at 14,000 x*g* for 10 minutes to remove insoluble material. A 25% Protein G-Sepharose slurry was washed 3 times with 1ml of immunoprecipitation buffer supplemented with 1% Tx-100. 1μg of anti-PKB (PH domain) antibody was added to every 20μl of 25% Protein G-Sepharose (5μl packed volume) and incubated in a total volume of 300-500μl on a rotating mixer for 2 hours at 4°C. After this time antibody-Protein G-Sepharose complex was pelleted by a pulse spin at 14000 x*g*, 4°C. Any unbound antibody was aspirated off and the antibody-bead complex was washed 3 times with 1ml of immunoprecipitation buffer supplemented with 1%Tx-100. 20μl of 25% Protein G-Sepharose-antibody conjugate was used per immunoprecipitation. 50-100μg of lysate was added to 20μl of 25% Protein G-Sepharose-antibody complex and the volume was made up to 300μl with IP buffer supplemented with 1% Tx-100 and mixed for 2 hours at 4°C on a rotating mixer. The mixture was centrifuged at 14,000 x*g*, 30 seconds, 4°C, and the pellet was washed three times with 1ml lysis buffer supplemented with 1M NaCl followed by two times with 1ml Kinase Assay buffer (KAB) at 4°C. Pellets were resuspended in 20μl KAB and assayed as follows. Reaction mixtures, with a total volume of 20μl, containing 10μl of KAB, 5μl of 150μM RPRAATF substrate peptide in KAB and 5μl of immunoprecipitate were prepared on ice and the reaction initiated by the addition of 5μl of [γ-^{32}P]ATP solution (250μM [γ-^{32}P]ATP with a specific activity in the range of 250,000 to 500,000 cpm/nmol (0.5 to 1 μCi [γ-^{32}P]ATP/reaction), 50mM $MgCl_2$). Blank reactions were prepared by substituting KAB for substrate peptide. After incubation with shaking at 30°C for 15 minutes, 15μl of the reaction mixture was removed and spotted onto 1cm^2 pieces of Whatman P-81 phosphocellulose paper and the paper dropped into 1% (v/v) phosphoric acid. The P-81 paper squares were washed for 10 minutes through three changes of 1% (v/v) phosphoric acid and then rinsed with water.

Rinsed squares were air dried and the incorporation of [γ-^{32}P]ATP into the substrate peptide determined by liquid scintillation counting.

2.3.8 SDS-PAGE

SDS/Polyacrylamide gel electrophoresis was carried out using Bio-Rad mini-PROTEAN II. The Bio-Rad mini-PROTEAN II slab gels had a stacking gel of 2cm composed of 5% acrylamide/0.136% bisacrylamide (v/v) in 125mM Tris-HCl (pH 6.8), 0.1% (w/v) SDS, polymerised with 0.1% (w/v) ammonium persulphate and 0.05% (v/v) TEMED. The resolving gel consisted of 6.5-10% acrylamide/0.18-0.28% bisacrylamide in 0.383mM Tris-HCl (pH 8.8), 0.1% (w/v) SDS, polymerised with 0.1% (w/v) ammonium persulphate and 0.01% (v/v) TEMED. Protein samples were solubilised in sample buffer and heated at 80°C in water bath for 3minutes. Samples were loaded into the wells in the stacking gel. 10µl of broad range pre-stained molecular weight markers were loaded into at least one well. Gels were immersed in electrode buffer and electrophorised until the dye front had reached the desired position or until adequate separation of pre-stained molecular weight markers. A constant voltage of 70 volts was applied through the stacking gel, which was increased to 120 volts through the resolving gel.

2.3.9 Western blotting

After separation of the proteins as described earlier, gels were removed from the plates and equilibrated in Towbin's buffer for 10 minutes. A sandwiched arrangement of components, individually soaked in Towbin's buffer, were made as follows from bottom to top: brillo pad, two pieces of Whatmann 3MM filter paper, nitrocellulose paper, equilibrated polyacrylamide gel, two pieces of Whatmann 3MM filter paper, brillo pad. The sandwich was placed in a cassette and slotted, bottom nearest to cathode, into a Bio-Rad mini trans-blot tank filled with Towbin's buffer. Transfer of proteins was performed at room temperature for 3 hours at a constant current of 250mA. Efficiency of transfer was determined by staining the nitrocellulose membrane with Ponceau S solution.

Membrane was incubated with 5% (w/v) non-fat milk (BioRad) made up in PBS-T for 1 hour to block non-specific binding sites. Primary antibodies were diluted in 1% (w/v) non-fat milk/PBS-T. Blots were incubated with primary antibody of interest overnight on a shaking platform at 4°C. The blot was washed three times over 15 minutes with PBS-T

and incubated for 1 hour with 1μg/ml of an HRP-linked secondary antibody raised to the (tail) Fc-region of primary antibody IgG molecule. The blot was washed for 15 minutes with PBS-T supplemented with 1 Molar NaCl, followed by 3 changes over 15 minutes with PBS-T.

2.3.10 Immunoblot analysis.

Immuno-labelled proteins were visualised using HRP-conjugated secondary antibody and the ECL system (Amersham, UK). Bands were quantified by densitometry using Tina Image software. In order to quantify the relative levels of expression, increasing loads of protein were loaded into adjacent lanes and the linearity of the immunoblot signal determined by densitometric analysis of blots developed using ECL. Multiple exposures of X-ray film were performed in order to insure linearity of response to film to signal. All immunoblot signals were quantified from linear regions of the protein titration curve.

2.3.11 Growth and Maintenance of L6 cultures.

L6 cells were seeded into 175cm^2 flasks and maintained at 37°C/5% CO_2 in a humidified incubator. On average the L6 cells from one 175cm^2 flask were seeded onto ten 10cm plates or six 6well plates. Cells were fed 24 hours after seeding and then every two days with α-modification Minimum Essential Medium (α-MEM) supplemented with 8% FBS and 100U/ml penicillin/streptomycin until 30% confluence.

2.3.12 Passage of skeletal muscle cultures

Rat skeletal muscle cultures and L6 cultures were passaged at 50% and 30% confluence, respectively, on the fourth day since seeding or last passage. Medium was aspirated from cells in a 75cm^2 flask and the cells then washed for 20 seconds with 5ml pre-warmed sterile trypsin EDTA. This trypsin was removed and replaced with 2ml of fresh trypsin. Cells were returned to the incubator and left for around 2-4 minutes to allow cells to detach. The trypsin was neutralised by the addition of 10ml of growth medium (defined in chapter4) or in the case of L6 cells, α-MEM supplemented with 8%FBS and cells seeded as desired.

2.3.13 Freezing down cultures

Three to four 75cm^2 flasks of rat skeletal muscle cultures or one to two 175cm^2 flasks of L6 cells were trypsinised as previously described. Cells were pelleted and resuspended to 1x10^6 cells per ml in 100%FBS-10%DMSO. 0.5ml aliquots of cell suspension were placed into cryovials. Cryovials were wrapped in blue roll and placed in a polystyrene box at -80°C overnight, after which vials were placed in the vapour phase of liquid nitrogen for long term storage.

2.3.14 Whole cell indirect immunofluorescence

Skeletal muscle cells were cultured on collagen coated coverslips placed in a 6 well culture dish. Cells were then transferred onto ice and washed three times with ice cold PBS and fixed using 3mls of para-formaldehyde per well. Cells were washed three times with PBS, followed by three washes in PBS/5% goat serum over a time period of 15 minutes, in order to block non-specific binding sites. Cells were incubated with primary antibody diluted in PBS/1% goat serum for 1 hour. After this time, cells were washed three times with PBS/0.1% (w/v) BSA and incubated with FITC-conjugated secondary antibodies diluted in PBS/1% goat serum. Finally, cells were washed with five changes of PBS over a 15-minute period and mounted on glass slides using Vector Laboratories mounting medium. Slides were visualised using a Zeiss fluorescent microscope.

2.3.15 2-Deoxy-D-glucose (deGlc) transport assays in cultured myotubes.

Cultured myotubes serum starved for 16 hours, were washed two times in 3 ml of Krebs Ringer Hepes buffer pH7.4 and incubated for 30 min at 37°C in the presence or absence of 1nM to 1μM insulin or 500μM AICAR (in the presence or absence of 100nM wortmannin as indicated in the figure legends). Uptake was initiated by addition of 10μM 2-deGlc (1μCi/ml) for 10 min. Specific carrier mediated deGlc uptake was determined by calculating the cell associated radioactivity in the presence of 10μM Cytochalasin B. Plates were washed rapidly by three changes in ice cold PBS. Cells were lysed in 1ml of 1% Tx-100. The lysate was transferred to scintillation tubes and cell associated radioactivity was determined by liquid scintillation spectrophotometry.

2.3.16 Recombinant protein kinase B (PKB) phosphorylation and activity microtitre plate assay

This is a two-step reaction. First, S473D-PKBα was combined with its allosteric activator, PIP_3 and/or the test compound, in the presence of its constitutively active upstream kinase, 3-phosphoinositide-dependent kinase-1 (PDK1) and unlabelled ATP. Phosphorylation/activation of S473D-PKB was then allowed to proceed for 30 min at 30°C. Secondly, radiolabelled ATP and a peptide substrate specific for S473D-PKB was added, and the incubation continued for a further 30 min. The reaction was then terminated by the addition of 20 mM EDTA and the extent of peptide phosphorylation (an index of PKB activation) measured upon capture of the peptide by p81 paper.

(i) Preparation of lipid vesicles

The following lipid stock solutions were made up and stored at -20°C in glass vials under N_2.

- 1mg/ml (0.837 mM) stearoyl, arachidonyl PIP_3 in distilled water (in opaque polypropylene tube).
- 25 mg/ml (32.89 mM) phosphatidycholine in chloroform/methanol (2:1)
- 10 mg/ml (12.31 mM) phosphatidylserine in chloroform/methanol (2:1)

For 2.2 ml of vesicles, 66.9 µl phosphatidylcholine and 178.2 µl of phosphatidylserine were mixed in a polypropylene tube. Solvent was removed under vacuum in a centrifugal evaporator (Howe GyroVap) for as short a time as possible. 26.5 µl PIP_3 was added to the dried lipids and the evaporation process repeated. When all the water was removed 2.2 ml 10 mM Hepes/NaOH pH 7.0 was added to the dried lipids, minimising exposure of the dried lipid to air (which can lead to oxidation). The mixture was incubated on ice for 1 hour with occasional brief vortexing (protected from light). Once the lipid has rehydrated and no longer adheres to the wall of the polypropylene tube it should appear to be an opaque, homogeneous suspension. This lipid suspension was sonicated for 20 min in a bath sonicator at 4°C. The prepared vesicles contain 1 mM phosphatidyl choline (PC), 1 mM phosphatidyl serine (PS) and 0.01 mM PIP_3. Once diluted 10-fold in the assay, the final lipid concentrations is 100 µM (PC/PS) and 1 µM PIP_3 (determined within GlaxoSmithkline as the optimal concentration for stimulation of recombinant PKB). The lipid vesicles from now on will be referred to as 'PIP_3 vesicles' and were stored at 4°C until use. Vesicles were aliquoted, snap-frozen under liquid nitrogen and stored at –80°C,

for storage periods longer than a week. They are good for 2-3 freeze-thaw cycles and were, prior to use, vortexed vigorously and sonicated briefly on thawing.

(ii) Assay

Activation reactions, with a total volume of 20 µl, containing 10 µl 2x KAB+Mg, 1 µl recombinant PKB (0.5 µg/µl), 4µl of unlabelled ATP (0.25 mM), 2 µl PIP_3 vesicles or compound (100 µM) and 2 µl water were prepared at room temperature. Activating reactions were initiated by addition of 1 µl recombinant PDK1 (0.02 µg/µl) and incubated at 30°C for 20 min. Blank reactions were prepared by prior addition of 5 µl EDTA (20 mM). Subsequently 10 µl of [γ^{32}P]-ATP (50 µM, 1 µCi/reaction) and RPRAATF substrate peptide (30 µM final) in 1x KAB+Mg was incubated at 30°C for 20 min. The reaction was terminated by addition of 5 µl EDTA (20mM). 17.5 µl of the reaction mixture was spotted onto P81 paper. The paper was dropped into 1% (v/v) phosphoric acid. The P-81 paper squares were washed for 10 min through three changes of 1% (v/v) phosphoric acid and then rinsed with water. Rinsed squares were air-dried and the incorporation of [γ^{32}P]-ATP into the substrate peptide was determined by liquid scintillation counting.

2.3.17 Statistical analysis.

Statistical analysis was performed using Student's t-test (2-tailed independent samples) with StatView software (Abacus Software, CA). A p value < 0.05 was taken as a significant difference between groups.

It should be noted that for clarity and conciseness of data, quantification of immunoreactivity from immunoblots in chapters three and five are presented as fold increase in protein expression in SHRSP/ZDF relative to WKY/lean Zucker.

Chapter 3.

A comparative analysis of glucose transport in skeletal muscle of WKY and SHRSP rat.

3.1 Introduction

Reduced insulin-stimulated glucose uptake (insulin resistance) by skeletal muscle and adipose tissue is of major pathogenic importance in several common human disorders including type 2 diabetes, hypertension, obesity and combined hyperlipidaemia, but the underlying mechanisms are unknown (Reaven, 1988). The primary nature of the link between insulin resistance and cardiovascular disorders is reinforced by the demonstration that the abnormality is also found in genetic models of hypertension. For example, Reaven and colleagues showed that the Spontaneously Hypertensive Rat (SHR) exhibited blunted insulin-stimulated glucose transport in adipose tissue compared to control normotensive animals (Reaven et al., 1989), while more recent studies have demonstrated grossly defective insulin inhibition of lipolysis (Aitman, 2001). These findings have been recently extended to a close relative of the SHR, the stroke-prone spontaneously hypertensive rat (SHRSP). The stroke-prone SHR represents a derivative of SHR that displays even higher blood pressures than the SHR and, as the name suggests, is more prone to cerebrovascular lesions resulting in stroke (Yamori et al., 1974). Studies on this sub-group have shown that adipocytes from these animals exhibit blunted insulin-stimulated glucose transport and a reduced ability of insulin to suppress isoproterenol-stimulated lipolysis (Collison et al., 2000). However, although such data clearly show that both SHR and SHRSP exhibit insulin resistance at the cellular level in adipocytes, they provide no information on whether this insulin resistance is also manifest in skeletal muscle, the major site of post-prandial glucose disposal (James et al., 1986).

3.1.1 Exercise-stimulated glucose transport

Exercise, like insulin, stimulates glucose disposal via glucose transporter-4 (Glut-4) translocation in skeletal muscle (introduction, section 1.5). However, insulin and exercise appear to promote Glut-4 translocation through distinct intracellular signalling cascades. Thus, in response to insulin, Glut-4 translocation is dependent upon the activation of phosphatidylinositol 3'-kinase (PI3K) and is sensitive to the PI3K inhibitor, wortmannin (Yeh et al., 1995). By contrast, exercise-stimulated Glut-4 translocation is wortmannin-resistant (Yeh et al., 1995) and appears to involve the activation of AMP-activated protein kinase (AMPK) (Hayashi et al., 1998); (Kurth-Kraczek et al., 1999). Moreover, these two

stimuli appear to act upon distinct intracellular pools of Glut4-containing vesicles (Ploug et al., 1998); (Aledo et al., 1997). Several studies have demonstrated defective insulin-stimulated Glut-4 translocation in patients with type 2 diabetes (Kahn, 1992), (Kahn et al., 1992); (Garvey et al., 1992); (Garvey et al., 1998). By contrast, it is noteworthy that several studies have suggested that normal exercise-stimulated Glut-4 translocation can often be observed in the face of insulin resistance in human type 2 diabetic populations (Goodyear et al., 1991); (Hughes et al., 1993); (Kennedy et al., 1999); (Wojtaszewski et al., 2000a).

3.1.2 Aims and objectives

The stroke prone spontaneously hypertensive rat (SHRSP) is a model of human insulin resistance and is characterised by reduced insulin-mediated glucose disposal and defective fatty acid metabolism in isolated adipocytes (Collison et al., 2000).

The aims of this study were:

(i) The assessment of insulin- and AICAR-stimulated glucose transport in isolated skeletal muscle from male SHRSP and WKY rats.

(ii) The quantification of total cellular expression and/or subcellular localisation of key proteins involved in insulin-signal transduction and glucose uptake namely (IRS-1/2, PI3K, caveolin, flotillin, SNAREs and Glut-4).

(iii) The measurement of the activity of PKB in SHRSP and WKY skeletal muscle.

3.2 Results.

3.2.1 The effect of insulin and AICAR on deGlc uptake by flexor digitorum brevis muscles.

The characteristics of the animals used in this study are shown in Table 3.1. Blood pressure was higher in the SHRSP compared to the WKY animals. (Collison et al., 2000) have previously shown that adipocytes from SHRSP animals exhibit reduced insulin-stimulated glucose transport in isolated adipocytes, and a blunted ability of insulin to suppress isoproterenol-stimulated lipolysis compared to the WKY strain. To further extend these findings, the ability of insulin to stimulate 2-deoxy-D-glucose (deGlc) uptake in isolated flexor digitorum brevis (FDB) muscles from these animals was examined. Figure 3.1 compares the effect of 1μM insulin and 500 μM AICAR (5-aminoimidazole-4-carboxamide ribonucleoside), an activator of AMPK, on deGlc transport into FDB muscle. As shown, muscles from SHRSP exhibit decreased insulin-stimulated deGlc uptake compared to WKY muscles, but the response to AICAR is essentially identical between the two groups.

3.2.2 Total cellular expression of Glut-4 in skeletal muscle from WKY and SHRSP animals.

The Glut-4 glucose transporter mediates the insulin-stimulated glucose transport in skeletal muscle (Ploug et al., 1998). I therefore determined the total cellular levels of Glut-4 in skeletal muscle membranes from SHRSP and WKY animals by quantitative immunoblotting. Figure 3.2 demonstrates that Glut-4 levels are similar in different muscles from SHRSP and WKY animals. These data indicate that reduced Glut-4 expression cannot explain the reduced ability of insulin to stimulate deGlc uptake in SHRSP muscle.

Table 3.1 Characteristics of the animal groups.

	Blood pressure systolic(mm Hg)	Blood pressure diastolic(mm Hg)	Serum glucose (mmol/L)	Weight (g)
WKY(n=16)	**126 ± 11**	**94 ± 10**	**8.3 ± 0.5**	**283.8 ± 26.5**
SHRSP(n=16)	**174 ± 12***	**128 ± 10***	**8.0 ± 0.6**	**227.6 ± 13.5***

Shown are the mean body weight, serum glucose and systolic and diastolic blood pressures of the 12 week old animals used in this study. * Indicates a statistical difference between the groups, $p<0.02$. Performed in collaboration with Dr. D. Graham, Dept. Medicine and Therapeutics, University of Glasgow.

Figure 3.1 The effect of insulin and AICAR on deGlc uptake in FDB muscle from SHRSP and WKY rats.

Flexor digitorum brevis muscles were incubated in Krebs Hensliet buffer for 30 min in the presence or absence of 1 μM insulin or 500 μM AICAR in 95 % air/5 % CO_2 prior to assay of deGlc uptake as described. The results are expressed as a fold stimulation over basal (typically between 0.6 - 0.9 pmol/min/mg wet weight muscle). Basal rates were not significantly different between the two strains. The results shown are the mean ± S.E.M. for three experiments. * indicates a statistically significant increase in response to insulin, p=0.02.** indicates a significant increase in response to AICAR, p=0.05. † indicates a significant increase in response to insulin compared to SHRSP basal (p<0.05) and also that the magnitude of the insulin response is lower in SHRSP compared to WKY muscles (p=0.02). †† indicates a statistically significant increase in response to AICAR (p=0.03) and also refers to no significant difference in the magnitude of the AICAR effects between the two strains.

Figure 3.1 The effect of insulin and AICAR on deGlc uptake in FDB muscle from SHRSP and WKY rats.

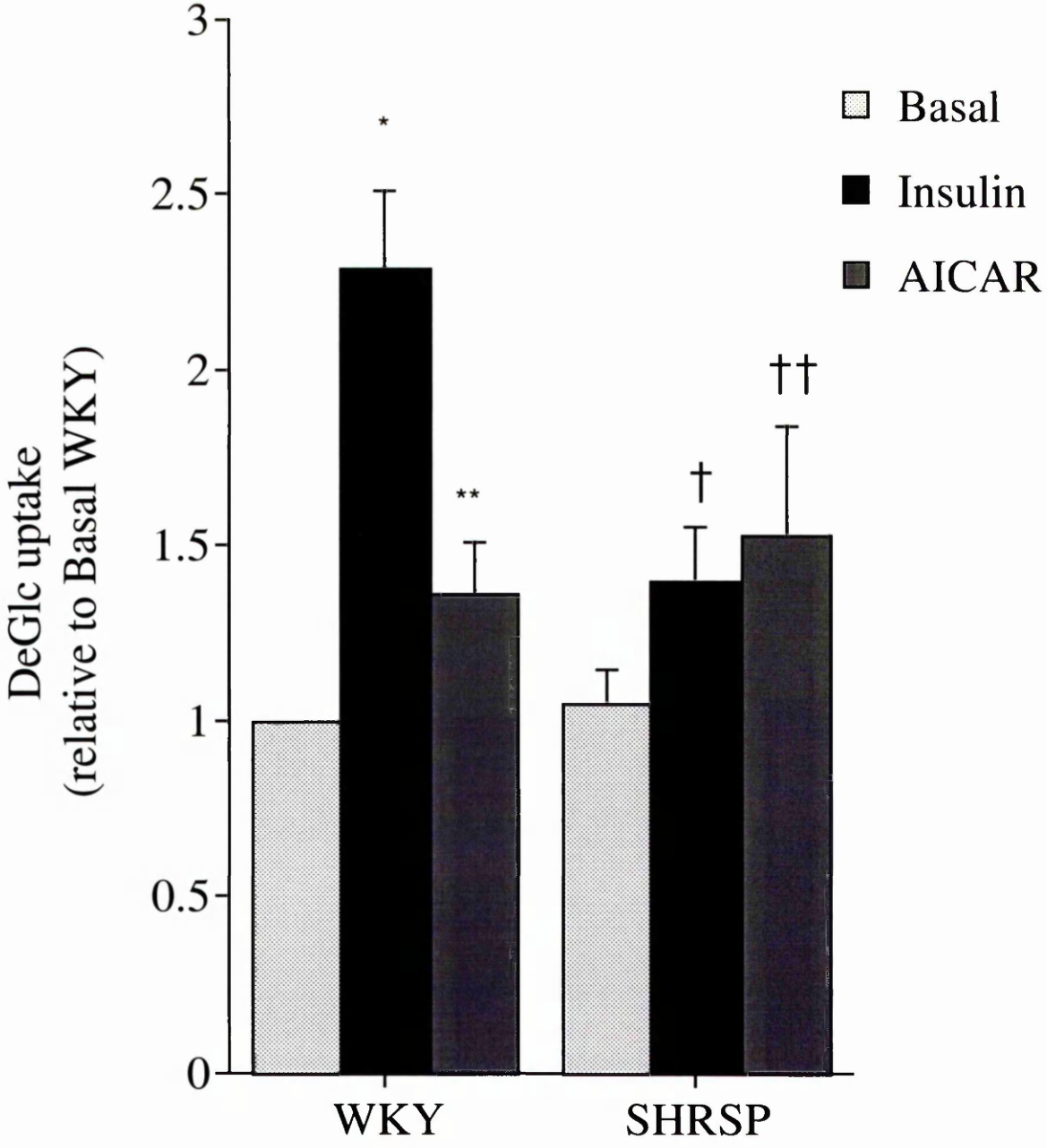

Figure 3.2 Immunoblot analysis of Glut4 levels in muscle from SHRSP and WKY animals.

Shown is a representative immunoblot for Glut4 levels in either tibialis or EDL muscles from SHRSP or WKY animals in which 20 μg of muscle lysate was loaded per lane. Shown are samples from two different animals. Quantification of Glut4 protein levels in these muscles from six different animals revealed no significant differences between the two strains.

Figure 3.2 Immunoblot analysis of Glut-4 levels in muscle from SHRSP and WKY animals.

(A)

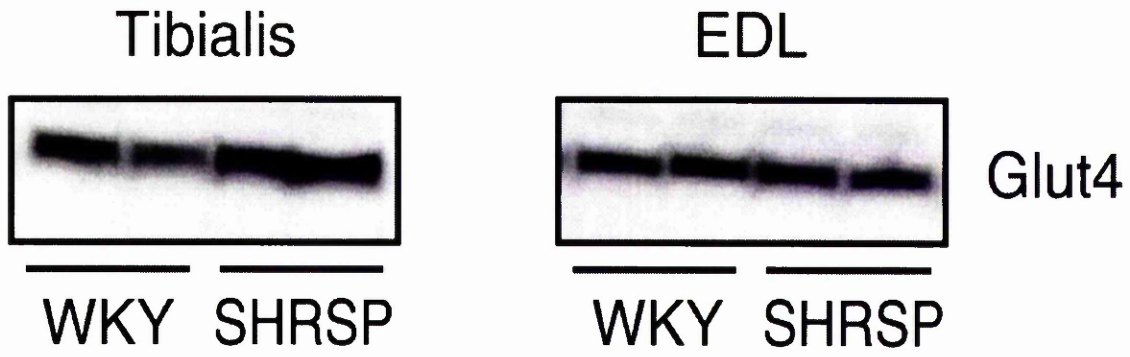

(B)

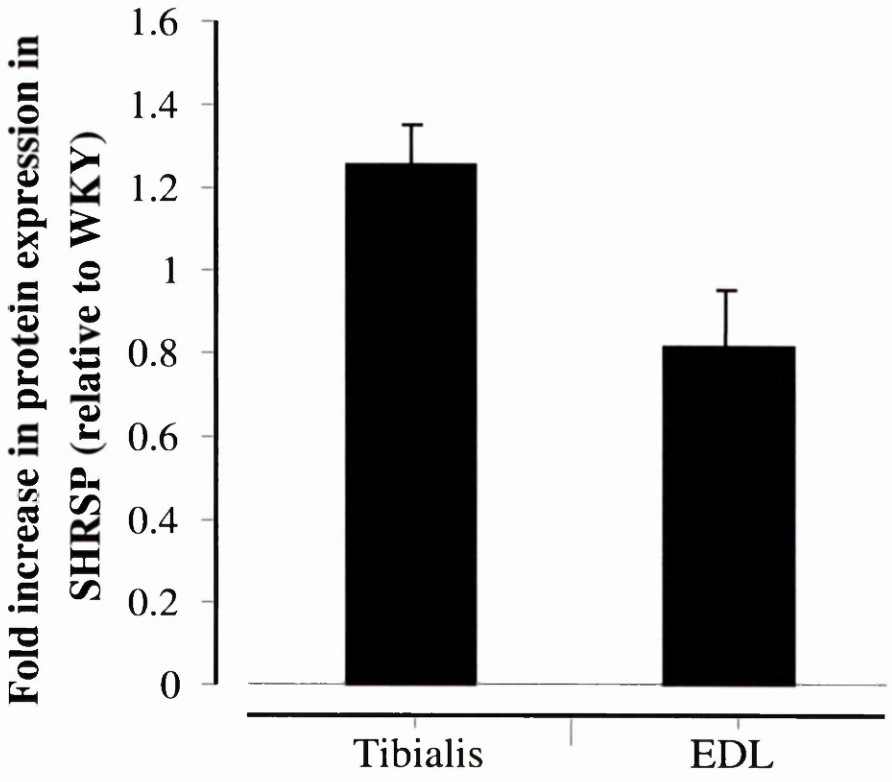

3.2.3 Immunoblot analysis of molecules involved in insulin-stimulated glucose transport.

In an attempt to identify differences between the SHRSP and WKY muscle that could account for the observed insulin resistance, the cellular content and distributions of proteins involved in insulin signalling and Glut-4 trafficking in muscles of these animals was assessed. Figure 3.3A shows an immunoblot analysis of the levels and distribution of IRS-1, IRS-2 and the p85α subunit of PI3K in muscle fractions. Expression levels of these proteins were examined in three crude subcellular fractions of muscle, specifically a heavy membrane fraction, a light membrane fraction (enriched in intracellular membranes, as evidenced by the majority of cellular Glut-4 being present in this fraction) and a soluble protein fraction (figure 3.3A and quantified in 3.3B). As has been reported in adipocytes (Clark et al., 1998); (Clark et al., 2000); (Whitehead et al., 2000), these key insulin-signalling molecules were found localised predominantly in the light membrane and soluble protein fractions of skeletal muscle. Neither the absolute level nor the distribution among these fractions was significantly different between SHRSP and WKY animals (Figure 3.3B). Hence, it would seem unlikely that defective expression of IRS-1, IRS-2 or PI3K can explain the insulin resistance observed in SHRSP muscles.

3.2.4 PKB Activity in EDL and soleus skeletal muscle from WKY and SHRSP animals.

In order to evaluate possible signalling defects associated with insulin action in these muscles, the ability of insulin to stimulate protein kinase B activity was examined. PKB has been suggested to be involved in the insulin-stimulated translocation of Glut-4 to the plasma membrane of both adipocytes and muscle (Alessi et al., 1996); (Coffer et al., 1998); (Foran et al., 1999); (Hill et al., 1999); (Wang et al., 1999). Figure 3.4 shows that no differences in the basal or insulin-stimulated PKB activity were observed in soleus or EDL muscles isolated from SHRSP and WKY animals. In addition, no differences in levels of serine phosphorylation of PKB at position 473 were observed between insulin-stimulated EDL muscles from WKY and SHRSP animals (Figure 3.5). Phosphorylation of the serine residues has been suggested to be required for PKB activation (Cohen, 1999). Thus, it appears that SHRSP muscles exhibit normal insulin-stimulation of PKB activity.

Figure 3.3 Immunoblot analysis of insulin signalling proteins in skeletal muscle from SHRSP and WKY rats.

The distribution of IRS-1, IRS-2 and the p85α subunit of PI3K in skeletal muscle fractions from SHRSP and WKY animals were analysed by quantitative immunoblotting (**A**). The light membrane (LM) fraction contains the majority of the intracellular membranes, as evidenced by the majority of the cellular Glut4 being present in this fraction. HM = heavy membranes, Cyt = soluble protein fraction. The data presented is representative of three separate experiments involving different rats in which 20 μg of each fraction was loaded on each lane of the gel. No significant differences in either expression level or subcellular distribution were observed for any of the proteins studied. **B** shows quantification of four experiments of this type, in which the distribution of these molecules among the different fractions is presented, expressed as a % of total immunoreactivity (mean value presented). Experiments were performed in collaboration with F. Cairns, Dept. Biochemistry and Molecular Biology, University of Glasgow

Figure 3.3 Immunoblot analysis of insulin signalling proteins in skeletal muscle from SHRSP and WKY rats.

(A)

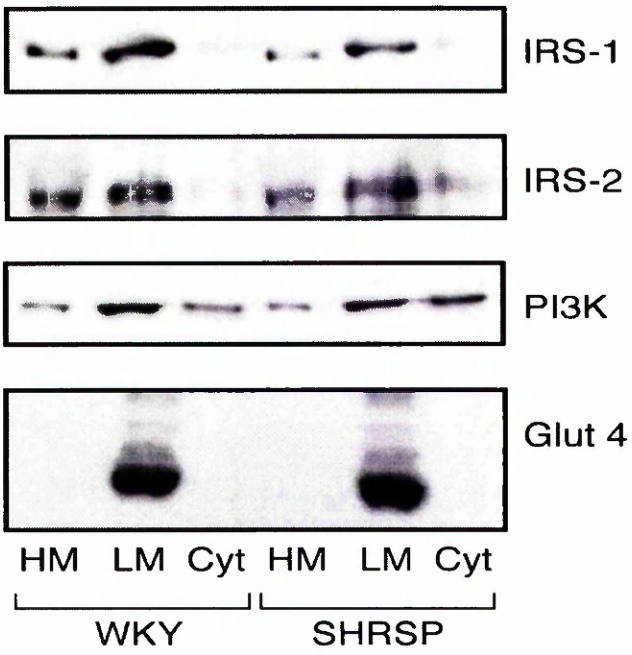

(B)

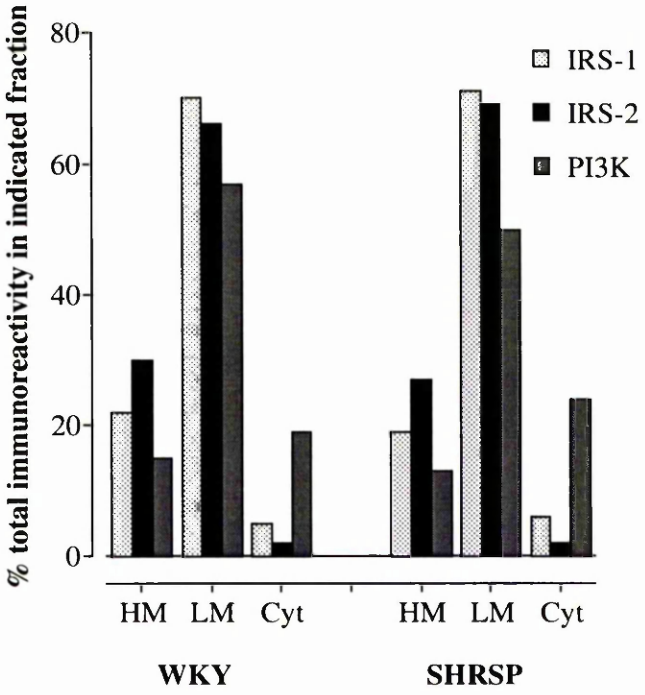

Figure 3.4 Protein kinase B activity in muscles from WKY and SHRSP rats.

EDL or soleus muscles were incubated with or without 1 μM insulin for 30 min and PKB activity determined as outlined methods. Shown is data from three experiments from six different animals (mean ± S.E.M.) with each condition performed in triplicate in each experiment. No significant differences were observed between the strains. Experiments were performed in collaboration with F. Cairns, Dept. Biochemistry and Molecular Biology, University of Glasgow

Figure 3.4 Protein kinase B activity in muscles from WKY and SHRSP rats.

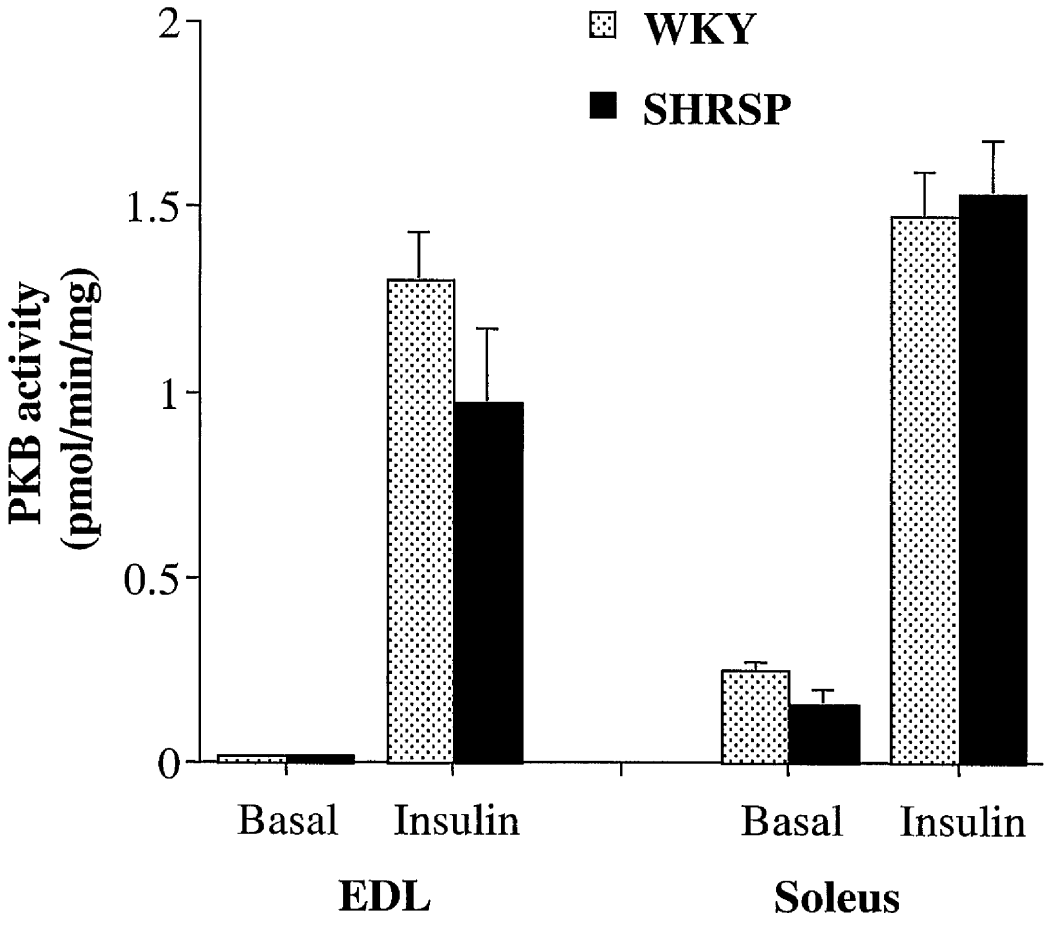

Figure 3.5 Immunoblot analysis of PKB serine-473 phosphorylation in EDL muscle lysates from WKY and SHRSP rats.

EDL muscles were incubated with or without 1 μM insulin for 30 min and whole muscle lysates were made as outlined in methods. Shown is a representative immunoblot for PKB-PH domain and phosphorylated serine-473 PKB levels in EDL muscles from SHRSP or WKY animals in which 10 μg of muscle lysate was loaded per lane. PKB–PH domain is shown to illustrate that the observed changes in PKB serine-473 phosphorylation is not a consequence of global changes in PKB expression. The experiment was repeated three times with similar results. No significant differences in PKB serine-473 phosphorylation were observed between the strains.

Figure 3.5 Immunoblot analysis of PKB serine-473 phosphorylation in EDL muscle lysates from WKY and SHRSP rats.

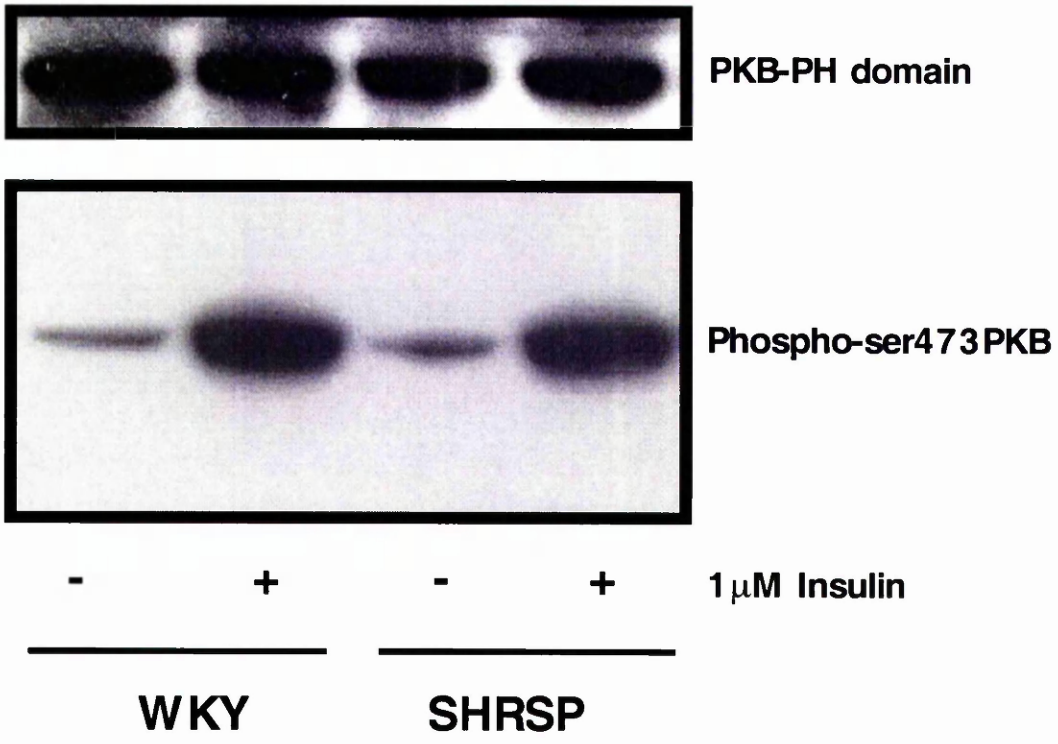

3.2.5 Immunoblot analysis of SNARE proteins in skeletal muscle from SHRSP and WKY rats.

To further elucidate the defects leading to insulin resistance in SHRSP muscle, I compared the total cellular content of VAMP2, VAMP3/cellubrevin and syntaxin 4, the SNARE proteins that mediate Glut-4 translocation (see (Rea and James, 1997) for review) in total muscle extracts. Quantification of this data revealed that VAMP2 expression was elevated 2.9 $\pm$ 0.2-fold in EDL and 2.7 $\pm$ 0.3-fold in tibialis muscles from the insulin resistant SHRSP strain compared to WKY animals (p=0.02 for both). VAMP3/cellubrevin levels was statistically significant only in the tibialis muscle (2.5 $\pm$ 0.13-fold in tibialis, p<0.05). Syntaxin 4 levels were also increased in EDL muscles from SHRSP animals (2.08 $\pm$ 0.2-fold, p=0.03) and tibialis (2.8 $\pm$ 0.05-fold, p=0.02). By contrast, cellular levels of AMPKα2, PKB/cAKT and eNOS did not differ significantly between strains in either muscle (Figure 3.6). AMPKα1 was barely detectable in these tissues, consistent with published results (data not shown) (Cheung et al., 2000).

3.2.6 Immunoblot analysis of caveolin and flotillin in skeletal muscle from SHRSP and WKY rats.

Recent studies have implicated caveolae and/or lipid rafts as possible components of the insulin signalling apparatus. I therefore examined the level of expression of caveolin isoforms in muscle tissue from SHRSP and WKY animals, and also the expression of flotillin, a protein enriched in membrane rafts and which has been implicated as a component of the insulin-signalling cascade. Levels of expression of caveolin-1 and flotillin were found to be markedly elevated in the SHRSP animals compared to controls (figure 3.7). In EDL muscle, caveolin expression was increased 3.4 $\pm$ 0.4-fold (p=0.005) and in tibialis by 4.34 $\pm$ 0.4-fold (p=0.002). Similarly, flotillin levels were also increased by 2.9 $\pm$ 0.05-fold and 2.7 $\pm$ 0.12-fold in EDL and tibialis muscles, respectively (p<0.05 for both).

Figure 3.6 Immunoblot analysis of SNARE protein levels in skeletal muscle from SHRSP and WKY rats.

Shown are representative immunoblots (**A**) in which 20 μg of protein lysates prepared from skeletal muscle of male SHRSP or WKY animals were analysed by SDS-PAGE and immunoblotting with the antibodies indicated. **B** presents quantification of 4 experiments of this type, with the relative level of expression in SHRSP muscle expressed as a fold of that observed in the corresponding WKY muscle (± S.E.M.). Data from two separate experiments is shown for each of EDL and tibialis muscles. Results obtained using antibodies specific for eNOS, AMPK and PKB-β are shown to illustrate that the observed changes in SNARE protein expression are not a consequence of global increases in the expression of proteins implicated in insulin or exercise signal transduction. Details of statistically significant differences are not presented on the graph for clarity but are included in the text.

Figure 3.6 Immunoblot analysis of SNARE protein levels in skeletal muscle from SHRSP and WKY rats.

(A)

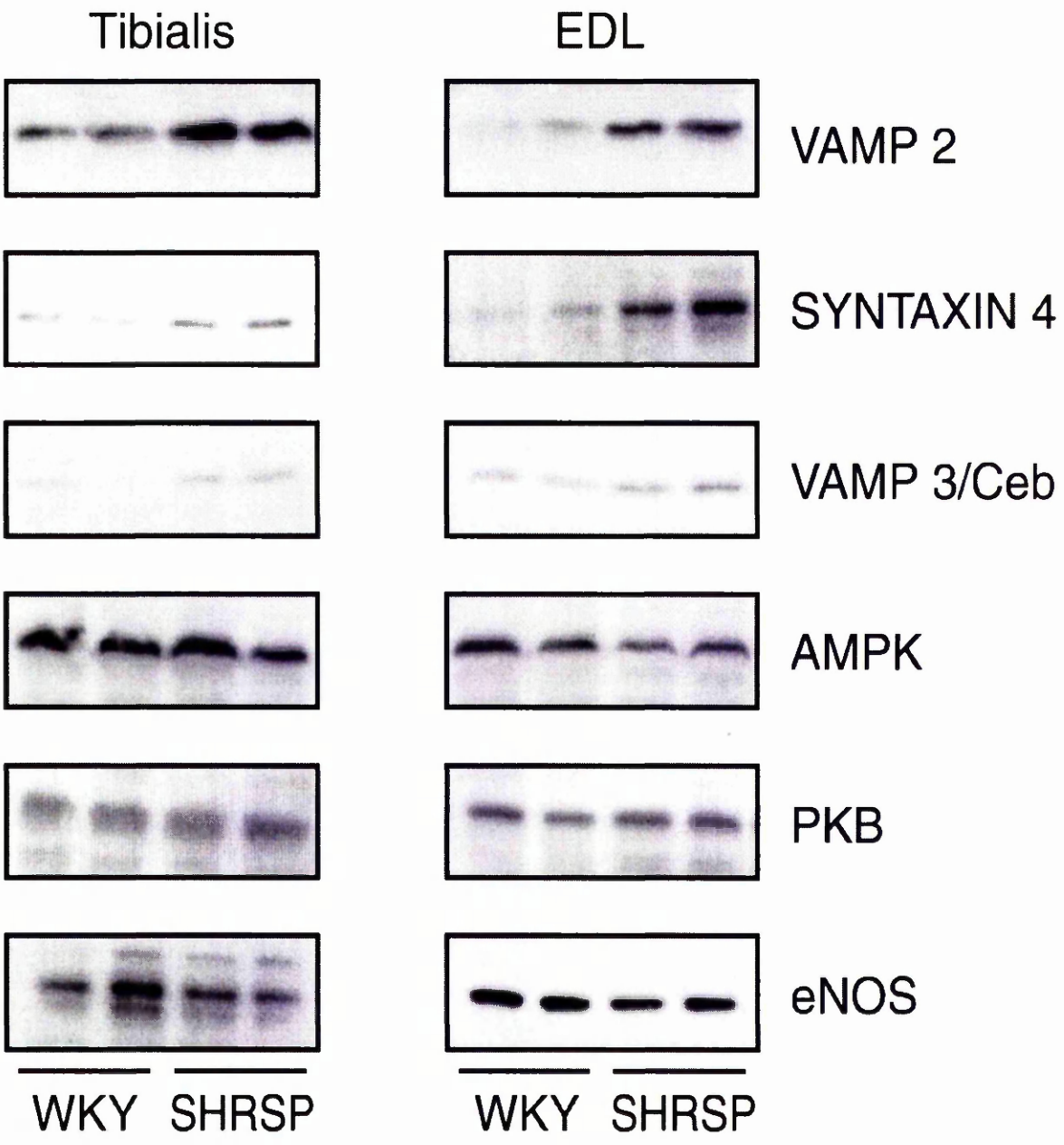

(B)

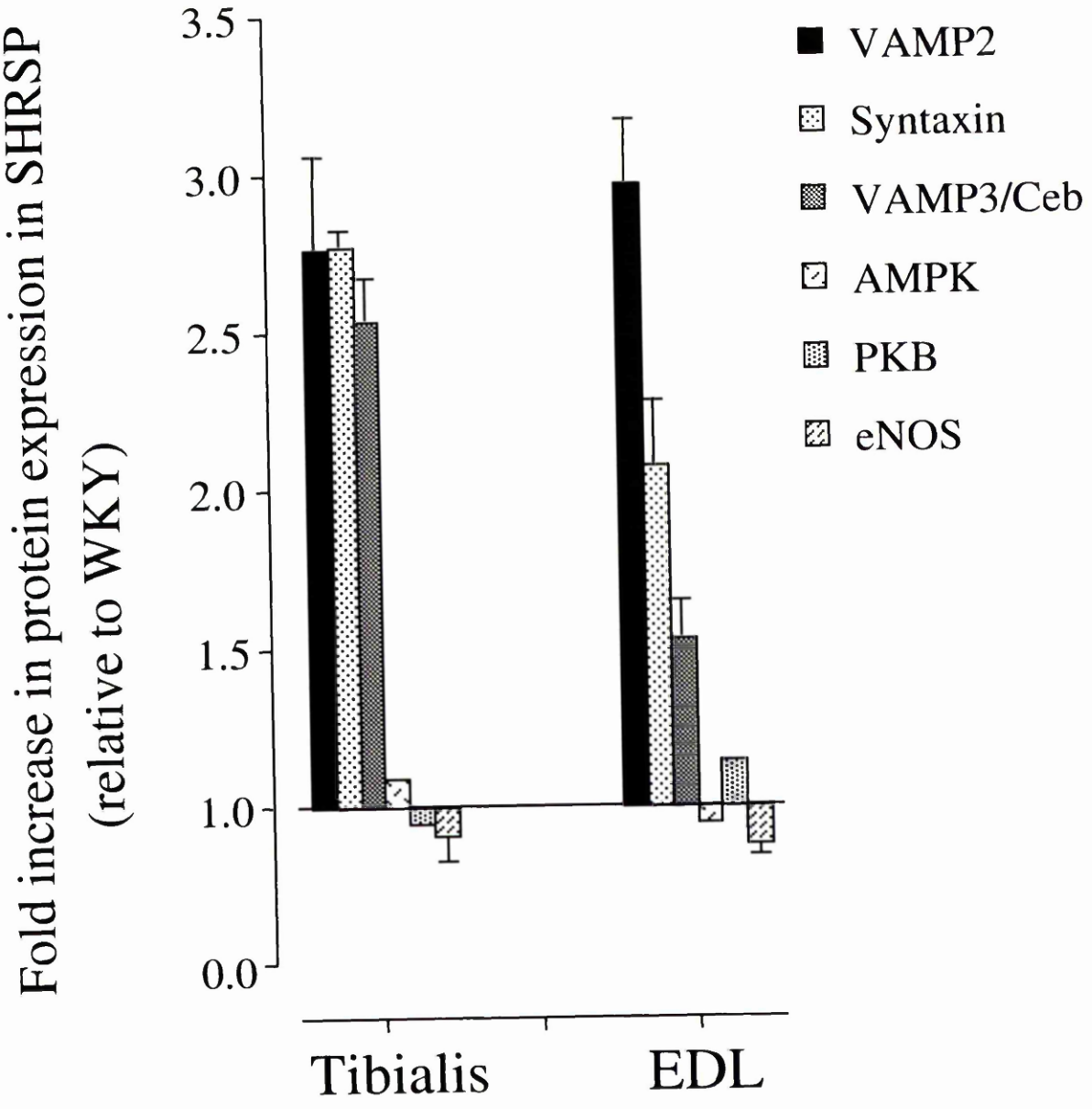
Fold increase in protein expression in SHRSP
(relative to WKY)
3.5
3.0
2.5
2.0
1.5
1.0
0.0
VAMP2
Syntaxin
VAMP3/Ceb
AMPK
PKB
eNOS
Tibialis
EDL

Figure 3.7 Immunoblot analysis of caveolin and flotillin in skeletal muscle from SHRSP and WKY rats.

Shown are representative immunoblots (**A**) in which 20 μg of protein lysates made from skeletal muscle of male SHRSP or WKY animals were analysed by SDS-PAGE and immunoblotting with the antibodies indicated. Shown is data from two separate animals of each strain; note that the blots presented are deliberately over-exposed in order to show the level of caveolin and flotillin present in WKY animals. **B** presents quantification of 4 experiments of this type, with the relative level of expression in SHRSP muscles expressed as a fold of that observed in the corresponding WKY muscle (± S.E.M.). Statistically significant increases in SHRSP compared to WKY are indicated by: * p=0.005, ** p=0.002, † p<0.05.

Figure 3.7 Immunoblot analysis of caveolin and flotillin in skeletal muscle from SHRSP and WKY rats.

(A)

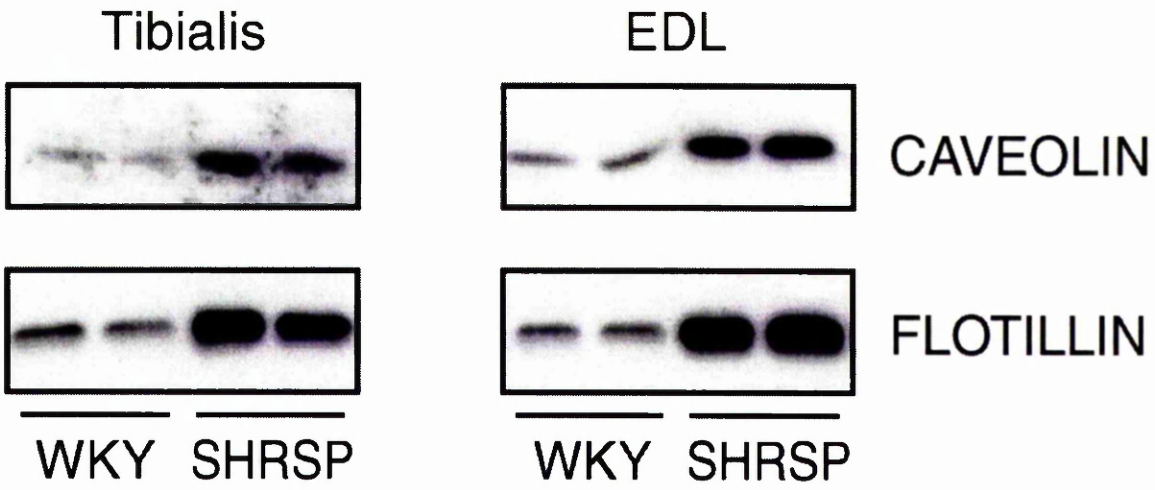

(B)

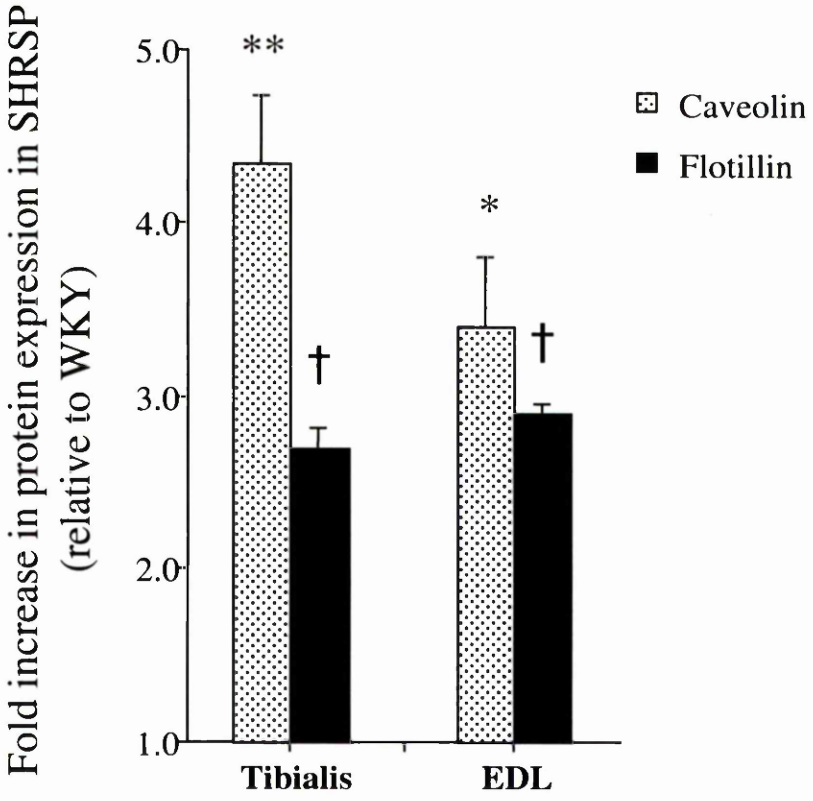

3.3 Discussion

Glucose transport in skeletal muscle is stimulated both by insulin and exercise. Insulin-stimulated glucose transport is reduced in type 2 diabetes and insulin resistance, but several studies have suggested that exercise-stimulated glucose transport is unaffected in these states (Hughes et al., 1993); (Kennedy et al., 1999); (Wojtaszewski et al., 2000a); (Houmard et al., 1995). Understanding the molecular basis for defective insulin action is of fundamental importance, given the greatly increased incidence of cardiovascular disease in individuals with type 2 diabetes (Yip et al., 1998); (Laakso, 1999). This study has examined the ability of insulin and AICAR (an activator of AMPK) to modulate glucose transport in skeletal muscle from SHRSP animals compared to the normotensive, insulin-sensitive WKY strain. I have shown that muscle from the SHRSP exhibits blunted insulin-stimulated glucose transport (figure 3.1), in agreement with the previous observation that adipocytes from these animals also exhibit defective insulin action (Collison et al., 2000).

AMPK is activated in response to exercise in both human and rodent muscle (Hayashi et al., 1998); (Kurth-Kraczek et al., 1999). AMPK has, therefore, been suggested to play a crucial role in exercise-stimulated glucose transport based upon studies showing that treatment of muscle with AICAR can activate glucose transport by a mechanism similar to that induced by exercise (Hayashi et al., 1998); (Kurth-Kraczek et al., 1999). Strikingly, AICAR is able to activate glucose transport to a similar extent in muscle from both SHRSP and WKY strains (Figure 3.1), suggesting that the insulin resistance observed in the SHRSP is confined to an insulin-specific step in the activation of glucose transport. This step is not expression of the major insulin-responsive glucose transporter, Glut-4, as levels of expression of this protein were found to be similar in all muscles examined (EDL, tibialis and FDB) (Figure 3.2).

In an attempt to identify possible sites of lesion in the insulin signalling cascade, the levels of expression and subcellular localisation of several key proteins implicated in insulin-stimulated glucose transport were examined, specifically IRS-1, IRS-2 and PI3K (Figures 3.3A/B) (White and Kahn, 1994); (White, 1997); (Inoue et al., 1998). The subcellular distribution of IRS-1 and IRS-2 is modulated by insulin (Inoue et al., 1998).

The association of IRS-1 with a cytoskeletal 'scaffold' adjacent to the plasma membrane has been suggested to be a fundamental aspect of insulin signalling in adipocytes (Clark et al., 1998); (Clark et al., 2000). In response to insulin treatment, IRS-1 is released from this scaffold and appears to behave as a soluble protein, moving from the particulate to the cytosolic fraction upon subcellular analysis (Clark et al., 1998). In an effort to address whether IRS proteins were cytosolic or particulate in muscle, we subjected muscle homogenates to subcellular fractionation. Analysis of the subcellular distribution of IRS-1 and IRS-2 revealed that these molecules were associated with both heavy and light membrane fractions, with some immunoreactivity evident in the cytosolic fraction (Figure 3.3A). However, comparison of these fractions from SHRSP and WKY strains revealed no differences in either total level of expression or subcellular distribution (Figure 3.3B). Hence, it would appear unlikely that the primary defect in insulin action in the SHRSP lies at the level of expression or localisation of these proteins. Similarly, levels of expression of AMPKα2 (the major isoform in skeletal muscle (Cheung et al., 2000), both PKB/cAKT and eNOS were similar between the two groups (Figure 3.6).

In an effort to address whether the extent of activation of downstream signalling molecules differed between the two strains, we assayed PKB/cAKT activity in both soleus and EDL muscles from SHRSP and WKY animals. As shown in Figure 3.4, no difference in either basal or insulin-stimulated PKB activity was observed between these strains. These data suggest that the defect in insulin action observed in the insulin-resistant SHRSP is not a consequence of defective activation of this important kinase.

Insulin-stimulated Glut-4 translocation represents a highly regulated vectorial delivery of defined intracellular cargo to the plasma membrane. The fidelity of this response is mediated, at least in part, by SNARE proteins (reviewed in (Rea and James, 1997) and (Pessin et al., 1999)). To examine potential defects in the translocation of Glut-4, total cellular expression of the SNARE proteins, syntaxin 4 and VAMP2, were quantified. GST-fusion proteins for each of these SNARE proteins inhibit insulin-stimulated Glut-4 translocation in muscle and fat cells, arguing cogently for a crucial functional role of these proteins in insulin action (Millar et al., 1999); (Tellam et al., 1997); (Martin et al., 1998); (Volchuk et al., 1996); (Olson et al., 1997); (Cheatham et al., 1996). Moreover, in the insulin resistant and diabetic ZDF rat VAMP2 and syntaxin 4 SNARE protein

expression is significantly up regulated compared with lean animals (Maier et al., 2000). Similar data was observed here, VAMP2 expression was doubled in both EDL and tibialis muscle from SHRSP compared to WKY ($p<0.01$ for both muscles), and syntaxin 4 levels were also increased. Such data suggest that up-regulation of SNARE proteins may be evident in a range of insulin resistant models. However, further work will be required to determine whether these changes are causal or adaptive.

One other major difference between these two strains was identified in this study. Specifically, the expression of caveolin-1 and flotillin were markedly elevated in muscle from the insulin resistant SHRSP compared to WKY animals (Figure 3.7A/B). Caveolin is the major structural protein of caveolae, flask-like invaginations of the cell surface (Smart et al., 1999). Caveolae have been implicated in the spatial organisation of intracellular signalling cascades, and several studies have reported localisation of insulin receptors to these structures (Baumann et al., 2000); (Mastick et al., 1995); (Mastick and Saltiel, 1997); (Gustavsson et al., 1999). Caveolin expression is induced upon differentiation of adipocytes (Scherer et al., 1994), and insulin stimulates tyrosine phosphorylation of caveolin in fat cells (Mastick and Saltiel, 1997). More recently, the localisation of insulin-regulated CAP proteins to caveolae has argued strongly for an important (but as yet undefined) role for caveolae in insulin signal transduction (Baumann et al., 2000); (Saltiel, 1996). The over-expression of caveolin observed in skeletal muscle of the SHRSP strain may therefore be an important contributory factor to the insulin resistance observed in these animals. Whether increased expression of caveolin could result in the sequestration of important insulin signalling components in an inactive environment or act as an inhibitor of down-stream effects remains to be determined. Strikingly, the lipid raft associated protein, flotillin is also markedly over-expressed in SHRSP muscles compared to WKY. Flotillin has been proposed to localise a protein complex of CAP-Cbl proteins to lipid rafts in adipocytes which may play a crucial role in propagation of the insulin signal, at least in adipocytes (Baumann et al., 2000). The fact that both caveolin and flotillin are over-expressed in muscle from the SHRSP suggests that over expression of caveolae-associated proteins may act to blunt the ability of insulin receptors to signal to proximal molecules in the insulin signalling cascade. Further studies will be required to test this hypothesis in a systematic fashion.

In summary, the data presented here shows that skeletal muscle of SHRSP exhibits reduced insulin-stimulated glucose transport compared to WKY isogenic controls. The response to activation of AMPK by AICAR treatment was, however, indistinguishable between the two strains, suggesting that the defect in insulin action lies on a specific arm of the machinery or signalling cascade activated by insulin. Furthermore, the SHRSP, like the insulin resistant ZDF rat, exhibits elevated VAMP2 and syntaxin 4 expression in skeletal muscle, suggesting that this defect may be common to a range of rodent models of insulin resistance. Finally, I report for the first time that caveolin and flotillin are over-expressed in the insulin resistant muscle tissue. This result may be of considerable importance, given the proposed central role of caveolae in the organisation of the insulin signalling system.

Chapter 4.

Establishment of skeletal muscle cell cultures from WKY and SHRSP rats and a comparison of the effects of insulin and AICAR on deGlc transport in these cultures.

4.1 Introduction

Skeletal muscle is the major site for insulin-stimulated glucose uptake facilitated by the glucose transporter 4 (Glut-4). DeFronzo et al and Katz et al highlighted the dominant role of skeletal muscle in whole body glucose disposal and its apparent pathophysiology in type 2 diabetes (DeFronzo et al., 1981); (Katz et al., 1983); (DeFronzo et al., 1985). Study of glucose uptake by intact muscle is prone to problems, such as uneven exposure of muscle cells to substrate and agonist. In addition, intact muscle will be composed of other tissues such as nerves, connective tissue, endothelial cells and fat, all of which add further ambiguity to results (Yaffe and Saxel, 1977). Use of cultured skeletal muscle cells offers the chance of isolating a relatively pure population of cells, which can be manipulated more easily, with greater scope for experimental analysis under better-defined conditions. This culture system though is not without its fair share of criticism and problems. Present methodologies for growth and differentiation of such cells do not fully recapitulate *in situ* conditions such as innervation (Smith and Lawrence, Jr., 1984); (Coderre et al., 1992), perfusion (Cleland et al., 1998) and coordinated contraction (Ploug and Ralston, 1998) all of which have been shown in animal studies to have dramatic effects on skeletal muscle glucose disposal. In defence, it seems clear that such systems, while not a perfect model of a working muscle, can begin to dissect out environmental effects from genetic ones, moreover by using both *in situ* and *in vitro* methodologies a greater understanding of this interplay can be achieved.

4.1.1 Skeletal muscle cell cultures

Rinaldini and Konigsberg were the first to culture skeletal muscle cells by isolating satellite cells from mature muscle (Konigsberg, 1979). Nowadays, skeletal muscle cell culture systems are widely used as experimental systems in many areas of research, from the study of the highly regulated process of myogenesis to the study of muscle disease states such as the muscular dystrophies and metabolic derangements that characterise insulin resistance (Cornelison and Wold, 1997); (Yeaman et al., 2001).

4.1.2 Regulators of myogenesis

Skeletal muscle develops from pluripotent mesodermal cells (reviewed in (Arnold and Winter, 1998); (Ordahl and Williams, 1998)). These cells give rise to embryonic myogenic cells, which in turn produce the myoblast pool that terminally differentiate and fuse to become myotubes (Arnold and Winter, 1998). These events are in part regulated by a group of transcription factors known as the muscle determining factors (MDFs). In mammals, there are four MDFs - (myoD, myf5, MRF4 and myogenin) (Weintraub, 1993). MyoD and myf5 expression in embryonic myogenic cells provoke differentiation of these cells into multiple myoblasts through mitotic expansion (Cornelison et al., 2000). In later stages of myoblast diversification and subsequent differentiation to form fused multinucleated myotubes, myogenin, MRF4 and other structural muscle proteins such as desmin and muscle-cadherin are expressed (Cornelison and Wold, 1997). A small minority of embryonic myogenic cells are mitotically quiescent and associate closely with the newly formed myotubes eventually residing between the basal lamina and sarcolemma of mature myofibres. These precursor cells are called satellite cells and do not express the four MDFs (Cornelison and Wold, 1997); (Ordahl et al., 2000). By taking advantage of the ability of satellite cells to proliferate along myogenic lines and differentiate into myotubes, the study of muscle cell biology has increased our understanding of the developmental and cellular processes of muscle.

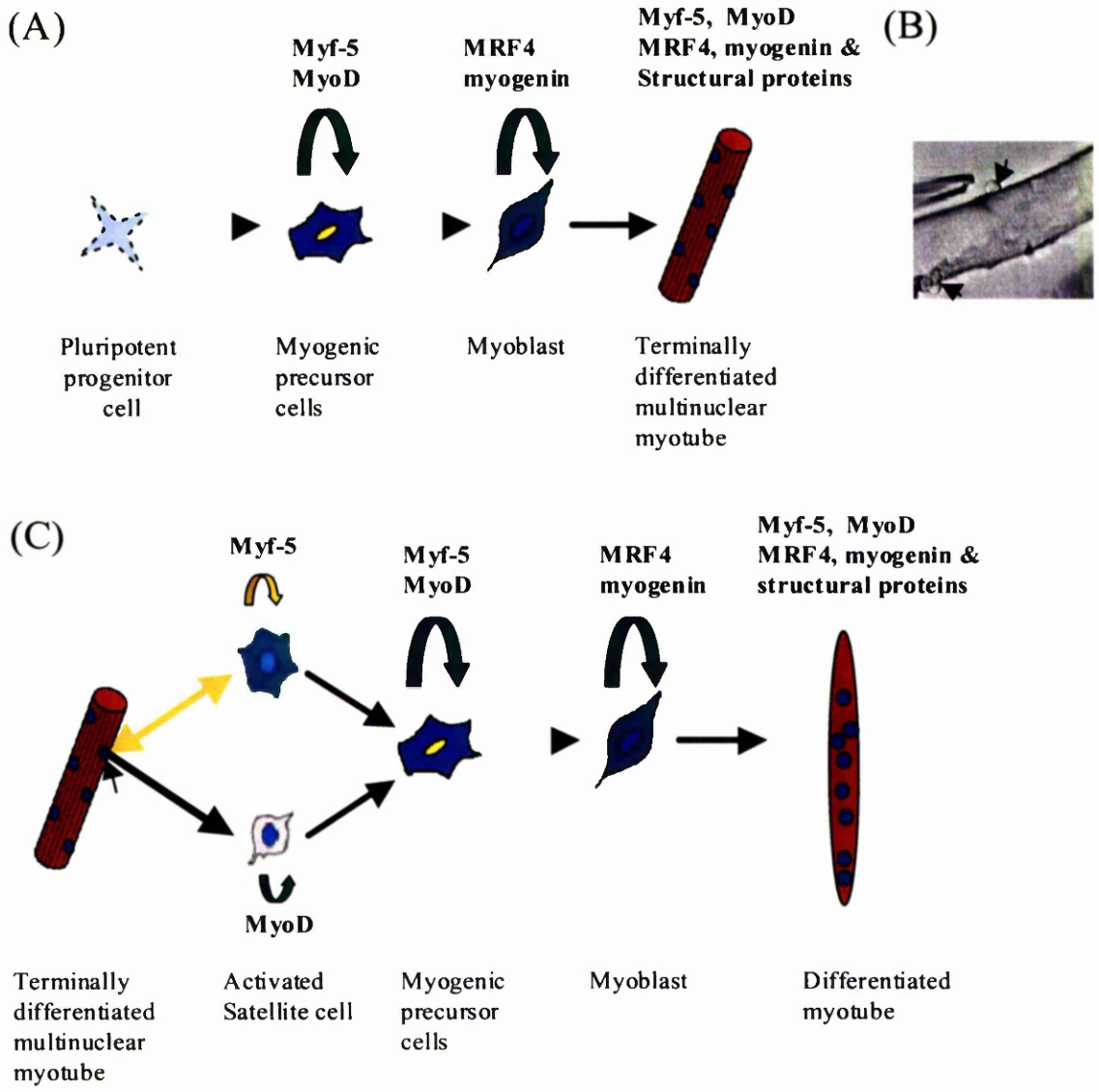

Figure 4.1 Molecular regulation of myogenesis.

(A) Targeted inactivation of the MDFs has defined two groups of factors. The primary MDFs, MyoD and Myf-5, are required at the determination step for commitment of the progenitor cell to the myogenic lineage. The committed cells (myoblasts) can proliferate and further differentiate into myotubes under the action of the secondary MDFs, myogenin and MRF4. *Adapated from Sabourin and Rudnicki, 2000.* (B) Phase image of myofibre with satellite cells arrowed. *Reproduced from Cornelison and Wold, 1997.* (C) Upon activation, quiescent satellite cells (indicated by arrow), first express Myf-5 and MyoD before co-expressing both and progressing through the developmental program to the differentiated multinucleated myotube. In the absence of MyoD or expression of Myf-5 alone, satellite cells appear to exhibit a propensity for self-renewal rather than progression through the differentiation program (yellow arrow). *Reproduced from Sabourin and Rudnicki, 2000.*

4.1.3 Role of skeletal muscle in carbohydrate metabolism

As mentioned earlier skeletal muscle by virtue of its considerable contribution to total body mass (approximately 35-45%) is responsible for a large part (approximately 80%) of the post-prandial glucose uptake (DeFronzo et al., 1981). In general, this glucose has two fates, it can be stored as glycogen through the process of glycogen synthesis or it can be used via the glycolytic pathway to produce energy. These are dynamic opposing processes and which one takes precedence is controlled to a large extent by the continually shifting cellular energy demand (Salway, 1994). Therefore, at times when the cellular energy demand is high as is the case during exercise, the glycolytic pathway will be dominant, as will pathways like glycogenolysis, which liberate glucose from intracellular glycogen stores. In contrast, at rest when energy demands are low glucose will be stored, thus storage pathways like glycogenesis are dominant (Salway, 1994). In addition, during times where glucose is not available and glycogen stores are depleted as in the extreme case of starvation alternative sources of energy must be found. An example of this is the *de novo* synthesis of glucose in the liver and kidneys from protein and other non-carbohydrate precursors by a process called gluconeogenesis. Usually the protein comes from muscle breakdown itself. This however is not advantageous since muscle protein is functionally important for survival. The preferred alternative energy source is fatty acids derived from fats, which produces energy via a process called β–oxidation. Fats, stored as triglycerides are a very good store of energy and by the action of lipases, fatty acids are liberated in a process called lipolysis (Salway, 1994). The opposite scenario to starvation would be that of excess food (carbohydrate) intake surplus to physical requirement. Under such conditions glycogen storage in muscle and liver are saturated and the process of lipogenesis favours a shift to storage as fats. Therefore, skeletal muscle in addition to its known structural and mechanical functions has an important role in the regulation of the organism's energy homeostasis.

4.1.4 Cultured skeletal muscle cells: a model for the study of insulin resistance.

A number of studies have shown that skeletal muscles from type 2 diabetic patients are insulin resistant and show a marked reduction in insulin-stimulated glucose transport (Dohm et al., 1988); (Andreasson et al., 1991); (Krook et al., 1998). In addition, skeletal muscle cells cultured from type 2 diabetic patients and non-diabetic relatives of type 2 diabetic families were found to be insulin resistant (Henry et al., 1995); (Jackson et al.,

2000). Such data strongly supports the view that inheritable factors predispose such individuals to peripheral insulin resistance and NIDDM at the cellular level in the absence of circulating factors. This maintenance, by cultured skeletal muscle cells, of the metabolic and biochemical properties of skeletal muscle further highlights the usefulness of this system in studying diseases such as insulin resistance.

4.1.5 Aims and objectives.

It is possible that the insulin resistance observed in the SHRSP may be secondary to changes in physiology, such as altered blood flow to the muscle beds by defective vasodilatation in response to insulin, or by changes in circulating factors which regulate peripheral insulin sensitivity. By way of addressing this, the objectives of this chapter were to:

(i) detail the methodology for the isolation and growth of muscle satellite cells from SHRSP and WKY animals.

(ii) provide evidence that these cells are of myogenic origin and possess the insulin sensitive facilitative glucose transporter Glut-4.

(iii) develop methodology for the measurement of deGlc transport stimulated by insulin and other agents.

(iv) examine the effect of various growth conditions and differentiation time periods on insulin-stimulated deGlc uptake.

(v) measure, under optimal conditions established above, the effect of insulin and AICAR on deGlc transport in the presence and absence of wortmannin in skeletal muscle cells derived from SHRSP and WKY rats.

In summary, this chapter details the methodological development and characterisation of skeletal muscle cell cultures from the insulin-sensitive WKY rat and the insulin-resistant SHRSP rat within the context of insulin- and non-insulin- mediated glucose transport.

4.2 Method development and Results

4.2.1 Isolation of myoblast cell cultures.

Primary skeletal muscle cultures were grown from satellite cells isolated from dissociated muscle tissue by methods adapted from (Yasin et al., 1977); (Konigsberg, 1979); (Blau and Webster, 1981); (Sarabia et al., 1990) and Yeaman S.J., University of Newcastle, UK, personal communication). Male 12-week-old rats were sacrificed by CO_2 overdose and the extensor digitorum longus (EDL) muscle was dissected and cleaned of connective tissue. All subsequent procedures were performed under sterile conditions. The muscles from one rat were washed twice in sterile PBS (room temperature) and minced finely with sterile scissors in a petri dish to aid enzymatic dissociation of satellite cells. The minced muscle was transferred to a foil-sealed 25ml sterile conical flask containing a sterile magnetic stirring bar. The muscle was enzymatically dissociated at 37°C by three 10-minute rounds of mixing with 10ml of 300Units/ml Collagenase (Type 1A) made up in 0.25% w/v trypsin on a magnetic stirrer set to 300 revolutions per minute. After each round the mixture was triturated 10 times using a sterile 12ml pipette and particulate matter was allowed to settle for 5 minutes. The supernatant containing the liberated cells from each round was carefully removed to a 50ml corning tube, taking care not to disturb the pellet of undigested tissue, neutralised with 2ml of 100% FBS and centrifuged at 1000 x g for 5 min. The resulting pellet containing the liberated cells was resuspended in 4 ml of growth medium (Hams-F10, 20% FBS, 1% Chick Embryo extract, 100U/ml penicillin/streptomycin, 1% L-glutamine) warmed to 37°C and pre-equilibrated in a tissue culture incubator set to a 5% CO_2 humidified atmosphere. The resuspended cells were pre-plated on a non-coated 75cm^2 tissue culture flask at 37°C in a 5% CO_2 humidified atmosphere for two hours. This step removes any contaminating fibroblast cells owing to the ability of fibroblast cells to bind more tenaciously to non-coated plasticware than muscle cells. Following this purification step the media containing unbound cells was transferred to 25cm^2 collagen-coated flasks as collagen coated substrata greatly benefit the growth of skeletal muscle cells (Hauschka and Konigsberg, 1966).

4.2.2 Maintenance of rat skeletal muscle cell cultures.

Cells were fed every third day with growth medium (4.2.1) and passaged once 50% confluent. Cells were seeded onto collagen-coated plasticware at $1.2x10^5$ cells per 6 well plate or $4x10^5$ cells per $75cm^2$ flask. Cells were differentiated when 70-80% confluent by replacing growth medium with differentiation medium (α-MEM, 2% FBS, 1% L-glutamine, 100 U/ml penicillin/streptomycin). Cells were used between six and eight days post differentiation.

4.2.3 Preparation of cultures prior to use.

Between six and eight days post differentiation when cultures had reached confluence and fused, differentiation medium was replaced with serum free α-MEM supplemented with 100U/ml penicillin/streptomycin and 1% L-glutamine for 24 hours prior to use.

4.2.4 Whole cell indirect immunofluorescence of cultured cells.

In order to ascertain whether these cultured cells were indeed myogenic, whole-cell indirect immunofluorescence was performed as outlined in section 2.3.14. MyoD and myogenin are exclusively expressed in myogenic cells and as such are considered muscle cell specific markers (Cornelison et al., 2000). These two transcription factors are localised in the nuclei where they are involved in the regulation of muscle cell development. The representative fluorescence microscope images illustrated in figure 4.2 clearly show positive fluorescence within the nuclei of these cells, indicating the presence of both MyoD and Myogenin in these putative muscle cells. It is noteworthy that these cells referred to as myotubes are highly elongated and multinucleated, a common feature of fused muscle cells. Positive staining of skeletal muscle α-actin and desmin, gold-standard skeletal muscle-specific structural proteins, are also seen in these cultured cells confirming that these are cultured skeletal muscle cells (data not shown).

Figure 4.2 Immunofluorescence detection of myogenic markers in skeletal muscle cell cultures from WKY and SHRSP rats.

Shown are representative fields of differentiated myotubes from SHRSP and WKY strains, stained with antibodies against Myogenin or Myo D. Note the presence of multinucleated cells, characteristic of myotubes.

Figure 4.2 Immunofluorescence detection of myogenic markers in skeletal muscle cell cultures from WKY and SHRSP rats.

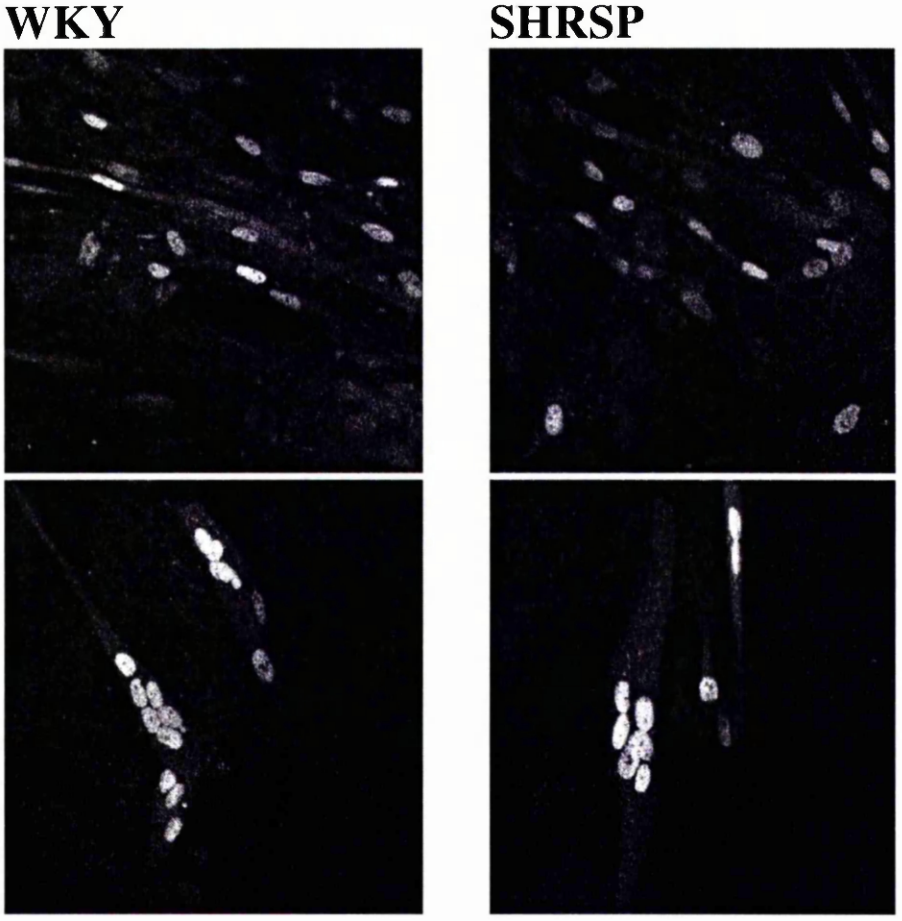

4.2.5 Insulin-stimulated uptake and metabolism of 2-deoxy-D-glucose by cultured skeletal muscle cells.

In order to utilise these cultured muscle cells in a comparative analysis of glucose transport in WKY and SHRSP animals, it was important to establish an optimised methodology for the measurement of glucose uptake. A number of groups have examined glucose transport in cultured skeletal muscle and adipocyte cells (Klip et al., 1984); (Sarabia et al., 1990); (Gould et al., 1994); (Blair et al., 1999). Using adaptations of these methods, coupled transport and phosphorylation of glucose was measured using the D-glucose analogue 2-deoxy-D-glucose (deGlc). DeGlc is transported into the cell by glucose transporters and is phosphorylated by hexokinase but cannot be further metabolised. In addition, phosphorylation of deGlc prevents exit from the cell and maintains a low concentration of deGlc that maintains unidirectional uptake uncomplicated by efflux, allowing simple kinetic measurements. Radiolabelled deGlc allows the quantitative measurement of cell accumulation via liquid scintillation spectrophotometry. In principle under conditions where transport of deGlc is not rate limiting, carrier-mediated transport is related to the amount of cell-associated radioactivity in the absence of any non-specific binding of radiolabelled deGlc to the cell surface.

In order to determine conditions where deGlc transport was not rate limiting, serum starved cultured myotubes (4.2.2-4.2.3) were washed two times in 3 ml of Krebs Ringer Hepes buffer pH7.4 and incubated for 30 min at 37°C in the presence or absence of 1μM insulin. Uptake was initiated by addition of 10μM deGlc (1μCi/ml) for 3-15 min. Specific carrier mediated deGlc uptake was determined by calculating the cell associated radioactivity in the presence of 10μM cytochalasin B. Cytochalasin B blocks carrier mediated transport and hence indicates non-carrier mediated but cell associated radioactivity. DeGlc uptake was stopped by rapidly washing the tissue culture plates with three changes of ice cold PBS. Cells were lysed in 1ml of 1% Tx-100. The lysate was transferred to scintillation tubes and cell associated radioactivity was determined by liquid scintillation spectrophotometry.

As shown in figure 4.3, deGlc uptake by WKY skeletal muscle cultures is linear up to 15 minutes in both the presence and absence of 1μM insulin, with a significant increase in

deGlc uptake over basal seen at 5, 10 and 15 minutes. This data clearly shows that from 3 to 15 minutes insulin-mediated deGlc transport is not rate limiting with respect to this concentration of 10μM of deGlc. Interestingly, in the absence of insulin, deGlc is transported into the cell but this non-insulin- yet time-dependent increase is not rate limiting up to 15 minutes. This basal uptake may be the result of Glut-1 activity that is present at the cell surface in muscle cells (Klip and Paquet, 1990); (Gaster et al., 2000). In summary, it is noteworthy that a 30-minute stimulation of insulin significantly increased deGlc uptake over basal transport after 5, 10 and 15 minutes incubation with deGlc. This increase over basal transport gave a better signal to noise ratio at the later time points of 10 and 15 minutes. All subsequent experiments utilised a 10-minute incubation time with deGlc. In comparison, deGlc uptake by the skeletal muscle L6 cell line is linear up to 30 minutes in both the presence and absence of 1μM insulin, with a significant increase in deGlc uptake over basal seen at the time points indicated (figure 4.4). However, the amount of glucose transported by L6 cells is approximately half that of WKY skeletal muscle cells at all corresponding time points studied (figure 4.4).

In order to determine optimal agonist treatment timings for maximal effects on a 10-minute deGlc uptake, increasing incubation times of 1μM insulin, 500μM AICAR and 500μM arsenite were examined. Arsenite is a metabolic poison and has been shown to increase glucose transport in muscle cells independently of PI3K activity (McDowell et al., 1997). Insulin caused a time-dependent increase in deGlc uptake, with significant maximal effects on deGlc uptake being observed by 20-30 minutes (figure 4.5). The magnitude and time courses are similar to those observed by others in response to insulin (Jackson et al., 2000); (Ciaraldi et al., 1995). Arsenite and AICAR also showed a time-dependent increase in deGlc uptake (figure 4.6), with significant effects on deGlc uptake being observed by 5 and 20 minutes, respectively. Both compounds showed maximal stimulation of deGlc transport by 30 minutes (figure 4.6). Therefore a 30-minute incubation with agonists, prior to a 10-minute deGlc uptake, was used in all subsequent experiments. Insulin also gave a time-dependent increase in deGlc uptake, with maximal effects on deGlc transport observed by 30 minutes in L6 cells (figure 4.7).

Figure 4.3 Time course analysis of deGlc uptake by WKY skeletal muscle cultures.

The effects of increasing incubation times (3-15 mins) of 10μM deGlc on uptake (pmol/min/well) by serum starved differentiated WKY skeletal muscle cells incubated for 30 mins in the presence (●) or absence (○) of 1μM insulin are shown. Data are the means ± S.E.M. from four separate experiments. Within each experiment, determinations were performed in triplicate. Methods used for treatment and uptake measurements are described in 4.2.5. * indicates a significant increase in response to insulin in WKY cultures at 5 mins, p=0.02. ** indicates a significant increase in response to insulin in WKY cultures at 10 mins, p=0.01. *** indicates a significant increase in response to insulin in WKY cultures at 15 mins, p=0.001.

Figure 4.3 Time course analysis of deGlc uptake by WKY skeletal muscle cultures.

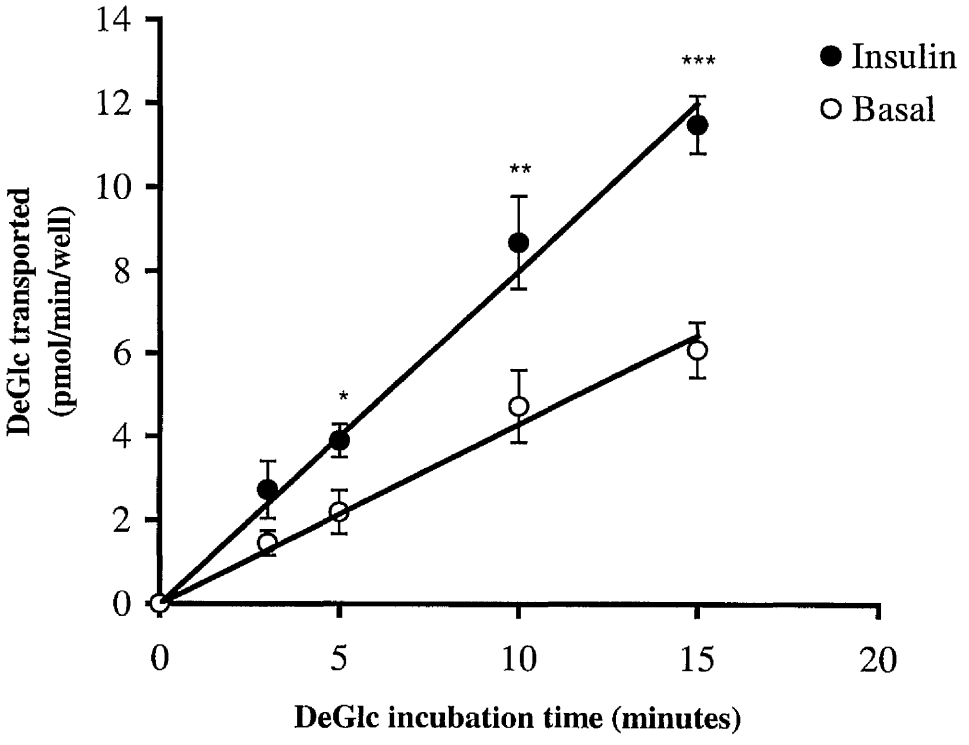

Figure 4.4 Time course analysis of deGlc uptake by L6 muscle cells.

Shown are the effects of increasing incubation times (3-60 mins) of 10μM deGlc on uptake (pmol/min/well) by serum starved differentiated L6 skeletal muscle cells incubated for 30 mins in the presence (■) or absence (□) of 1μM insulin. Data are the means ± S.E.M. from three independent experiments. Within each experiment, determinations were performed in triplicate. Methods used for treatment and uptake measurements are described in 4.2.5. *, **, ***, **** indicates a significant increase in response to insulin over corresponding basal at 5, 10, 20, 30 mins, p=0.005, p=0.01, p=0.0006, p=0.0001, respectively.

Figure 4.4 Time course analysis of deGlc uptake by L6 cells.

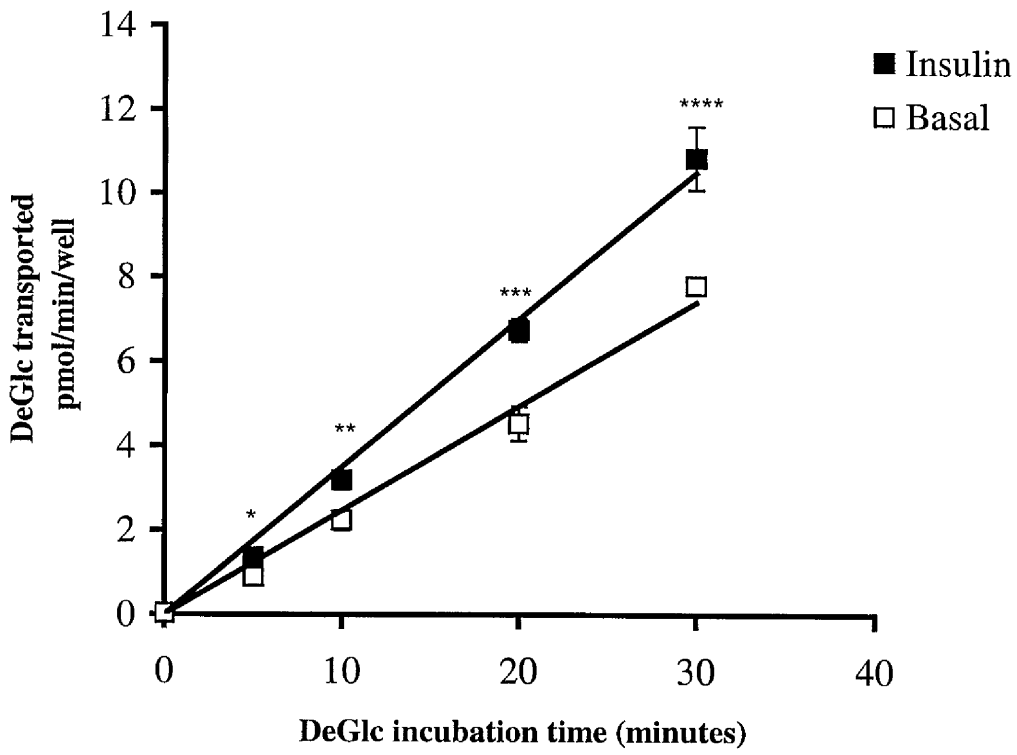

Figure 4.5 Time course analysis of insulin-mediated deGlc uptake by WKY skeletal muscle cultures.

Shown are the effects of increasing insulin (1μM) incubation times (as indicated) on a 10 min deGlc uptake (pmol/min/well) by serum starved differentiated WKY skeletal muscle cells. Data are the means ± S.E.M. from four independent experiments. Within each experiment, determinations were performed in triplicate. Methods used for treatment and uptake measurements are described in 4.2.5. * indicates a significant increase in response to a 20 min insulin stimulation in WKY cultures, p=0.01. ** indicates a significant increase in response to a 30 min insulin stimulation in WKY cultures, p=0.003.

Figure 4.5 Time course analysis of insulin-mediated deGlc uptake by WKY skeletal muscle cultures.

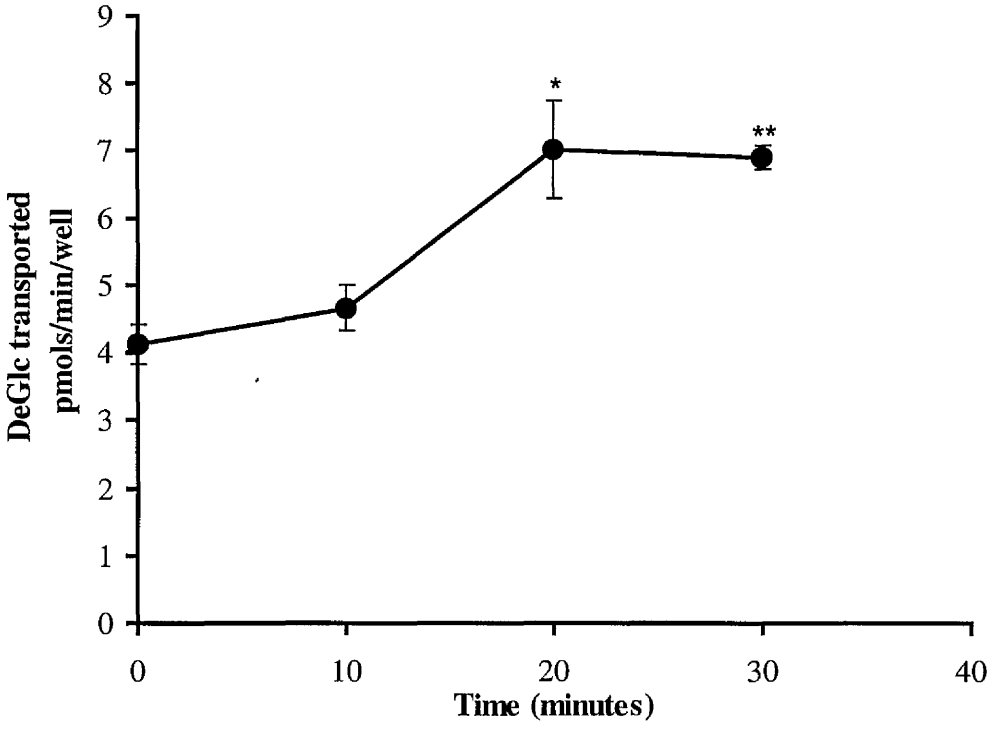

Figure 4.6 Time course analysis of AICAR- and arsenite-mediated deGlc uptake by WKY skeletal muscle cultures.

Shown are the effects of increasing AICAR (500μM) and arsenite (500μM) incubation times on a 10 min deGlc uptake (pmol/min/well) in serum starved differentiated WKY skeletal muscle cells. Data are the means ± S.E.M. from four independent experiments. Within each experiment, determinations were performed in triplicate. Methods used for treatment and uptake measurements are described in 4.2.5. ** indicate a significant increase in response to arsenite over corresponding basal at 5, 10, 20, 30, 60 min, $p<0.005$. †, †† indicate a significant increase in response to a AICAR over corresponding basal at 20, 30 and 60 min, $p=0.05$ and $p=0.01$, respectively.

Figure 4.6 Time course analysis of AICAR- and arsenite-mediated deGlc uptake by WKY skeletal muscle cultures.

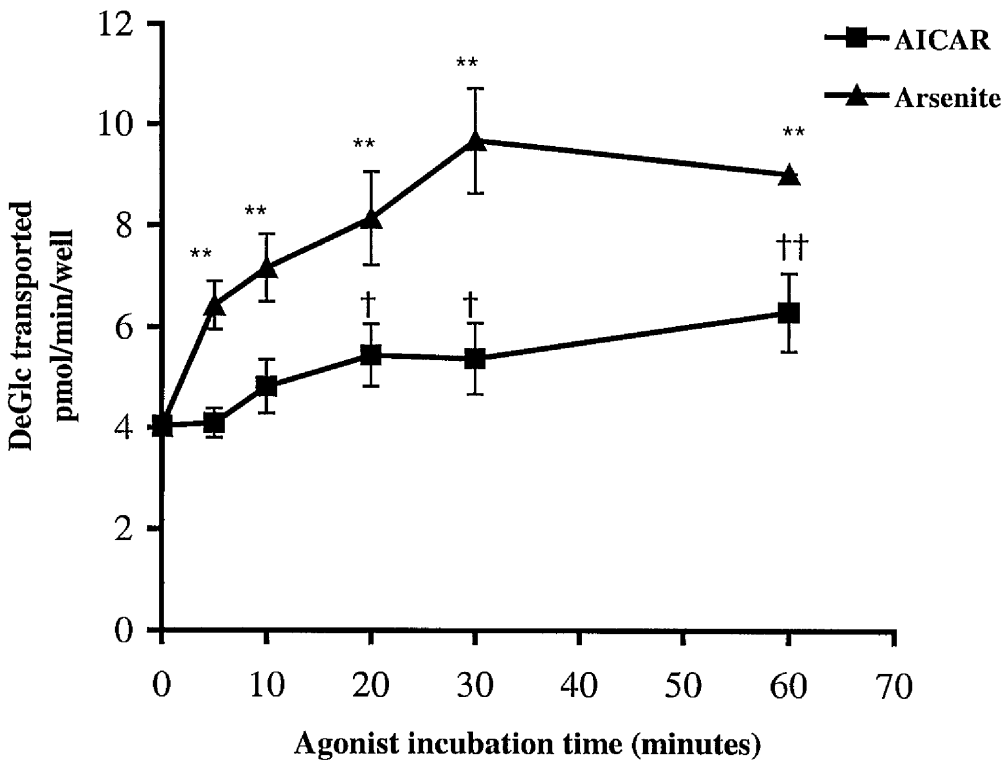

Figure 4.7 Time course analysis of insulin-mediated deGlc uptake by L6 muscle cultures.

Shown are the effects of increasing insulin (1μM) incubation times (as indicated) on deGlc uptake (pmol/min/well) by serum starved differentiated L6 skeletal muscle cells. Data are the means ± S.E.M. from three independent experiments. Within each experiment, determinations were performed in triplicate. Methods used for treatment and uptake measurements are described in 4.2.5. * indicates a significant increase in response to insulin in L6 cultures at 30 min compared to 0 min.

Figure 4.7 Time course analysis of insulin-mediated deGlc uptake by L6 muscle cultures.

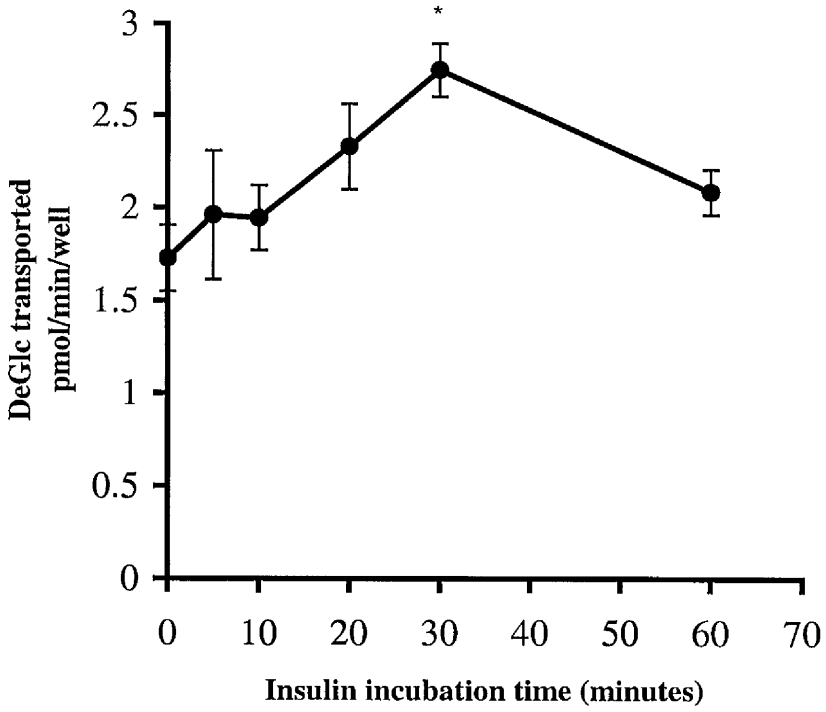

4.2.6 Assessment of growth media on insulin-stimulated deGlc uptake.

A number of variations on the growth and differentiation conditions have been reported to contribute to overall cellular health and responsiveness of skeletal muscle cells. Of particular interest here are the semi-defined serum-free media of Allen and colleagues and that of Ham and colleagues, which support the growth and proliferation or cultured rat and human skeletal muscle cells, respectively (Allen et al., 1985); (Ham et al., 1988). Both of these media do not require chick-embryo-extract (CEE). Allen et al and Ham et al found that their media gave better growth results in comparison to the widely used CEE containing growth medium described in 4.2.1. Both these media have in common the requirement of a cocktail of various growth factors and supplements, which within their respective systems are shown to be beneficial in the growth of those muscle cells. I have taken supplements common to both recipes to replace the requirement for CEE in the present growth medium. This medium will be termed CEE-free growth medium and contains Ham's-F10 nutrient medium, 20% FBS, 1% penicillin/streptomycin, 1% L-glutamine, 500 mg/l BSA fraction (V), 500mg/l Pederson fetuin, 1 μM dexamethasone, 1 nM insulin.

Growth of skeletal muscle cells requires a two-step media change (Konigsberg, 1979). The first is optimised for the proliferation of cells whilst minimising differentiation and is therefore termed growth medium. The second is optimised for fusion of the cultured unicellular myoblast to the multinucleated syncytial myotube and is termed differentiation medium (Konigsberg, 1979). Some groups routinely use DMEM nutrient based differentiation medium, whereas others use α-MEM nutrient medium.

In order to examine the effect variations in cell growth and differentiation conditions have on deGlc transport, cells were grown in CEE containing or CEE-free growth media, and fed as described in 4.2.2. Cells were differentiated once 70-80% confluent as described in 4.2.2. Cells grown in CEE-free growth medium were differentiated as described in 4.2.2 using α-MEM based nutrient medium. Cells grown in the CEE containing growth medium were differentiated using either α-MEM based nutrient medium described in 4.2.2 or DMEM based nutrient medium. Media changes and all other supplements such as antibiotics and serum were maintained as described in 4.2.2. Figure 4.8 shows that of all the variations tested, cells grown in CEE-free growth medium (C) gave the best

response to 1μM insulin (2.5 ± 0.21 fold increase over basal), a significant $p<0.05$ increase over the previously used CEE containing growth media (A), which also gave a significant 1.57 ± 0.06, $p=0.0007$, fold increase over basal in response to insulin. However, substitution of α-MEM- for DMEM-based nutrient differentiation media (B) abolishes insulin-stimulated glucose transport in cultured myotubes, showing no significant increase in deGlc transport compared to basal transport. In this system, the present experiment suggests that cells grown in CEE-free growth media perform better with respect to insulin-stimulated glucose transport in contrast to cells grown in CEE containing growth media or differentiated using DMEM based nutrient media. Cells grown in CEE-free growth media retained, morphologically, all the characteristics of muscle cells previously seen (see figure 4.2). All subsequent experiments were performed using CEE-free growth media and α-MEM differentiation media.

Figure 4.8 The effects of various growth and differentiation media on insulin-stimulated deGlc uptake by WKY skeletal muscle cultures.

The effects of various media manoeuvres on insulin-stimulated deGlc uptake in cultured WKY skeletal muscle cells using methods described in 4.2.5 for treatment and measurement of uptake are shown. Data presented are the means ± S.E.M. from three independent determinations. **(A)** represents cells grown in CEE supplemented growth media defined in 4.2.1 and differentiated in α-MEM defined in 4.2.2. * indicates a significant increase over basal transport in response to insulin, p=0.0007. **(B)** represents cells grown in CEE supplemented growth media defined in 4.2.1 and differentiated in DMEM defined in 4.2.2. † indicates no significant difference over basal transport in response to insulin. **(C)** represents cells grown in CEE-free growth media described in 4.2.6 and differentiated in α-MEM defined in 4.2.2. ** indicates a significant difference in magnitude of the insulin response between C and A, p=0.04, and also that the insulin response is significantly increased over basal, p=0.002.

Figure 4.8 The effects of various growth and differentiation media on insulin-stimulated deGlc uptake by WKY skeletal muscle cultures.

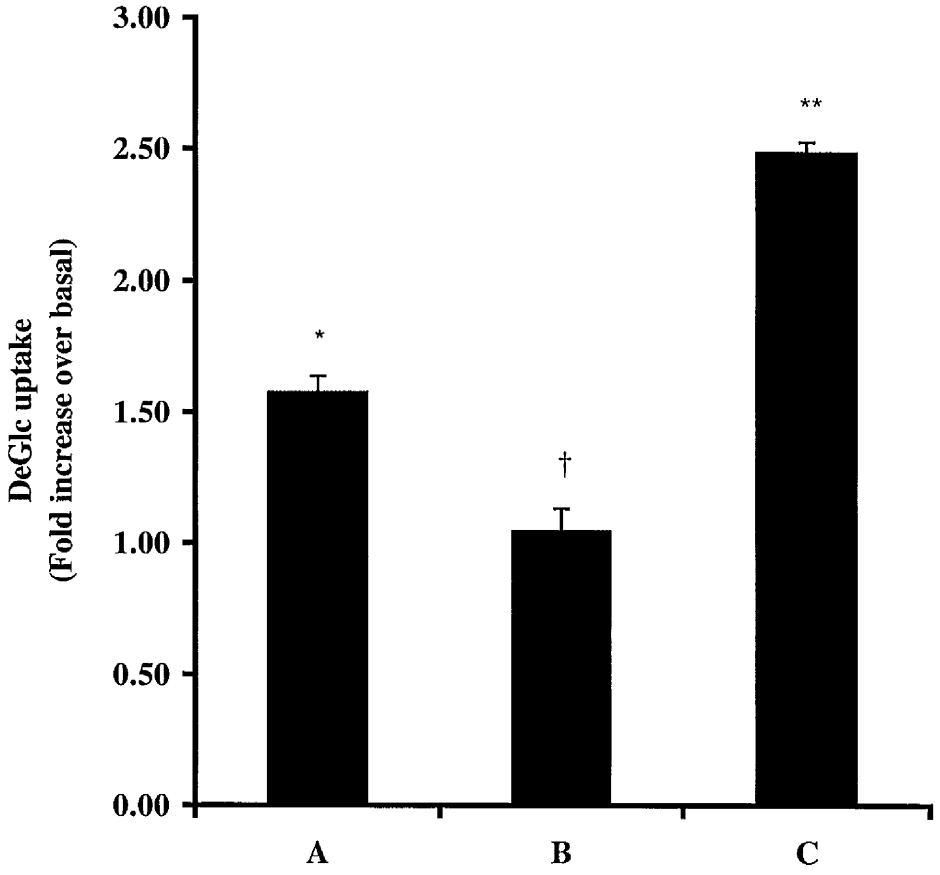

4.2.7 Influence of differentiation time-period on insulin-stimulated deGlc uptake.

Achieving adequate insulin responsiveness is critical to the use of cultured muscle cells to study defects in deGlc transport. This will be influenced by the time post-differentiation when the cells are assayed. For example in the C2 skeletal muscle cell line, Ploug and colleagues observed maturation of Glut-4 enriched compartments residing intracellularly as cells are differentiated from day 0 to day 6 (Ploug et al., 1998). Glut-4 reached maximal levels of staining by day 6. Such studies prompted an examination of the impact of time post differentiation on insulin-stimulated deGlc uptake in these cells. Myoblasts grown in CEE-free growth media (4.2.6) were differentiated for 0-16 days. Insulin-stimulated deGlc uptake was performed on cells fused for the number of days indicated in figure 4.9. The insulin-stimulated fold increase over basal deGlc transport reached significance in all 4 and 6 day differentiated cells, $p<0.05$. In addition, a significant increase in the magnitude of the insulin response was seen in 4 and 6 day differentiated cells compared to undifferentiated and 16 day differentiated cells, $p<0.05$. It should be noted that the unstimulated (basal) rate of deGlc transport was not significantly different between all time points (3.7 ± 0.32 pmol/min/well). Moreover, in 4 and 6 day differentiated cells, significant reductions in the insulin to basal ratio were observed in cultures derived from SHRSP animals with respect to WKY cultures (see 4.2.8 and figure 4.9). All subsequent deGlc uptake measurements were performed on cells that had been differentiated for 6 days in conjunction with all the prior modifications.

Figure 4.9 Influence of differentiation time period on insulin-stimulated glucose uptake.

Cells were grown in CEE-free growth media described in 4.2.6 and differentiated using media described in 4.2.2. Cells not differentiated and on the days indicated after addition of differentiation media were acutely insulin-stimulated (1μM insulin for 30min) and a 10 min deGlc transport assay was performed as outlined in 4.2.5. Results shown are the means ± S.E.M. of 3 separate experiments. * indicates a significant fold-increase over basal p=0.001. ** indicates a significant fold-increase over basal p=0.005, and also indicates a significant fold-increase over corresponding SHRSP fold stimulation. † indicates a significant fold-increase over basal p=0.02. †† indicates a significant fold-increase over basal p=0.02.

Figure 4.9 Influence of differentiation time period on insulin-stimulated glucose uptake.

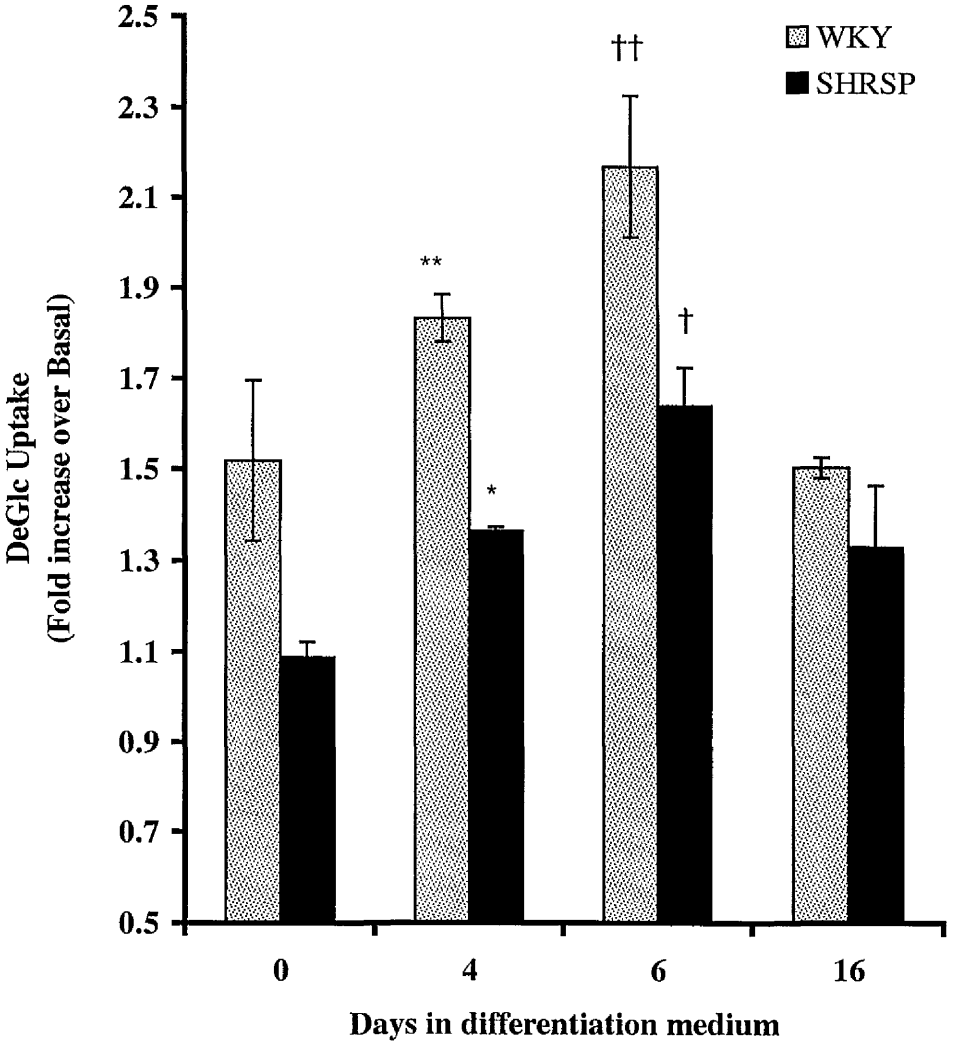

4.2.8 Dose-dependent effect of insulin on deGlc uptake in skeletal muscle cells from WKY and SHRSP animals.

Using methods outlined in 2.3.15 under optimised conditions of growth and differentiation (4.2.6, 4.2.7) skeletal muscle cells were treated with insulin doses ranging from 1nM to 1μM. A dose-dependent increase in deGlc uptake was observed in all skeletal muscle cells as illustrated in figure 4.10. I observed both a decreased maximal rate of insulin-stimulated deGlc uptake and a rightward shift of the dose-response curve in myotubes from SHRSP compared to WKY rats (figure 4.10). Such data suggest that while all skeletal muscle cells respond to insulin in a time and dose-dependent manner, SHRSP skeletal muscle cells are insulin resistant and exhibit a diminished ability of insulin to stimulate deGlc uptake compared with WKY muscle cells. The time- and dose-dependent increase in glucose transport observed in WKY and SHRSP skeletal muscle cells is indicative of a Glut-4 mediated event. The insulin-regulated glucose transporter, Glut-4, is responsible for the bulk of both insulin- and contraction-mediated glucose transport by skeletal muscle (Ploug et al., 1998); (Gaster et al., 2000). Both WKY and SHRSP cultured skeletal muscle cells lysates express the insulin-regulated glucose transporter, Glut-4. In agreement with results seen in whole muscle from these animals (chapter 3) there were no significant differences in total Glut-4 levels between WKY and SHRSP skeletal muscle cells as seen in the representative immunoblot of figure 4.11.

Figure 4.10 The effect of increasing insulin concentrations on deGlc uptake by WKY and SHRSP skeletal muscle cultures.

A typical dose response curve for insulin in cultured myoblasts from SHRSP or WKY strains. Serum starved myoblast were washed two times in KRH buffer then incubated in KRH for 30 min in the presence or absence of the indicated concentration of insulin. Each point is the mean of triplicate determinations and is corrected for the non-specific association of deGlc uptake with the cells. Data from a representative experiment is shown, expressed as a fold increase relative to Basal WKY-derived cultures. A significant difference between SHRSP and WKY points is illustrated by * p=0.05 and ** p=0.01. The experiment was repeated three times with similar results. The basal rates of transport were not significantly different between WKY- and SHRSP- derived cultures.

Figure 4.11 Immunoblot analysis of Glut4 levels in skeletal muscle cultures from SHRSP and WKY animals.

Shown is a representative immunoblot in which 20 μg/lane of muscle lysate, made from SHRSP and WKY EDL muscles, were analysed by SDS-PAGE/immunoblotting with an antibody specific for Glut-4. Quantification of Glut4 protein levels in these muscles from six different animals revealed no significant differences between the two strains (data not shown).

Figure 4.10 The effect of increasing insulin concentrations on deGlc uptake by WKY and SHRSP skeletal muscle cultures.

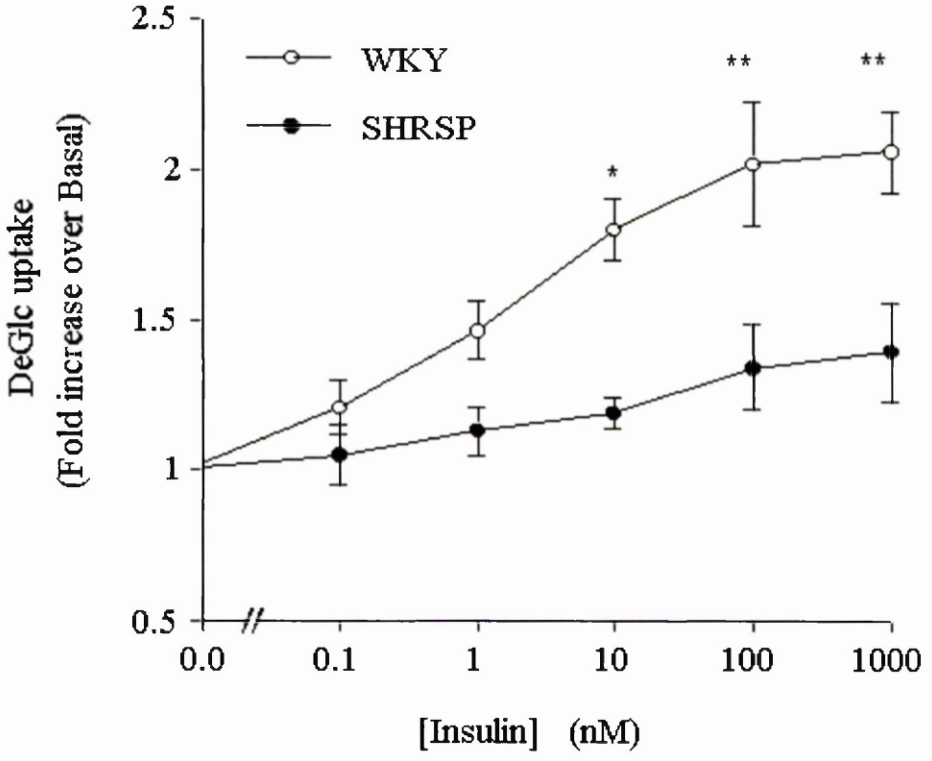

Figure 4.11 Immunoblot analysis of Glut-4 levels in skeletal muscle cultures from SHRSP and WKY animals.

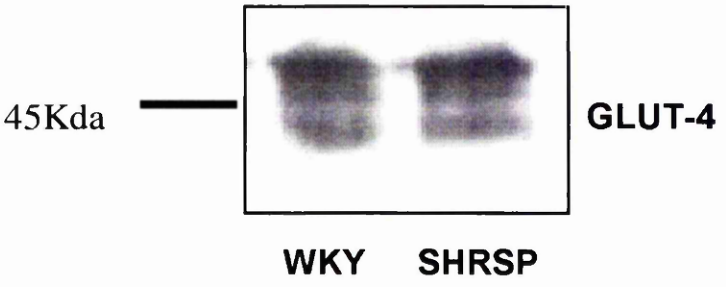

4.2.9 Ability of insulin and AICAR to stimulate deGlc uptake in WKY and SHRSP skeletal muscle cells.

Stimulation of skeletal muscle cells with 1μM insulin or 500μM AICAR demonstrates that muscle cell cultures from SHRSP skeletal muscle exhibit blunted insulin-stimulated deGlc uptake compared to WKY, but the response to AICAR was similar between the two cultures (figure 4.12). This is consistent with data on intact muscle (see chapter 3). Moreover, it is noteworthy that similar experimental results were obtained from cultures between passage 5-8 (data not shown), indicating a stably maintained trait. In addition, and consistent with data from intact muscle, treatment with 100nM wortmannin two minutes prior to agonist completely blocked insulin-stimulated deGlc uptake but was without effect on AICAR-stimulated deGlc uptake (figure 4.12).

Figure 4.12 DeGlc uptake in skeletal muscle cultures - the effects of insulin, AICAR and wortmannin.

Shown are the effects of a 30 min incubation with either 1 μM insulin or 500 μM AICAR on deGlc uptake. The effect of pre-treatment of the cells with 100 nM wortmannin on these stimulations is also shown. The data are presented as mean ± S.E.M. from 3 separate experiments, expressed as a fold increase over the basal WKY rate. * indicates a significant increase in transport in response to insulin, p=0.01. ** indicates a reduction in insulin-stimulated glucose transport compared to WKY strain, p=0.04. † indicates a significant increase in response to AICAR in WKY cultures, p=0.05. †† indicates no significant difference in the magnitude of the AICAR response between the WKY and SHRSP strains, and also that the AICAR response in SHRSP cultures is significantly increased over basal, p=0.05. Wortmannin inhibited insulin-stimulated deGlc uptake significantly in both WKY and SHRSP cultures (p=0.01 in both) and had no significant effect on AICAR stimulated deGlc transport.

Figure 4.12 DeGlc uptake in skeletal muscle cultures - the effects of insulin, AICAR and wortmannin.

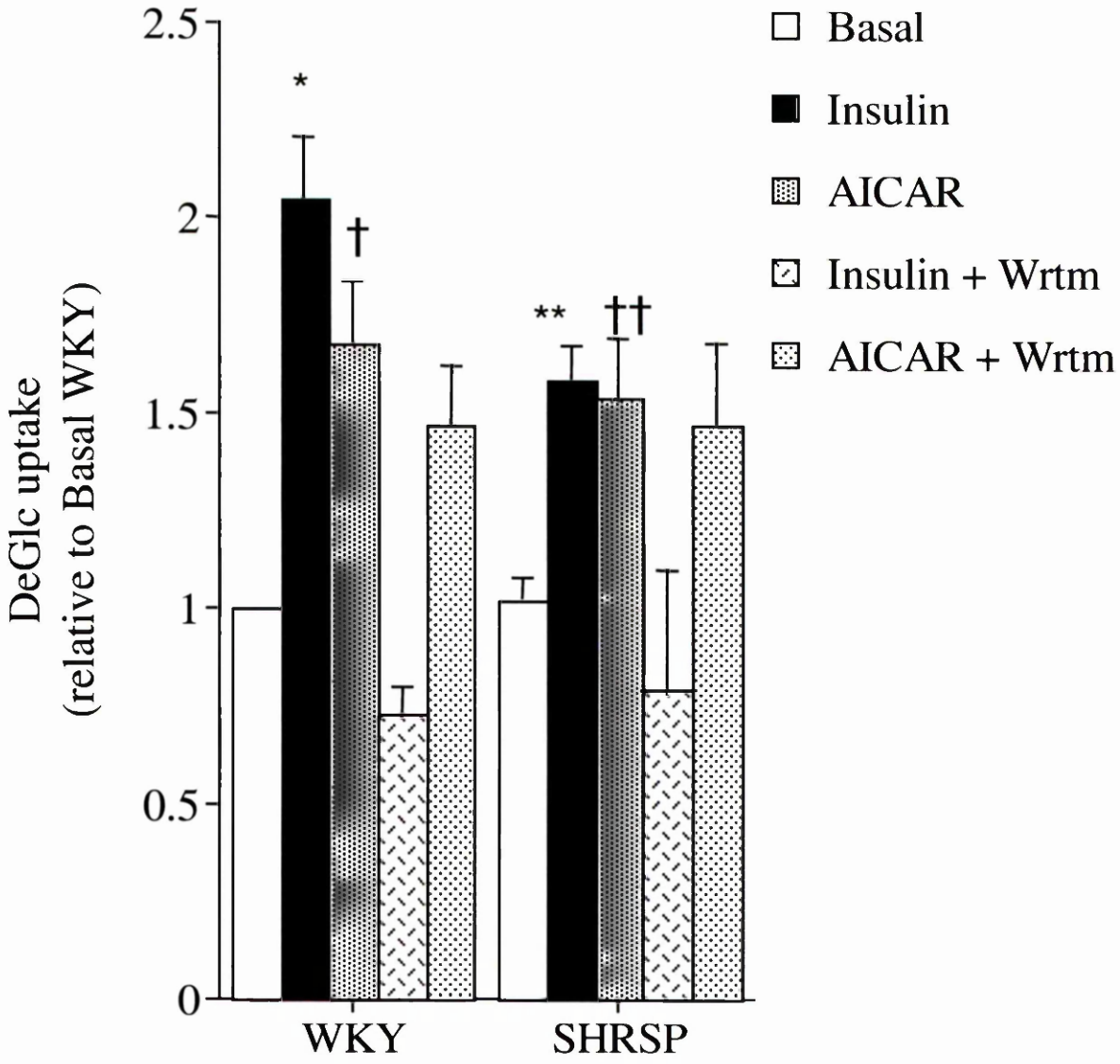

4.3 Discussion

This chapter expands upon the findings in chapter three by assessing insulin- and AICAR-stimulated glucose transport in cultured skeletal muscle cells isolated from WKY and SHRSP extensor digitorum longus muscle. Using established cell culture techniques, skeletal muscle satellite cells were isolated and cultured. Once differentiated these cells possessed the muscle determining factors myoD and myogenin and were morphologically distinct from myoblasts in that they were multinucleated and highly elongated indicative of myotubes (figure 4.2). In addition, these myotubes expressed the insulin regulated glucose transporter, Glut-4 (figure 4.11).

In order to assess glucose transport, the development of adequate methods is necessary so as to achieve reproducible and significant results within skeletal muscle cells. As previously shown in chapter three and reported by (Sarabia et al., 1990); (Jackson et al., 2000) skeletal muscle cells give a modest but characteristic two- to four-fold increase of insulin-stimulated glucose uptake. As documented here, both growth media composition and differentiation timings were important factors that significantly affected insulin-stimulated glucose uptake in the present system (figure 4.8). After methodical alteration of growth and differentiation media in the present system, I have found that the replacement of chick-embryo-extract (CEE) with the supplements common to the semi-defined human and rat skeletal muscle cell growth media of Ham et al and Allen et al respectively, in conjunction with the α-MEM based differentiation media, gave better insulin-stimulated glucose uptake responses compared to cells grown in CEE-containing growth medium or differentiated in DMEM medium (figure 4.8) (Allen et al., 1985); (Ham et al., 1988). Furthermore, both WKY and SHRSP muscle cells when differentiated for four to six days gave significantly better insulin-stimulated glucose fold uptake responses compared to undifferentiated or 16-day differentiated cells (figure 4.9). A likely explanation for this lack of an insulin response at early time points maybe due to the lack of Glut-4 protein (Guillet-Deniau et al., 1994); (Gaster et al., 2000). Indeed Ralston et al has shown that Glut-4 is virtually undetectable in C2 myoblasts but is highly expressed and intracellularly located in three-day-old C2 myotubes (Ralston and Ploug, 1996). The decreased insulin-stimulated glucose transport seen in 16 days-old myotubes

may be due to an age-related effect. In addition, agonist and deGlc incubation times were optimised for this culture system.

The development of this skeletal muscle cell culture system permits the comparison of insulin- and AICAR-stimulated glucose transport between SHRSP and WKY cells without the confusion of physiological factors such as altered blood flow or circulating paracrine factors. As discussed earlier in 1.5.1 and chapter three, AICAR is able to activate AMPK, an important mediator of the effects of exercise on glucose transport (Corton et al., 1994); (Goodyear, 2000). Consequently, the use of AICAR provides the opportunity to study the effects of exercise on glucose uptake *in vitro*. By way of optimising deGlc assay conditions, I have determined that these cells display a linear uptake of deGlc over 15 minutes in the presence and absence of insulin. In addition, these cells gave a time-dependent increase in deGlc uptake in the presence of insulin, AICAR and arsenite, with maximal deGlc transport seen at 30 minutes under stimulated conditions. Therefore, under the chosen 30-minute agonist stimulation and 10-minute deGlc uptake conditions, glucose transport is the rate-limiting step.

The novel and remarkable finding in this study is that the defect observed in insulin-stimulated glucose transport in intact muscles from the SHRSP (chapter 3) was also observed in cultured myotubes (figure 4.10 and 4.12). Specifically both WKY and SHRSP skeletal muscle cells exhibit a time- and dose-dependent response to insulin. However, SHRSP skeletal muscle cells show a decreased maximal rate of insulin-stimulated deGlc uptake and a rightward shift of the dose-response curve. This diminution of insulin sensitivity is evident throughout all passages of cells. Moreover, AICAR-stimulated deGlc transport was not significantly different between WKY and SHRSP skeletal muscle cells, in agreement with data seen in intact FDB muscle (chapter 3). Consistent with data on intact muscle, pre-treatment with 100 nM of the PI3K inhibitor wortmannin, completely blocked insulin-stimulated deGlc uptake but was without effect on AICAR-stimulated deGlc uptake. Such data suggest that AICAR stimulates glucose uptake via a wortmannin insensitive/ PI3K-independent pathway.

In conclusion, these data clearly demonstrate that at the level of skeletal muscle cells, the SHRSP exhibits a noticeable primary defect in insulin-stimulated deGlc uptake compared

with WKY rats. This defect is confined to an insulin-specific step in the activation of glucose transport since it is not observed in AICAR-stimulated deGlc uptake.

Chapter 5.

Analysis of glucose transport in skeletal muscle from the Zucker diabetic fatty rat – The effect of hyperglycaemia and thiazolidinedione treatment on glucose transport.

5.1 Introduction

5.1.1 The Zucker diabetic fatty rat as a model of human type 2 diabetes.

The data presented in chapters three and four have demonstrated that the spontaneously hypertensive rat model (SHRSP) is insulin resistant at the level of skeletal muscle, and that this insulin resistance is maintained in cultured skeletal muscle cells over several passages indicating genetic predisposition. It is now of interest to determine whether the sustained insulin resistance observed in the hypertensive SHRSP rat myocytes is common to other rat models of insulin resistance.

The Zucker diabetic fatty (ZDF) rat is a model of type 2 diabetes, useful for studies of insulin- and non-insulin-stimulated glucose uptake in skeletal muscle *in vitro* and *in situ*. This model was derived from the genetically obese (*fa/fa*) Zucker rat characterised by a mutation in the leptin receptor (OB-R), which was initially identified in Eli Lilly Research labs in 1974 (Unger and Orci, 2001). These rats were obese and insulin resistant, but did not develop overt diabetes (fasting hyperglycaemia) until a late age. Inbreeding of selected pairs with diabetic lineage lead to the establishment of the ZDF rat line in 1985 (Peterson et al., 1990). This animal exhibits symptoms of type 2 diabetes and cardiovascular disease that are very similar to those seen in humans with type 2 diabetes and other obesity-related diseases. Moreover, from a practical point of view, this model is particularly convenient, as type 2 diabetes-related pathologies such as fasting hyperglycaemia and cardiovascular disease develop rapidly, usually by 14 weeks of age in males. The course of the disease begins with the hyperphagic ZDF rat becoming obese and insulin-resistant, and develops into the formation of a hyperglycaemic animal that exhibits signs of hypo-insulinaemia due to β-cell decompensation. This progression of events is strikingly similar to those seen in human type 2 diabetic patients who, as in the case of the rat model, are characterised by hyperinsulinaemic-compensated normoglycaemia leading to low blood insulin and hyperglycaemia due to β-cell decompensation (Unger and Orci, 2001).

Since a number of studies have shown that chronic hyperglycaemia can impair insulin-stimulated glucose uptake and utilisation and exacerbate secondary disease, the hyperglycaemia observed in the obese ZDF rat provides a extremely useful model for the

investigation of glucose transport under this potentially deleterious condition (Rossetti et al., 1987); (Hager et al., 1991); (Davidson et al., 1994a).

5.1.2 Potential molecular defects in hyperglycaemia

The precise mechanism by which hyperglycaemia leads to peripheral insulin resistance is not fully understood however it has been demonstrated that diet/drug-induced restoration of blood glucose to normal levels improves insulin sensitivity and insulin-stimulated glucose uptake in adipocytes or muscle from diabetic rats or Type 2 diabetic humans (Henry et al., 1986); (Kahn et al., 1991); (Greenfield et al., 1982); (Kolterman and Olefsky, 1984). It is thought that increased biosynthetic activity and production of metabolites from the hexosamine pathway, which subsequently impair the function of the insulin signalling pathway are associated with the development of insulin resistance (Davidson et al., 1994b); (Rossetti, 2000). Studies on skeletal muscle from diabetic rodents and humans have shown defects in the insulin signalling pathways at the steps involving IRS-1, PI-3K and Glut 4 translocation (Anai et al., 1998); (Heydrick et al., 1995); (Heydrick et al., 1993); (Folli et al., 1993); (Saad et al., 1992); (Krook et al., 1998); (Bjornholm et al., 1997); (Goodyear et al., 1995); (Kim et al., 1999); (Friedman et al., 1999). These molecules are therefore likely to be involved in the mechanism by which restoration of glycaemia improves insulin sensitivity.

Another potential defect in insulin signalling may involve protein kinase B (PKB). Defective skeletal muscle PKB activity is observed in human diabetics and the ZDF rat (Krook et al., 1998); (Oku et al., 2001). Protein kinase B performs an important role in insulin signal transduction, being involved in the regulation of glycogen synthesis and implicated in the regulation of glucose transport (Hajduch et al., 2001). Activation of endogenous PKB occurs via a two-step process consisting of membrane localisation and binding of PIP_3 (the product of PI3K activity) and phosphorylation of threonine308 by PDK1 and serine473 possibly by an as yet undefined PDK2 (Alessi et al., 1997b). To address the significance of defects in PKB activity, a novel PKB agonist in development at GlaxoSmithkline was used to assess the effect of direct PKB activation on skeletal muscle glucose transport.

5.1.3 Pharmacological management of NIDDM- The thiazolidinediones

The primary goal for all diabetics is to maintain normoglycaemia. Some type 2 diabetics can achieve this by diet and exercise, however others require pharmacological intervention. In general, marketed drugs either stimulate the pancreas to produce more insulin or sensitise tissues such as muscle and fat to the action of insulin. The latter recent drugs which re-sensitise the insulin-resistant peripheral glucose storage tissues of fat and muscle to the actions of insulin include the thiazolidinediones of which Rosiglitazone is an example (Murphy and Holder, 2000). Clinically, Rosiglitazone is able to reduce fasting blood glucose and triglycerides. It achieves this by increasing Glut-4 expression in adipocytes and re-sensitising these cells to the antilipolytic action of insulin on the inhibition of hormone sensitive lipase (Young et al., 1995). It has also been shown to improve insulin sensitivity with respect to glucose uptake in muscle. At a molecular level, thiazolidinediones are high affinity ligands for the transcription factor Peroxisome Proliferator Activator Receptor gamma (PPARγ) (Murphy and Holder, 2000). PPARγ usually act as heterodimers with Retinoid X receptors (RXR) on their cognate response elements (Murphy and Holder, 2000). Interestingly PPARγ response elements control adipogenic genes, and evidence is accumulating that this transcription factor may also regulate muscle specific gene expression.

5.1.4 Aims and objectives.

(i) To compare insulin- and AICAR-stimulated glucose transport and components of the insulin-signalling network in isolated skeletal muscle from the diabetic ZDF rat model and its normal lean litter-mate.

(ii) To investigate the effect of novel PKB agonists on skeletal muscle glucose transport.

(iii) To examine insulin-stimulated glucose transport in cultured skeletal muscle cells obtained from ZDF and lean rats.

(iv) To examine the effects of hyperglycaemia on glucose transport in ZDF and lean Zucker skeletal muscle cells and the ability of rosiglitazone treatment to modulate the effects of hyperglycaemia on glucose transport.

5.2 Results

5.2.1 The effect of insulin and AICAR on deGlc uptake by flexor digitorum brevis (FDB) muscles.

ZDF rats are insulin resistant and a model of type 2 diabetes (Peterson et al., 1990). Hyperinsulinaemic-euglycaemic clamp studies and glucose transport measurements on isolated epididymal fat cells show an impaired insulin response to stimulate glucose disposal and glucose transport, respectively, in these animals (Unger and Orci, 2001). As the hyperinsulinaemic-euglycaemic clamp suppresses hepatic glucose output, these studies indicate that the defects must arise predominantly from impaired skeletal muscle glucose disposal (Unger and Orci, 2001). The characteristics of the animals used in this study are shown in Table 5.1. Fasting blood glucose levels and body weight were higher in the ZDF compared to the lean Zucker animals. In order to compare skeletal muscle insulin sensitivity in ZDF rats and lean Zucker rats, FDB muscles were isolated and the insulin-stimulated glucose transport was then measured using methods described in 2.3.2. Isolated FDB muscles were stimulated with 1μM insulin for 30 minutes prior to 2-deoxy-D-glucose uptake measurement. Figure 5.1 shows that maximal insulin-mediated deGlc uptake was significantly lower (p=0.002) in FDB muscles from ZDF rats (1.6 ± 0.3-fold) compared to lean Zuckers (3.2 ± 0.2-fold). This clearly indicates a diminished ability of insulin to stimulate deGlc uptake in isolated skeletal muscle of ZDF rats. These results support evidence of muscular insulin resistance in ZDF rats obtained by whole-body hyperinsulinaemic-euglycaemic clamp studies.

As described in studies utilising the SHRSP rat model, muscle glucose uptake can also be elicited in a non-insulin dependent manner by the AMPK agonist AICAR. To assess the effect of AICAR on deGlc transport, lean Zucker and ZDF FDB muscles were treated as outlined in section 3.2. Figure 5.1 demonstrates that AICAR stimulates deGlc transport in both ZDF (2.8 ± 0.08-fold) and lean (2.6 ± 0.12-fold) to a similar extent. These results are in keeping with those seen in SHRSP versus WKY rats (figure 3.1). Insulin-stimulated skeletal muscle deGlc uptake is diminished in both ZDF and SHRSP with respect to their lean controls but AICAR elicits deGlc uptake to the same extent in both insulin sensitive (WKY and lean Zuckers) and insulin insensitive (SHRSP and ZDF) animals.

Table 5.1 Characteristics of the animal groups.

	Serum glucose (mmol/L)	Weight (g)
Lean (n=15)	**5.2 ± 1**	**275 ± 11**
Zucker ZDF(n=15)	**17 ± 3***	**345 ± 20***

Shown are the mean body weight and fasted serum glucose of the 12 week-old animals used in this study. * indicates a statistical significant difference between the groups, $p<0.01$. Performed in collaboration with Dr. Greg Murphy and Dr. Carolyn Lister, Department of Vascular Biology, GlaxoSmithkline, Harlow, UK.

Figure 5.1 The effect of insulin and AICAR on deGlc uptake in FDB muscle from ZDF and lean Zucker rats.

Shown are the effects of 30 min incubation with either 1μM insulin or 500μM AICAR on glucose uptake in FDB muscles exposed to deGlc for 10 min. The data are presented as mean ± S.E.M. from 3 separate experiments, expressed as a fold increase over the basal lean rate. * indicates a significant increase in deGlc transport over basal in response to insulin, p=0.01. ** indicates no significant fold-increase in response to insulin with respect to basal and a significant difference *vs* corresponding value in lean Zucker strain, p=0.04. † indicates a significant increase in response to AICAR in lean Zucker muscles, p=0.05. †† indicates no significant difference in the magnitude of the AICAR response between the lean Zucker and ZDF strains, and also that the AICAR response in ZDF rats is significantly increased over basal, p=0.05. Basal deGlc transport was not significantly different between ZDF and lean Zucker rats.

Figure 5.1 The effect of insulin and AICAR on deGlc uptake in FDB muscle from ZDF and lean Zucker rats.

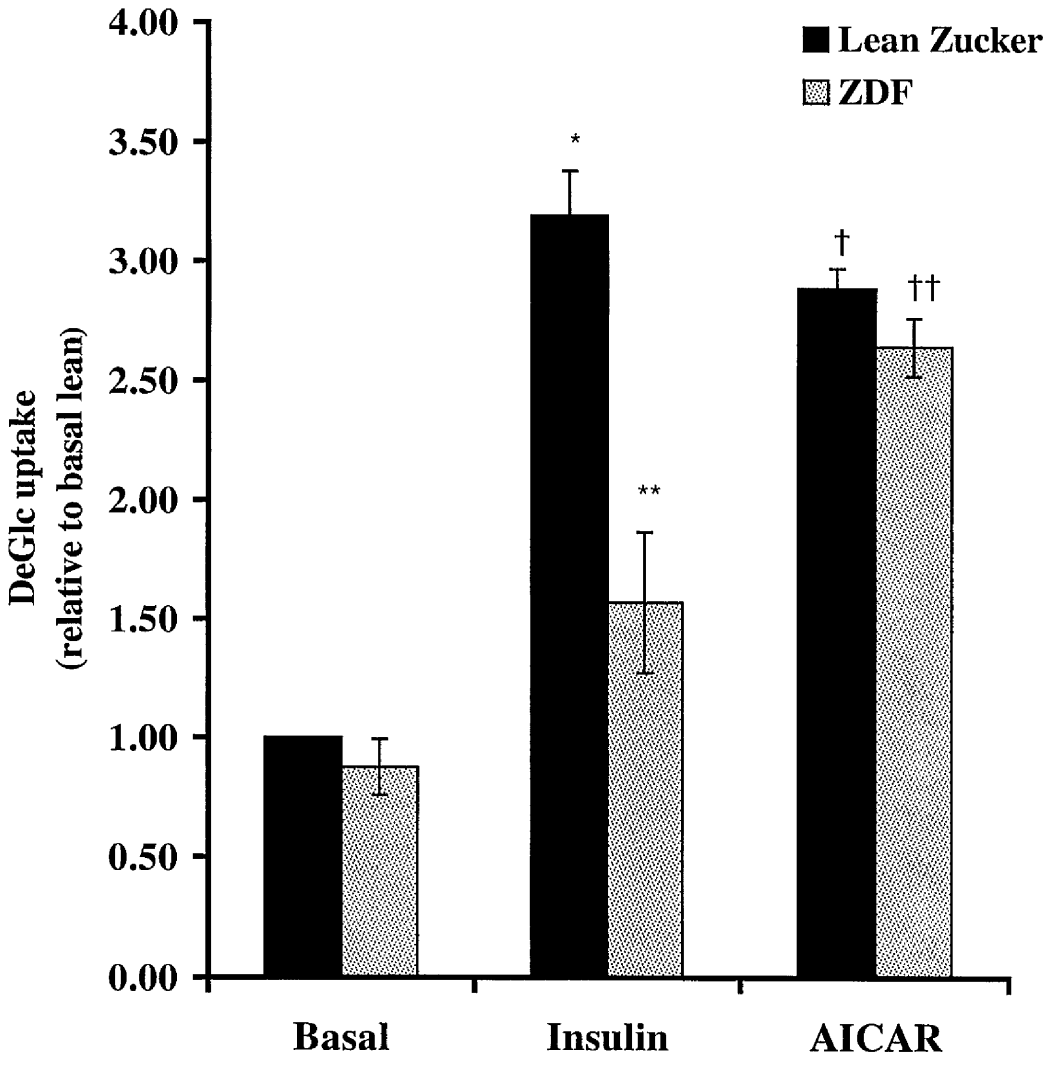

5.2.2 Immunoblot analysis of molecules involved in insulin-stimulated glucose transport.

Whole skeletal muscle lysates of EDL, soleus, tibialis and gastrocnemius muscles from ZDF and lean Zucker rats were prepared and immunoblotted as described (2.3.3, 2.3.8 - 2.3.10). As shown in figure 5.2A and quantified in figure 5.2B no significant differences were detected in total cellular levels of IRS-1 and the p85 subunit of PI3K between ZDF and lean Zucker animals. Similarly, there was no noticeable difference in the total cellular expression levels of PKB, as detected by an antibody raised to the PKB pleckstrin homology domain (figure 5.3A). However, significant differences ($p<0.05$) are observed in the insulin-stimulated S473 phosphorylation of PKB in ZDF rats compared with lean Zuckers (figure 5.3B). In addition, insulin-stimulated EDL muscle PKB activity from ZDF rats is significantly decreased compared with lean Zuckers as shown in figure 5.4. Such data support the view that the insulin resistance observed in ZDF rats with respect to the lean Zuckers cannot be due to the altered cellular expression of these key proteins involved in glucose transport. However, the diminished activity of PKB is indicative of a defect in the insulin-signalling pathway. This result suggests that PKB could be a possible target for pharmacological modulation.

Figure 5.2 Immunoblot analysis of IRS-1 and p85 in various hind limb muscles from the ZDF and lean Zucker rat.

Representative immunoblots (**A**) in which 20 & 10 μg of protein lysates made from EDL, soleus and tibialis skeletal muscle of male lean Zucker and ZDF rats were analysed by SDS-PAGE/immunoblotting with the antibodies specific for the IRS-1 carboxyl terminus domain and p85 subunit of PI3K. Data from one animal of each strain is shown. (**B**) represents quantification of 4 experiments of this type from 4 animals from each strain, with the relative level of expression in ZDF muscles expressed as a % of that observed in the corresponding lean Zucker muscle taken as 100% (means ± S.E.M.). No significant differences in protein expression levels were found in lysates from all muscles studied between lean Zucker and ZDF rats.

Figure 5.2 Immunoblot analysis of IRS-1 and p85 in various hind limb muscles from the ZDF and lean Zucker rat.

A

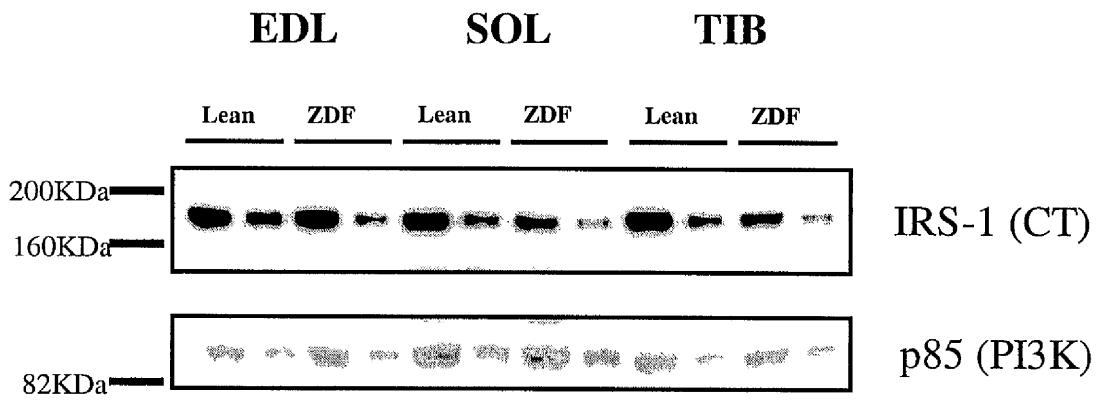

B

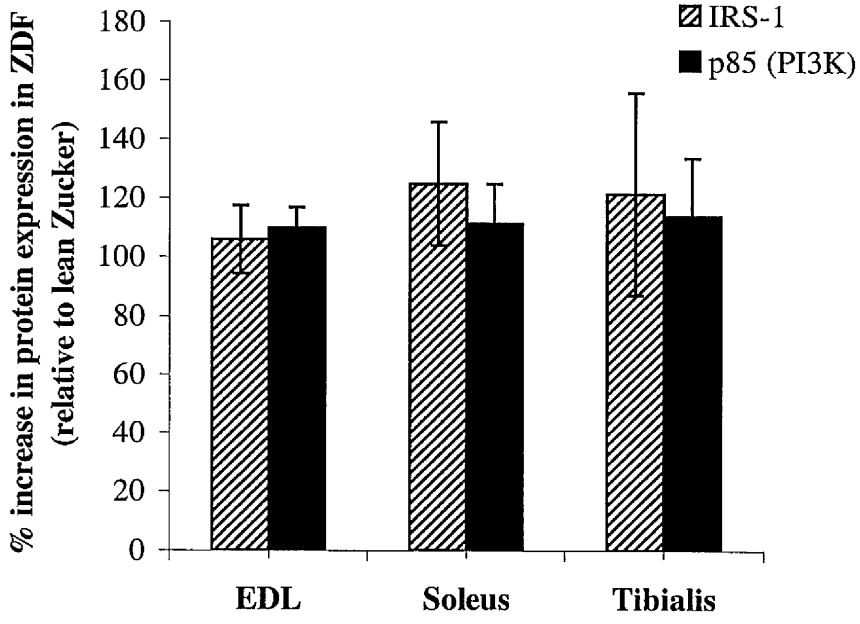

Figure 5.3 Immunoblot analysis of PKB serine-473 phosphorylation in EDL muscles lysates from ZDF and lean Zucker rats.

EDL muscles from lean Zucker and ZDF rats were incubated with or without 1 μM insulin for 30 min and whole muscle lysates prepared as outlined in 2.3.3. Equal amounts of protein (10 μg/lane) were subjected to SDS-PAGE/immunoblot analysis using antibodies specific for PKB-PH domain and PKB phosphorylated at serine-473. **(A)** is a representative immunoblot for PKB-PH domain. No significant difference was observed between basal or insulin-stimulated muscle lysates of lean Zucker and ZDF rats. **(B)** indicates phosphorylated serine-473 PKB levels in EDL muscle lysates in the absence or presence of 1μM insulin from ZDF and lean Zucker animals. Insulin causes a significant increase ($p<0.05$, $n=3$) in serine phosphorylated PKB in lean Zucker muscle lysates only. PKB–PH domain is also shown to illustrate that the observed changes in PKB serine-473 phosphorylation is not a consequence of global changes in PKB expression.

Figure 5.3 Immunoblot analysis of PKB serine-473 phosphorylation in EDL muscles lysates from ZDF and lean Zucker rats.

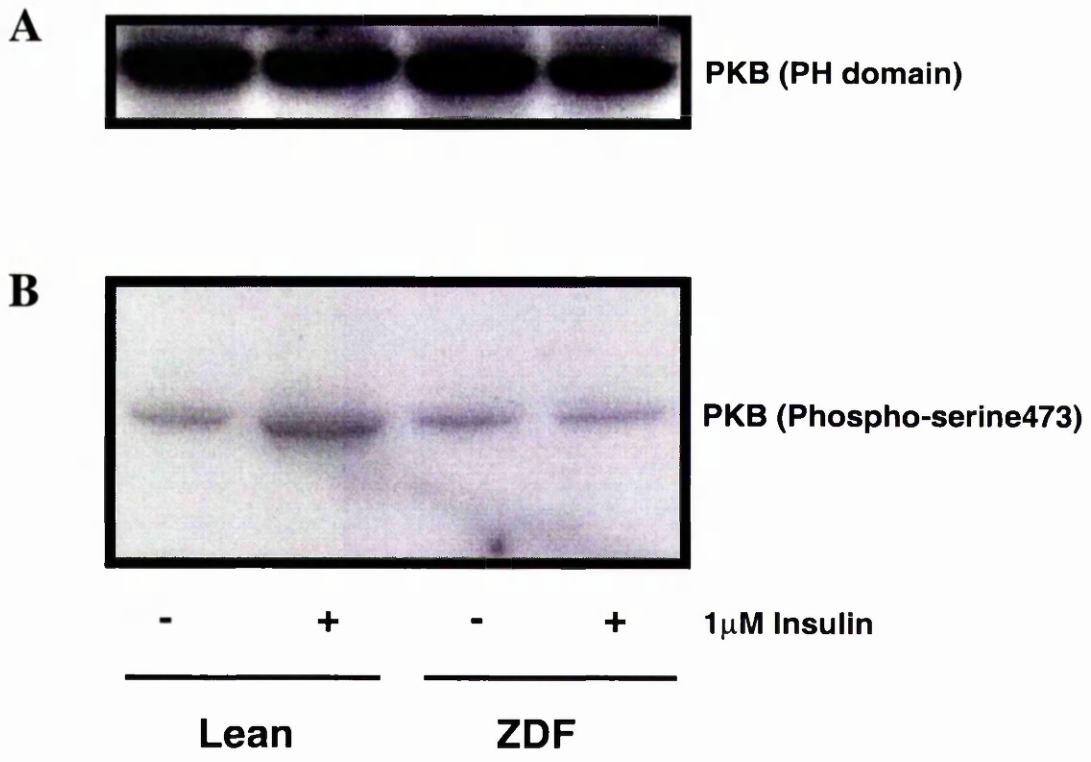

Figure 5.4 Effect of insulin on PKB activity in EDL muscle lysates from ZDF and lean Zucker rats.

EDL muscles were incubated at 37°C in the presence or absence of 1 μM insulin for 30 minutes. Muscles lysates were prepared as described in 2.3.3. PKB activity in muscle lysates was measured against a peptide substrate based on a motif from GSK3 as outlined in 2.3.7. PKB activity is expressed as picomoles of substrate phosphorylated /min/mg protein. Shown is data from three experiments (means ± S.E.M.), with each condition performed in triplicate in each experiment. *Significantly different ($p<0.01$) *vs* unstimulated muscle lysates and ZDF muscle lysates. In ZDF muscle lysates insulin did not stimulate a significant increase in PKB activity over basal. No significant differences in basal activity were observed between lean Zucker and ZDF muscle lysates.

Figure 5.4 Effect of insulin on PKB activity in EDL muscle lysates from ZDF and lean Zucker rats.

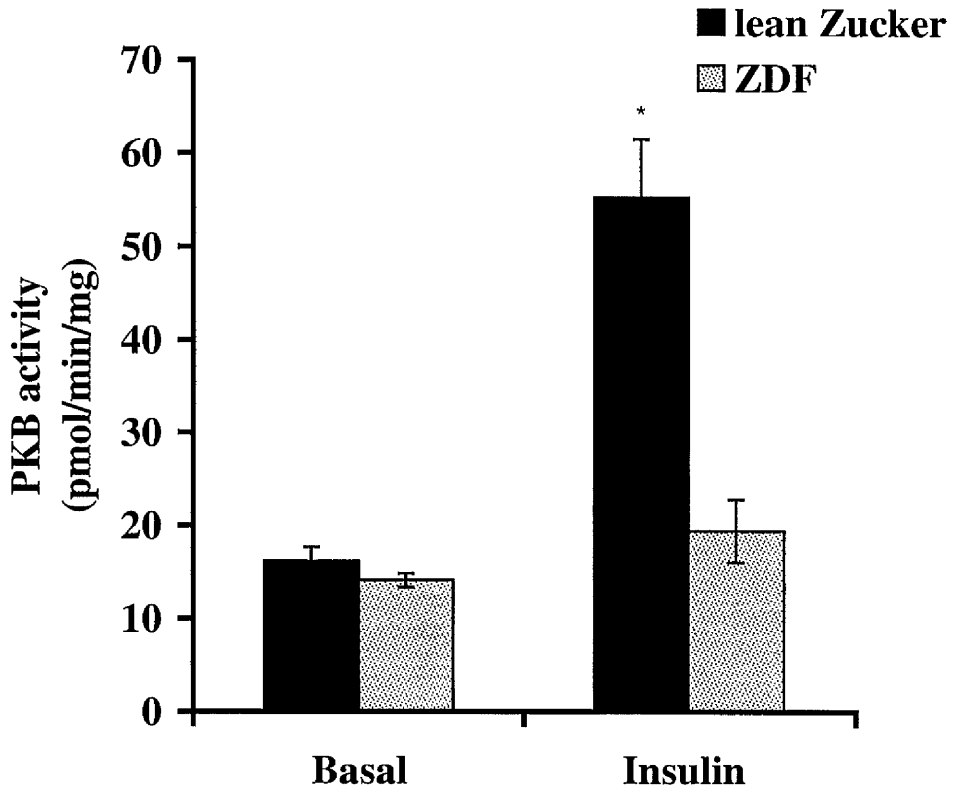

5.2.3 Effect of pharmacological agonists on *in vitro* phosphorylation of PKBS473D.

GlaxoSmithkline has identified pharmacological agents able to activate *in vitro* recombinant PKBS473D. PKBS473D is a PKB mutant in which serine (S) in the second regulatory phosphorylation site at position 473, is replaced by an aspartic acid (D) residue, mimicking the *in vivo* partially-activating phosphorylation of S473 (Alessi et al., 1996). This phosphorylation partially reveals the PDK1 phosphorylation site at threonine (T) 308, which is positioned in the activation loop of the catalytic/kinase domain of PKB. Phosphorylation of T308 and S473 fully activates PKB kinase activity toward intracellular substrates (Alessi et al., 1996). The pharmacological agents which activate PKBS473D are designed to functionally mimic PKB's PH domain binding of PIP_3, which is a necessary but not a sufficient step towards the activation of endogenous PKB (Kohn et al., 1996b).

Previous screens of GlaxoSmithkline compound bank for pharmacological agents which are able to stimulate recombinant PKBS473D kinase activity toward a PKB specific substrate peptide sequence has revealed a number of promising leads. Of those, two compounds SB456672 and SB437478 were selected as most worthy of further investigation and development. In particular, *in vitro* analyses show these compounds are lipophilic and therefore potentially cell permeable, an important prerequisite for drugs that must traverse the cell plasma membrane to reach their target. In addition, these compounds possess a low binding affinity for serum albumin. Serum albumin is the most abundant blood protein and is able to bind and sequester many drugs thus lowering the concentration of available drug capable of acting on its target. This lowered 'biological-availability' limits drug action.

Before investigating the action of these putative PKB agonists on skeletal muscle glucose uptake, their effects were examined on recombinant PKB phosphorylation and on their ability to activate PKB activity toward a synthetic peptide substrate using systems and methods developed within GlaxoSmithkline and described in 2.3.16. Figure 5.5 illustrates that in the presence of recombinant PDK1 and PIP_3 vesicles, recombinant PKBS473D is phosphorylated on T308 (lanes 3 and 4). This is detected using an antibody that specifically recognises the phosphorylated T308 of PKB. This phosphorylation is abolished in the presence of 20mM EDTA, which chelates Mg^{2+}, an

ion absolutely required for kinase activity (lanes 1 and 2). In addition, removal of either PIP_3 vesicles (lanes 5-6) or recombinant PDK1 (lanes 7-8) effectively abolishes PKB T308 phosphorylation.

It should be noted that in the absence of PIP_3 (lanes 5-6), there is a slight phosphorylation of T308 in recombinant PKBS473D. This low-level phosphorylation of T308 could be due to the more accessible nature of the PDK1 phosphorylation site in the partially primed, recombinant PKBS473D protein, compared to the native enzyme. However, in the absence of PDK1 there is no detectable phosphorylation of recombinant PKBS473D on T308 (lanes 7-8), indicating that T308 phosphorylation is absolutely dependent on PDK1 in this *in vitro* system.

In the presence of PDK1 but absence of PIP_3 vesicles both SB456672 and SB437478 restore T308 phosphorylation of PKBS473D (lanes 11-12). Indeed, SB437478 was shown to elicit T308 phosphorylation in the absence of both PDK1 and PIP_3 vesicles (lanes 9-10). This phosphorylation is further enhanced by addition of PDK1 (lanes 11-12). These data show that both putative PKB agonists facilitate PDK1-dependent but PIP_3-independent phosphorylation of T308 in recombinant PKBS473D. This indicates that these compounds can substitute PIP_3 function in exposing the PDK1 phosphorylation site of PKB. Moreover, SB437478 but not SB456672 can elicit PDK1-independent PKBS473D T308 phosphorylation. Perhaps the simplest interpretation of this result is that this implies a further level of pharmacological interaction with PKB enabling PKB auto-phosphorylation.

Figure 5.5 Effect of PKB agonist SB456672 and SB437478 on the *in vitro* threonine308 phosphorylation of recombinant S473D-PKBα.

The effects of PIP_3 vesicles, PDK1 and PKB agonists on *in vitro* recombinant S473D-PKBα threonine308 phosphorylation were independently assessed. Shown is a representative immunoblot of two separate experiments carried out as described in 2.3.16 and run in duplicate. 10μl of each reaction mixture was resolved by SDS-PAGE/immunoblotting and probed with an antibody that specifically recognises phosphorylated threonine-308 in PKBα. As indicated, lanes 1-2 represent the effect of 20 mM EDTA on Thr-308 phosphorylation status in the presence of PIP_3 vesicles and PDK1 and are labelled 'kinase dead'. Lanes 3-4 represent PKBS473D Thr-308 phosphorylation in the presence of purified recombinant PDK1 and PIP_3 vesicles and are labelled 'fully active'. Lanes 5-6 and 7-8 represent the effect of removal of PIP_3 vesicles or recombinant PDK1 on PKBS473D Thr-phosphorylation respectively, and are therefore labelled 'PIP_3-independent' or 'PDK1-independent' respectively. Lanes 9-10 represents the effect of either SB456672 (upper panel) or SB437478 (lower panel) on thr-308 PKBS473D phosphorylation in the absence of recombinant PDK1 and PIP_3 vesicles. Lanes 11-12 represents the effect of compounds [abbreviated CPD in figure] (SB456672 upper panel and SB437478 lower panel) on Thr-308 PKBS473D phosphorylation in the presence of recombinant PDK1. PIP_3 in the presence of compounds gave similar results to that seen in lanes 9-10 (data not shown). Experiments were repeated once more with similar results.

Figure 5.5 Effect of PKB agonist SB456672 and SB437478 on the *in vitro* phosphorylation of recombinant S473D-PKB.

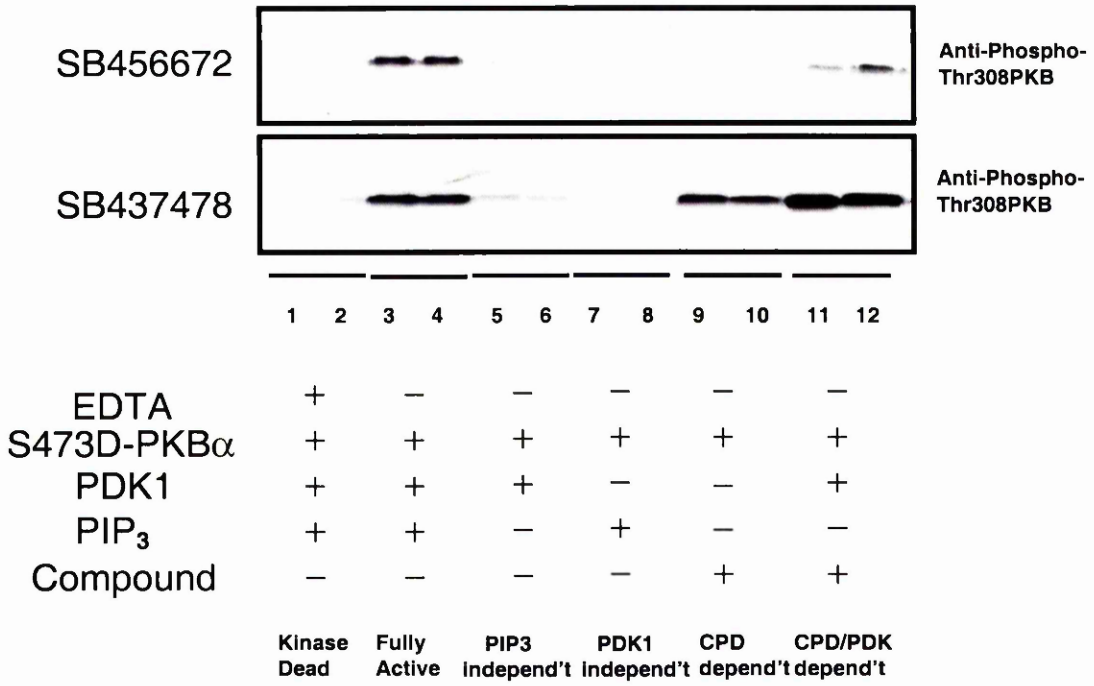

5.2.4 Effect of SB456672 and SB437478 on *in vitro* PKBS473D-dependent phosphorylation of PKB peptide substrate.

As shown above in 5.2.3, SB456672 and SB437478 both elicit T308 phosphorylation of recombinant PKB by a PIP_3-independent but PDK1-dependent mechanism. However, such data does not directly establish the effect of these putative agonists on PKB activity. To examine this, the ability of recombinant PKBS473D to phosphorylate a synthetic peptide substrate (KRPRAATF) was measured after being treated as described in 5.2.3. For a full description of methods, refer to 2.3.16. As shown in figure 5.6 SB437478 and SB456672 in the absence and presence of PIP_3 vesicles significantly increased PKBS473D activity compared to vehicle. These data demonstrate that increased T308 phosphorylation directly correlates with increased activity toward a specific peptide substrate.

5.2.5 The effect of PKB agonist on deGlc uptake.

As described earlier, SB456672 was able to reconstitute *in vitro* PDK1-dependent phosphorylation of T308 on PKBS473D in the absence of PIP_3 vesicles. This compound was also able to stimulate *in vitro* PKB activity toward a peptide substrate. In addition, its lipophilicity and low serum albumin binding profile make it a good candidate for *in situ* analysis of a putative PKB agonist effect on glucose transport in skeletal muscle (GlaxoSmithkline data). Therefore, the effect of SB456672 on deGlc uptake in lean Zucker and ZDF rat muscles was assessed. Figure 5.7 shows that acute stimulation with 10μM SB456672 for 30 min did not significantly stimulate deGlc uptake over basal values in lean Zucker or ZDF rat muscles.

Figure 5.6 Effects of putative PKB agonists on S473D-PKBα-dependent phosphorylation of substrate peptide.

Recombinant S473D-PKBα protein was pre-incubated at 30°C for 60 min with recombinant PDK1 and ATP in the presence or absence of 10 μM PKB agonist (open bar) or PIP_3 vesicles, recombinant PDK1 and ATP in the presence or absence of 10 μM PKB agonist (closed bar). *In vitro* PKB activity was subsequently measured against a peptide substrate based on a motif from GSK-3. Methods used are outlined in 2.3.16. Values are the mean ± S.E.M. from three separate experiments each carried out in triplicate. §indicates a statistically significant increase in S473DPKBα activity in the presence of PIP_3 vesicles compared with no PIP_3 vesicles ($p<0.0001$). *indicates a significant increase *vs* corresponding vehicle value, and also indicates no significant difference in activity *vs* vehicle activity in the presence of PIP_3 vesicles ($p<0.001$). **indicates a significant increase *vs* corresponding vehicle value ($p<0.000001$), and corresponding SB437438 value in the absence of PIP_3 vesicles ($p<0.0001$). †indicates a significant increase in activity compared to corresponding vehicle activity ($p=0.01$), and also indicates a significant decrease compared to SB437438 value in the absence of PIP_3 vesicles ($p<0.001$). ††indicates a significant increase compared to corresponding vehicle activity ($p=0.03$) and also indicates a significant increase vs corresponding SB456672 value in the absence of PIP_3 vesicles ($p<0.01$).

Figure 5.6 Effects of putative PKB agonists on S473D-PKBα-dependent phosphorylation of substrate peptide.

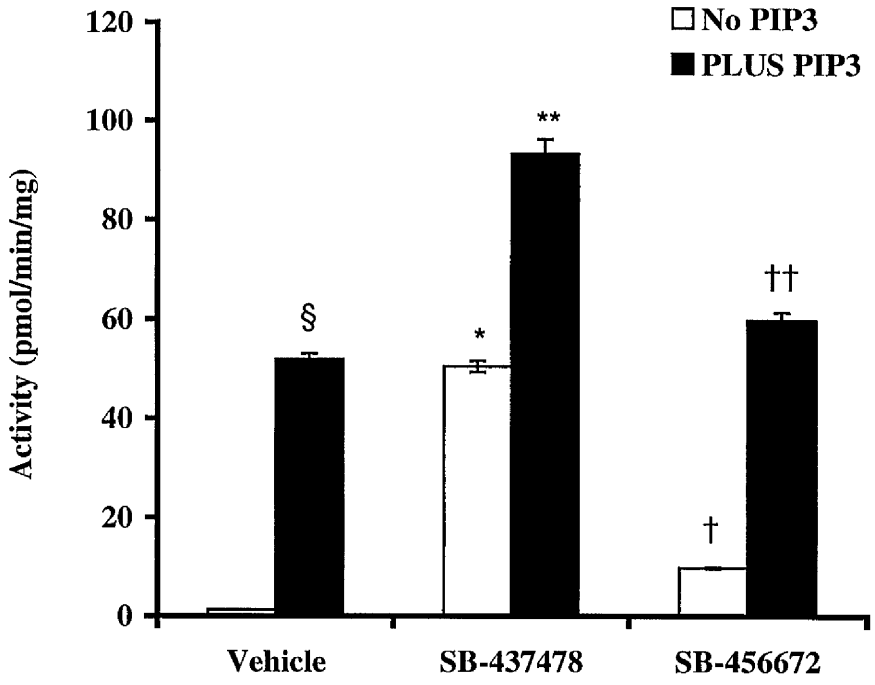

Figure 5.7 The effect of PKB agonist SB456672 on deGlc uptake in FDB muscle from lean Zucker and ZDF muscle.

The effects of acute stimulation of 30 min incubation with SB456672 on a 10 min deGlc uptake in lean Zucker and ZDF FDB muscles are shown. The data are presented as mean ± S.E.M. from 3 separate experiments, expressed as a fold increase over the basal lean rate. SB456672 did not significantly increase deGlc fold uptake over basal in ZDF or lean Zucker rats. Basal deGlc transport was not significantly different between ZDF and lean Zucker rats.

Figure 5.7 The effect of PKB agonist SB456672 on deGlc uptake in FDB muscle from lean Zucker and ZDF muscle.

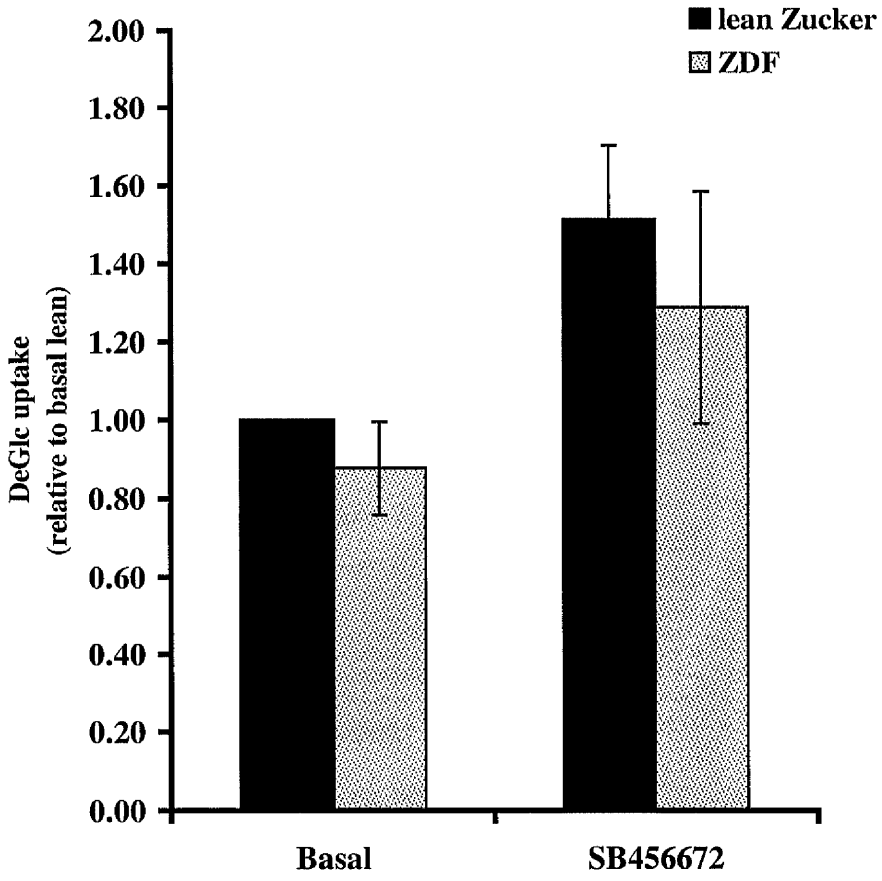

5.2.6 Immunoblot analysis of c-Cbl, flotillin and caveolin expression in lean Zucker and ZDF muscles.

As discussed in 1.4 there is evidence that insulin via the insulin receptor co-stimulates an alternative PI3K-independent pathway required for the stimulation of glucose transport. This proposed pathway thus far includes CAP/c-Cbl/C3G/TC-10, all of which localise to plasma membrane domains involved in cell signalling known as caveolae (Baumann et al., 2000); (Chiang et al., 2001); (Watson et al., 2001). Caveolae are a subset of lipid rafts consisting of membranous invaginations enriched in the structural protein caveolin. Caveolin forms homo-oligomers and hetero-oligomers with another structural protein named flotillin (Galbiati et al., 2001). As previously shown in figure 3.7, both caveolin and flotillin are significantly overexpressed in the insulin-resistant SHRSP with respect to the WKY rat. This may contribute to impaired insulin-dependent glucose uptake in that animal. In order to investigate whether expression of these proteins is also increased in ZDF relative to lean Zuckers, immunoblot analysis of EDL, soleus and tibialis muscle lysates were performed. As shown in figure 5.8 A/B no significant differences were detected in total cellular expression of c-Cbl, caveolin-1 and flotillin from ZDF or lean Zucker skeletal muscle lysates. Therefore, it is unlikely that the impairment of insulin-dependent glucose uptake in this animal model is due to altered expression of caveolin, flotillin-1 or c-Cbl.

Figure 5.8 Immunoblot analysis of c-Cbl, flotillin and caveolin-1 expression in lean Zucker and ZDF muscle.

Shown are representative immunoblots **(A)** in which 20 & 10 μg of protein lysates from EDL, soleus and tibialis skeletal muscle of male lean Zucker or ZDF rats were analysed by SDS-PAGE/immunoblotting with the antibodies specific for c-Cbl, flotillin and caveolin-1. Data from one animal of each strain is shown; note that the blots presented are deliberately over-exposed in order to show the level of c-Cbl and caveolin present in muscles with weaker signals. **(B)** represents quantification of 4 experiments of this type from 4 animals from each strain, with the relative level of expression in ZDF muscles expressed as a % of that observed in the corresponding lean Zucker muscle taken as 100% (means ± S.E.M.). No significant change in c-Cbl, flotillin or caveolin-1 protein expression levels were observed between lean Zucker or ZDF muscles.

Figure 5.8 Immunoblot analysis of c-Cbl, flotillin and caveolin-1 expression in lean Zucker and ZDF muscle.

A

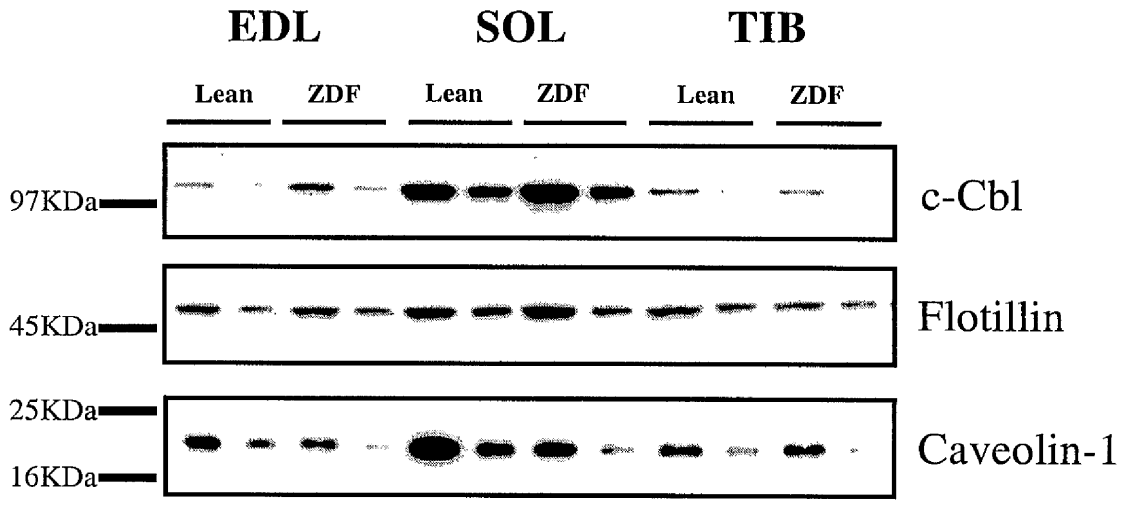

B

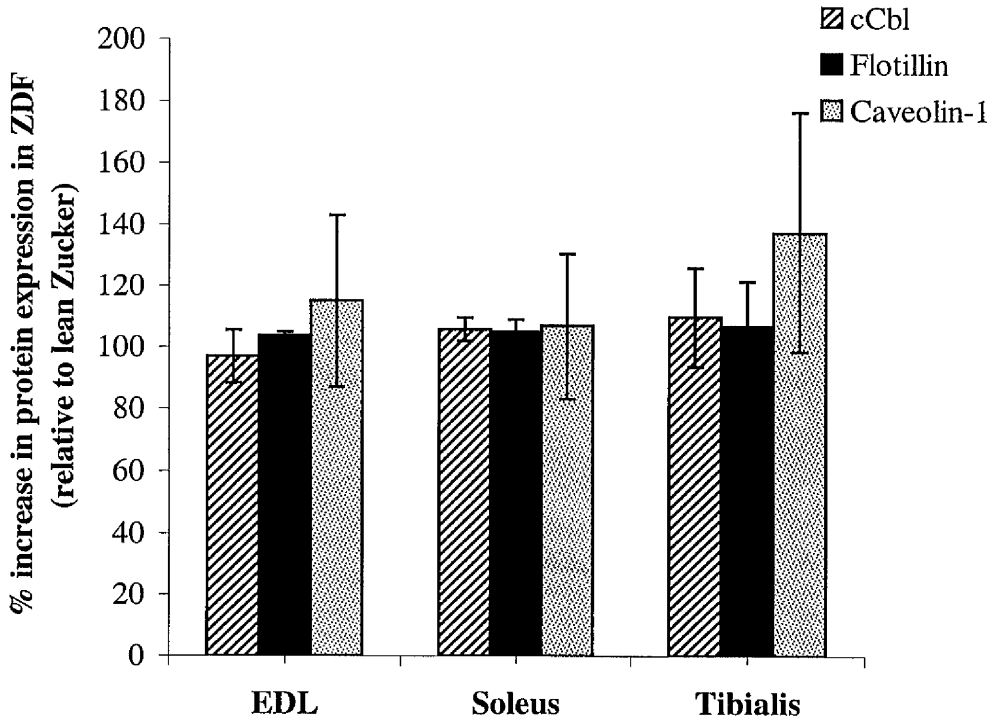

5.2.7 The effect of insulin on deGlc transport in EDL and soleus skeletal muscle cell cultures from ZDF and lean Zucker rats.

As shown in chapter 4 an impairment of deGlc transport in the skeletal muscle from the insulin resistant SHRSP rat persists in cells cultured from SHRSP muscle. To investigate whether this is also observed in ZDF and lean Zuckers rats, primary skeletal muscle cells were isolated and cultured from EDL and soleus muscles as previously described in 4.2.1 and modified in 4.2.6. The immunoblot analysis in figure 5.9 illustrates that these cells contain the myogenic marker myogenin. They also express Glut-4 (data not shown). As shown previously in figure 5.1 skeletal muscle from the insulin resistant ZDF animals exhibit a marked impairment of insulin-stimulated deGlc transport compared with the insulin-sensitive lean Zuckers. Acute insulin treatment (1 μM for 30 min) significantly increased deGlc transport in EDL (2.70 ± 0.4-fold over basal; $p<0.05$) and in soleus (2.5 ± 0.3-fold over basal; $p<0.05$) skeletal muscle cells from lean Zuckers (figure 5.10). The mean basal transport rate was 2.4 ± 0.01 pmol/min/well and was not significantly different in both lean Zucker and ZDF rat. Acute insulin stimulation of ZDF EDL and soleus skeletal muscle cell cultures failed to significantly increase deGlc uptake over basal (figure 5.10).

Figure 5.9 Immunoblot analysis of Myogenin expression in lean Zucker and ZDF skeletal muscle cultures.

A representative immunoblot is shown in which 10 μg of protein lysates made from four different differentiated (day 4) skeletal muscle cell cultures from lean Zucker or ZDF rats were analysed by SDS-PAGE/immunoblotting with an antibody specific for myogenin. The experiment was repeated twice with similar results.

Figure 5.10 The effect of insulin on deGlc uptake in skeletal muscle cultures from lean Zuckers and ZDF rats.

The effects of acute insulin stimulation (1 μM for 30 min) on a 10 min deGlc uptake in EDL and soleus skeletal muscle cells cultured from 12 week old lean Zucker and ZDF rats are shown. Using methods described in 4.2.1-4.2.3 with optimisations defined in 4.2.6-4.2.7 cells were isolated and cultured. DeGlc uptake was measured as outlined in 2.3.15. This graph represents data obtained from cells between passages 5-8. The data are presented as mean ± S.E.M. from 4 separate experiments, expressed as a fold increase over the basal rate. Basal rates of transport were not significantly different between lean Zucker and ZDF rat. * indicates a significant fold-increase in deGlc transport in response to insulin, p=0.01. ** indicates a significant fold-increase in deGlc transport in response to insulin, p=0.04. Acute insulin stimulation failed to significantly increase deGlc transport above basal levels in ZDF muscle cells cultures.

Figure 5.9 Immunoblot analysis of Myogenin expression in lean Zucker and ZDF skeletal muscle cultures.

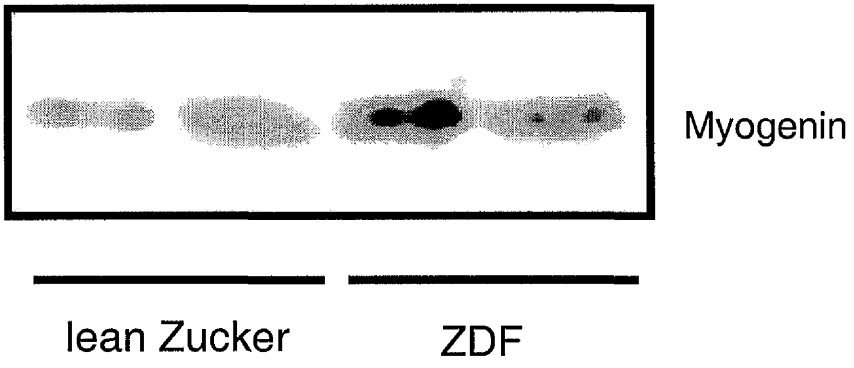

Figure 5.10 The effect of insulin on deGlc uptake in skeletal muscle cultures from lean Zuckers and ZDF rats.

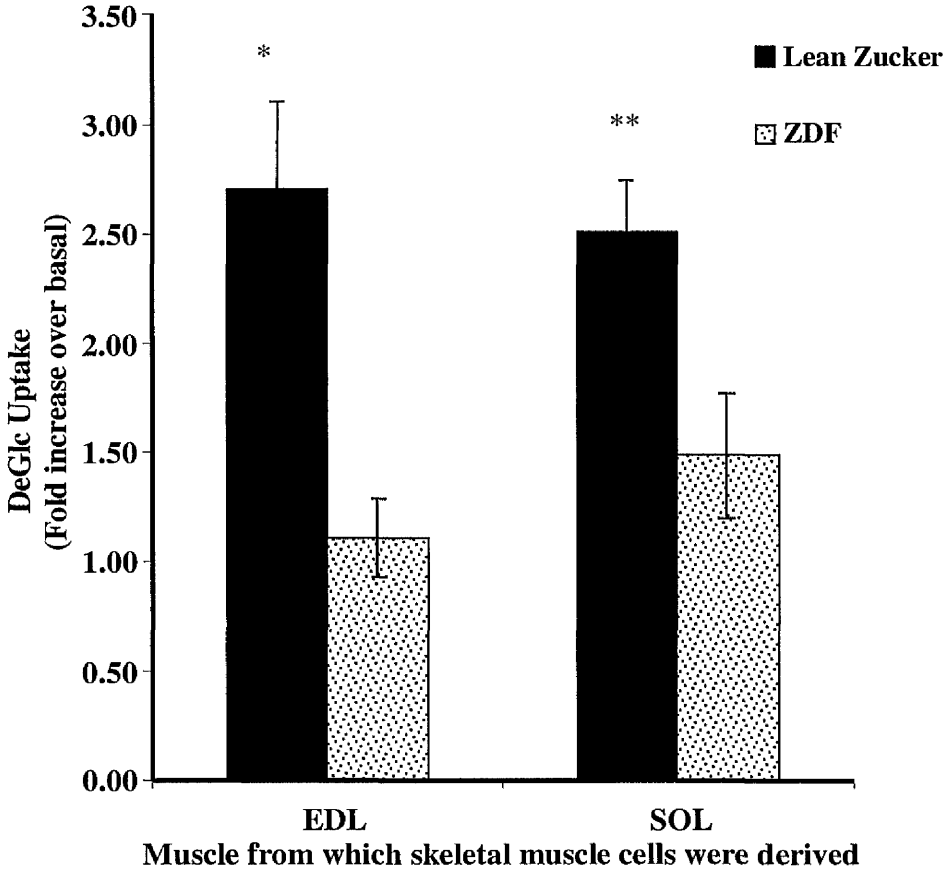

5.2.8 The effect of hyperglycaemia on insulin-stimulated deGlc transport in EDL skeletal muscle cell cultures isolated from ZDF and lean Zucker rats.

The diabetic ZDF rat displays fasting hyperglycaemia associated with dyslipidaemia and obesity (Unger and Orci, 2001). As observed in figures 5.1 and 5.10, the insulin resistance seen in ZDF muscle is maintained in cultured muscle cells implying a genetic predisposition to skeletal muscle insulin resistance. To examine the effect of hyperglycaemia on insulin-stimulated deGlc transport, cells were grown in chick embryo extract (CEE)-free growth medium as described in 4.2.6 and differentiated in α-MEM differentiation medium with a final D-glucose concentration of 5mM or 30mM. Cells were fed every 24 hours for 5 days with this medium and serum starved for 24 hours in serum-free medium containing 5mM or 30mM D-glucose, prior to measurement of insulin-stimulated deGlc uptake. The assay for insulin-stimulated deGlc uptake was performed as described in 4.2.5. In cells cultured under normoglycaemic conditions, acute insulin treatment (1μM for 30 min) increased deGlc uptake in lean Zucker cultures from 2.2 ± 0.09 to 6.1 ± 0.4 pmol/min/well ($p<0.001$), but failed to significantly stimulate deGlc uptake in ZDF cultures (figure 5.11). In contrast, in cells cultured under hyperglycaemic conditions (30mM D-glucose) acute insulin treatment failed to significantly stimulate glucose transport above basal in either lean Zucker or ZDF muscle cultures. Basal transport levels did not significantly change between lean Zucker or ZDF cultures in the presence of 5 or 30 mM D-glucose.

Figure 5.11 The effect of hyperglycaemia on insulin-stimulated deGlc uptake in skeletal muscle cultures from lean Zucker and ZDF rats.

Muscle cultures were grown using media outlined in 4.2.6 and differentiated with α-MEM differentiation medium outlined in 4.2.2 supplemented with or without 25mM D-glucose, giving a final D-glucose concentration of 30 mM or 5 mM, respectively. Cells were fed every 24 hours for 5 days with this differentiation medium and serum starved for 24 hours in serum-free medium containing 30 mM or 5 mM D-glucose, prior to measurement of insulin-stimulated deGlc uptake. Cells were incubated in the presence or absence of 1 μM insulin for 20 min prior to a 10 min deGlc uptake assay (insulin stimulation was maintained throughout uptake assay) that was performed as described in 4.2.5. Basal transport levels were not significantly different between lean Zucker or ZDF cultures in the presence of 5 or 30 mM D-glucose. *indicates a statistically significant increase in deGlc transport in lean Zucker muscle cultures ($p<0.001$). Acute insulin stimulation failed to significantly increase deGlc transport above basal levels in ZDF muscle cells cultured under 5 or 30 mM D-glucose, and lean Zuckers muscle cells cultured under 30mM D-glucose. The results shown are obtained from two independent ZDF and lean Zucker skeletal muscle cultures and are the mean ± S.E.M. from 3 separate experiments on each.

Figure 5.11 The effect of hyperglycaemia on insulin-stimulated deGlc uptake in skeletal muscle cultures from lean Zucker and ZDF rats.

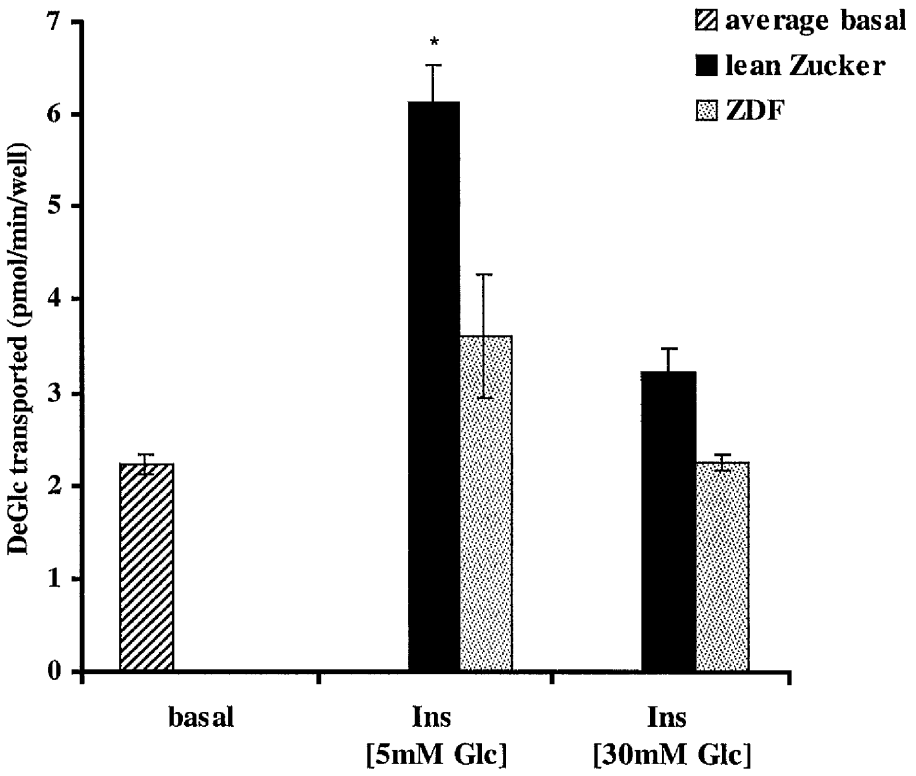

5.2.9 The effect of chronic Rosiglitazone treatment on insulin-stimulated deGlc transport in muscle cells chronically treated with low (5mM) and high (30mM) D-glucose.

Cells differentiated for 5 days (as in 5.2.9) in the presence of 5mM or 30 mM D-glucose were treated with 1 μM Rosiglitazone over the last 3 days of differentiation essentially as (Park et al., 1998b). Prior to deGlc assay (described in 4.2.5), cells were incubated in serum-free media containing 5 or 30 mM D-glucose with 1μM Rosiglitazone for 24 hours. Under normoglycaemic conditions, cells chronically treated with 1μM rosiglitazone, basal glucose transport drug (basal=4.9 $\pm$ 0.4 pmol/min/well; figure 5.12) was significantly increased ($p<0.001$) approximately 2-fold compared to cells, which were not exposed to the drug (basal=2.2 $\pm$ 0.09 pmol/min/well; figure 5.11). In these lean Zucker skeletal muscle cells, acute insulin stimulation (1 μM for 30 min), gave a similar fold increase from this elevated basal value (from 4.9 $\pm$ 0.42 to 10.6 $\pm$ 0.4 pmol/min/well ($p<0.001$)) but did not significantly increase deGlc uptake in ZDF cultures (figure 5.12). However, chronic exposure of the cells to hyperglycaemic conditions (30mM glucose) abrogated insulin-dependent glucose uptake whether or not the cells had been treated with Rosiglitazone, but did not abolish the increased basal deGlc uptake elicited by treatment with the drug. Therefore, the amelioration of hyperglycaemia induced by thiazolidinediones (Park et al., 1998a); (Park et al., 1998b) appears to be independent of enhanced insulin sensitivity in this *in vitro* muscle system, but rather a consequence of a direct effect of the drug on basal glucose uptake.

Figure 5.12 The effects of chronic Rosiglitazone treatment on insulin-stimulated deGlc uptake in skeletal muscle cultures chronically treated with 5 mM and 30 mM D-glucose.

Cells differentiated for 5 days (as in figure 5.11) in the presence of 5mM or 30 mM D-glucose were chronically treated with 1 μM Rosiglitazone over the last 3 days of differentiation. Prior to acute insulin stimulation (1μM insulin for 30 min) and 10 min deGlc uptake assay (described in 4.2.5), cells were incubated in serum-free media containing 5 or 30mM D-glucose with 1μM Rosiglitazone for 24 hours. Basal transport levels did not significantly change between lean Zucker or ZDF cultures in the presence of 5 or 30 mM D-glucose. ††indicates that basal deGlc transport in Rosiglitazone treated cells is significantly elevated compared to untreated cells (figure 5.11); (p<0.01). †indicates a significant increase in glucose transport rates compared to non-drug treated cells (Figure 5.12); (p<0.01). *indicates a statistically significant increase in deGlc transport in lean Zucker cultures; (p<0.001).. Acute insulin stimulation failed to significantly increase deGlc transport over basal transport rates in ZDF muscle cells chronically treated with 5 or 30mM D-glucose and 1μM Rosiglitazone. Lean Zucker muscle cells chronically treated with 30mM D-glucose and 1μM Rosiglitazone also failed to significantly respond to insulin. The results shown are obtained from two independent ZDF and lean Zucker skeletal muscle cultures and are the mean ± S.E.M. from 3 separate experiments on each.

Figure 5.12 The effects of chronic Rosiglitazone treatment on insulin-stimulated deGlc uptake in skeletal muscle cultures chronically treated with 5mM and 30mM D-glucose.

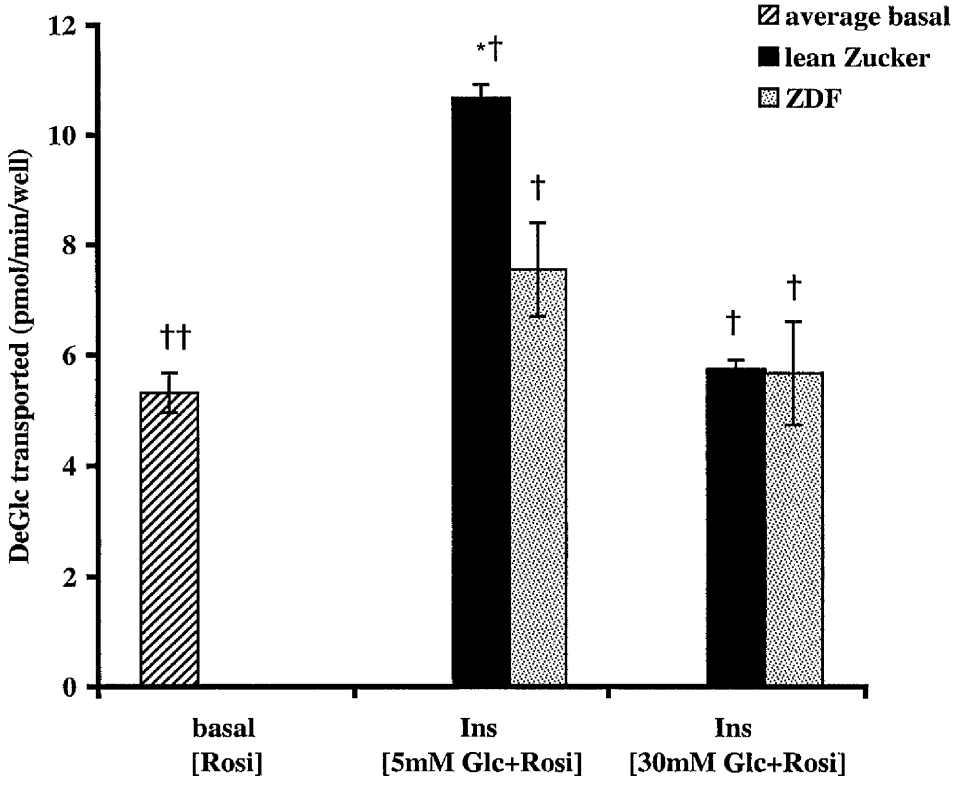

5.3 Discussion

This study was designed to extend the findings of the previous chapters, so as to test the hypothesis that the major cause of insulin resistance in the ZDF rat is a consequence of impaired insulin-dependent glucose uptake in skeletal muscle. I have shown that in the flexor digitorum brevis (FDB) muscle of the ZDF rat there is a marked decrease in the magnitude of insulin-stimulated deGlc transport with respect to the lean Zucker control muscles (see figure 5.1). Moreover, this diminished insulin response is also maintained in skeletal muscle cells cultured from extensor digitorum brevis (EDL) and soleus muscles, and persists in these cells throughout all passages (figure 5.10). These results strongly suggest that the defect in ZDF rats is due to a genetic predisposition, and is not due to an acute physiological change such as altered blood flow to the muscle or paracrine effects.

Given the importance of skeletal muscle in the post-prandial disposal of blood glucose, such a defect will greatly contribute to the overall diabetic phenotype of the ZDF rat. A number of studies on rats have suggested that while insulin-stimulated glucose transport is impaired in NIDDM and insulin-resistant states, exercise-stimulated glucose transport is unaffected (Goodyear et al., 1988); (Brozinick, Jr. et al., 1992); (King et al., 1993); (Brozinick, Jr. et al., 1994). As discussed earlier in 1.5.1 and chapter three, AMPK is implicated as a crucial mediator of the effects of exercise on glucose transport (Hayashi et al., 1998); (Fujii et al., 2000). Consequently, AICAR, which is able to activate AMPK, significantly increased glucose transport to a similar extent in both ZDF and lean Zucker animals (see figure 5.1). This result is in agreement with that of chapter three and suggests that the insulin resistance observed in the ZDF rat like the SHRSP rat is confined to an insulin-dependent event in the activation of glucose transport.

To further analyse this insulin-specific defect, I have examined the levels of expression of key proteins involved in the insulin-signalling transduction cascade namely, IRS-1, PI3K, caveolin-1, flotillin and c-Cbl. No significant difference was found in the expression levels of these proteins in EDL, soleus or tibialis muscles between ZDF and lean Zucker rats (see figure 5.2 and 5.8). The lack of significant difference in caveolin-1 and flotillin levels is in contrast to the observed increase in expression of these molecules seen in the insulin-resistant SHRSP rat (chapter three). However the similar protein expression levels

of PI3K and IRS-1 in lean Zucker and ZDF rats is in agreement with the analysis of these protein levels in WKY and SHRSP. These data may suggest that the caveolae-associated molecules do not influence the observed insulin resistance seen in the ZDF rat skeletal muscle. On the other hand, while PKB cellular expression is unchanged in EDL muscle in both ZDF and lean Zucker rats (see figure 5.3A), the insulin-stimulated activity of PKB in the EDL muscle lysates from ZDF rats is markedly diminished compared to lean Zuckers (see figure 5.4). I have also found that the insulin-dependent phosphorylation of the PKB serine 473 residue is reduced in ZDF rats compared to lean Zuckers (see figure 5.3B). Hence, defective insulin-dependent activation of PKB appears to underlie the diminished insulin-stimulated deGlc uptake. These observations are consistent with studies involving overexpression of constitutively active PKB, which leads to a significant increase in glycogen and protein synthesis and also glucose transport (Hajduch et al., 1998); (Kohn et al., 1996a); (Ueki et al., 1998); (Foran et al., 1999) all of which suggests PKB plays an important role in insulin-stimulated glucose uptake. However, overexpression of a putative dominant negative mutant of PKB was reported to inhibit protein synthesis but did not affect glucose transport (Kitamura et al., 1998), possibly due to some endogenous PKB activity remaining. Thus a mandatory role for PKB in insulin action on glucose transport has been implied but remains controversial. Nevertheless, the observed defect in insulin action on glucose transport may be partly due to the defective PKB activity and/or elements upstream of this kinase. Pharmacological activation of PKB may therefore be of potential therapeutic utility in the treatment of diabetes.

PKB agonists may have positive effects on responses further downstream, similar to those seen when constitutively active PKB is overexpressed in cells. In trying to address this, GlaxoSmithKline has isolated two compounds able to specifically activate PKB *in vitro*, SB456672 and SB437478. These compounds are thought to act by functionally mimicking PIP_3 binding to PKB, exposing the PDK1/2 phosphorylation sites. I have confirmed that both compounds are able to stimulate PDK1-dependent but PIP_3-independent, threonine-308 phosphorylation of recombinant PKBS473D (see figure 5.5). Intriguingly, SB437478 could also stimulate PKBS473D threonine-308 phosphorylation independently of PDK1, probably by allowing PKB autophosphorylation although activation of a contaminating kinase by this compound cannot be excluded (see figure 5.5). In addition, both compounds are able to significantly stimulate PKBS473D kinase activity *in vitro* (see figure 5.6).

In an effort to address whether PKB agonists in isolation could stimulate glucose transport, I treated FDB muscles from ZDF and lean Zucker rats with SB456672. As shown in figure 5.7, a small but non-significant enhancement in deGlc uptake was observed in muscle from each animal model. Both SB456672 and SB437478 are highly specific for PKB and allow activation of PKB *in vitro* of the compounds isolated from the *in vitro* screen. These compounds were characterised as lipophilic and as possessing low serum protein binding activity (GlaxoSmithkline data). However, in recent subsequent experiments no activation of PKB in response to these agents was observed in the Chang liver cell line, until the cells were ruptured by freeze thawing (GlaxoSmithkline data). This implies that these compounds lacked sufficient cell penetrance to support activation of endogenous PKB, therefore, unfortunately, cannot be used at this time to unanimously demonstrate the absolute requirement for PKB activation in insulin-dependent stimulation of glucose transport. Accordingly, the priority in developing these compounds as drugs would be to demonstrate that they are capable of supporting phosphorylation and therefore activation of endogenous PKB in cells. A demonstration of this will be essential in providing evidence for a direct co-relation between PKB activation and increase in deGlc uptake.

There has been increasing evidence that whole-body hyperglycaemia induces insulin resistance in muscle (Rossetti et al., 1987); (Rossetti, 2000). In an attempt to determine whether glucose acts directly on the muscle cell to impair insulin action I evaluated the effect of normo- and hyper-glycaemia on deGlc transport in cultured lean/ZDF muscle cells. Figure 5.11, demonstrates that in cells derived from lean Zucker, (30mM) D-glucose administration caused the glucose uptake efficiency to fall to levels similar to that observed in cells derived from the ZDF. This finding agrees with data showing that hyperglycaemia directly inhibits insulin-stimulated glucose utilisation and glucose transport in rat skeletal muscle (Richter et al., 1988); (Kurowski et al., 1999). No such decrease was observed in glucose uptake in ZDF skeletal muscle cells. However, it was suggested that the decrease in skeletal muscle glucose utilisation during hyperglycaemia is directly linked to inhibition of PKB (Kurowski et al., 1999); (Oku et al., 2001). As ZDF rats display ineffective activation of PKB activity by insulin (see figure 5.3 and 5.4), this finding could explain why hyperglycaemia fails to have a further effect on the glucose uptake in ZDF muscles. In agreement with these observations, recent data (Nawano et al., 2000) have shown that while hyperglycaemia can induce further insulin

resistance in adipose and hepatic tissue, it does not appreciably worsen the insulin resistant skeletal muscle of the ZDF rat.

As demonstrated in figure 5.11 the 3-fold insulin-dependent stimulation of deGlc uptake in cells derived from lean Zucker rats was abolished by hyperglycaemic conditions (30mM D-glucose for 6 days). No insulin-dependent stimulation was detectable (above basal) in cells derived from ZDF animals, and this was unaffected by hyperglycaemia, indicating that the ZDF-derived cells are already insulin-insensitive.

In order to assess the reversibility of the hyperglycaemic-induced insulin-resistance in lean Zucker muscle cells, I used Rosiglitazone, a member of the thiazolidinedione class of compounds known to reduce hyperglycaemia, hyperinsulinaemia and hypertriglyceridaemia (Park et al., 1998b). Chronic Rosiglitazone treatment (1μM for 3 days) caused an approximate 2.5-fold elevation in basal glucose transport (figure 5.12). The fold-stimulation elicited by insulin in these cells was not significantly altered (approximately 2.2-fold in the presence of Rosiglitazone *vs* 2.8-fold in the absence of Rosiglitazone). However, hyperglycaemic treatment abolished the insulin-dependent stimulation of glucose uptake. Again, no insulin-dependent glucose uptake was observed in cells from ZDF muscle (figure 5.12), and this was not further affected by hyperglycaemia.

Rosiglitazone treatment neither restored the insulin response in hyperglycaemic lean Zucker cells nor in ZDF cells. However, in all cases Rosiglitazone treatment significantly elevated basal glucose uptake rates. This suggests that the whole-body insulin-sensitising effects of the thiazolidinedione drugs are in part mediated in their enhancement of insulin-independent glucose uptake in skeletal muscle. These findings are in agreement with those reported in muscle cultures derived from diabetic patients (Park et al., 1998a). They found that treatment of human skeletal muscle cultures from obese Type 2 diabetic patients with Troglitazone was followed by a 2-fold increase in mRNA and protein expression of Glut-1 (the basal glucose transporter) but not Glut-4.

Chapter 6

Overview and conclusions.

6.1 General conclusions

Skeletal muscle plays a crucial role in the insulin-mediated post-prandial disposal of blood glucose. In addition, it is a highly specialised tissue that is well adapted to respond to the continually shifting, and at times disproportionate, energy demands required during exercise/contraction. To this extent, skeletal muscle is able to take up glucose in response to both the anabolic stimulus of insulin and the catabolic action of exercise. Insulin resistance, which manifests itself as a reduction in insulin's ability to stimulate glucose uptake, is of major pathogenic importance in several prevalent human disorders, including type 2 diabetes, hypertension and obesity. Interestingly, there is strong evidence to suggest that in these insulin-resistant individuals exercise stimulated glucose uptake is unaffected. It is therefore the purpose of much current research to make a distinction between the two individual mechanisms by which insulin and exercise elicit their action on skeletal muscle glucose uptake.

In an effort to explore these two mechanisms, I have examined insulin- and AICAR-stimulated glucose uptake in isolated skeletal muscle and cultured myocytes from the insulin-resistant hypertensive rat SHRSP and the obese type II diabetic ZDF rat. The insulin- and AICAR-stimulated deGlc uptake pattern from these two disease models was compared to that from their normal equivalent, WKY and lean Zucker rat respectively. AICAR has been used as an exercise-effect substitute due to its ability to activate AMPK, a molecule that is acutely activated during exercise in both human and rodent muscle. Present findings indicate that AMPK serves as a "cellular energy sensor" that inhibits non-essential ATP consuming biosynthetic pathways, thereby conserving ATP for more immediate cellular functions involved with survival such as muscle contraction. In addition, treatment of muscle with AICAR has been shown to activate glucose transport by a similar mechanism to exercise.

The results from deGlc transport experiments, reported in chapters three and four show that the SHRSP rat displays a blunted insulin-stimulated glucose transport at the level of skeletal muscle when compared to the normotensive WKY rat. This is in agreement with the previous observation by (Collison et al., 2000), who found that isolated adipocytes from the SHRSP were also markedly insulin resistant, displaying defective insulin-stimulated glucose transport and suppression of lipolysis. Taken together, such data

indicates that the SHRSP displays a marked insulin-resistance in fat and muscle, key insulin-sensitive peripheral tissues responsible for the disposal of the majority of the post-prandial blood glucose. However, AICAR-stimulated glucose transport was unaffected in skeletal muscle, suggesting that the defect responsible for the observed insulin resistance is confined to an insulin-specific step in the activation of glucose transport. By examining the overtly diabetic rat model, the Zucker diabetic fatty (ZDF) rat, some key similarities were found. Importantly, a marked decrease in skeletal muscle insulin-stimulated glucose transport is observed in the ZDF rat compared with the insulin-sensitive lean Zucker rat. In addition, AICAR is able to activate glucose transport to a similar extent in both ZDF and lean Zucker rats. The profile of insulin-stimulated glucose transport is maintained *in vitro*, in cultured skeletal muscle cells from ZDF and lean Zucker rats. Taken together these results suggest that like the SHRSP, the ZDF rat has a defect in the insulin-stimulated glucose transport in skeletal muscle and that *in situ* this insulin-resistance is also restricted to an insulin-specific step in the activation of glucose transport. These results are in agreement with current findings showing that exercise-stimulated glucose transport is unimpaired in insulin-resistant individuals and that insulin and exercise stimuli contribute to glucose uptake through two distinct pathways.

Following this initial characterisation, I focussed on examining possible causes of the observed skeletal muscle insulin resistance. Analysis of the expression levels of key proteins involved in insulin signalling and insulin-stimulated glucose transport starting with the insulin-responsive glucose transporter, Glut-4 were performed. On comparing SHRSP and WKY rats, no difference was found in the total cellular levels of this transporter and therefore decreased Glut-4 expression cannot explain the defect in SHRSP. Similar data were reported from a similar study on ZDF animals (Maier et al., 2000).

In addition, the expression or cellular localisation of other molecules such as IRS-1/2 and PI3K is unchanged between SHRSP and WKY. PKB expression and activity was also unaffected. In the ZDF and lean Zucker rat, expression of IRS-1, PI3K and PKB was found to be similar between the two animal types. However, PKB activity in conjunction with PKB ser473 phosphorylation was markedly decreased in ZDF skeletal muscle compared with lean Zucker skeletal muscle. This implies that the genetic defect in ZDF

rats is upstream of PKB. This result would support claims that PKB is potential pharmacological target in treatment of insulin resistance (Cohen, 1999); (Alessi, 2001).

Intriguingly, the total cellular expression levels of caveolin and flotillin are increased in the skeletal muscle from SHRSP compared to WKY. These proteins are important in insulin signal transduction and compartmentalisation. Caveolin is a structural protein and a key component of small flask-like invaginations of the plasma membrane called caveolae. Caveolae are important mediators of insulin receptor signalling. Indeed, the insulin receptor has been found to localise to caveolae and overexpression of caveolin enhances insulin receptor tyrosine kinase phosphorylation of IRS-1. Therefore, increased expression of caveolin positively modulates signalling through the insulin receptor. In this respect the observation of increased levels of caveolin in SHRSP compared to WKY skeletal muscle may be a consequence of defective insulin signalling, and so perhaps a means of compensation by the skeletal muscle cells by overexpressing an element that may enhance insulin action. Furthermore, insulin stimulation leads to the phosphorylation of caveolin and expression of caveolin increases as 3T3-L1 fibroblasts are differentiated into insulin-sensitive adipocytes. However, it cannot be ruled out that overexpression of caveolin seen here could result in a sequestration of important insulin signalling molecules in an inactive environment, thereby acting as an inhibitor of further downstream events resulting in decreased glucose transport. Intriguingly, the lipid raft protein flotillin is also markedly overexpressed in SHRSP muscle compared with WKY. Flotillin is able to form heterodimers with caveolin and has been proposed to localise the insulin receptor phosphorylated c-Cbl via the c-Cbl-associated protein (CAP) to caveolae. Recent studies suggest that CAP-c-Cbl localisation to caveolae is critical for insulin-stimulated glucose transport. Therefore, the closely associated caveolae molecules, flotillin and caveolin positively modulate insulin action. This close association may indicate a dual regulation of these proteins, in that overexpression of one may force or co-ordinately regulate the overexpression of the other. In preliminary experiments using real-time quantification of messenger RNA for caveolin and flotillin, I have found a two-fold increase in both flotillin and caveolin mRNA in SHRSP skeletal muscle compared with WKY. Although this data did not satisfy the criteria for inclusion in chapter three, it does potentially indicate that the regulation of flotillin and caveolin overexpression in SHRSP occurs at the level of mRNA and may not be due to decreased degradation of these proteins. However, further study is required to test whether the overexpression of

caveolin and flotillin act to blunt insulin-stimulated glucose transport. In contrast to the SHRSP model, in ZDF skeletal muscle lysates there was no significant increase in the lipid raft associated proteins c-Cbl, caveolin-1 or flotillin total cellular protein expression compared with that observed in normal lean Zuckers. These data may suggest that these molecules do not influence the observed insulin resistance seen in the ZDF rat skeletal muscle.

The SNARE proteins VAMP2 and syntaxin-4 were also markedly overexpressed in SHRSP skeletal muscle compared to WKY rats. These proteins are crucial in mediating insulin-stimulated Glut-4 vesicle translocation. They are also found to be overexpressed in other rat models of insulin resistance. Previous work from our laboratory has illustrated increased expression of the SNAREs VAMP2, cellubrevin and syntaxin-4 in ZDF muscles (Maier et al., 2000). However, like flotillin and caveolin further analysis is required to determine whether their overexpression is causal or adaptive to the observed skeletal muscle insulin resistance.

It is possible that the insulin resistance observed in the SHRSP and ZDF animals may be secondary to changes in physiology, such as altered blood flow to the muscle beds by defective vasodilatation in response to insulin, or by changes in circulating factors which regulate peripheral insulin sensitivity. In order to investigate this possibility, myotubes from SHRSP and ZDF animals were cultured through eight passages and were subjected to deGlc uptake assays in the presence of insulin. SHRSP myotubes were also tested for their ability to transport deGlc in the presence of AICAR. The first important finding is that the impaired insulin stimulation of glucose uptake is maintained in cultured myotubes from both SHRSP and ZDF rats. Moreover, AICAR-stimulated glucose transport in SHRSP myotubes is also unimpaired compared with WKY myotubes in agreement with the *in situ* data. Taken together these data suggest that the observed skeletal muscle insulin resistance constitutes a hereditary trait, characteristic to ZDF and SHRSP and is not due to altered blood flow or circulating factors. In addition, the observation that the AMPK-activator AICAR can stimulate glucose uptake in both SHRSP and WKY myotubes to the same extent further support the suggestion that the insulin resistance is confined to an insulin specific step in the activation of glucose transport. Moreover, in agreement with previous reports, AICAR-stimulated glucose transport, like exercise, is insensitive to the PI3K inhibitor wortmannin. In contrast, insulin-stimulated glucose

transport is completely abrogated by wortmannin. These data strongly indicate that like exercise, AICAR- stimulated glucose transport occurs via a PI3K-independent pathway.

Since the diabetic ZDF rat displays fasting hyperglycaemia associated with dyslipidaemia and obesity, the effect of hyperglycaemia on insulin-stimulated deGlc transport was also tested. The results showed that in the lean Zucker but not in the ZDF rat, hyperglycaemia inhibited insulin-stimulated glucose utilisation and glucose transport in agreement with other studies (Richter et al., 1988); (Kurowski et al., 1999). Since it has been shown that ZDF rats are characterised by low levels of PKB activity in response to insulin, this finding suggests that the decrease in skeletal muscle glucose utilisation during hyperglycaemia could be directly linked to inhibition of PKB. This may explain why hyperglycaemia fails to have a further effect on the glucose uptake in ZDF muscles, as illustrated in 5.11.

It might be speculated that pharmacological agents in the form of PKB agonists would have positive effects on responses further downstream, similar to those seen when constitutively active PKB is overexpressed in cells. I tested the ability of novel agonists SB456672 and SB437478 to influence downstream events, and I verified that these compounds can achieve PDK1-dependent but PIP_3-independent, threonine-308 phosphorylation and significant increases in activity of recombinant PKBS473D in a microtitre plate assay. Intriguingly, SB437478 could also stimulate PKBS473D threonine-308 phosphorylation independently of PDK1, probably by allowing PKB autophosphorylation although activation of a contaminating kinase by this compound cannot be excluded.

I then treated FDB muscles from ZDF and lean Zucker rats with SB456672 in an effort to address whether PKB agonists in isolation could stimulate glucose transport. However, the muscles were unresponsive to this drug, as was indicated by the non-significant increase in deGlc uptake, probably due to insufficient cell penetrance of this compound. New cell permeable agonists need to be developed with proven ability to specifically phosphorylate and therefore activate endogenous PKB. Such compounds could assist in further studies aimed at providing evidence for a direct co-relation between PKB activation and increase in deGlc uptake.

Type 2 diabetes mellitus is commonly managed with diet and exercise but in some cases pharmacological intervention is required. In general, these pharmacological compounds either stimulate the pancreas to produce more insulin or sensitise tissues such as muscle and fat to the action of insulin. The latter group of compounds able to re-sensitise the insulin-insensitive peripheral glucose storage tissues of fat and muscle to the actions of insulin is known as the thiazolidinediones. Rosiglitazone, an example of a thiazolidinedione, is able to reduce fasting blood glucose and triglycerides by increasing Glut-4 expression and re-sensitising fat cells to the action of insulin on the inhibition of hormone sensitive lipase. Rosiglitazone was used in the skeletal muscle cell cultures from ZDF and lean Zucker rats in order to assess the ability of this drug to ameliorate the defect in glucose transport observed in this system. Rosiglitazone was found to significantly increase the basal glucose uptake in skeletal muscle cells by approximately two-fold but had no further effect on insulin-stimulated glucose transport in lean or ZDF muscle cells cultured under normoglycaemic or hyperglycaemic conditions. This suggests that the whole-body insulin-sensitising effects of the thiazolidinedione drugs are in part mediated in their enhancement of insulin-independent glucose uptake in skeletal muscle. These findings are in agreement with those reported in muscle cultures derived from diabetic patients (Park et al., 1998a). They found that treatment of human skeletal muscle cultures from obese Type 2 diabetic patients with Troglitazone was followed by a 2-fold increase in mRNA and protein expression of Glut-1 (the basal glucose transporter) but not Glut-4.

6.2 Concluding remarks and suggestions for the future.

In summary, the findings of this thesis show that hypertensive SHRSP and type 2 diabetic ZDF rat models display a marked skeletal muscle insulin resistance. Furthermore, this insulin resistance is maintained in cultured skeletal muscle cells. Using these skeletal muscle systems, this study aimed at identifying intermediate molecules that could potentially be part of a defective step in the impaired insulin-stimulated deGlc uptake pathway, and it also aimed at the assessment of novel therapeutic agents such as PKB agonists. Using this system the possibility of two distinct pathways between insulin and exercise–mediated glucose uptake was investigated.

The conclusions drawn from these studies are the following:
Firstly, the data suggests that the ZDF and SHRSP models used in this project owe their skeletal muscle insulin-resistance phenotype to genetic make up rather than secondary pathophysiological effects. In addition, in the lean Zucker animal, hyperglycaemia, a characteristic of the ZDF rat was found from *in vitro* experiments to be a contributing/determining factor to the insulin-stimulated deGlc uptake defect.

Moreover, in support of accumulating data this system provided evidence for a distinction between insulin- and exercise-mediated deGlc transport pathways. In particular the data suggests that apart from the insulin-mediated pathway, AICAR through a PI3K-independent pathway can also significantly activate deGlc transport in skeletal muscle.

It would be interesting to pursue the analysis of the overexpression of caveolin and flotillin. Such analysis may indicate whether or not the overexpression of these molecules is primary or secondary to the defective insulin-stimulated glucose transport seen in SHRSP rats. In addition, it may also be of interest to examine the effect of insulin on the caveolae association of important signalling molecules, such as c-Cbl, in SHRSP and WKY animals.

Finally, assessment of lead compounds from the GlaxoSmithkline PKB activator screen lead to the conclusion that these particular compounds are unsuitable as therapeutic candidates and are not effective in experimental practice as endogenous biochemical component activators. There is therefore immediate need for the development of new cell-penetrant agents that will assist in the investigation of the specific components that comprise the insulin- and the exercise- stimulated glucose uptake pathway. Only by the complete identification of the downstream molecules and their roles, can the defective steps in insulin signalling pathway, as seen in type 2 diabetes, be completely elucidated in order for satisfactory therapy to be achieved.

Publications arising from this thesis

Declan J. James, Fiona Cairns, Ian P. Salt, Gregory J. Murphy, Anna F. Dominiczak, John M.C. Connell, and Gwyn W. Gould. (2001). Skeletal muscle of Stroke-Prone Spontaneously Hypertensive Rats exhibits reduced insulin-stimulated glucose transport and elevated levels of caveolin and flotillin. Diabetes. *50*(9), 2148-56.

Declan J. James, Mary Collison, Ian P. Salt, Anna F. Dominiczak, John M.C. Connell, and Gwyn W. Gould. (2000). Insulin- and AICA Riboside-stimulated glucose transport in primary muscle cultures from control and insulin resistant rats. Diabetes. *49* SUPP1, A240.

Reference List

Abbud, W., Habinowski, S., Zhang, J.Z., Kendrew, J., Elkairi, F.S., Kemp, B.E., Witters, L.A., and Ismail-Beigi, F. (2000). Stimulation of AMP-activated protein kinase (AMPK) is associated with enhancement of Glut1-mediated glucose transport. Arch. Biochem. Biophys. *380*, 347-352.

Ahmed, Z., Smith, B.J., and Pillay, T.S. (2000). The APS adapter protein couples the insulin receptor to the phosphorylation of c-Cbl and facilitates ligand-stimulated ubiquitination of the insulin receptor. FEBS Lett. *475*, 31-34.

Aitman, T.J. (2001). CD36, insulin resistance, and coronary heart disease. Lancet *357*, 651-652.

Aledo, J.C., Lavoie, L., Volchuk, A., Keller, S.R., Klip, A., and Hundal, H.S. (1997). Identification and characterisation of two distinct intracellular Glut-4 pools in rat skeletal muscle: evidence for an endosomal and an insulin- sensitive Glut-4 compartment. Biochem. J. *325 (Pt 3)*, 727-732.

Alessi, D.R. (2001). Discovery of PDK1, one of the missing links in insulin signal transduction. Colworth Medal Lecture. Biochem. Soc. Trans. *29*, 1-14.

Alessi, D.R., Andjelkovic, M., Caudwell, B., Cron, P., Morrice, N., Cohen, P., and Hemmings, B.A. (1996). Mechanism of activation of protein kinase B by insulin and IGF-1. EMBO J. *15*, 6541-6551.

Alessi, D.R., Deak, M., Casamayor, A., Caudwell, F.B., Morrice, N., Norman, D.G., Gaffney, P., Reese, C.B., MacDougall, C.N., Harbison, D., Ashworth, A., and Bownes, M. (1997a). 3-Phosphoinositide-dependent protein kinase-1 (PDK1): structural and functional homology with the Drosophila DSTPK61 kinase. Curr. Biol. *7*, 776-789.

Alessi, D.R., James, S.R., Downes, C.P., Holmes, A.B., Gaffney, P.R., Reese, C.B., and Cohen, P. (1997b). Characterisation of a 3-phosphoinositide-dependent protein kinase which phosphorylates and activates protein kinase B alpha. Curr. Biol. *7*, 261-269.

Allen, R.E., Dodson, M.V., Luiten, L.S., and Boxhorn, L.K. (1985). A serum-free medium that supports the growth of cultured skeletal muscle satellite cells. In Vitro Cell Dev. Biol. *21*, 636-640.

Anai, M., Funaki, M., Ogihara, T., Terasaki, J., Inukai, K., Katagiri, H., Fukushima, Y., Yazaki, Y., Kikuchi, M., Oka, Y., and Asano, T. (1998). Altered expression levels and impaired steps in the pathway to phosphatidylinositol 3-kinase activation via insulin receptor substrates 1 and 2 in Zucker fatty rats. Diabetes *47*, 13-23.

Andreasson, K., Galuska, D., Thorne, A., Sonnenfeld, T., and Wallberg-Henriksson, H. (1991). Decreased insulin-stimulated 3-0-methylglucose transport *in-vitro* incubated muscle strips from type 2 diabetic subjects. Acta Physiol Scand. *142*, 255-260.

Araki, E., Lipes, M.A., Patti, M.E., Bruning, J.C., Haag, B., Johnson, R.S., and Kahn, C.R. (1994). Alternative pathway of insulin signalling in mice with targeted disruption of the IRS-1 gene. Nature *372*, 186-190.

Arnold, H.H. and Winter, B. (1998). Muscle differentiation: more complexity to the network of myogenic regulators. Curr. Opin. Genet. Dev. *8*, 539-544.

Atkinson, M.A. and Eisenbarth, G.S. (2001). Type 1 diabetes: new perspectives on disease pathogenesis and treatment. Lancet *358,* 221-229.

Baldwin, S.A., Baldwin, J.M., Gorga, F.R., and Lienhard, G.E. (1979). Purification of the cytochalasin B binding component of the human erythrocyte monosaccharide transport system. Biochim. Biophys. Acta *552*, 183-188.

Balon, T.W. and Nadler, J.L. (1994). Nitric oxide release is present from incubated skeletal muscle preparations. J. Appl. Physiol *77*, 2519-2521.

Balon, T.W. and Nadler, J.L. (1996). Nitric oxide mediates skeletal glucose transport. Am. J. Physiol *270*, E1058-E1059.

Balon, T.W. and Nadler, J.L. (1997). Evidence that nitric oxide increases glucose transport in skeletal muscle. J. Appl. Physiol *82*, 359-363.

Bandyopadhyay, G., Kanoh, Y., Sajan, M.P., Standaert, M.L., and Farese, R.V. (2000). Effects of adenoviral gene transfer of wild-type, constitutively active, and kinase-defective protein kinase C-lambda on insulin-stimulated glucose transport in L6 myotubes. Endocrinology *141*, 4120-4127.

Bandyopadhyay, G., Standaert, M.L., Galloway, L., Moscat, J., and Farese, R.V. (1997). Evidence for involvement of protein kinase C (PKC)-zeta and non-involvement of diacylglycerol-sensitive PKCs in insulin-stimulated glucose transport in L6 myotubes. Endocrinology *138*, 4721-4731.

Banks, P., Bartley, W., and Birt, L.M. (1976). The biochemistry of the tissues. John Wiley & Sons Ltd.).

Baron, A.D. (1994). Haemodynamic actions of insulin. Am. J. Physiol *267*, E187-E202.

Barrett, M.P., Walmsley, A.R., and Gould, G.W. (1999). Structure and function of facilitative sugar transporters. Curr. Opin. Cell Biol. *11*, 496-502.

Baumann, C.A., Ribon, V., Kanzaki, M., Thurmond, D.C., Mora, S., Shigematsu, S., Bickel, P.E., Pessin, J.E., and Saltiel, A.R. (2000). CAP defines a second signalling pathway required for insulin-stimulated glucose transport. Nature *407*, 202-207.

Bergeron, R., Russell, R.R., III, Young, L.H., Ren, J.M., Marcucci, M., Lee, A., and Shulman, G.I. (1999). Effect of AMPK activation on muscle glucose metabolism in conscious rats. Am. J. Physiol *276*, E938-E944.

Birnbaum, M.J. (1989). Identification of a novel gene encoding an insulin-responsive glucose transporter protein. Cell *57*, 305-315.

Bjornholm, M., Kawano, Y., Lehtihet, M., and Zierath, J.R. (1997). Insulin receptor substrate-1 phosphorylation and phosphatidylinositol 3-kinase activity in skeletal muscle from NIDDM subjects after in vivo insulin stimulation. Diabetes *46*, 524-527.

Blair, A.S., Hajduch, E., Litherland, G.J., and Hundal, H.S. (1999). Regulation of glucose transport and glycogen synthesis in L6 muscle cells during oxidative stress. Evidence for cross-talk between the insulin and SAPK2/p38 mitogen-activated protein kinase signalling pathways. J. Biol. Chem. *274*, 36293-36299.

Blau, H.M. and Webster, C. (1981). Isolation and characterisation of human muscle cells. Proc. Natl. Acad. Sci. U. S. A *78*, 5623-5627.

Brozinick, J.T., Jr., Etgen, G.J., Jr., Yaspelkis, B.B. and Ivy, J.L. (1992). Contraction-activated glucose uptake is normal in insulin-resistant muscle of the obese Zucker rat. J. Appl. Physiol *73*, 382-387.

Brozinick, J.T., Jr., Etgen, G.J., Jr., Yaspelkis, B.B. and Ivy, J.L. (1994). Glucose uptake and Glut-4 protein distribution in skeletal muscle of the obese Zucker rat. Am. J. Physiol *267*, R236-R243.

Burgering, B.M. and Coffer, P.J. (1995). Protein kinase B (c-Akt) in phosphatidylinositol-3-OH kinase signal transduction. Nature *376*, 599-602.

Cain, C.C., Trimble, W.S., and Lienhard, G.E. (1992). Members of the VAMP family of synaptic vesicle proteins are components of glucose transporter-containing vesicles from rat adipocytes. J. Biol. Chem. *267* , 11681-11684.

Calera, M.R., Martinez, C., Liu, H., Jack, A.K., Birnbaum, M.J., and Pilch, P.F. (1998). Insulin increases the association of Akt-2 with Glut4-containing vesicles. J. Biol. Chem. *273*, 7201-7204.

Carling, D., Clarke, P.R., Zammit, V.A., and Hardie, D.G. (1989). Purification and characterisation of the AMP-activated protein kinase. Copurification of acetyl-CoA carboxylase kinase and 3-hydroxy-3- methylglutaryl-CoA reductase kinase activities. Eur. J. Biochem. *186*, 129-136.

Cheatham, B. and Kahn, C.R. (1995). Insulin action and the insulin signalling network. Endocr. Rev. *16*, 117-142.

Cheatham, B., Vlahos, C.J., Cheatham, L., Wang, L., Blenis, J., and Kahn, C.R. (1994). Phosphatidylinositol 3-kinase activation is required for insulin stimulation of pp70 S6 kinase, DNA synthesis, and glucose transporter translocation. Mol. Cell Biol. *14*, 4902-4911.

Cheatham, B., Volchuk, A., Kahn, C.R., Wang, L., Rhodes, C.J., and Klip, A. (1996). Insulin-stimulated translocation of Glut-4 glucose transporters requires SNARE-complex proteins. Proc. Natl. Acad. Sci. U. S. A *93*, 15169-15173.

Chen, D., Van Horn, D.J., White, M.F., and Backer, J.M. (1995). Insulin receptor substrate 1 rescues insulin action in CHO cells expressing mutant insulin receptors that lack a juxtamembrane NPXY motif. Mol. Cell Biol. *15*, 4711-4717.

Chen, Y.A. and Scheller, R.H. (2001). SNARE-mediated membrane fusion. Nat. Rev. Mol. Cell Biol. *2*, 98-106.

Chen, Z.P., McConell, G.K., Michell, B.J., Snow, R.J., Canny, B.J., and Kemp, B.E. (2000). AMPK signalling in contracting human skeletal muscle: acetyl-CoA carboxylase and NO synthase phosphorylation. Am. J. Physiol Endocrinol. Metab *279*, E1202-E1206.

Cheung, P.C., Salt, I.P., Davies, S.P., Hardie, D.G., and Carling, D. (2000). Characterisation of AMP-activated protein kinase gamma-subunit isoforms and their role in AMP binding. Biochem. J. *346 Pt 3*, 659-669.

Chiang, S.H., Baumann, C.A., Kanzaki, M., Thurmond, D.C., Watson, R.T., Neudauer, C.L., Macara, I.G., Pessin, J.E., and Saltiel, A.R. (2001). Insulin-stimulated Glut-4 translocation requires the CAP-dependent activation of TC10. Nature *410*, 944-948.

Chou, C.K., Dull, T.J., Russell, D.S., Gherzi, R., Lebwohl, D., Ullrich, A., and Rosen, O.M. (1987). Human insulin receptors mutated at the ATP-binding site lack protein tyrosine kinase activity and fail to mediate postreceptor effects of insulin. J. Biol. Chem. *262*, 1842-1847.

Ciaraldi, T.P., Abrams, L., Nikoulina, S., Mudaliar, S., and Henry, R.R. (1995). Glucose transport in cultured human skeletal muscle cells. Regulation by insulin and glucose in nondiabetic and non-insulin-dependent diabetes mellitus subjects. J. Clin. Invest *96*, 2820-2827.

Clark, S.F., Martin, S., Carozzi, A.J., Hill, M.M., and James, D.E. (1998). Intracellular localisation of phosphatidylinositide 3-kinase and insulin receptor substrate-1 in adipocytes: potential involvement of a membrane skeleton. J. Cell Biol. *140*, 1211-1225.

Clark, S.F., Molero, J.C., and James, D.E. (2000). Release of insulin receptor substrate proteins from an intracellular complex coincides with the development of insulin resistance. J. Biol. Chem. *275*, 3819-3826.

Clarke, J.F., Young, P.W., Yonezawa, K., Kasuga, M., and Holman, G.D. (1994). Inhibition of the translocation of Glut-1 and Glut-4 in 3T3-L1 cells by the phosphatidylinositol 3-kinase inhibitor, wortmannin. Biochem. J. *300 (Pt 3)*, 631-635.

Cleland, S.J., Petrie, J.R., Ueda, S., Elliott, H.L., and Connell, J.M. (1998). Insulin as a vascular hormone: implications for the pathophysiology of cardiovascular disease. Clin. Exp. Pharmacol. Physiol *25*, 175-184.

Coderre, L., Kandror, K.V., Vallega, G., and Pilch, P.F. (1995). Identification and characterisation of an exercise-sensitive pool of glucose transporters in skeletal muscle. J. Biol. Chem. *270*, 27584-27588.

Coderre, L., Monfar, M.M., Chen, K.S., Heydrick, S.J., Kurowski, T.G., Ruderman, N.B., and Pilch, P.F. (1992). Alteration in the expression of Glut-1 and Glut-4 protein and messenger RNA levels in denervated rat muscles. Endocrinology *131*, 1821-1825.

Coffer, P.J., Jin, J., and Woodgett, J.R. (1998). Protein kinase B (c-Akt): a multifunctional mediator of phosphatidylinositol 3-kinase activation. Biochem. J. *335 (Pt 1)*, 1-13.

Cohen, P. (1999). The Croonian Lecture 1998. Identification of a protein kinase cascade of major importance in insulin signal transduction. Philos. Trans. R. Soc. Lond B Biol. Sci. *354*, 485-495.

Collison, M., Glazier, A.M., Graham, D., Morton, J.J., Dominiczak, M.H., Aitman, T.J., Connell, J.M., Gould, G.W., and Dominiczak, A.F. (2000). Cd36 and molecular mechanisms of insulin resistance in the stroke-prone spontaneously hypertensive rat. Diabetes *49*, 2222-2226.

Colville, C.A., Seatter, M.J., Jess, T.J., Gould, G.W., and Thomas, H.M. (1993). Kinetic analysis of the liver-type (GLUT2) and brain-type (GLUT3) glucose transporters in Xenopus oocytes: substrate specificities and effects of transport inhibitors. Biochem. J. *290 (Pt 3)*, 701-706.

Cornelison, D.D., Olwin, B.B., Rudnicki, M.A., and Wold, B.J. (2000). MyoD(-/-) satellite cells in single-fibre culture are differentiation defective and MRF4 deficient. Dev. Biol. *224*, 122-137.

Cornelison, D.D. and Wold, B.J. (1997). Single-cell analysis of regulatory gene expression in quiescent and activated mouse skeletal muscle satellite cells. Dev. Biol. *191*, 270-283.

Corton, J.M., Gillespie, J.G., and Hardie, D.G. (1994). Role of the AMP-activated protein kinase in the cellular stress response. Curr. Biol. *4*, 315-324.

Cross, D.A., Alessi, D.R., Cohen, P., Andjelkovich, M., and Hemmings, B.A. (1995). Inhibition of glycogen synthase kinase-3 by insulin mediated by protein kinase B. Nature *378*, 785-789.

Cushman, S.W. and Wardzala, L.J. (1980). Potential mechanism of insulin action on glucose transport in the isolated rat adipose cell. Apparent translocation of intracellular transport systems to the plasma membrane. J. Biol. Chem. *255*, 4758-4762.

Czech, M.P. and Corvera, S. (1999). Signalling mechanisms that regulate glucose transport. J. Biol. Chem. *274*, 1865-1868.

Darakhshan, F., Kristiansen, S., Richter, E., and Hundal, H.S. (1997). GLUT5 and fructose transport in human skeletal muscle. Biochem. Soc. Trans. *25*, 473S.

Davidson, M.B., Bouch, C., Venkatesan, N., and Karjala, R.G. (1994a). Impaired glucose transport in skeletal muscle but normal Glut-4 tissue distribution in glucose-infused rats. Am. J. Physiol *267*, E808-E813.

Davidson, M.B., Hunt, K., and Fernandez-Mejia, C. (1994b). The hexosamine biosynthetic pathway and glucose-induced down regulation of glucose transport in L6 myotubes. Biochim. Biophys. Acta *1201*, 113-117.

DeFronzo, R.A., Ferrannini, E., Sato, Y., Felig, P., and Wahren, J. (1981). Synergistic interaction between exercise and insulin on peripheral glucose uptake. J. Clin. Invest *68*, 1468-1474.

DeFronzo, R.A., Gunnarsson, R., Bjorkman, O., Olsson, M., and Wahren, J. (1985). Effects of insulin on peripheral and splanchnic glucose metabolism in non-insulin-dependent (type 2) diabetes mellitus. J. Clin. Invest *76*, 149-155.

Dohm, G.L., Tapscott, E.B., Pories, W.J., Dabbs, D.J., Flickinger, E.G., Meelheim, D., Fushiki, T., Atkinson, S.M., Elton, C.W., and Caro, J.F. (1988). An in vitro human muscle preparation suitable for metabolic studies. Decreased insulin stimulation of glucose transport in muscle from morbidly obese and diabetic subjects. J. Clin. Invest *82*, 486-494.

Donnelly, R. and Connell, J.M. (1992). Insulin resistance: possible role in the aetiology and clinical course of hypertension. Clin. Sci. (Colch.) *83*, 265-275.

Douen, A.G., Ramlal, T., Rastogi, S., Bilan, P.J., Cartee, G.D., Vranic, M., Holloszy, J.O., and Klip, A. (1990). Exercise induces recruitment of the "insulin-responsive glucose transporter". Evidence for distinct intracellular insulin- and exercise- recruitable transporter pools in skeletal muscle. J. Biol. Chem. *265*, 13427-13430.

Ebina, Y., Araki, E., Taira, M., Shimada, F., Mori, M., Craik, C.S., Siddle, K., Pierce, S.B., Roth, R.A., and Rutter, W.J. (1987). Replacement of lysine residue 1030 in the putative ATP-binding region of the insulin receptor abolishes insulin- and antibody-stimulated glucose uptake and receptor kinase activity. Proc. Natl. Acad. Sci. U. S. A *84*, 704-708.

Folli, F., Saad, M.J., Backer, J.M., and Kahn, C.R. (1993). Regulation of phosphatidylinositol 3-kinase activity in liver and muscle of animal models of insulin-resistant and insulin-deficient diabetes mellitus. J. Clin. Invest *92*, 1787-1794.

Foran, P.G., Fletcher, L.M., Oatey, P.B., Mohammed, N., Dolly, J.O., and Tavare, J.M. (1999). Protein kinase B stimulates the translocation of Glut-4 but not Glut-1 or transferrin receptors in 3T3-L1 adipocytes by a pathway involving SNAP- 23, synaptobrevin-2, and/or cellubrevin. J. Biol. Chem. *274*, 28087-28095.

Frech, M., Andjelkovic, M., Ingley, E., Reddy, K.K., Falck, J.R., and Hemmings, B.A. (1997). High affinity binding of inositol phosphates and phosphoinositides to the

pleckstrin homology domain of RAC/protein kinase B and their influence on kinase activity. J. Biol. Chem. *272*, 8474-8481.

Friedman, J.E., Dudek, R.W., Whitehead, D.S., Downes, D.L., Frisell, W.R., Caro, J.F., and Dohm, G.L. (1991). Immunolocalisation of glucose transporter Glut-4 within human skeletal muscle. Diabetes *40*, 150-154.

Friedman, J.E., Ishizuka, T., Shao, J., Huston, L., Highman, T., and Catalano, P. (1999). Impaired glucose transport and insulin receptor tyrosine phosphorylation in skeletal muscle from obese women with gestational diabetes. Diabetes *48*, 1807-1814.

Fujii, N., Hayashi, T., Hirshman, M.F., Smith, J.T., Habinowski, S.A., Kaijser, L., Mu, J., Ljungqvist, O., Birnbaum, M.J., Witters, L.A., Thorell, A., and Goodyear, L.J. (2000). Exercise induces isoform-specific increase in 5'AMP-activated protein kinase activity in human skeletal muscle. Biochem. Biophys. Res. Commun. *273*, 1150-1155.

Fukumoto, H., Kayano, T., Buse, J.B., Edwards, Y., Pilch, P.F., Bell, G.I., and Seino, S. (1989). Cloning and characterisation of the major insulin-responsive glucose transporter expressed in human skeletal muscle and other insulin- responsive tissues. J. Biol. Chem. *264*, 7776-7779.

Fushiki, T., Wells, J.A., Tapscott, E.B., and Dohm, G.L. (1989). Changes in glucose transporters in muscle in response to exercise. Am. J. Physiol *256*, E580-E587.

Galbiati, F., Razani, B., and Lisanti, M.P. (2001). Emerging themes in lipid rafts and caveolae. Cell *106*, 403-411.

Garvey, W.T., Maianu, L., Hancock, J.A., Golichowski, A.M., and Baron, A. (1992). Gene expression of Glut-4 in skeletal muscle from insulin-resistant patients with obesity, IGT, GDM, and NIDDM. Diabetes *41*, 465-475.

Garvey, W.T., Maianu, L., Zhu, J.H., Brechtel-Hook, G., Wallace, P., and Baron, A.D. (1998). Evidence for defects in the trafficking and translocation of Glut-4 glucose transporters in skeletal muscle as a cause of human insulin resistance. J. Clin. Invest *101*, 2377-2386.

Gaster, M., Handberg, A., Beck-Nielsen, H., and Schroder, H.D. (2000). Glucose transporter expression in human skeletal muscle fibers. Am. J. Physiol Endocrinol. Metab *279*, E529-E538.

Goodyear, L.J. (2000). AMP-activated protein kinase: a critical signalling intermediary for exercise-stimulated glucose transport? Exerc. Sport Sci. Rev. *28*, 113-116.

Goodyear, L.J., Giorgino, F., Sherman, L.A., Carey, J., Smith, R.J., and Dohm, G.L. (1995). Insulin receptor phosphorylation, insulin receptor substrate-1 phosphorylation, and phosphatidylinositol 3-kinase activity are decreased in intact skeletal muscle strips from obese subjects. J. Clin. Invest *95*, 2195-2204.

Goodyear, L.J., Hirshman, M.F., and Horton, E.S. (1991). Exercise-induced translocation of skeletal muscle glucose transporters. Am. J. Physiol *261*, E795-E799.

Goodyear, L.J., Hirshman, M.F., Knutson, S.M., Horton, E.D., and Horton, E.S. (1988). Effect of exercise training on glucose homeostasis in normal and insulin-deficient diabetic rats. J. Appl. Physiol *65*, 844-851.

Goodyear, L.J. and Kahn, B.B. (1998). Exercise, glucose transport, and insulin sensitivity. Annu. Rev. Med. *49*, 235-261.

Gorga, F.R., Baldwin, S.A., and Lienhard, G.E. (1979). The monosaccharide transporter from human erythrocytes is heterogeneously glycosylated. Biochem. Biophys. Res. Commun. *91*, 955-961.

Gould, G.W., Merrall, N.W., Martin, S., Jess, T.J., Campbell, I.W., Calderhead, D.M., Gibbs, E.M., Holman, G.D., and Plevin, R.J. (1994). Growth factor-induced stimulation of hexose transport in 3T3-L1 adipocytes: evidence that insulin-induced translocation of Glut-4 is independent of activation of MAP kinase. Cell Signal. *6*, 313-320.

Gould, G.W. and Seatter, M.J. (1997). Introduction to the facilitative glucose transporter family. In Facilitative glucose transporters, G.W.Gould, ed. R.G.Landes), pp. 1-37.

Greenfield, M.S., Doberne, L., Rosenthal, M., Schulz, B., Widstrom, A., and Reaven, G.M. (1982). Effect of sulfonylurea treatment on in vivo insulin secretion and action in patients with non-insulin-dependent diabetes mellitus. Diabetes *31*, 307-312.

Guilherme, A. and Czech, M.P. (1998). Stimulation of IRS-1-associated phosphatidylinositol 3-kinase and Akt/protein kinase B but not glucose transport by beta1-integrin signalling in rat adipocytes. J. Biol. Chem. *273*, 33119-33122.

Guillet-Deniau, I., Leturque, A., and Girard, J. (1994). Expression and cellular localisation of glucose transporters (Glut-1, Glut-3, Glut-4) during differentiation of myogenic cells isolated from rat foetuses. J. Cell Sci. *107 (Pt 3)*, 487-496.

Gustavsson, J., Parpal, S., Karlsson, M., Ramsing, C., Thorn, H., Borg, M., Lindroth, M., Peterson, K.H., Magnusson, K.E., and Stralfors, P. (1999). Localisation of the insulin receptor in caveolae of adipocyte plasma membrane. FASEB J. *13*, 1961-1971.

Hager, S.R., Jochen, A.L., and Kalkhoff, R.K. (1991). Insulin resistance in normal rats infused with glucose for 72 h. Am. J. Physiol *260*, E353-E362.

Hajduch, E., Alessi, D.R., Hemmings, B.A., and Hundal, H.S. (1998). Constitutive activation of protein kinase B alpha by membrane targeting promotes glucose and system A amino acid transport, protein synthesis, and inactivation of glycogen synthase kinase 3 in L6 muscle cells. Diabetes *47*, 1006-1013.

Hajduch, E., Litherland, G.J., and Hundal, H.S. (2001). Protein kinase B (PKB/Akt)--a key regulator of glucose transport? FEBS Lett. *492*, 199-203.

Ham, R.G., St Clair, J.A., Webster, C., and Blau, H.M. (1988). Improved media for normal human muscle satellite cells: serum-free clonal growth and enhanced growth with low serum. In Vitro Cell Dev. Biol. *24*, 833-844.

Hansen, T., Andersen, C.B., Echwald, S.M., Urhammer, S.A., Clausen, J.O., Vestergaard, H., Owens, D., Hansen, L., and Pedersen, O. (1997). Identification of a common amino acid polymorphism in the p85alpha regulatory subunit of phosphatidylinositol 3-kinase: effects on glucose disappearance constant, glucose effectiveness, and the insulin sensitivity index. Diabetes *46*, 494-501.

Hara, K., Yonezawa, K., Sakaue, H., Ando, A., Kotani, K., Kitamura, T., Kitamura, Y., Ueda, H., Stephens, L., and Jackson, T.R. (1994). 1-Phosphatidylinositol 3-kinase activity is required for insulin- stimulated glucose transport but not for RAS activation in CHO cells. Proc. Natl. Acad. Sci. U. S. A *91*, 7415-7419.

Hardie, D.G. and Carling, D. (1997). The AMP-activated protein kinase--fuel gauge of the mammalian cell? Eur. J. Biochem. *246*, 259-273.

Hashiramoto, M.; James, D.E. (2000). Characterization of insulin-responsive GLUT4 storage vesicles isolated from 3T3-L1 adipocytes. Mol.Cell Biol. *20*, 416- 427

Hauschka, S.D. and Konigsberg, I.R. (1966). The influence of collagen on the development of muscle clones. Proc. Natl. Acad. Sci. U. S. A *55*, 119-126.

Hawley, S.A., Selbert, M.A., Goldstein, E.G., Edelman, A.M., Carling, D., and Hardie, D.G. (1995). 5'-AMP activates the AMP-activated protein kinase cascade, and Ca2+/calmodulin activates the calmodulin-dependent protein kinase I cascade, via three independent mechanisms. J. Biol. Chem. *270*, 27186-27191.

Hayashi, T., Hirshman, M.F., Kurth, E.J., Winder, W.W., and Goodyear, L.J. (1998). Evidence for 5' AMP-activated protein kinase mediation of the effect of muscle contraction on glucose transport. Diabetes *47*, 1369-1373.

Hayashi, T., Wojtaszewski, J.F., and Goodyear, L.J. (1997). Exercise regulation of glucose transport in skeletal muscle. Am. J. Physiol *273*, E1039-E1051.

Heller-Harrison, R.A., Morin, M., Guilherme, A., and Czech, M.P. (1996). Insulin-mediated targeting of phosphatidylinositol 3-kinase to Glut4-containing vesicles. J. Biol. Chem. *271*, 10200-10204.

Henry, R.R., Abrams, L., Nikoulina, S., and Ciaraldi, T.P. (1995). Insulin action and glucose metabolism in nondiabetic control and NIDDM subjects. Comparison using human skeletal muscle cell cultures. Diabetes *44*, 936-946.

Henry, R.R., Wallace, P., and Olefsky, J.M. (1986). Effects of weight loss on mechanisms of hyperglycaemia in obese non- insulin-dependent diabetes mellitus. Diabetes *35*, 990-998.

Heydrick, S.J., Gautier, N., Olichon-Berthe, C., Van Obberghen, E., and Marchand-Brustel, Y. (1995). Early alteration of insulin stimulation of PI 3-kinase in muscle and adipocyte from gold thioglucose obese mice. Am. J. Physiol *268*, E604-E612.

Heydrick, S.J., Jullien, D., Gautier, N., Tanti, J.F., Giorgetti, S., Van Obberghen, E., and Marchand-Brustel, Y. (1993). Defect in skeletal muscle phosphatidylinositol-3-kinase in obese insulin-resistant mice. J. Clin. Invest *91*, 1358-1366.

Hill, M.M., Clark, S.F., Tucker, D.F., Birnbaum, M.J., James, D.E., and Macaulay, S.L. (1999). A role for protein kinase B beta/Akt2 in insulin-stimulated Glut-4 translocation in adipocytes. Mol. Cell Biol. *19*, 7771-7781.

Himsworth, H.P. (1936). Diabetes mellitus: Its differentiation into insulin-sensitive and insulin-insensitive types. Lancet *1* , 127-130.

Holman, G.D. and Cushman, S.W. (1994). Subcellular localisation and trafficking of the Glut-4 glucose transporter isoform in insulin-responsive cells. Bioessays *16*, 753-759.

Holman, G.D., Lo, L.L., and Cushman, S.W. (1994). Insulin-stimulated Glut-4 glucose transporter recycling. A problem in membrane protein subcellular trafficking through multiple pools. J. Biol. Chem. *269*, 17516-17524.

Holman, G.D. and Sandoval, I.V. (2001). Moving the insulin-regulated glucose transporter Glut-4 into and out of storage. Trends Cell Biol. *11*, 173-179.

Houmard, J.A., Hickey, M.S., Tyndall, G.L., Gavigan, K.E., and Dohm, G.L. (1995). Seven days of exercise increase Glut-4 protein content in human skeletal muscle. J. Appl. Physiol *79*, 1936-1938.

Hubbard, S.R. (1997). Crystal structure of the activated insulin receptor tyrosine kinase in complex with peptide substrate and ATP analogue. EMBO J. *16*, 5572-5581.

Hubbard, S.R., Wei, L., Ellis, L., and Hendrickson, W.A. (1994). Crystal structure of the tyrosine kinase domain of the human insulin receptor. Nature *372*, 746-754.

Hughes, V.A., Fiatarone, M.A., Fielding, R.A., Kahn, B.B., Ferrara, C.M., Shepherd, P., Fisher, E.C., Wolfe, R.R., Elahi, D., and Evans, W.J. (1993). Exercise increases muscle Glut-4 levels and insulin action in subjects with impaired glucose tolerance. Am. J. Physiol *264*, E855-E862.

Hundal, H.S., Ahmed, A., Guma, A., Mitsumoto, Y., Marette, A., Rennie, M.J., and Klip, A. (1992). Biochemical and immunocytochemical localisation of the 'GLUT5 glucose transporter' in human skeletal muscle. Biochem. J. *286 (Pt 2)*, 339-343.

Hutber, C.A., Hardie, D.G., and Winder, W.W. (1997). Electrical stimulation inactivates muscle acetyl-CoA carboxylase and increases AMP-activated protein kinase. Am. J. Physiol *272*, E262-E266.

Inoue, G., Cheatham, B., Emkey, R., and Kahn, C.R. (1998). Dynamics of insulin signalling in 3T3-L1 adipocytes. Differential compartmentalisation and trafficking of insulin receptor substrate (IRS)-1 and IRS-2. J. Biol. Chem. *273*, 11548-11555.

Isakoff, S.J., Taha, C., Rose, E., Marcusohn, J., Klip, A., and Skolnik, E.Y. (1995). The inability of phosphatidylinositol 3-kinase activation to stimulate Glut-4 translocation indicates additional signalling pathways are required for insulin-stimulated glucose uptake. Proc. Natl. Acad. Sci. U. S. A *92*, 10247-10251.

Jackson, S., Bagstaff, S.M., Lynn, S., Yeaman, S.J., Turnbull, D.M., and Walker, M. (2000). Decreased insulin responsiveness of glucose uptake in cultured human skeletal muscle cells from insulin-resistant nondiabetic relatives of type 2 diabetic families. Diabetes *49*, 1169-1177.

James, D.E., Burleigh, K.M., and Kraegen, E.W. (1986). In vivo glucose metabolism in individual tissues of the rat. Interaction between epinephrine and insulin. J. Biol. Chem. *261*, 6366-6374.

James, D.E., Strube, M., and Mueckler, M. (1989). Molecular cloning and characterisation of an insulin-regulatable glucose transporter. Nature *338*, 83-87.

Jeffs, B., Clark, J.S., Anderson, N.H., Gratton, J., Brosnan, M.J., Gauguier, D., Reid, J.L., Macrae, I.M., Dominiczak, A.F. (1997). Sensitivity to cerebral ischaemic insult in a rat model of stroke is determined by a single genetic locus. Nat. Genet. *16*: 364-367.

Jiang, T., Sweeney, G., Rudolf, M.T., Klip, A., Traynor-Kaplan, A., and Tsien, R.Y. (1998). Membrane-permeant esters of phosphatidylinositol 3,4,5-trisphosphate. J. Biol. Chem. *273*, 11017-11024.

Joost, H.G. and Thorens, B. (2001). The extended GLUT-family of sugar/polyol transport facilitators: nomenclature, sequence characteristics, and potential function of its novel members (review). Mol. Membr. Biol. *18*, 247-256.

Julius, S., Gudbrandsson, T., Jamerson, K., Tariq, S.S., and Andersson, O. (1991). The haemodynamic link between insulin resistance and hypertension. J. Hypertens. *9*, 983-986.

Kahn, B.B. (1992). Alterations in glucose transporter expression and function in diabetes: mechanisms for insulin resistance. J. Cell Biochem. *48*, 122-128.

Kahn, B.B., Rosen, A.S., Bak, J.F., Andersen, P.H., Damsbo, P., Lund, S., and Pedersen, O. (1992). Expression of Glut-1 and Glut-4 glucose transporters in skeletal muscle of humans with insulin-dependent diabetes mellitus: regulatory effects of metabolic factors. J. Clin. Endocrinol. Metab *74* , 1101-1109.

Kahn, B.B., Shulman, G.I., DeFronzo, R.A., Cushman, S.W., and Rossetti, L. (1991). Normalisation of blood glucose in diabetic rats with phlorizin treatment reverses insulin-resistant glucose transport in adipose cells without restoring glucose transporter gene expression. J. Clin. Invest *87*, 561-570.

Kaliman, P., Vinals, F., Testar, X., Palacin, M., and Zorzano, A. (1995). Disruption of Glut-1 glucose carrier trafficking in L6E9 and Sol8 myoblasts by the phosphatidylinositol 3-kinase inhibitor wortmannin. Biochem. J. *312 (Pt 2)*, 471-477.

Kasahara, M. and Hinkle, P.C. (1977). Reconstitution and purification of the D-glucose transporter from human erythrocytes. J. Biol. Chem. *252*, 7384-7390.

Kasuga, M., Karlsson, F.A., and Kahn, C.R. (1982a). Insulin stimulates the phosphorylation of the 95,000-dalton subunit of its own receptor. Science *215*, 185-187.

Kasuga, M., Hedo, J.A., Yamada, K.M., and Kahn, C.R. (1982b). The structure of insulin receptor and its subunits. Evidence for multiple nonreduced forms and a 210,000 possible proreceptor. J. Biol. Chem. *257*, 10392-10399.

Kasuga, M., Zick, Y., Blith, D.L., Karlsson, F.A., Haring, H.U., and Kahn, C.R. (1982c). Insulin stimulation of phosphorylation of the beta subunit of the insulin receptor. Formation of both phosphoserine and phosphotyrosine. J. Biol. Chem. *257*, 9891-9894.

Katz, L.D., Glickman, M.G., Rapoport, S., Ferrannini, E., and DeFronzo, R.A. (1983). Splanchnic and peripheral disposal of oral glucose in man. Diabetes *32*, 675-679.

Kayano, T., Burant, C.F., Fukumoto, H., Gould, G.W., Fan, Y.S., Eddy, R.L., Byers, M.G., Shows, T.B., Seino, S., and Bell, G.I. (1990). Human facilitative glucose transporters. Isolation, functional characterisation, and gene localisation of cDNAs encoding an isoform (GLUT5) expressed in small intestine, kidney, muscle, and adipose tissue and an unusual glucose transporter pseudogene-like sequence (GLUT6). J. Biol. Chem. *265*, 13276-13282.

Kayano, T., Fukumoto, H., Eddy, R.L., Fan, Y.S., Byers, M.G., Shows, T.B., and Bell, G.I. (1988). Evidence for a family of human glucose transporter-like proteins. Sequence and gene localisation of a protein expressed in foetal skeletal muscle and other tissues. J. Biol. Chem. *263*, 15245-15248.

Kennedy, J.W., Hirshman, M.F., Gervino, E.V., Ocel, J.V., Forse, R.A., Hoenig, S.J., Aronson, D., Goodyear, L.J., and Horton, E.S. (1999). Acute exercise induces Glut-4 translocation in skeletal muscle of normal human subjects and subjects with type 2 diabetes. Diabetes *48*, 1192-1197.

Khan, A.H., Thurmond, D.C., Yang, C., Ceresa, B.P., Sigmund, C.D., and Pessin, J.E. (2001). Munc18c regulates insulin-stimulated Glut-4 translocation to the transverse tubules in skeletal muscle. J. Biol. Chem. *276*, 4063-4069.

Khayat, Z.A., Tong, P., Yaworsky, K., Bloch, R.J., and Klip, A. (2000). Insulin-induced actin filament remodelling colocalizes actin with phosphatidylinositol 3-kinase and Glut-4 in L6 myotubes. J. Cell Sci. *113 Pt 2*, 279-290.

Kim, Y.B., Nikoulina, S.E., Ciaraldi, T.P., Henry, R.R., and Kahn, B.B. (1999). Normal insulin-dependent activation of Akt/protein kinase B, with diminished activation of phosphoinositide 3-kinase, in muscle in type 2 diabetes. J. Clin. Invest *104*, 733-741.

King, P.A., Betts, J.J., Horton, E.D., and Horton, E.S. (1993). Exercise, unlike insulin, promotes glucose transporter translocation in obese Zucker rat muscle. Am. J. Physiol *265*, R447-R452.

Kitamura, T., Ogawa, W., Sakaue, H., Hino, Y., Kuroda, S., Takata, M., Matsumoto, M., Maeda, T., Konishi, H., Kikkawa, U., and Kasuga, M. (1998). Requirement for activation of the serine-threonine kinase Akt (protein kinase B) in insulin stimulation of protein synthesis but not of glucose transport. Mol. Cell Biol. *18*, 3708-3717.

Klip, A., Li, G., and Logan, W.J. (1984). Induction of sugar uptake response to insulin by serum depletion in fusing L6 myoblasts. Am. J. Physiol *247*, E291-E296.

Klip, A. and Paquet, M.R. (1990). Glucose transport and glucose transporters in muscle and their metabolic regulation. Diabetes Care *13*, 228-243.

Kohn, A.D., Summers, S.A., Birnbaum, M.J., and Roth, R.A. (1996a). Expression of a constitutively active Akt Ser/Thr kinase in 3T3-L1 adipocytes stimulates glucose uptake and glucose transporter 4 translocation. J. Biol. Chem. *271*, 31372-31378.

Kohn, A.D., Takeuchi, F., and Roth, R.A. (1996b). Akt, a pleckstrin homology domain containing kinase, is activated primarily by phosphorylation. J. Biol. Chem. *271*, 21920-21926.

Kolterman, O.G. and Olefsky, J.M. (1984). The impact of sulfonylurea treatment upon the mechanisms responsible for the insulin resistance in type 2 diabetes. Diabetes Care *7 Suppl 1*, 81-88.

Konigsberg, I.R. (1979). Skeletal myoblasts in culture. Methods Enzymol. *58*, 511-527.

Kotani, K., Ogawa, W., Matsumoto, M., Kitamura, T., Sakaue, H., Hino, Y., Miyake, K., Sano, W., Akimoto, K., Ohno, S., and Kasuga, M. (1998). Requirement of atypical protein kinase C lambda for insulin stimulation of glucose uptake but not for Akt activation in 3T3-L1 adipocytes. Mol. Cell Biol. *18*, 6971-6982.

Kristiansen, S., Darakhshan, F., Richter, E.A., and Hundal, H.S. (1997). Fructose transport and GLUT-5 protein in human sarcolemmal vesicles. Am. J. Physiol *273*, E543-E548.

Krook, A. and O'Rahilly, S. (1996). Mutant insulin receptors in syndromes of insulin resistance. Baillieres Clin. Endocrinol. Metab *10*, 97-122.

Krook, A., Roth, R.A., Jiang, X.J., Zierath, J.R., and Wallberg-Henriksson, H. (1998). Insulin-stimulated Akt kinase activity is reduced in skeletal muscle from NIDDM subjects. Diabetes *47*, 1281-1286.

Kurowski, T.G., Lin, Y., Luo, Z., Tsichlis, P.N., Buse, M.G., Heydrick, S.J., and Ruderman, N.B. (1999). Hyperglycaemia inhibits insulin activation of Akt/protein kinase B but not phosphatidylinositol 3-kinase in rat skeletal muscle. Diabetes *48*, 658-663.

Kurth-Kraczek, E.J., Hirshman, M.F., Goodyear, L.J., and Winder, W.W. (1999). 5' AMP-activated protein kinase activation causes Glut-4 translocation in skeletal muscle. Diabetes *48*, 1667-1671.

Laakso, M. (1999). Hyperglycaemia and cardiovascular disease in type 2 diabetes. Diabetes *48*, 937-942.

Lavan, B.E., Lane, W.S., and Lienhard, G.E. (1997a). The 60-kDa phosphotyrosine protein in insulin-treated adipocytes is a new member of the insulin receptor substrate family. J. Biol. Chem. *272*, 11439-11443.

Lavan, B.E., Fantin, V.R., Chang, E.T., Lane, W.S., Keller, S.R., and Lienhard, G.E. (1997b). A novel 160-kDa phosphotyrosine protein in insulin-treated embryonic kidney cells is a new member of the insulin receptor substrate family. J. Biol. Chem. *272*, 21403-21407.

Livingstone, C., James, D.E., Rice, J.E., Hanpeter, D., and Gould, G.W. (1996). Compartment ablation analysis of the insulin-responsive glucose transporter (Glut-4) in 3T3-L1 adipocytes. Biochem. J. *315 (Pt 2)* , 487-495.

Lund, S., Holman, G.D., Schmitz, O., and Pedersen, O. (1995). Contraction stimulates translocation of glucose transporter Glut-4 in skeletal muscle through a mechanism distinct from that of insulin. Proc. Natl. Acad. Sci. U. S. A *92*, 5817-5821.

Maier, V.H., Melvin, D.R., Lister, C.A., Chapman, H., Gould, G.W., and Murphy, G.J. (2000). v- and t-SNARE protein expression in models of insulin resistance: normalisation

of glycaemia by rosiglitazone treatment corrects overexpression of cellubrevin, vesicle-associated membrane protein-2, and syntaxin-4 in skeletal muscle of Zucker diabetic fatty rats. Diabetes *49*, 618-625.

Malide, D., Dwyer, N.K., Blanchette-Mackie, E.J., and Cushman, S.W. (1997). Immunocytochemical evidence that Glut-4 resides in a specialised translocation post-endosomal VAMP2-positive compartment in rat adipose cells in the absence of insulin. J. Histochem. Cytochem. *45*, 1083-1096.

Mantych, G.J., James, D.E., and Devaskar, S.U. (1993). Jejunal/kidney glucose transporter isoform (Glut-5) is expressed in the human blood-brain barrier. Endocrinology *132*, 35-40.

Marletta, M.A. (1994). Nitric oxide synthase: aspects concerning structure and catalysis. Cell *78*, 927-930.

Martin, L.B., Shewan, A., Millar, C.A., Gould, G.W., and James, D.E. (1998). Vesicle-associated membrane protein 2 plays a specific role in the insulin-dependent trafficking of the facilitative glucose transporter Glut-4 in 3T3-L1 adipocytes. J. Biol. Chem. *273*, 1444-1452.

Martin, S., Tellam, J., Livingstone, C., Slot, J.W., Gould, G.W., and James, D.E. (1996). The glucose transporter (Glut-4) and vesicle-associated membrane protein-2 (VAMP-2) are segregated from recycling endosomes in insulin- sensitive cells. J. Cell Biol. *134*, 625-635.

Mastick, C.C., Brady, M.J., and Saltiel, A.R. (1995). Insulin stimulates the tyrosine phosphorylation of caveolin. J. Cell Biol. *129*, 1523-1531.

Mastick, C.C. and Saltiel, A.R. (1997). Insulin-stimulated tyrosine phosphorylation of caveolin is specific for the differentiated adipocyte phenotype in 3T3-L1 cells. J. Biol. Chem. *272*, 20706-20714.

McDowell, H.E., Walker, T., Hajduch, E., Christie, G., Batty, I.H., Downes, C.P., and Hundal, H.S. (1997). Inositol phospholipid 3-kinase is activated by cellular stress but is not required for the stress-induced activation of glucose transport in L6 rat skeletal muscle cells. Eur. J. Biochem. *247*, 306-313.

McMahon, H.T., Ushkaryov, Y.A., Edelmann, L., Link, E., Binz, T., Niemann, H., Jahn, R., and Sudhof, T.C. (1993). Cellubrevin is a ubiquitous tetanus-toxin substrate homologous to a putative synaptic vesicle fusion protein. Nature *364*, 346-349.

Merrill, G.F., Kurth, E.J., Hardie, D.G., and Winder, W.W. (1997). AICA riboside increases AMP-activated protein kinase, fatty acid oxidation, and glucose uptake in rat muscle. Am. J. Physiol *273*, E1107-E1112.

Millar, C.A., Shewan, A., Hickson, G.R., James, D.E., and Gould, G.W. (1999). Differential regulation of secretory compartments containing the insulin-responsive glucose transporter 4 in 3T3-L1 adipocytes. Mol. Biol. Cell *10*, 3675-3688.

Moller, D.E. (2001). New drug targets for type 2 diabetes and the metabolic syndrome. Nature *414*, 821-827.

Moncada, V.Y., Hedo, J.A., Serrano-Rios, M., and Taylor, S.I. (1986). Insulin-receptor biosynthesis in cultured lymphocytes from an insulin- resistant patient (Rabson-Mendenhall syndrome). Evidence for defect before insertion of receptor into plasma membrane. Diabetes *35*, 802-807.

Morris, A.D., Petrie, J.R., and Connell, J.M. (1994). Insulin and hypertension. J. Hypertens. *12*, 633-642.

Murphy, G.J. and Holder, J.C. (2000). PPAR-gamma agonists: therapeutic role in diabetes, inflammation and cancer. Trends Pharmacol. Sci. *21*, 469-474.

Musi, N., Fujii, N., Hirshman, M.F., Ekberg, I., Froberg, S., Ljungqvist, O., Thorell, A., and Goodyear, L.J. (2001). AMP-activated protein kinase (AMPK) is activated in muscle of subjects with type 2 diabetes during exercise. Diabetes *50*, 921-927.

Nakanishi, H., Brewer, K.A., and Exton, J.H. (1993). Activation of the zeta isozyme of protein kinase C by phosphatidylinositol 3,4,5-trisphosphate. J. Biol. Chem. *268*, 13-16.

Nakashima, N., Sharma, P.M., Imamura, T., Bookstein, R., and Olefsky, J.M. (2000). The tumor suppressor PTEN negatively regulates insulin signalling in 3T3-L1 adipocytes. J. Biol. Chem. *275*, 12889-12895.

Nawano, M., Oku, A., Ueta, K., Umebayashi, I., Ishirahara, T., Arakawa, K., Saito, A., Anai, M., Kikuchi, M., and Asano, T. (2000). Hyperglycaemia contributes insulin resistance in hepatic and adipose tissue but not skeletal muscle of ZDF rats. Am. J. Physiol Endocrinol. Metab *278*, E535-E543.

Nystrom, F.H., Chen, H., Cong,L. N., Li, Y., and Quon, M.J. (1999). Caveolin-1 interacts with the insulin receptor and can differentially modulate insulin signalling in transfected Cos-7 cells and rat adipose cells. Mol. Endocrinol. *13*, 2013-2024.

O'Doherty, R.M., Halseth, A.E., Granner, D.K., Bracy, D.P., and Wasserman, D.H. (1998). Analysis of insulin-stimulated skeletal muscle glucose uptake in conscious rat using isotopic glucose analogues. Am. J. Physiol *274*, E287-E296.

Okada, T., Kawano, Y., Sakakibara, T., Hazeki, O., and Ui, M.(1994). Essential role of phosphatidylinositol 3-kinase in insulin-induced glucose transport and antilipolysis in rat adipocytes. Studies with a selective inhibitor wortmannin. J. Biol. Chem. *269*, 3568-3573.

Oku, A., Nawano, M., Ueta, K., Fujita, T., Umebayashi, I., Arakawa, K., Kano-Ishihara, T., Saito, A., Anai, M., Funaki, M., Kikuchi, M., Oka, Y., and Asano, T. (2001). Inhibitory effect of hyperglycaemia on insulin-induced Akt/protein kinase B activation in skeletal muscle. Am. J. Physiol Endocrinol. Metab *280*, E816-E824.

Olson, A.L., Knight, J.B., and Pessin, J.E. (1997). Syntaxin-4, VAMP2, and/or VAMP3/cellubrevin are functional target membrane and vesicle SNAP receptors for insulin-stimulated Glut-4 translocation in adipocytes. Mol. Cell Biol. *17*, 2425-2435.

Ono, H., Katagiri, H., Funaki, M., Anai, M., Inukai, K., Fukushima, Y., Sakoda, H., Ogihara, T., Onishi, Y., Fujishiro, M., Kikuchi, M., Oka, Y., and Asano, T. (2001). Regulation of phosphoinositide metabolism, Akt phosphorylation, and glucose transport by PTEN (phosphatase and tensin homologue deleted on chromosome 10) in 3T3-L1 adipocytes. Mol. Endocrinol. *15*, 1411-1422.

Ordahl, C.P. and Williams, B.A. (1998). Knowing chops from chuck: roasting myoD redundancy. Bioessays *20*, 357-362.

Ordahl, C.P., Williams, B.A., and Denetclaw, W. (2000). Determination and morphogenesis in myogenic progenitor cells: an experimental embryological approach. Curr. Top. Dev. Biol. *48*, 319-367.

Palmer, R.M., Ashton, D.S., and Moncada, S. (1988). Vascular endothelial cells synthesise nitric oxide from L-arginine. Nature *333*, 664-666.

Park, K.S., Ciaraldi, T.P., Lindgren, K., Abrams-Carter, L., Mudaliar, S., Nikoulina, S.E., Tufari, S.R., Veerkamp, J.H., Vidal-Puig, A., and Henry, R.R. (1998a). Troglitazone effects on gene expression in human skeletal muscle of type 2 diabetes involve up-regulation of peroxisome proliferator- activated receptor-gamma. J. Clin. Endocrinol. Metab *83*, 2830-2835.

Park, K.S., Ciaraldi, T.P., Abrams-Carter, L., Mudaliar, S., Nikoulina, S.E., and Henry, R.R. (1998b). Troglitazone regulation of glucose metabolism in human skeletal muscle cultures from obese type II diabetic subjects. J. Clin. Endocrinol. Metab *83*, 1636-1643.

Perry, M.A. (1980). Capillary filtration and permeability coefficients calculated from measurements of interendothelial cell junctions in rabbit lung and skeletal muscle. Microvasc. Res. *19*, 142-157.

Pessin, J.E., Thurmond, D.C., Elmendorf, J.S., Coker, K.J., and Okada, S. (1999). Molecular basis of insulin-stimulated Glut-4 vesicle trafficking. Location! Location! Location! J. Biol. Chem. *274*, 2593-2596.

Peterson, R.G., Shaw, W.N., Neel, M.A., Little, L.A., and Eichberg, J. (1990). Zucker diabetic fatty rat as a model for non-insulin-dependent diabetes mellitus. ILAR News *32*, 16-19.

Ploug, T. and Ralston, E. (1998). Anatomy of glucose transporters in skeletal muscle. Effects of insulin and contractions. Adv. Exp. Med. Biol. *441*, 17-26.

Ploug, T., van Deurs, B., Ai, H., Cushman, S.W., and Ralston, E. (1998). Analysis of Glut-4 distribution in whole skeletal muscle fibers: identification of distinct storage compartments that are recruited by insulin and muscle contractions. J. Cell Biol. *142*, 1429-1446.

Ponka, P. and Lok, C.N. (1999). The transferrin receptor: role in health and disease. Int. J. Biochem. Cell Biol. *31*, 1111-1137.

Rabson, S.M. and Mendenhall, E.N. (1956). Familial hypertrophy of pineal body, hyperplasia of adrenal cortex and diabetes mellitus. J. Clin. Path. *26*, 283-290.

Ralston, E. and Ploug, T. (1996). Glut-4 in cultured skeletal myotubes is segregated from the transferrin receptor and stored in vesicles associated with TGN. J. Cell Sci. *109 (Pt 13)*, 2967-2978.

Rand, E.B., Depaoli, A.M., Davidson, N.O., Bell, G.I., and Burant, C.F. (1993). Sequence, tissue distribution, and functional characterisation of the rat fructose transporter GLUT5. Am. J. Physiol *264*, G1169-G1176.

Randhawa, V.K., Bilan, P.J., Khayat, Z.A., Daneman, N., Liu, Z., Ramlal, T., Volchuk, A., Peng, X.R., Coppola, T., Regazzi, R., Trimble, W.S., and Klip, A. (2000). VAMP2, but not VAMP3/cellubrevin, mediates insulin-dependent incorporation of Glut-4 into the plasma membrane of L6 myoblasts. Mol. Biol. Cell *11*, 2403-2417.

Rasmussen, B.B. and Winder, W.W. (1997). Effect of exercise intensity on skeletal muscle malonyl-CoA and acetyl- CoA carboxylase. J. Appl. Physiol *83*, 1104-1109.

Rea, S. and James, D.E. (1997). Moving Glut-4: the biogenesis and trafficking of Glut-4 storage vesicles. Diabetes *46*, 1667-1677.

Reaven, G.M. (1988). Banting lecture 1988. Role of insulin resistance in human disease. Diabetes *37*, 1595-1607.

Reaven, G.M., Chang, H., Hoffman, B.B., and Azhar, S. (1989). Resistance to insulin-stimulated glucose uptake in adipocytes isolated from spontaneously hypertensive rats. Diabetes *38*, 1155-1160.

Reaves, B.J., Bright, N.A., Mullock, B.M., and Luzio, J.P. (1996). The effect of wortmannin on the localisation of lysosomal type I integral membrane glycoproteins suggests a role for phosphoinositide 3- kinase activity in regulating membrane traffic late in the endocytic pathway. J. Cell Sci. *109 (Pt 4)*, 749-762.

Reedquist, K.A., Fukazawa, T., Panchamoorthy, G., Langdon, W.Y., Shoelson, S.E., Druker, B.J., and Band, H. (1996). Stimulation through the T cell receptor induces Cbl association with Crk proteins and the guanine nucleotide exchange protein C3G. J. Biol. Chem. *271*, 8435-8442.

Reid, M.B. (1998). Role of nitric oxide in skeletal muscle: synthesis, distribution and functional importance. Acta Physiol Scand. *162*, 401-409.

Ribon, V., Hubbell, S., Herrera, R., and Saltiel, A.R. (1996). The product of the Cbl oncogene forms stable complexes in vivo with endogenous Crk in a tyrosine phosphorylation-dependent manner. Mol. Cell Biol. *16*, 45-52.

Ribon, V. and Saltiel, A.R. (1997). Insulin stimulates tyrosine phosphorylation of the proto-oncogene product of c-Cbl in 3T3-L1 adipocytes. Biochem. J. *324 (Pt 3)*, 839-845.

Richter, E.A., Hansen, B.F., and Hansen, S.A. (1988). Glucose-induced insulin resistance of skeletal-muscle glucose transport and uptake. Biochem. J. *252*, 733-737.

Roberts, C.K., Barnard, R.J., Scheck, S.H., and Balon, T.W. (1997). Exercise-stimulated glucose transport in skeletal muscle is nitric oxide dependent. Am. J. Physiol *273*, E220-E225.

Roberts, C.K., Barnard, R.J., Jasman, A., and Balon, T.W. (1999). Acute exercise increases nitric oxide synthase activity in skeletal muscle. Am. J. Physiol *277*, E390-E394.

Rordorf-Nikolic, T., Van Horn, D.J., Chen, D., White, M.F., and Backer,J.M. (1995). Regulation of phosphatidylinositol 3'-kinase by tyrosyl phosphoproteins. Full activation requires occupancy of both SH2 domains in the 85-kDa regulatory subunit. J. Biol. Chem. *270*, 3662-3666.

Rossetti, L. (2000). Perspective: Hexosamines and nutrient sensing. Endocrinology *141*, 1922-1925.

Rossetti, L., Smith, D., Shulman, G.I., Papachristou, D., and DeFronzo, R.A. (1987). Correction of hyperglycaemia with phlorizin normalises tissue sensitivity to insulin in diabetic rats. J. Clin. Invest *79*, 1510-1515.

Rothenberg, P.L., Lane, W.S., Karasik, A., Backer, J., White, M., and Kahn, C.R. (1991). Purification and partial sequence analysis of pp185, the major cellular substrate of the insulin receptor tyrosine kinase. J. Biol. Chem. *266*, 8302-8311.

Rothman, D.L., Magnusson, I., Cline, G., Gerard, D., Kahn, C.R., Shulman, R.G., and Shulman, G.I. (1995). Decreased muscle glucose transport/phosphorylation is an early defect in the pathogenesis of non-insulin-dependent diabetes mellitus. Proc. Natl. Acad. Sci. U. S. A *92*, 983-987.

Rothman, J.E. and Warren, G. (1994). Implications of the SNARE hypothesis for intracellular membrane topology and dynamics. Curr. Biol. *4*, 220-233.

Roy, D. and Marette, A. (1996). Exercise induces the translocation of Glut-4 to transverse tubules from an intracellular pool in rat skeletal muscle. Biochem. Biophys. Res. Commun. *223*, 147-152.

Ryder, J.W., Chibalin, A.V., and Zierath, J.R. (2001). Intracellular mechanisms underlying increases in glucose uptake in response to insulin or exercise in skeletal muscle. Acta Physiol Scand. *171*, 249-257.

Saad, M.J., Araki, E., Miralpeix, M., Rothenberg, P.L., White, M.F., and Kahn, C.R. (1992). Regulation of insulin receptor substrate-1 in liver and muscle of animal models of insulin resistance. J. Clin. Invest *90*, 1839-1849.

Salt, I., Celler, J.W., Hawley, S.A., Prescott, A., Woods, A., Carling, D., and Hardie, D.G. (1998). AMP-activated protein kinase: greater AMP dependence, and preferential nuclear localisation, of complexes containing the alpha2 isoform. Biochem. J. *334 (Pt 1)*, 177-187.

Saltiel, A.R. (1996). Diverse signalling pathways in the cellular actions of insulin. Am. J. Physiol *270*, E375-E385.

Salway, J.G. (1994). Glycogen metabolism. In Metabolism at a glance, (Oxford: Blackwell Scientific Publications), pp. 60-61.

Sarabia, V., Ramlal, T., and Klip, A. (1990). Glucose uptake in human and animal muscle cells in culture. Biochem. Cell Biol. *68*, 536-542.

Scherer, P.E., Lisanti, M.P., Baldini, G., Sargiacomo, M., Mastick, C.C., and Lodish, H.F. (1994). Induction of caveolin during adipogenesis and association of Glut-4 with caveolin-rich vesicles. J. Cell Biol. *127*, 1233-1243.

Schu, P.V., Takegawa, K., Fry, M.J., Stack, J.H., Waterfield, M.D., and Emr, S.D. (1993). Phosphatidylinositol 3-kinase encoded by yeast VPS34 gene essential for protein sorting. Science *260*, 88-91.

Sharma, P.M., Egawa, K., Huang, Y., Martin, J.L., Huvar, I., Boss, G.R., and Olefsky, J.M. (1998). Inhibition of phosphatidylinositol 3-kinase activity by adenovirus-mediated gene transfer and its effect on insulin action. J. Biol. Chem. *273*, 18528-18537.

Shepherd, P.R., Nave, B.T., and Siddle, K. (1995). Insulin stimulation of glycogen synthesis and glycogen synthase activity is blocked by wortmannin and rapamycin in 3T3-L1 adipocytes: evidence for the involvement of phosphoinositide 3-kinase and p70 ribosomal protein-S6 kinase. Biochem. J. *305 (Pt 1)*, 25-28.

Shepherd, P.R., Withers, D.J., and Siddle, K. (1998). Phosphoinositide 3-kinase: the key switch mechanism in insulin signalling. Biochem. J. *333 (Pt 3)*, 471-490.

Shulman, G.I., Rothman, D.L., Jue, T., Stein, P., DeFronzo, R.A., and Shulman, R.G. (1990). Quantitation of muscle glycogen synthesis in normal subjects and subjects with non-insulin-dependent diabetes by 13C nuclear magnetic resonance spectroscopy. N. Engl. J. Med. *322*, 223-228.

Shulman, R.G. and Rothman, D.L. (2001). ^{13}C NMR of intermediary metabolism: implications for systemic physiology. Annu. Rev. Physiol *63*, 15-48.

Siddle, K., Urso, B., Niesler, C.A., Cope, D.L., Molina, L., Surinya, K.H., and Soos, M.A. (2001). Specificity in ligand binding and intracellular signalling by insulin and insulin-like growth factor receptors. Biochem. Soc. Trans. *29*, 513-525.

Simpson, F., Whitehead, J.P., and James, D.E. (2001). Glut-4 at the cross roads between membrane trafficking and signal transduction. Traffic. *2*, 2-11.

Slot, J.W., Geuze, H.J., Gigengack, S., James, D.E., and Lienhard, G.E. (1991a). Translocation of the glucose transporter Glut-4 in cardiac myocytes of the rat. Proc. Natl. Acad. Sci. U. S. A *88*, 7815-7819.

Slot, J.W., Geuze, H.J., Gigengack, S., Lienhard, G.E., and James, D.E. (1991b). Immuno-localisation of the insulin regulatable glucose transporter in brown adipose tissue of the rat. J. Cell Biol. *113*, 123-135.

Smart, E.J., Graf, G.A., McNiven, M.A., Sessa, W.C., Engelman, J.A., Scherer, P.E., Okamoto, T., and Lisanti, M.P. (1999). Caveolins, liquid-ordered domains, and signal transduction. Mol. Cell Biol. *19*, 7289-7304.

Smith, R.L. and Lawrence, J.C., Jr. (1984). Insulin action in denervated rat hemidiaphragms. Decreased hormonal stimulation of glycogen synthesis involves both glycogen synthase and glucose transport. J. Biol. Chem. *259*, 2201-2207.

Sollner, T., Whiteheart, S.W., Brunner, M., Erdjument-Bromage, H., Geromanos, S., Tempst, P., and Rothman, J.E. (1993). SNAP receptors implicated in vesicle targeting and fusion. Nature *362*, 318-324.

Spiegelman, B.M. (1998). PPAR-gamma: adipogenic regulator and thiazolidinedione receptor. Diabetes *47*, 507-514.

Standaert, M.L., Galloway, L., Karnam, P., Bandyopadhyay, G., Moscat, J., and Farese, R.V. (1997). Protein kinase C-zeta as a downstream effector of phosphatidylinositol 3-kinase during insulin stimulation in rat adipocytes. Potential role in glucose transport. J. Biol. Chem. *272*, 30075-30082.

Stephens, L., Anderson, K., Stokoe, D., Erdjument-Bromage, H., Painter, G.F., Holmes, A.B., Gaffney, P.R., Reese, C.B., McCormick, F., Tempst, P., Coadwell, J., and Hawkins, P.T. (1998). Protein kinase B kinases that mediate phosphatidylinositol 3,4,5-trisphosphate-dependent activation of protein kinase B. Science *279*, 710-714.

Sudhof, T.C. (1995). The synaptic vesicle cycle: a cascade of protein-protein interactions. Nature *375*, 645-653.

Sun, X.J., Miralpeix, M., Myers, M.G., Jr., Glasheen, E.M., Backer, J.M., Kahn, C.R., and White, M.F. (1992). Expression and function of IRS-1 in insulin signal transmission. J. Biol. Chem. *267*, 22662-22672.

Sun, X.J., Wang, L.M., Zhang, Y., Yenush, L., Myers, M.G., Jr., Glasheen, E., Lane, W.S., Pierce, J.H., and White, M.F. (1995). Role of IRS-2 in insulin and cytokine signalling. Nature *377*, 173-177.

Suzuki, K. and Kono, T. (1980). Evidence that insulin causes translocation of glucose transport activity to the plasma membrane from an intracellular storage site. Proc. Natl. Acad. Sci. U. S. A *77*, 2542-2545.

Taira, M., Taira, M., Hashimoto, N., Shimada, F., Suzuki, Y., Kanatsuka, A., Nakamura, F., Ebina, Y., Tatibana, M., and Makino, H. (1989). Human diabetes associated with a deletion of the tyrosine kinase domain of the insulin receptor. Science *245*, 63-66.

Tamemoto, H., Kadowaki, T., Tobe, K., Yagi, T., Sakura, H., Hayakawa, T., Terauchi, Y., Ueki, K., Kaburagi, Y., and Satoh, S. (1994). Insulin resistance and growth retardation in mice lacking insulin receptor substrate-1. Nature *372*, 182-186.

Tanner, L.I. and Lienhard, G.E. (1989). Localisation of transferrin receptors and insulin-like growth factor II receptors in vesicles from 3T3-L1 adipocytes that contain intracellular glucose transporters. J. Cell Biol. *108*, 1537-1545.

Tellam, J.T., Macaulay, S.L., McIntosh, S., Hewish, D.R., Ward, C.W., and James, D.E. (1997). Characterisation of Munc-18c and syntaxin-4 in 3T3-L1 adipocytes. Putative role in insulin-dependent movement of Glut-4. J. Biol. Chem. *272*, 6179-6186.

Thien, C.B. and Langdon, W.Y. (2001). Cbl: many adaptations to regulate protein tyrosine kinases. Nat. Rev. Mol. Cell Biol. *2*, 294-307.

Tsakiridis, T., McDowell, H.E., Walker, T., Downes, C.P., Hundal, H.S., Vranic, M., and Klip, A. (1995). Multiple roles of phosphatidylinositol 3-kinase in regulation of glucose transport, amino acid transport, and glucose transporters in L6 skeletal muscle cells. Endocrinology *136*, 4315-4322.

Ueki, K., Yamamoto-Honda, R., Kaburagi, Y., Yamauchi, T., Tobe, K., Burgering, B.M., Coffer, P.J., Komuro, I., Akanuma, Y., Yazaki, Y., and Kadowaki, T. (1998). Potential role of protein kinase B in insulin-induced glucose transport, glycogen synthesis, and protein synthesis. J. Biol. Chem. *273*, 5315-5322.

Unger, R.H. and Orci, L. (2001). Diseases of liporegulation: new perspective on obesity and related disorders. FASEB J. *15*, 312-321.

Van Obberghen, E., Ksauga, M., Le Cam, A., Hedo, J.A., Itin, A., and Harrison, L.C. (1981). Biosynthetic labelling of insulin receptor: studies of subunits in cultured human IM-9 lymphocytes. Proc. Natl. Acad. Sci. U. S. A *78*, 1052-1056.

Vanhaesebroeck, B., Leevers, S.J., Panayotou, G., and Waterfield, M.D. (1997). Phosphoinositide 3-kinases: a conserved family of signal transducers. Trends Biochem. Sci. *22*, 267-272.

Virkamaki, A., Ueki, K., and Kahn, C.R. (1999). Protein-protein interaction in insulin signalling and the molecular mechanisms of insulin resistance. J. Clin. Invest *103*, 931-943.

Vock, R., Weibel, E.R., Hoppeler, H., Ordway, G., Weber, J.M., and Taylor, C.R. (1996). Design of the oxygen and substrate pathways. V. Structural basis of vascular substrate supply to muscle cells. J. Exp. Biol. *199 (Pt 8)*, 1675-1688.

Volchuk, A., Mitsumoto, Y., He, L., Liu, Z., Habermann, E., Trimble, W., and Klip, A. (1994). Expression of vesicle-associated membrane protein 2 (VAMP- 2)/synaptobrevin II and cellubrevin in rat skeletal muscle and in a muscle cell line. Biochem. J. *304 (Pt 1)*, 139-145.

Volchuk, A., Wang, Q., Ewart, H.S., Liu, Z., He, L., Bennett, M.K., and Klip, A. (1996). Syntaxin 4 in 3T3-L1 adipocytes: regulation by insulin and participation in insulin-dependent glucose transport. Mol. Biol. Cell *7*, 1075-1082.

Walker, K.S., Deak, M., Paterson, A., Hudson, K., Cohen, P., and Alessi, D.R. (1998). Activation of protein kinase B beta and gamma isoforms by insulin in vivo and by 3-phosphoinositide-dependent protein kinase-1 in vitro: comparison with protein kinase B alpha. Biochem. J. *331 (Pt 1)*, 299-308.

Wang, Q., Bilan, P.J., Tsakiridis, T., Hinek, A., and Klip, A. (1998). Actin filaments participate in the relocalisation of phosphatidylinositol3-kinase to glucose transporter-containing compartments and in the stimulation of glucose uptake in 3T3-L1 adipocytes. Biochem. J. *331 (Pt 3)*, 917-928.

Wang, Q., Somwar, R., Bilan, P.J., Liu, Z., Jin, J., Woodgett, J.R., and Klip, A. (1999). Protein kinase B/Akt participates in Glut-4 translocation by insulin in L6 myoblasts. Mol. Cell Biol. *19*, 4008-4018.

Wasserman, D.H. and Halseth, A.E. (1998). An overview of muscle glucose uptake during exercise. In Advances in experimental medicine and biology, N.Back, I.R.Cohen, A.Lajtha, and R.Paoletti, eds. (New York & London: Plenum), pp. 1-17.

Watson, R.T. and Pessin, J.E. (2001). Subcellular Compartmentalisation and Trafficking of the Insulin- Responsive Glucose Transporter, Glut-4. Exp. Cell Res. *271*, 75-83.

Watson, R.T., Shigematsu, S., Chiang, S.H., Mora, S., Kanzaki, M., Macara, I.G., Saltiel, A.R., and Pessin, J.E. (2001). Lipid raft microdomain compartmentalisation of TC10 is required for insulin signalling and Glut-4 translocation. J. Cell Biol. *154*, 829-840.

Weintraub, H. (1993). The MyoD family and myogenesis: redundancy, networks, and thresholds. Cell *75*, 1241-1244.

White, M.F. (1997). The insulin signalling system and the IRS proteins. Diabetologia *40 Suppl 2*, S2-17.

White, M.F. (1998). The IRS-signalling system: a network of docking proteins that mediate insulin action. Mol. Cell Biochem. *182*, 3-11.

White, M.F. and Kahn, C.R. (1994). The insulin signalling system. J. Biol. Chem. *269*, 1-4.

White, M.F., Livingston, J.N., Backer, J.M., Lauris, V., Dull, T.J., Ullrich, A., and Kahn, C.R. (1988a). Mutation of the insulin receptor at tyrosine 960 inhibits signal transmission but does not affect its tyrosine kinase activity. Cell *54*, 641-649.

White, M.F., Maron, R., and Kahn, C.R. (1985). Insulin rapidly stimulates tyrosine phosphorylation of a Mr-185,000 protein in intact cells. Nature *318*, 183-186.

White, M.F., Shoelson, S.E., Keutmann, H., and Kahn, C.R. (1988b). A cascade of tyrosine autophosphorylation in the beta-subunit activates the phosphotransferase of the insulin receptor. J. Biol. Chem. *263*, 2969-2980.

Whitehead, J.P., Clark, S.F., Urso, B., and James, D.E. (2000). Signalling through the insulin receptor. Curr. Opin. Cell Biol. *12*, 222-228.

Whitman, M., Downes, C.P., Keeler, M., Keller, T., and Cantley, L. (1988). Type I phosphatidylinositol kinase makes a novel inositol phospholipid, phosphatidylinositol-3-phosphate. Nature *332*, 644-646.

Wiese, R.J., Mastick, C.C., Lazar, D.F., and Saltiel, A.R. (1995). Activation of mitogen-activated protein kinase and phosphatidylinositol 3'-kinase is not sufficient for the hormonal stimulation of glucose uptake, lipogenesis, or glycogen synthesis in 3T3-L1 adipocytes. J. Biol. Chem. *270*, 3442-3446.

Williams, J.F., McClain, D.A., Dull, T.J., Ullrich, A., and Olefsky, J.M. (1990). Characterization of an insulin receptor mutant lacking the subunit processing site. J. Biol. Chem. *265*, 8463-8469.

Winder, W.W. (2001). Energy-sensing and signalling by AMP-activated protein kinase in skeletal muscle. J. Appl. Physiol *91*, 1017-1028.

Winder, W.W. and Hardie, D.G. (1996). Inactivation of acetyl-CoA carboxylase and activation of AMP-activated protein kinase in muscle during exercise. Am. J. Physiol *270*, E299-E304.

Winder, W.W. and Hardie, D.G. (1999). AMP-activated protein kinase, a metabolic master switch: possible roles in type 2 diabetes. Am. J. Physiol *277*, E1-10.

Withers, D.J., Gutierrez, J.S., Towery, H., Burks, D.J., Ren, J.M., Previs, S., Zhang, Y., Bernal, D., Pons, S., Shulman, G.I., Bonner-Weir, S., and White, M.F. (1998). Disruption of IRS-2 causes type 2 diabetes in mice. Nature *391*, 900-904.

Wojtaszewski, J.F., Hansen, B.F., Gade, Kiens, B., Markuns, J.F., Goodyear, L.J., and Richter, E.A. (2000a). Insulin signalling and insulin sensitivity after exercise in human skeletal muscle. Diabetes *49*, 325-331.

Wojtaszewski, J.F., Nielsen, P., Hansen, B.F., Richter, E.A., and Kiens, B. (2000b). Isoform-specific and exercise intensity-dependent activation of 5'-AMP-activated protein kinase in human skeletal muscle. J. Physiol *528 Pt 1*, 221-226.

Yaffe, D. and Saxel, O. (1977). Serial passaging and differentiation of myogenic cells isolated from dystrophic mouse muscle. Nature *270*, 725-727.

Yamamoto-Honda, R., Tobe, K., Kaburagi, Y., Ueki, K., Asai, S., Yachi, M., Shirouzu, M., Yodoi, J., Akanuma, Y., and Yokoyama, S. (1995). Upstream mechanisms of glycogen synthase activation by insulin and insulin-like growth factor-I. Glycogen synthase activation is antagonised by wortmannin or LY294002 but not by rapamycin or by inhibiting p21ras. J. Biol. Chem. *270*, 2729-2734.

Yamori, Y., Tomimoto, K., Ooshima, A., Hazama, F., and Okamoto, K. (1974). Proceedings: Developmental course of hypertension in the SHR-substrains susceptible to hypertensive cerebrovascular lesions. Jpn. Heart J. *15*, 209-210.

Yang, J., Clarke, J.F., Ester, C.J., Young, P.W., Kasuga, M., and Holman, G.D. (1996). Phosphatidylinositol 3-kinase acts at an intracellular membrane site to enhance Glut-4 exocytosis in 3T3-L1 cells. Biochem. J. *313 (Pt 1)*, 125-131.

Yang, J., and Holman, G.D. (1993). Comparison of Glut-4 and Glut-1 subcellular trafficking in basal and insulin-stimulated 3T3-L1 cells. J. Biol. Chem. *268*, 4600-4603.

Yasin, R., Van Beers, G., Nurse, K.C., Al Ani, S., Landon, D.N., and Thompson, E.J. (1977). A quantitative technique for growing human adult skeletal muscle in culture starting from mononucleated cells. J. Neurol. Sci. *32*, 347-360.

Yeaman, S.J., Armstrong, J.L., Bonavaud, S.M., Poinasamy, D., Pickersgill, L., and Halse, R. (2001). Regulation of glycogen synthesis in human muscle cells. Biochem. Soc. Trans. *29*, 537-541.

Yeh, J.I., Gulve, E.A., Rameh, L., and Birnbaum, M.J. (1995). The effects of wortmannin on rat skeletal muscle. Dissociation of signalling pathways for insulin- and contraction-activated hexose transport. J. Biol. Chem. *270*, 2107-2111.

Yip, J., Facchini, F.S., and Reaven, G.M. (1998). Resistance to insulin-mediated glucose disposal as a predictor of cardiovascular disease. J. Clin. Endocrinol. Metab *83*, 2773-2776.

Young, M.E. and Leighton, B. (1998). Evidence for altered sensitivity of the nitric oxide/cGMP signalling cascade in insulin-resistant skeletal muscle. Biochem. J. *329 (Pt 1)*, 73-79.

Young, M.E., Radda, G.K., and Leighton, B. (1997). Nitric oxide stimulates glucose transport and metabolism in rat skeletal muscle in vitro. Biochem. J. *322 (Pt 1)*, 223-228.

Young, P.W., Cawthorne, M.A., Coyle, P.J., Holder, J.C., Holman, G.D., Kozka, I.J., Kirkham, D.M., Lister, C.A., and Smith, S.A. (1995). Repeat treatment of obese mice with BRL 49653, a new potent insulin sensitiser, enhances insulin action in white adipocytes. Association with increased insulin binding and cell-surface Glut-4 as measured by photoaffinity labelling. Diabetes *44*, 1087-1092.

Zheng, D., MacLean, P.S., Pohnert, S.C., Knight, J.B., Olson, A.L., Winder, W.W., and Dohm, G.L. (2001). Regulation of muscle Glut-4 transcription by AMP-activated protein kinase. J. Appl. Physiol *91*, 1073-1083.

Zimmet, P., Alberti, K.G., and Shaw, J. (2001). Global and societal implications of the diabetes epidemic. Nature *414*, 782-787.

Zorzano, A., Munoz, P., Camps, M., Mora, C., Testar, X., and Palacin, M. (1996). Insulin-induced redistribution of Glut-4 glucose carriers in the muscle fiber. In search of Glut-4 trafficking pathways. Diabetes *45 Suppl 1*, S70-S81.